THE UNIVERSITY OF QUEENSLAND

AUSTRALIA

Establishment, optimization and characterization of a rat model of breast cancer induced bone pain

Priyank Ashok Shenoy

B. Pharm., M. Pharm.(Pharmacology)

A thesis submitted for the degree of Doctor of Philosophy at

The University of Queensland in year 2017

Faculty of Medicine

Abstract

In the majority of patients with advanced breast cancer, there is metastatic spread to bones resulting in pain. Clinically available drug treatments for alleviation of breast cancer-induced bone pain (BCIBP) often produce inadequate pain relief due to dose-limiting side-effects. A major impediment to the discovery of novel well-tolerated analgesic agents for the relief of pain due to bony metastases is the fact that most rodent models of cancer induced bone pain were induced by systemic injection of cancer cells, resulting in widespread formation of cancer metastases and poor general animal health necessitating early euthanasia on welfare grounds.

In my thesis, Chapter 1 explores briefly the literature on concepts involving pain processing, pathophysiology of breast cancer and Walker 256 breast cancer cell- induced bone pain model in rats.

My first aim was to establish and comprehensively characterise a clinically relevant and optimised Wistar Han female rat model of BCIBP involving unilateral intra-tibial injection (ITI) of Walker 256 breast carcinoma cells. The results described in Chapter 2 portray the establishment and optimisation of this model. I found the optimum number of Walker 256 cells producing bilateral hypersensitivity in the hind paws of rats whilst maintaining satisfactory animal health to be 4.5 x 10^5 cells / 10 µL. The rats unilaterally injected with cancer cells developed bilateral mechanical allodynia and mechanical hyperalgesia, but not thermal hyperalgesia. I further characterised this model using tibial bone histology and micro-computed tomography (µCT) scans, which confirmed the presence of osteolytic lesions due to cancer induced bone destruction. Interestingly, the pain hypersensitivity in the hind paws of rats given an ITI of Walker 256 cells resolved after approximately 25 days, which was reversed by administration of the opioid receptor antagonist, naloxone, suggesting a possible role of endogenous opioid system. Further, I fully validated the model pharmacologically by testing the clinically used standard analgesic drugs viz. morphine, gabapentin, amitriptyline and meloxicam and found their corresponding $ED_{50\text{-Ipsilateral}}$ values for anti-allodynia to be 1.3 mg/kg, 47.1 mg/kg, 20.1 mg/kg and 3.9 mg/kg, respectively.

Although, Walker 256 cell line is one of the most commonly used rat breast cancer cell lines in experimental research, the molecular genetic profile of this cell line is not known. One of the aims of Chapter 3 was therefore to perform gene expression characterisation of Walker 256 cell line using next-generation RNA sequencing. The gene expression profile of Walker 256 cell line resembled to Basal-B subtype of human breast cancer cell lines. Specifically, Walker 256 cells

express the marker Her2 (Erbb2), but not estrogen or androgen receptors, and also lack progesterone receptor typically found in human Her2-positive breast cancers. To gain additional insight into the pathophysiological mechanisms contributing to the development of BCIBP, in this Chapter, I also assessed gene expression changes in dorsal root ganglia (DRGs) and spinal cord of rats using next-generation sequencing. In the spinal cord of BCIBP rats during the pain state (day 10 post-ITI), 294 genes were differentially expressed in the spinal cord compared to sham rats, including several genes known to have roles in pain processing pathway. In addition, 25 genes were differentially expressed in the DRGs of BCIBP rats at the resolved-pain state (day 48 post-ITI) compared to BCIBP rats in pain state.

The last aim of my project, described in Chapter 4, was to assess the analgesic efficacy of J-2156, a somatostatin receptor– 4 (SST4) agonist, in the optimized rat model of BCIBP. J-2156 elicited anti-allodynia and anti-hyperalgesia in the BCIBP model in a dose-dependent manner. In BCIBP rats, the vast majority of cell bodies of small peptidergic (77 %) and non-peptidergic C fibre neurons (86 %) as well as medium-large diameter neurons (92 %) in the DRGs expressed the SST4 receptor. This distribution in BCIBP rats did not significantly differ from that in the sham rats. Consistent with a peripheral mechanism of action, treatment with J-2156 caused a decrease in phosphorylated extracellular signal-regulated kinase (pERK) expression in the spinal dorsal horn.

In summary, in my PhD project, I have successfully established, optimized and characterized a rat model of BCIBP, which is well-suited for probing the mechanisms underpinning BCIBP and for efficacy profiling of new molecules. I have performed transcriptomic characterization of Walker 256 rat breast cancer cell line, which gave detailed insights into the potentials and limitations of Walker 256 as a breast cancer cell line. I have also performed transcriptomic characterization of the DRGs and spinal cord of BCIBP rats compared to sham rats, which has given important information on gene-level changes associated with BCIBP. Lastly, I have found that J-2156 has potential to alleviate BCIBP and hence, this provides valuable insight into the role of SST4 receptor as an analgesic drug target in the pathophysiological state of BCIBP.

Declaration by author

This thesis is composed of my original work, and contains no material previously published or written by another person except where due reference has been made in the text. I have clearly stated the contribution by others to jointly-authored works that I have included in my thesis.

I have clearly stated the contribution of others to my thesis as a whole, including statistical assistance, survey design, data analysis, significant technical procedures, professional editorial advice, and any other original research work used or reported in my thesis. The content of my thesis is the result of work I have carried out since the commencement of my research higher degree candidature and does not include a substantial part of work that has been submitted to qualify for the award of any other degree or diploma in any university or other tertiary institution. I have clearly stated which parts of my thesis, if any, have been submitted to qualify for another award.

I acknowledge that an electronic copy of my thesis must be lodged with the University Library and, subject to the policy and procedures of The University of Queensland, the thesis be made available for research and study in accordance with the Copyright Act 1968 unless a period of embargo has been approved by the Dean of the Graduate School.

I acknowledge that copyright of all material contained in my thesis resides with the copyright holder(s) of that material. Where appropriate I have obtained copyright permission from the copyright holder to reproduce material in this thesis.

Publications during candidature

Peer-reviewed papers:

- SHENOY, P. A., KUO, A., VETTER, I. & SMITH, M. T. 2016. The Walker 256 Breast Cancer Cell- Induced Bone Pain Model in Rats. *Frontiers in Pharmacology*, 7.

- SHENOY, P., KUO, A., VETTER, I. & SMITH, M. T. 2017. Optimization and In Vivo Profiling of a Refined Rat Model of Walker 256 Breast Cancer Cell-Induced Bone Pain Using Behavioral, Radiological, Histological, Immunohistochemical and Pharmacological Methods. *Frontiers in Pharmacology*, 8.

Conference presentations:

- Presented Poster entitled "Establishment, Optimization and Characterization of a Rat Model of Breast Cancer -induced Bone Pain" in "7th International Postgraduate Symposium in Biomedical Sciences", School of Biomedical Sciences, The University of Queensland, Brisbane, Australia held during 31st October – 01st November 2016.

- Presented Poster entitled "Establishment, Optimization and Characterization of a Rat Model of Breast Cancer -induced Bone Pain" in "International Association for the Study of Pain's World Congress on Pain", Yokohama, Japan held during 26-30th September 2016.

- Presented talk entitled "Establishment, Optimization and Characterization of a Rat Model of Breast Cancer Induced Bone Pain" in "6th International Postgraduate Symposium in Biomedical Sciences", School of Biomedical Sciences, The University of Queensland, Brisbane, Australia held during 02nd-04th November 2015.

- Presented Poster entitled "Establishment and Optimization of a Rat Model of Breast Cancer -induced Bone Pain" in "2015 Australian Pain Society 35th Annual Scientific Meeting", Brisbane, Australia held during 15-18th March 2015.

- Presented talk entitled "Breast Cancer induced Bone Pain" in "Three Minute Thesis (3 MT) Competition", School of Pharmacy, The University of Queensland, Brisbane, Australia held on 22nd July 2014.

Publications included in this thesis

1. **SHENOY, P. A.**, KUO, A., VETTER, I. & SMITH, M. T. 2016. The Walker 256 Breast Cancer Cell- Induced Bone Pain Model in Rats. *Frontiers in Pharmacology,* 7. – incorporated in Chapter 1.

Contributor	Statement of contribution
Priyank A. Shenoy (Candidate)	Wrote (100 %) Edited paper (25 %)
Andy Kuo	Edited paper (25 %)
Irina Vetter	Edited paper (25 %)
Maree T. Smith	Edited paper (25 %)

2. **SHENOY, P. A.**, KUO, A., VETTER, I. & SMITH, M. T. 2017. Optimization and In Vivo Profiling of a Refined Rat Model of Walker 256 Breast Cancer Cell-Induced Bone Pain Using Behavioral, Radiological, Histological, Immunohistochemical and Pharmacological Methods. *Frontiers in Pharmacology*, 8. – incorporated as Chapter 2.

Contributor	**Statement of contribution**
Priyank A. Shenoy (Candidate)	Designed experiments (30 %) Laboratory work (100 %) Analysis and interpretation of data (50 %) Wrote paper (100 %) Edited paper (20 %)
Andy Kuo	Designed experiments (10 %) Analysis and interpretation of data (15 %) Edited paper (10 %)
Irina Vetter	Designed experiments (10 %) Analysis and interpretation of data (15 %) Edited paper (20 %)
Maree T. Smith	Designed experiments (50 %) Analysis and interpretation of data (20 %) Edited paper (50 %)

Contributions by others to the thesis

My PhD Advisors, Dr Irina Vetter, Professor Maree T. Smith and Dr Andy Kuo have made significant contributions towards the work presented in this thesis including conception and design of the project, interpretation of data and drafting and revising the written parts of this work. RNA-seq samples of Walker 256 cell line were processed by Institute for Molecular Bioscience, the University of Queensland (Australia). Boehringer Ingelheim Pharma Gmbh & Co. KG (Germany) processed the RNA-seq samples of neural tissues and supplied the data of affinity/potency experiments on J-2156. Dr John Mackie and Dr Karine Mardon kindly helped me with histopathological analysis and radiological analysis of rat tibial bones, respectively.

Statement of parts of the thesis submitted to qualify for the award of another degree

None

Acknowledgements

I would firstly thank Lord Hanuman, whose limitless power and grace drives my life. I am very thankful to my Advisors, Dr Irina Vetter, Professor Maree T. Smith and Dr Andy Kuo, for providing me necessary infrastructure, funds and all the guidance and support required throughout my PhD candidature. I will always remain very thankful to Dr Vetter who chose me as a PhD student and provided me with a life-changing opportunity of studying in Australia. My PhD project work was conducted in Professor Smith's laboratory at Centre for Integrated Preclinical Drug Development (CIPDD/TetraQ) (Centre for Clinical Research, Faculty of Medicine). I have seen Professor Smith as a strict mentor, yet certainly one of the kindest, most compassionate and revered persons I have ever met. These years of my professional associations with Professor Smith have left deep positive imprints on me, and I will cherish them for the rest of my life. Without Professor Smith's solid support throughout my candidature, I would have never seen this day of my life. Words will never be enough to express my feelings, but all I can very genuinenly say is that I have experienced the Almighty God in Professor Smith. I am grateful to Dr Kuo for his persistent support in my candidature.

I am thankful to the University of Queensland for providing me with an International PhD Scholarship. I acknowledge the Queensland Government Smart State Research Programme for supporting CIPDD research infrastructure. CIPDD is also supported by Therapeutic Innovation Australia (TIA). TIA is supported by the Australian Government through the National Collaborative Research Infrastructure Strategy (NCRIS) program.

I would specially thank Dr Ai-Leen Lam and Dr Nemat Khan, who stood by me when I needed them the most; I owe them a lot. I am thankful to Dr Felicity Han, Dr Jia Yu Peppermint Lee and Dr Drew Brockman from CIPDD for their expert guidance in various parts of my research. I am also thankful to Ms Suzanne O'Hagan, Dr Arjun Muralidharan, Mr Michael Osborne, Ms Kelly Sweeney, Ms Angela Raboczyj and all the students and staff members from Professor Smith's laboratory at CIPDD/TetraQ for their continuous support. I am also grateful to Dr Kathleen Yin, Mr Bryan Tay and all other members from Dr Vetter's laboratory at IMB for their kind assistance in my project.

Finally, I am very thankful to my mother, father, brother and all other family, friends and well-wishers who have been persistently supporting me through these years of my PhD.

Keywords

Breast cancer induced bone pain, bony metastases, Walker 256 cell, Wistar Han female rat model, transcriptomic characterisation, somatostatin receptor 4, J-2156

Australian and New Zealand Standard Research Classifications (ANZSRC)

ANZSRC code: 111501, Basic Pharmacology, 55%

ANZSRC code: 110905, Peripheral Nervous System, 30%

ANZSRC code: 110903, Central Nervous System, 15%

Fields of Research (FoR) Classification

FoR code: 1115, Pharmacology and Pharmaceutical Sciences, 60%

FoR code: 1109, Neurosciences, 30%

FoR code: 1112, Oncology and Carcinogenesis, 10%

Table of Contents

List of Figures

Chapter 1

Chapter 2

256 cells. *p<0.05 (Two-way ANOVA, *posthoc* Bonferroni test) *c.f.* rats given an ITI of HK W256 cells.

Figure 2.5. Paw thermal thresholds (PTTs) of ipsilateral and contralateral hindpaws of rats. Panels in the figure show mean (±SEM) PTTs of rats from (A) experiment 2, (B) experiment 3 and (C) experiment 6. HK, heat-killed; W256, Walker 256 cells. There were no statistically significant differences in PTTs between the treatment groups in any of these experiments (p>0.05; Two-way ANOVA, *posthoc* Bonferroni test).

Figure 2.6. Effect of naloxone on ipsilateral and contralateral paw withdrawal thresholds (PWTs) of rats. Panels in the figure show mean (±SEM) PWT versus time curves from experiment 5 following naloxone or vehicle injection between (A) day 43-51 post-ITI and (B) day 53-66 post-ITI. The dotted line indicates the threshold PWT value at / below which the rats were considered to have fully developed mechanical allodynia. BCIBP (4 x 10^5), group of rats given an ITI of 4 x 10^5 W256 cells; HK, heat-killed; NAL, naloxone (15 mg/kg s.c.); Sham (4 x 10^5), group of rats given an ITI of 4 x 10^5 HK W256 cells; VEH, vehicle; W256, Walker 256 cells. *p<0.05 (Two-way ANOVA, *posthoc* Bonferroni test) *c.f.* rats given an ITI of HK W256 cells.

Figure 2.7. Temporal changes in the paw withdrawal thresholds (PWTs) of BCIBP rats in the ipsilateral hindpaws following the administration of single bolus doses of analgesic and adjuvant drugs. Panels in the figure show temporal changes in mean (±SEM) PWT versus time curves following injection of (A) morphine, (B) gabapentin, (C) amitriptyline and (D) meloxicam.

Figure 2.8. Dose response curves of morphine and gabapentin in BCIBP rats. Panels in the figure show % MAX AUC ΔPWT (representative of response) versus $\log_{10}$ dose (representative of dose) curves of (A) morphine and (B) gabapentin in the ipsilateral and contralateral hindpaws. $ED_{50\text{-IPSI}}$ and $ED_{50\text{-CONTRA}}$ values for morphine were found to be 1.3 and 1.4 mg/kg, respectively, and for gabapentin were found to be 47.1 and 30.8 mg/kg, respectively.

Figure 2.9. Dose response curves of amitriptyline and meloxicam in BCIBP rats. Panels in the figure show % MAX AUC ΔPWT (representative of response) versus $\log_{10}$ dose (representative of dose) curves of (A) amitriptyline and (B) meloxicam in the ipsilateral and contralateral hindpaws. $ED_{50\text{-IPSI}}$ and $ED_{50\text{-CONTRA}}$ values for amitriptyline were found to be 20.1 and 21.4 mg/kg, respectively, and for meloxicam were found to be 3.9 and 3.5 mg/kg, respectively.

Figure 2.10. Temporal changes in the paw pressure thresholds (PPTs) of BCIBP rats in the ipsilateral hindpaws following administration of single bolus doses of analgesic and adjuvant drugs. Panels in the figure show temporal changes in mean (±SEM) PPT versus time curves following injection of (A) morphine, (B) gabapentin, (C) amitriptyline and (D) meloxicam.

Figure 2.11. Radiological assessment of tibiae from BCIBP rats and the corresponding sham rats. Panels in the figure show (A) 3D-µCT radiological image of a sham rat's tibia at day 10 post-ITI, (B) trabecular bone of a sham rat's tibia at day 10 post-ITI, (C) 3D-µCT radiological image of a BCIBP rat's tibia at day 10 post-ITI, (D) trabecular bone of a BCIBP rat's tibia at day 10 post-ITI, (E-H) morphometric changes in BCIBP rats' tibiae relative to sham rats' tibiae at day 10 post-ITI, (I) 3D-µCT radiological image of a sham rat's tibia at day 48 post-ITI, (J) trabecular bone of a sham rat's tibia at day 48 post-ITI, (K) 3D-µCT radiological image of a BCIBP rat's tibia at day 48 post-ITI, (L) trabecular bone of a BCIBP rat's tibia at day 48 post-ITI, (M-P) morphometric changes in BCIBP rats' tibiae relative to sham rats' tibiae at day 48 post-ITI. *$p<0.05$ (Two-way ANOVA, *posthoc* Bonferroni test). Scale bar – 5 mm.

Figure 2.12. Histological assessment of tibiae from BCIBP rats and corresponding sham rats. Panels in the figure show representative images of H&E staining of tibial sections of (A) sham rat at day 10 post-ITI, (B) BCIBP rat at day 10 post-ITI, (C) sham rat at day 48 post-ITI and (D) BCIBP rat at day 48 post-ITI. Black arrowheads show destruction of cortical bone of tibiae. Scale bar – 1 mm.

Figure 2.13. Immunocytochemical staining of the Walker 256 cell line for Cytokeratin 18 using the ab187573 (Abcam) antibody. Panels in the figure show (A) cytokeratin 18 (B) DAPI and (C) A and B merged.

Figure 2.14. Immunohistochemical staining of Cytokeratin 18 in tibial sections of BCIBP rats and the corresponding sections from sham rats using the ab187573 (Abcam) antibody. Panels in the figure show immunofluorescence imaging of tibial sections of (A) sham rat at day 7 post-ITI, (B) BCIBP rat at day 7 post-ITI, (C) sham rat at day 38 post-ITI and (D) BCIBP rat at day 38 post-ITI.

Supplementary Figure 2.1. Form used to record clinical observations in rats.

Supplementary Figure 2.2. Body weight of rats from various experiments. Panels in the figure show mean (±SEM) body weight of rats from (A) experiment 1, (B) experiment 4, (C) experiment 6, (D) experiment 7, (E) experiment 8, (F) experiment 9, (G) experiment 10, (H) experiment 11, (I)

experiment 12, (J) experiment 13, (K) experiment 14, (L) experiment 15 and (M) experiment 16. HK, heat-killed; W256, Walker 256 cells.

Supplementary Figure 2.3. Paw withdrawal thresholds (PWTs) of ipsilateral and contralateral hindpaws of rats. Panels in the figure show mean (±SEM) PWTs of rats from (A) experiment 4, (B) experiment 8, (C) experiment 9, (D) experiment 15 and (E) experiment 16. HK, heat-killed; W256, Walker 256 cells.

Supplementary Figure 2.4. Paw pressure thresholds (PPTs) of the ipsilateral and contralateral hindpaws of rats from experiment 4.

Supplementary Figure 2.5. Paw thermal thresholds (PTTs) of the ipsilateral and contralateral hindpaws of rats. Panels in the figure show mean (±SEM) PTTs of rats from (A) experiment 4 and (B) experiment 5. HK, heat-killed; W256, Walker 256 cells.

Supplementary Figure 2.6. Effect of naloxone on ipsilateral and contralateral PWT / PPT / PTT values of rats. Panels in the figure show changes in mean (±SEM) (A) PWTs in experiment 3 following naloxone injection between day 81-91 post-ITI, (B) PPTs in experiment 3 following naloxone injection between day 82-92 post-ITI, (C) PWTs in experiment 4 following naloxone injection between days 81-93 post-ITI, (D) PPTs in experiment 4 following naloxone injection between days 82-94 post-ITI and (E) PTTs in experiment 7 following naloxone injection between days 21-24 post-ITI. BCIBP (1.5×10^5), group of rats given an ITI of 1.5×10^5 W256 cells; BCIBP (4×10^5), group of rats given an ITI of 4×10^5 W256 cells; DPBS, group of rats given an ITI of 10 µL DPBS; HK, heat-killed; NAL, naloxone (15 mg/kg s.c.); Sham (1.5×10^5), group of rats given an ITI of 1.5×10^5 HK W256 cells; Sham (4×10^5), group of rats given an ITI of 4×10^5 HK W256 cells; VEH, vehicle; W256, Walker 256.

Supplementary Figure 2.7. Temporal changes in the paw withdrawal thresholds (PWTs) of the contralateral hindpaws for BCIBP rats following administration of single bolus doses of analgesic and adjuvant drugs. Panels in the figure show temporal changes in mean (±SEM) PWTs versus time curves following injection of (A) morphine, (B) gabapentin, (C) amitriptyline and (D) meloxicam.

Supplementary Figure 2.8. Temporal changes in the paw pressure thresholds (PPTs) of the contralateral hindpaws for BCIBP rats following administration of single bolus doses of analgesic

Chapter 4

Figure 4.1. Temporal changes in mean (±SEM) paw withdrawal thresholds (PWTs) and paw pressure thresholds (PPTs) in the hindpaws of rats following a unilateral ITI of 4 x 10^5 Walker 256 cells (BCIBP group) and 4 x 10^5 heat-killed Walker 256 cells (sham group). Panels in the figure show (A) PWTs in the ipsilateral hindpaws, (B) PWTs in the contralateral hindpaws, (C) PPTs in the ipsilateral hindpaws and (D) PPTs in the contralateral hindpaws. The dotted line shows the threshold criterion for full development of mechanical allodynia (PWTs ≤ 6 g, panel A-B) and mechanical hyperalgesia (PPTs ≤ 80 g, panel C-D). *p≤0.05 (Two-way ANOVA, *posthoc* Bonferroni test) *c.f.* sham rats.

Figure 4.2. Anti-allodynic effect of single bolus doses (i.p.) of J-2156 on ipsilateral and contralateral hindpaw withdrawal thresholds (PWTs) in BCIBP-rats. Panels in the figure show mean (±SEM) (A) ipsilateral PWT versus time curves and (B) contralateral PWT versus time curves. The dotted line shows the threshold criterion of fully developed mechanical allodynia (≤ 6 g).

Figure 4.3. Anti-hyperalgesic effect of single bolus doses (i.p.) of J-2156 on ipsilateral and contralateral hindpaw pressure thresholds (PPTs) in BCIBP rats. Panels in the figure show mean (±SEM) (A) ipsilateral PPT versus time curves and (B) contralateral PPT versus time curves. The dotted line shows the threshold criterion of fully developed mechanical hyperalgesia (≤ 80 g).

Figure 4.4. Expression levels of the SST4 receptor in sections of ipsilateral lumbar L4-L6 dorsal root ganglia (DRGs) and in sections of the lumbar spinal dorsal horns of BCIBP-rats and the corresponding sections from sham rats (n=3-4/group). Panels in the figure show representative sections of (A) DRG of a sham rat, (B) DRG of a BCIBP-rat, (C) spinal dorsal horn of a sham rat and (D) spinal dorsal horn of a BCIBP-rat. Panel (E) shows fold-change in immunofluorescence of ipsilateral lumbar DRG sections of the BCIBP group relative to the sham group and (F) shows fold-change in immunofluorescence of lumbar spinal cord sections of the BCIBP group relative to the sham group. ns, statistically not significant (p>0.05, Mann-Whitney test).

Figure 4.5. Expression levels of somatostatin in sections of ipsilateral lumbar L4-L6 dorsal root ganglia (DRGs) and spinal dorsal horns of BCIBP-rats and the corresponding sections from sham rats (n=3-4/group). Panels in the figure show representative sections of (A) a lumbar DRG from a sham rat, (B) a lumbar DRG from a BCIBP-rat, (C) a lumbar spinal dorsal horn from a sham rat and

(D) a lumbar spinal dorsal horn from a BCIBP-rat. Panel (E) shows fold-change in immunofluorescence of ipsilateral lumbar DRG sections from the BCIBP group relative to the corresponding sections from the sham group and (F) shows the fold-change in immunofluorescence of lumbar spinal cord sections from the BCIBP group relative to the sham group. ns, statistically not significant ($p>0.05$, Mann-Whitney test).

Figure 4.6. Immunostaining showing co-localization of the SST4 receptor with (A) substance P (SP), (B) isolectin B4 (IB4) and (C) neurofilament 200 kDa (NF200) in representative sections from ipsilateral lumbar L4-L6 dorsal root ganglia (DRGs) of BCIBP-rats (n=3-4/group).

Figure 4.7. Effect of a single bolus dose of J-2156 (10 mg/kg, i.p.) on expression levels of phosphorylated extracellular signal-regulated kinase (pERK) in lumbar L4-L6 spinal dorsal horns of BCIBP-rats (n=3-4/group). Panels in the figure show (A) representative section from a drug-naïve BCIBP-rat, (B) representative section from a BCIBP-rat administered J-2156 (10 mg/kg, i.p.) and (C) fold-change in immunofluorescence of sections from the BCIBP group administered J-2156 relative to the corresponding sections from the drug-naïve BCIBP group. *$p\leq0.05$ (Mann-Whitney test).

Supplementary Figure 4.1. Anti-allodynic effect of single bolus doses (i.p.) of J-2156 on ipsilateral and contralateral ΔPWT and % MAX ΔPWT AUC values in BCIBP-rats. Panels in the figure show (A) ipsilateral ΔPWT versus time curves, (B) ipsilateral % MAX ΔPWT AUC at each dose, (C) contralateral ΔPWT versus time curves and (D) contralateral % MAX ΔPWT AUC at each dose. Panel B: *$p\leq0.05$ ($F_{(3,20)} = 11.0$) and Panel D: *$p\leq0.05$ ($F_{(3,20)} = 6.6$), One-way ANOVA, *posthoc* Dunnett's multiple comparisons test *c.f.* BCIBP-rats that received single bolus doses of vehicle.

Supplementary Figure 4.2. Anti-hyperalgesic effect of single bolus doses (i.p.) of J-2156 on ipsilateral and contralateral ΔPPT and % MAX ΔPPT AUC values in BCIBP-rats. Panels in the figure show (A) ipsilateral ΔPPT versus time curves, (B) ipsilateral % MAX ΔPPT AUC at each dose, (C) contralateral ΔPPT versus time curves and (D) contralateral % MAX ΔPPT AUC at each dose. Panel B: *$p\leq0.05$ ($F_{(3,20)} = 10.1$) and Panel D: *$p\leq0.05$ ($F_{(3,20)} = 14.5$), One-way ANOVA, *posthoc* Dunnett's multiple comparisons test *c.f.* BCIBP-rats that received single bolus doses of vehicle.

Supplementary Figure 4.3. Validation of the anti-SST4 receptor antibody using IHC staining. Panels in the figure show (A) a representative coronal section of rat brain used as a positive control

for the SST4 receptor and (B) a representative rat liver section used as a negative control for the SST4 receptor.

List of Tables

Chapter 1

Chapter 2

Chapter 3

List of Abbreviations

5-HT	5-Hydroxytryptamine
Aβ	A-beta
Aδ	A-delta
AMPA	A-Amino-3-Hydroxy-5-Methyl-4-Isoxazolepropionic Acid
ANO1	Anoctamin-1
ATP	Adenosine Triphosphate
AUC	Area Under Curve
BCIBP	Breast Cancer Induced Bone Pain
BDNF	Brain-Derived Neurotrophic Factor
Ca^{2+}	Calcium
CaMKIV	Calcium/Calmodulin- Dependent- Protein Kinase Type IV
cAMP	Cyclic Adenosine Monophosphate
Ca_v	Voltage Dependant Calcium Channels
CCL2	Chemokine C-C Motif Ligand 2
CCR2	Chemokine C-C Motif Receptor 2
c-GMP	Cyclic Guanosine Monophosphate
CGRP	Calcitonin Gene Related Peptide
CIBP	Cancer Induced Bone Pain
Cl^-	Chloride
COX	Cyclooxygenase
CREB	c-AMP Response Element Binding Protein
CX3CL	Fractalkine/ Chemokine (C-X3-C motif) Ligand
CX3CR	Fractalkine/ Chemokine (C-X3-C motif) Receptor
DREAM	Downstream Regulatory Element Antagonistic Modulator
DRG	Dorsal Root Ganglion
EAAT	Excitatory Amino Acid Transporter
EAE	Autoimmune Encephalitis
EphB1	Erythropoietin Producing Human Hepatocellular Carcinoma B1
EphrinB1	Eph-Receptor-Interacting Protein B1
ERK	Extracellular Signal-Regulated Kinase
FKN	Fractalkine
GABA	Gamma Amino Butyric Acid

G-CSF	Granulocyte Colony Stimulating Factor
GIRK	G-Protein-Gated Inwardly Rectifying K+
GM-CSF	Granulocyte Macrophage Colony Stimulating Factor
GPCR	G-Protein-Coupled Receptor
GTPase	Family of Hydrolase enzymes that can bind and hydrolyse Guanosine Triphosphate
HK	Heat-Killed
HMGB1	High Mobility Group Box 1
IASP	International Association for the Study of Pain
IL-6	Interleukin 6
IL-1β	Interleukin 1β
i.p.	Intraperitoneal
IP3	Inositol Triphosphate
ITI	Intra-Tibial Injection
JAK-STAT	Janus Kinase and Signal Transducer and Activator of Transcription
JNK	Jun N-Terminal Kinase
K^+	Potassium
KCC2	K-Cl (Potassium Chloride) Cotransporter 2
KEGG	Kyoto Encyclopedia of Genes and Genomes
K_V	Voltage Gated Potassium Channel
LPA	Lysophosphatidic Acid
MAPK	Mitogen Activated Protein Kinase
MCP-1	Chemokine Monocyte Chemoattractant Protein 1
MeCP2	Methyl-CpG-Binding Protein 2
MEK	Inhibitors of MAPK enzymes
mGluR	Metabotropic Glutamate Receptor
MMP2	Matrix Metalloproteinase 2
mRNA	Messenger Ribonucleic Acid
MS	Multiple Sclerosis
Na^+	Sodium
Na_V	Voltage Gated Sodium Channel
NE	Norepinephrine
NGF	Nerve Growth Factor
NMDA	N-Methly-D-Aspartate

NOS	Nitric Oxide Synthase
NSAIDs	Non-Steroidal Anti-inflammatory Drugs
ORL1	Opioid Receptor-Like 1
PBS	Phosphate Buffered Saline
p-CREB	Transcriptional Factor cAMP Response Element Binding Protein
pERK	Phosphorylated Extracellular Signal-Regulated Kinase
PGE2	Prostaglandin E2
PI3K	Phosphoinositide 3-Kinase
PKA	Protein Kinase A
PLC	Phospholipase C
PPT	Paw Pressure Threshold
PTT	Paw Thermal Threshold
PWT	Paw Withdrawal Threshold
RAGE	Receptor for Advanced Glycation End Products
RhoA	Ras Homolog Gene Family Membrane A
RhoGTPase	Any member of Rho family of GTPases
ROCK	Rho Kinase
SP	Substance P
s.c.	Subcutaneous
TAASK	TWIK- related acid sensitive potassium channel
TLR	Toll Like Receptor
TNF-α	Tumour Necrosis Factor- α
TRAAK1	TWIK- related arachidonic acid- stimulated channels
TREK	Mechanogated and arachidonic acid activated TWIK-related K^+ 1
TrkA	Tyrosine Kinase Receptor A
TrkB	Tyrosine Kinase Receptor B
TRP	Transient Receptor Potential (transducer protein molecules)
TRPA1	Transient Receptor Potential Ankyrin 1
TRPC5	Transient Receptor Potential Canonical (protein) 5
TRPM3	Transient Receptor Potential Melastatin 3
TRPM8	Transient Receptor Potential Melastatin 8
TRPV1	Transient Receptor Potential Vanilloid 1
TRPV2	Transient Receptor Potential Vanilloid 2
TRPV3	Transient Receptor Potential Vanilloid 3

TRPV4	Transient Receptor Potential Vanilloid 4 (cation channel)
TTX	Tetrodotoxin
TWIK	Tandem of p domains in a weak inwardly rectifying potassium channel
W256	Walker 256

Chapter 1

Literature review

1.1. Foreword

Pain is a significant health problem and a huge socio-economic burden across the world. This chapter gives a brief introduction to the concept of pain as well as pathways and signalling involved in pain pathophysiology in cancer and other diseases. Metastases of cancer cells to the skeleton, in particular breast cancer in the advanced stages, causes excruciating pain in patients so affected. This is because clinically available medications to treat this type of pain are not efficacious enough and also exhibit severe dose-limiting side effects. Hence it is very important to seek new analgesic drugs that are more efficacious and safer than those currently available. One of the very important steps in discovery of new analgesic drugs for treating this condition is employing suitable preclinical animal models of breast cancer-induced bone pain. Walker 256 breast cancer cell induced bone pain model in rats is one of the highly used models in experimental research and closely mimics the pathophysiology of human breast cancer-induced bone pain. Hence, this chapter also reviews various aspects of prevailing studies in the literature that have used this model.

A part of this chapter has been adopted with permission from a previously published review article that arose from this thesis (Shenoy et al., 2016), published by Frontiers in Pharmacology (http://journal.frontiersin.org/article/10.3389/fphar.2016.00286/full).

1.2. Breast cancer

Breast cancer, a leading cause of cancer death worldwide among females, is the most frequently diagnosed type of cancer (Torre et al., 2015). Amongst numerous cancer types, breast cancer by itself accounts for around 25 % of all cancer occurrence cases in females (Torre et al., 2015). Breast cancer is a group of heterogeneous diseases with diverse histopathological, genetic and clinical (outcomes) features, rather than a single disease (Vargo-Gogola and Rosen, 2007) (Figure 1.1). Clinically, there are five molecular subtypes of breast cancer tumours: luminal-A, luminal-B, Erbb2, basal-like and normal-like (Kao et al., 2009).

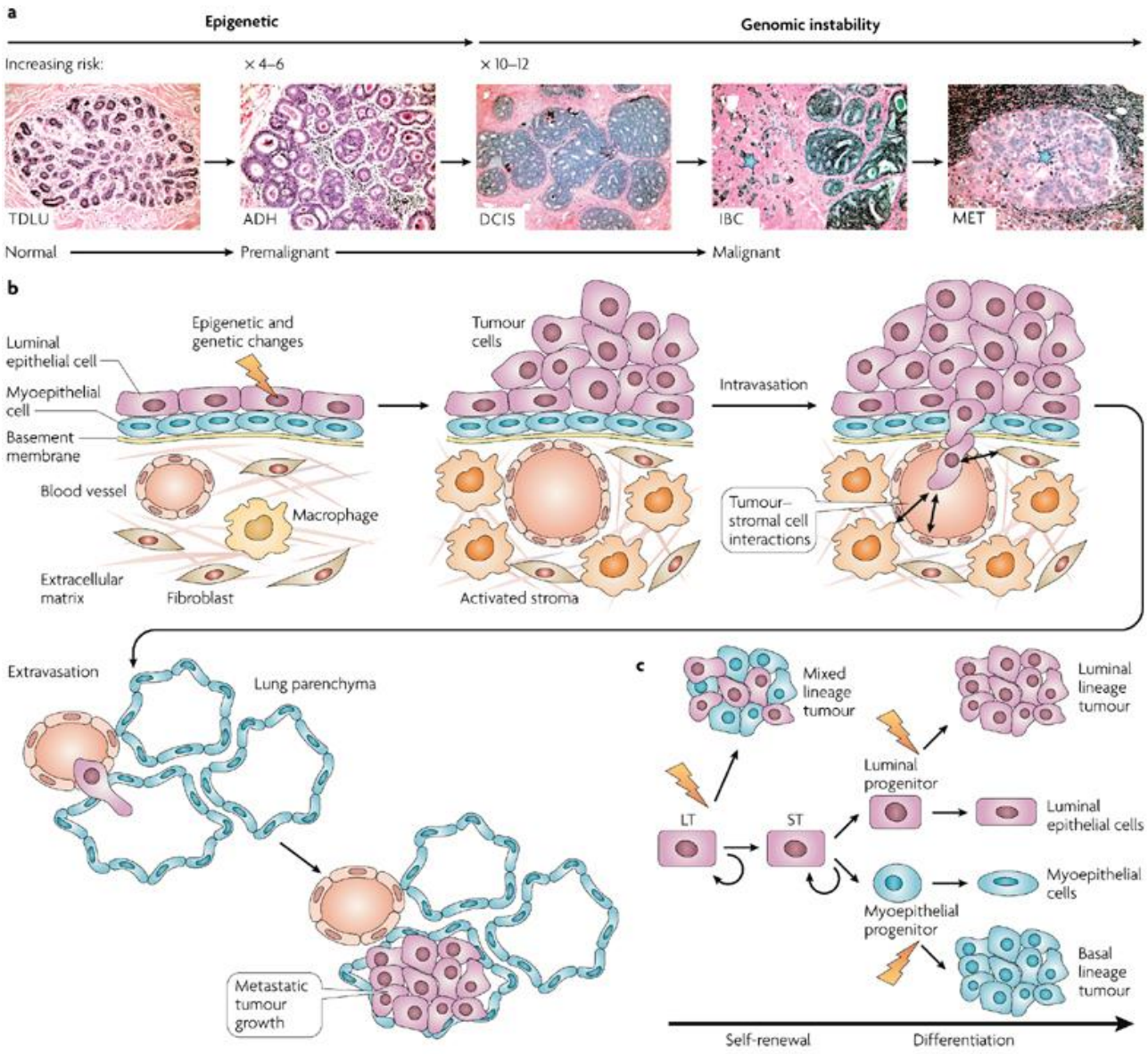

Figure 1.1. The biology of breast cancer. Adapted by permission from Macmillan Publishers Ltd: [Nature Reviews Cancer] (Vargo-Gogola and Rosen, 2007), copyright (2007). **a)** In breast cancer, the cells can exhibit continuous genotypic and phenotypic changes as the disease progresses. Lobules and ducts in the normal breast terminal ductal lobular unit (TDLU) are made of bi-layered epithelium consisting of luminal and myoepithelial cells. Certain abnormility in the layers of cells within the ducts / lobules can manifest as a premalignant lesion called atypical ductal hyperplasia (ADH). ADH might be considered to be the precursor of ductal carcinoma in situ (DCIS). DCIS is a non-invasive breast cancer lesion. As the disease progresses, there is an increase in the risk of conversion into a malignant state or invasive breast cancer (IBC). DCIS can have the potential to worsen to IBC (shown by a blue star adjacent to a DCIS lesion). Breast cancer cells very often metastasize to the lymph nodes (MET; shown by a blue star). **b)** The panel shows a schematic representation to demonstrate how the breast cancer progresses. Different genetic and epigenetic

changes and interactions of cells with the microenvironment drive the transformation of epithelial cells of breast to metastatic breast cancer. Via invasion through the basement membrane and the vasculature, cells establish themselves as a metastasized tumour in the new microenvironment, away from the tissue of origin. **c)** Due to the similarities between normal breast stem or progenitor cells and cancer cells, it is proposed that cancer cells having stem cell-like characteristics, known as 'cancer stem cells' or 'tumour-initiating cells', are the drivers of breast cancer progression. The given hypothesis is potrayed as epigenetic and genetic changes that occur in various stem or progenitor cells, including the long term (LT), short term (ST) and luminal or basal / myoepithelial progenitors, and leads to production of tumour subtypes consisting of different cell types (mixed, luminal or basal lineage). These may exhibit characteristic genetic profiles and have distinct prognoses.

1.3. Cancer-induced bone pain

Pain is a necessary, physiological phenomenon which is important for survival of the animals (including human beings). Simultaneously, pain is one of the most common symptoms of a wide variety of diseases and disorders and hence may be a severe clinical encounter (Gangadharan and Kuner, 2013). It is a subjective experience which varies individually for different persons (Coghill et al., 2003). In Australia, chronic pain is a huge public health burden and the cost associated with chronic pain has been estimated to be near $34.3 billion per year, or around $11,000 per person suffering from chronic pain (The MBF Foundation, 2007) (Miller et al., 2017, Henderson et al., 2013). Knowledge on the multiplicity of cellular and molecular mechanisms underpinning acute (physiological) pain as well as that in a pathophysiological context (persistent pain), has increased significantly in the past two decades (Argoff, 2011, Basbaum et al., 2009, Julius and Basbaum, 2001). Additionally, our collective understanding of various signalling pathways participating in the development of pain hypersensitivity induced by various diseases, is improving (Gangadharan and Kuner, 2013). The most common cause of pain in cancer arises from bone metastasis, and around 73% of patients with terminal breast cancer exhibit indications of bone metastases (Currie et al., 2013, Coleman, 2006, Bu et al., 2014). Of these, 75% suffer severe bone pain and pathological fractures (Ibrahim et al., 2013). This is in contrast to primary breast tumors in the tissue of origin that cause very little or no pain at all (Lozano-Ondoua et al., 2013b). Clinically, nonsteroidal anti-inflammatory drugs are the mainstay of treatment, often in combination with strong opioid analgesics, radiotherapy in the initial stages of metastasis, and adjuvant agents that inhibit osteoclast activity such as bisphosphonates and denosumab (Mantyh et al., 2002, Colvin and Fallon, 2008, Fallon et al., 2016, Fernandes et al., 2016). The principal challenge in understanding the pathophysiological mechanisms of cancer-induced bone pain (CIBP) is the development of an

animal model which has characteristics in common with that of human CIBP (Slosky et al., 2015). It is only recently that preclinical studies have begun to determine how metastatic cancers may interact with the bone microenvironment resulting in pain (Lozano-Ondoua et al., 2013b). Until the late twentieth century, all animal models of CIBP relied on systemic injection of carcinoma cells, which resulted in poor animal health because of metastases in vital organs such as the liver, lungs, brain and multiple sites in bone (Urch, 2004, Simmons et al., 2015). Subsequently, the more efficient method of local infusion of cancer cells into a single bone was developed, thereby avoiding systemic spread of cancer cells and the maintenance of good general animal health (Schwei et al., 1999). Although multiple breast cancer cell lines have been used to induce bone tumors in rats and mice, the focus of this mini-review (Shenoy et al., 2016) is confined to research in which Walker 256 rat breast cancer cells have been used to induce bone pain in rats.

1.4. Overview of signalling pathways

The International Association for the Study of Pain (IASP) defines pain as "an unpleasant sensory and emotional experience associated with actual or potential tissue damage, or described in terms of such damage" (Katz et al., 2015). While the term 'nociception' is defined as "the neural process of encoding noxious stimuli" (IASP). Peripheral sensory neurons that are involved in nociception form the nociceptive system (Schaible, 2007). Peripheral nociceptive neurons sense the noxious stimuli like mechanical, thermal and chemical stimuli and are classified as C or A-delta (Aδ) fibre types based upon the level of myelination and hence velocity of action potential conduction along the nerve fiber, the size of the cell somata, and the axon diameter (Albrecht and Rice, 2010). A-beta (Aβ) fibers, a third type, are responsible for conducting the non-nociceptive impulses generated by light touch, vibration and movement in the normal conditions of physiology (Gangadharan and Kuner, 2013) but can transmit nociceptive signals under pathophysiological conditions (Figure 1.2).

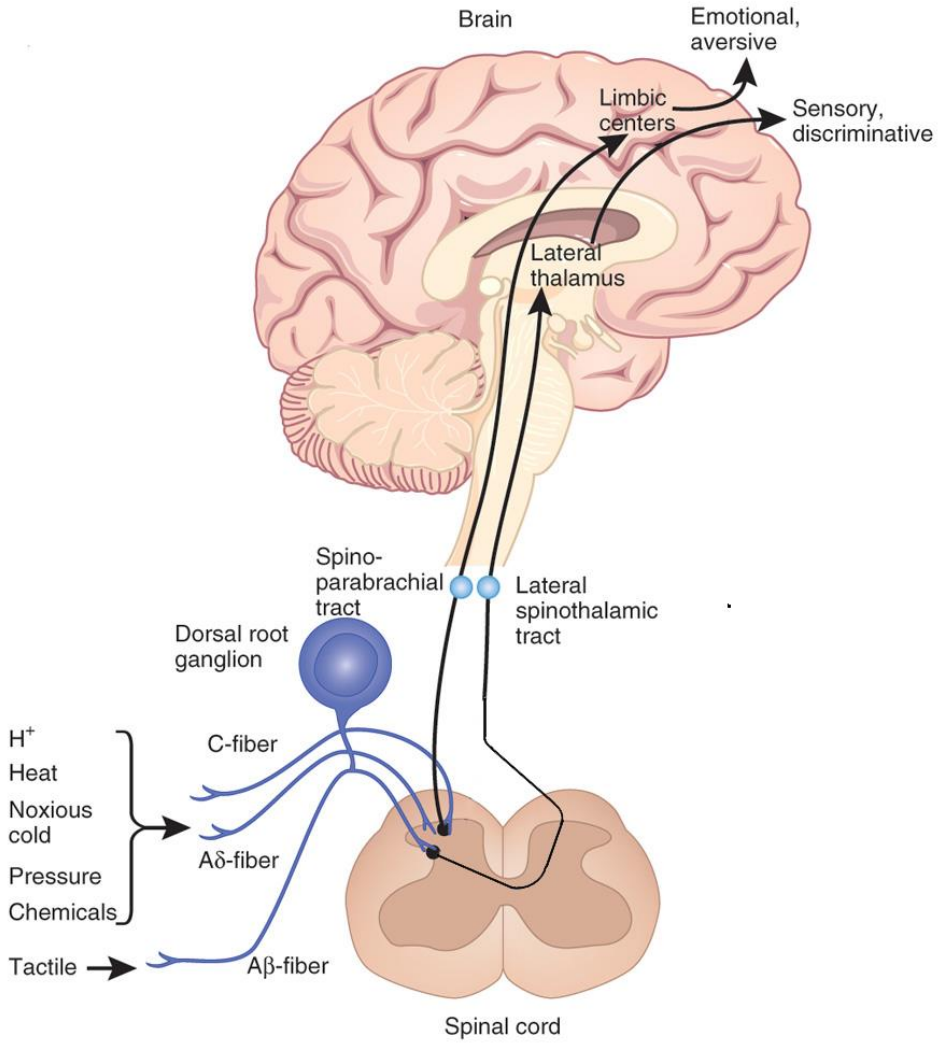

Figure 1.2. Ascending circuits involved in physiological pain. Adapted (and modified) by permission from Macmillan Publishers Ltd: [Nature Medicine] (Kuner, 2010), copyright (2010).

Peripheral C-, Aδ, and Aβ-fibers, the peripheral axons of sensory neurons having their cell bodies in the dorsal root ganglion (DRG), transform chemical, mechanical and thermal stimuli into electrical signals that are conducted to the spinal cord (Albrecht and Rice, 2010). Besides DRGs, other somatosensory neurons also have their cell bodies residing in the trigeminal ganglia, at the base of the skull (Le Pichon and Chesler, 2014). In the spinal cord, central projections synapse with neurons forming the spinoparabrachial and lateral spinothalamic tract to transmit pain signals to higher pain centres (Kuner, 2010).

Most nociceptors are activated by noxious mechanical, thermal, and chemical stimuli and are hence polymodal (Dubin and Patapoutian, 2010). Nociceptors can also have efferent functions by the release of neuropeptides like substance P (SP) and calcitonin gene-related peptide (CGRP) from their terminals and are responsible for induction of vasodilatation, plasma extravasation, attracting

macrophages or inducing mast cell degranulation, etcetera, which is known as a neurogenic inflammatory response (Lynn, 1996, Schaible et al., 2005). Nociceptors project into the spinal cord and they form synaptic junctions with second order neurons in the grey matter of the spinal dorsal horn (Abraira and Ginty, 2013). Nociceptors from nerves having their cell bodies in trigeminal ganglia synapse on second order neurons in the trigeminal subnucleus caudalis (Dubin and Patapoutian, 2010). A fraction of second-order neurons project to the higher centres that process pain as a response to noxious stimuli (Mantyh, 2006). There are other spinal cord neurons that have involvement in nociceptive motor reflexes and complex motor behaviour such as avoiding movement, and also generating the autonomic reflexes which are produced by noxious stimulation (Fitzgerald, 2005). The role of the somata of somatosensory neurons is not restricted to neuronal survival and synthesis of proteins which impart or alter cell function (Delmas et al., 2011). It is now recognised that the somata of DRG neurons are an important centre of various mechanisms regulating aberrant excitation and cell-cell interactions especially in chronic pain states (Devor, 2006). Descending tracts may curtail or enhance the processing of spinal nociception (Millan, 2002). The descending tracts are made up of pathways which originate from brain stem nuclei, specifically the periaqueductal grey and the rostral ventromedial medulla and subsequently descend in the spinal cord's dorsolateral funiculus (D'Mello and Dickenson, 2008). Descending inhibition is an important aspect of intrinsic antinociception (Schaible, 2007).

1.5. Involvement of ion channels in signalling mechanisms

Different stimuli act on variety of ion channels and receptors which leads to depolarisation of the membrane, and this is termed as the generator potential (Muroi and Undem, 2014). As a consequence, the voltage-gated sodium channels are activated, that are responsible for generation of action potential and the conduction of impulses to the central terminals (Muroi and Undem, 2014). Calcium channels are activated on membrane depolarisation and drive the influx of calcium as a response to action potentials and subthreshold depolarising signals (Catterall, 2011). Calcium that enters the cell through the voltage gated calcium channels serves as a second messenger in conduction of electrical impulses (Catterall, 2011). Similarly, a negative membrane potential is crucial for inhibition of peripheral excitability, and potassium ion channels are key contributors to resting membrane potential (Li and Toyoda, 2015). Choride ion channels are also important affectors of resting membrane potential (De Koninck, 2007). The intracellular concentration of chloride ions in neurons is low, and the potential of reversal for chloride ion currents is close to the resting potential of the membrane, hence, even small changes in intracellular choride concentration can significantly affect the transmission (De Koninck, 2007). In most chronic pain conditions arising from peripheral nerve damage or inflammatory processes, peripheral nerve block using non-

selective Na_V inhibitors can achieve complete pain relief in humans, proving that peripheral input is critical to chronic pain (Aguirre et al., 2012). Non-specific blockade of sodium channels, results into blockade of complete sensory and motor impulses leading to loss of all the senses and development of numbness, paralysis and loss of autonomic function (Roberson et al., 2011). Accordingly, voltage-gated sodium channels (Na_V) have received considerable interest in regards to their role in the pathogenesis of pain as they are involved in action potential generation and propagation (Dib-Hajj et al., 2010). However, the precise role of specific Na_V isoforms in modality- and disease-specific pain pathways remains unclear. Nine Na_V α-subunits, designated $Na_V1.1$–$Na_V1.9$, have been functionally characterised (Devor, 2006). Classifying between different isoforms has been made easier with the discovery of subtype selective neurotoxins like tetrodotoxin (TTX), which distinguishes TTX-sensitive ($Na_V1.1$, 1.2, 1.3, 1.4, 1.6 and 1.7) from TTX-resistant subtypes ($Na_V1.5$, 1.8, 1.9) (Catterall, 2000). $Na_V1.3$ is normally expressed during embryogenesis, but its expression is continued in sympathetic neurons in adults. It is upregulated in DRG neurons after injury (Dib-Hajj et al., 2010). This isoform plays an important role in pain sensation. Peripheral nerve injury leads to upregulated $Na_V1.3$ expression in the DRG (Black et al., 1999, Dib-Hajj et al., 1996, Kim et al., 2001, Lindia et al., 2005), dorsal horn (Hains et al., 2004), and also thalamic neurons (Zhao et al., 2006). Also, spinal cord injury causes increased expression of $Na_V1.3$ within the dorsal horn (Hains et al., 2003). Nav1.3 channel produces rapid-repriming TTX-sensitive current and quickly recovers from inactivation (Cummins et al., 2001, Yang et al., 2016). $Na_V1.7$ is expressed in DRG and sympathetic ganglion neurons (Dib-Hajj et al., 2010). Nav1.7 generates a fast-activating and –inactivating and slow-repriming, TTX-sensitive current (Klugbauer et al., 1995). Also, slow closed-state $Na_V1.7$ inactivation produces a significant ramp current as a response to small and slow depolarizations (Cummins et al., 1998, Herzog et al., 2003). Studies of human monogenic disorders of pain perception have drawn particular attention to $Na_V1.7$, because loss of function in this channel leads to chronic insensitivity to pain (Cox et al., 2006, Goldberg et al., 2007). However, the deletion of $Na_V1.7$ specifically in nociceptors, did not eliminate the neuropathic pain in mice (Nassar et al., 2005). $Na_V1.8$ ion channels are selectively expressed in DRG neurons and trigeminal ganglia, and are also present along the peripheral axon shafts. The biophysical properties of $Na_V1.8$, together with its important contribution in repetitive firing, and the fact that it is also located in free nerve terminals where pain-signalling is initiated, indicate that $Na_V1.8$ can critically influence nociceptor activity and thus contribute towards pain (Dib-Hajj et al., 2010). $Na_V1.8$ mediates inflammatory pain as documented by studies in $Na_V1.8$-null mice showing diminished responses to carrageenan- and nerve growth factor (NGF)-induced hyperalgesia (Akopian et al., 1999, Kerr et al., 2001), as well as diminished visceral pain sensitivities, which remains consistent with the fact that $Na_V1.8$ channels are expresses in all DRG neurons innervating

the colon (Gold et al., 2002). Similarly, $Na_V1.8$-gene deleted mice show a drastic decrease in ectopic discharge in A- and C-fibers which are associated with formation of neuroma after transection of the saphenous nerve (Roza et al., 2003). Behavioural experiments have proven that $Na_V1.8$-null animals are less sensitive to noxious cold, consistent with an important role of $Na_V1.8$ in action potential generation at cold temperatures (Zimmermann et al., 2007). However, $Na_V1.8$ knock-out mice were not devoid of neuropathic pain, indicating that there are other ion channels and proteins that concurrently contribute to the pain signalling, depending on the pathophysiology (Nassar et al., 2005, Kerr et al., 2001). $Na_V1.9$ is expressed in small diameter, nonpeptidergic DRG neurons, and in the trigeminal ganglion and myenteric neurons (Dib-Hajj et al., 2010). Experimental data suggest that $Na_V1.9$ has an important role in the sensation of pain (Chen et al., 2012a). Expression of $Na_V1.9$ in DRG neurons innervating the inflamed rat hindpaw is increased (Tate et al., 1998). PGE2, acting via G-protein–coupled receptors (GPCRs), enhances the current density of $Na_V1.9$ in DRG neurons in vitro, along with hyperpolarised shifts of activation and inactivation (Rush and Waxman, 2004), and treatment with IL-1β enhances persistent TTX-R mediated current by a p38 MAPK-dependent mechanism (Binshtok et al., 2008).

A wide variety of ion channels which are expressed on sensory nerve terminals mediate the transduction of various stimuli into membrane potential changes (Cho et al., 2012, Julius and Basbaum, 2001). A graded local change in membrane potential usually occurs in response to physicochemical stimuli, for example through activation of Transient Receptor Potential (transducer protein molecules) (TRP) channels, and once a threshold of depolarisation is achieved, this leads to the generation of action potentials (Zhao and Boulant, 2005). Voltage-gated ion channels that are present in the plasma membrane of the cell generate action potentials (Waszkielewicz et al., 2013). Na_V channels in particular are responsible for the upstroke of the action potential (Kress and Mennerick, 2009). These channels remain closed when the membrane potential is around the resting potential of the cell, however, they begin to rapidly open when the membrane potential reaches to the threshold value (Carter and Bean, 2009). When the channels open (as a response to depolarising transmembrane potential), they allow sodium ions to flow inwards. This changes the electrochemical gradient, and produces a further rise in the membrane potential. This then leads to opening of more channels, thereby producing greater electric current across the cell membrane. This self-growing process goes on rapidly, until all the ion channels are opened. This results in a large increase in the membrane potential (Endo, 2000). The rapid influx of sodium ions is responsible for reversing the polarity of the plasma membrane, and subsequently the ion channels are rapidly inactivated. With the closure of sodium channels, sodium ions cannot enter the neuron any longer, and they get transported actively across the plasma membrane (Ashrafuzzaman and Tuszynski,

2013). The large membrane depolarisation that occurs as a result of activation of Na_V channels in turn triggers activation of voltage-gated potassium (K_V) channels. An outward current of potassium ions is observed, thereby returning the electrochemical gradient to the resting state. Following the occurrence of an action potential, a negative shift is generated in a transient manner, which is called the after hyperpolarisation or refractory period, because of the additional potassium currents (Bean, 2007).

Hot and warm temperatures are detected by TRP channels like TRPV1 and TRPV2 (Transient Receptor Potential Vanilloid 2) along with the calcium-gated chloride channel, ANO1 (Anoctamin-1) (Cho et al., 2012, Julius and Basbaum, 2001, Roberts and Connor, 2006). TRPV3 (Transient Receptor Potential Vanilloid 3), TRPV4 (Transient Receptor Potential Vanilloid 4 (cation channel)) and TRPM3 (Transient Receptor Potential Melastatin 3) also play important roles in transduction of warm temperatures (Chung et al., 2004, Vriens et al., 2011, Watanabe et al., 2002). Protons are predominantly sensed by acid-sensing ion channels along with TRPV1 (Julius and Basbaum, 2001). There are also proton-sensitive GPCRs (Tomura et al., 2005). TRPM8 (Transient Receptor Potential Melastatin 8) senses cold temperatures, while $Na_V1.8$ is essential for cold-associated pain (Bautista et al., 2007, Zimmermann et al., 2007). TRPA1 (Transient Receptor Potential Ankyrin 1) and TRPC5 (Transient Receptor Potential Canonical (protein) 5) also play an important role in cold sensation (Kwan and Corey, 2009, Zimmermann et al., 2011). Piezo1 and Piezo2 act as mechanical transducers (Coste et al., 2010), though TRPA1 and the ATP-gated purinergic ion-channel P2X3 also act as mediators of mechanical hyperalgesia (Kwan et al., 2006, Petrus et al., 2007, Tsuda et al., 2000). When these ion channels are activated, they cause the generation of a transient potential, which amplifies in the form of a regenerative potential by sodium (Na^+) channels like $Na_V1.7$, $Na_V1.8$ and $Na_V1.9$ (Raouf et al., 2010). At this point, the signal may be curbed by endogenous inhibition occurring by the mediation of potassium (K^+) channels like the two-pore channels TREK1 (mechanogated and arachidonic acid- activated TWIK-related K^+ 1) and TRAAK1 (TWIK-related arachidonic acid- stimulated channels). TWIK channels comprise a tandem of p domains and produce a weak inwardly rectifying K^+ channel (Honore, 2007). The activation of other voltage gated Na^+ channels like $Na_V1.7$ initiates an action potential which transduces nociceptive signals from the periphery to the central nervous system (Raouf et al., 2010, Wood et al., 2004). A mutation in the *SCN9A* gene encoding the $Na_V1.7$ ion channel resulting in loss of its function causes complete inability to sense pain in humans (Cox et al., 2006). Conversely, another mutation in *SCN9A* resulting in gain of function leads to congenital paroxysmal disorders with extreme pain and congenital erythromelalgia (Fertleman et al., 2006). Analogous to these clinical findings, nociceptor-specific deletion of $Na_V1.7$ in mice causes reduced hypersensitivity (Nassar et al., 2004).

A Na^{+}-channel blocker, XEN402, is also known to relieve $Na_V1.7$ mediated spontaneous pain in patients with inherited erythromelalgia (Goldberg et al., 2012).

Sodium channels may be important contributors in the pathology of cancer induced bone pain (Liu et al., 2014c). Increased expression levels of $Na_V1.8$ and $Na_V1.9$ point towards possible involvement of these Na_V isoforms in breast cancer induced bone pain (Qiu et al., 2012). It has been observed that enhanced *SCN7A/Nax* expression, a gene that encodes an atypical sodium channel named 'Nax', contributes to bone cancer pain by increasing excitability of DRG neurons in a rat model of breast cancer induced bone pain (Ke et al., 2012). It is becoming increasingly evident that different pain phenotypes, although seemingly similar at the symptom level, can differ vastly in the signalling pathways and underlying molecular mechanisms involved (Baron, 2006). Recently a study found abolition of constriction injury dependent neuropathic pain in mice with sensory neurons-specific deletion of $Na_V1.7$, while pain-relief of nerve transection related pain required deletion of $Na_V1.7$ from sensory neurons and sympathetic neurons (Minett et al., 2014). Similarly, oxaliplatin induced pain and cancer induced bone pain, did not require the presence of $Na_V1.7$ sodium ion channels or nociceptors positive for $Na_V1.8$ (Minett et al., 2014). Na_V 1.6 is a very important and major sodium channel isoform present at the nodes of Ranvier in myelinated axons and also distributed along the unmyelinated C-fibers of sensory neurons. Modulation of the sodium channel current by $Na_V1.6$ may critically impact axonal conduction. $Na_V1.6$ is modulated by MAPKs that are expressed in neurons and are activated subsequent to injury, such as after sciatic nerve transection and hypoxia (Wittmack et al., 2005). $Na_V1.6$ has been found to accumulate along the degenerating axons in demyelinated regions of the central nervous system of the autoimmune encephalitis (EAE) mouse model of multiple sclerosis and also in patients suffering from multiple sclerosis (MS) (Craner et al., 2004a, Craner et al., 2004b). Moreover, $Na_V1.6$ is upregulated in activated microglia and macrophages in EAE mice and also in acute MS lesions (Craner et al., 2005). Hence, $Na_V1.6$ has a major role in normal axonal conduction and can significantly influence the pathophysiological condition of the nervous system that is injured. Some preclinical studies found, that expression of $Na_V1.6$ at mRNA (Messenger Ribonucleic Acid) and protein levels remained unchanged in the DRGs in the carrageenan induced inflammatory pain, while the $Na_V1.6$ mRNA levels decreased in the neuropathic pain models (Wang et al., 2011c). However, the assessment of global gene level and protein level changes in different models might provide key insights into the pathophysiology of pain in different conditions.

Some of the key ion channels known to be involved in processing of CIBP include Na_V 1.8 and 1.9, acid-sensing ion channels and TRPV1 channels (Mantyh, 2014). Other ion channels including

potassium ion channels and high-voltage activated calcium channels have also been implicated in CIBP (Shenoy et al., 2016).

1.6. Signalling molecules of peripheral pain sensitivity

In conditions of chronic pain like cancer and inflammation, nociceptive and non-nociceptive sensory afferent neurons are sensitised (Lozano-Ondoua et al., 2013b). Peripheral sensitisation is characterised by increased response of the peripheral sensory nerve endings, which are activated by chemical mediators released from nociceptors and cells of non-neuronal origin like mast cells, basophils, platelets, neutrophils, macrophages, endothelial cells, fibroblasts and keratinocytes at the site of inflammation or tissue damage (Gangadharan and Kuner, 2013). A wide variety of signalling molecules like protons, adenosine triphosphate (ATP), prostaglandins (PGE2), leukotrienes, thromboxanes, endocannabinoids, growth factors such as neurotrophins (NGF) and granulocyte- or granulocyte-macrophage colony stimulating factors (G-CSF, GM-CSF), cytokines (interleukin 6 (IL-6), interleukin 1β (IL-1β), tumour necrosis factor-α (TNFα)), chemokines, neuropeptides [CGRP, SP, bradykinin, histamine], proteases and lipids take part in mediation of peripheral pain sensitisation (Binshtok et al., 2008, Gangadharan and Kuner, 2013, Gold and Gebhart, 2010, Julius and Basbaum, 2001, Schweizerhof et al., 2009). Glutamate, a major excitatory amino acid neurotransmitter at central synapses, might also act in the peripheral nervous system by modulating the activation properties of nociceptive neurons, and by controlling the conduction of nociceptive impulses from periphery to the central nervous system (Gangadharan et al., 2011). Upon activation by chemical mediators, the activity of transduction proteins controlling the signalling of nociceptor terminals is altered at the transcriptional or post-translational level (Woolf and Ma, 2007). For instance, growth factors like NGF acting through its high affinity receptor, the tyrosine kinase A receptor (TrkA), or GM-CSF acting through tyrosine kinase receptors and Janus Kinase and Signal Transducer and Activator of Transcription (JAK-STAT) signalling, employ various downstream enzymes like phospholipase C (PLC), phosphoinositide 3-kinase (PI3K) and mitogen-activated protein kinase (MAPK). These enzymes are responsible for phosphorylation of transducer and amplifier molecules like TRPV1 (Transient Receptor Potential Vanilloid 1) and voltage gated sodium ion channel 1.8 ($Na_V1.8$) and also increase the expression of such molecules by transcriptional regulation through employment of STAT transcription factors. This leads to both short term and long term enhancement of the excitability of nociceptors (Dib-Hajj et al., 1998, Julius and Basbaum, 2001, Schweizerhof et al., 2009, Zhang et al., 2005, Wu et al., 2012a). In summary, there is a close interaction between the external signals generated by mechanical, chemical and thermal stimuli and the intrinsic factors, and this interface leads to the functional plasticity of neurons, which underpins the development of a response to the noxious stimuli that is

mediated by the higher centres of pain processing pathway (Woolf and Ma, 2007). Cancer cells and the associated immune cells are also responsible for secreting mediators like prostaglandins (Urch, 2004). Tumor cells also mediate the release other pro-nociceptive compounds like NGF, endothelins, bradykinins, histamine, etc. that assist in maintaining the associated pain (Middlemiss et al., 2011, Mantyh, 2014).

1.7. Role of G-protein-coupled receptors

GPCRs are cell surface targets that are highly important in normal cell signalling and mediate the physiological response to a variety of stimuli from light, odorants, hormones, neurotransmitters, etc. as well as clinically used drugs to treat ailments (Gurevich and Gurevich, 2017). Signalling mediated by GPCRs makes an important contribution in peripheral sensitisation (Gold and Gebhart, 2010). Various peptides, bioactive lipids and metabolic products are responsible for activating GPCRs in sensory neurons. These receptors couple with various G-proteins like Gq, G11, Gs, Gi, Go, G12 and G13. Gq/G11 signalling causes the activation of PLC-β and protein kinase C, releases Ca^{2+} from intracellular storage, and modulates extracellular regulated kinases ERK1 and ERK2 (Kuner, 2010). Gs signalling is connected to cAMP–protein-kinase-A -mediated sensitisation mechanisms (Hucho and Levine, 2007). Gs proteins act mainly through the activation of adenylyl cyclase, leading to increased intracellular levels of cAMP, which consequentially leads to the activation of downstream effectors like PKA (Stone and Molliver, 2009). The functional role of Gq/G11 signalling in nociceptors *in vivo* not only governs sensitisation mechanisms in pathological conditions of pain but also governs basal nociception along with acute pain conditions (Tappe-Theodor et al., 2012). This consists of tonic modulation of TREK channels (Chen et al., 2006), Na^{+} channels (Tappe-Theodor et al., 2012), TRPV1 (Zhang et al., 2012) and mechanosensory currents (Lechner and Lewin, 2009). Generally, GPCRs which signal via Gq and G11 also couple with G12 and G13 proteins, which activate the RhoGTPase RhoA (RhoGTPase = any member of Rho family of GTPases; RhoA = Ras homolog gene family member A; GTPase = family of hydrolase enzyme that can bind and hydrolyse guanosine triphosphate) and subsequently, a downstream kinase, ROCK (Rho Kinase). The contribution of RhoA-ROCK signalling in nociception is not clearly established. It is well known that Gq/11 coupled receptors process via the activation of ERK (Extracellular Signal-Regulated Kinase) (Della Rocca et al., 1997). Gi-mediated inhibition is an important barrier that determines nociceptor excitability. Gi/o proteins participate in the inhibitory effects of several neurotransmitters (Stone and Molliver, 2009). Several mechanisms of actions of the dimer Gi/o proteins have been proposed, like inhibition of adenylyl cyclase, inhibition of voltage dependent calcium channels and direct hyperpolarisation of neurons by activation of GIRK (G-Protein-Gated Inwardly Rectifying K+) channels (Stone and Molliver, 2009). The anti-

nociceptive activities of cannabinoids and opioids that bind to GPCRs are mediated through peripheral mechanisms as well (Agarwal et al., 2007, Kinsey et al., 2009, Lever et al., 2009, Stein and Lang, 2009). While ERK activation is reputed to be pro-nociceptive (Kawasaki et al., 2006, Ji et al., 2009a), drugs like opioids and cannabinoids might activate the molecular players of the ERK cascade (Korzh et al., 2008). Several molecular and cellular features of receptors like opioid receptors might not easily be co-related to any physiological or behavioural effects and hence need further investigations (Al-Hasani and Bruchas, 2011). Opioids and cannabinoids induce analgesia by inhibition of adenylyl cyclase, inhibition of voltage dependent calcium channels and activation of GIRK channels (Korzh et al., 2008). An agonist acting through a receptor can activate multiple signalling pathways (Ibsen et al., 2017). On these grounds, transactivation of other targets like vascular endothelial growth factor receptors (Rubovitch et al., 2004), epidermal growth factor receptors (Belcheva et al., 2001) and fibroblast growth factor receptors (Belcheva et al., 2002) might be involved in cannabinoid and opioid receptors- mediated activation of ERK. Similarly, different agonists can activate different pathways to activate ERK, consequentially (Korzh et al., 2008). Accordingly, other than analgesia, opioids are known to underpin a variety of behavioural and physiological effects like reward, depression, anxiety and addiction (Al-Hasani and Bruchas, 2011). Hence, the behavioural and physiological implication of the agonist-induced modulation of a signalling pathway could probably depend on how the pathway is triggered, the upstream and downstream contributors and the other parallel pathways involved. Some of the key GPCRs involved in processing CIBP include prostaglandin receptors, bradykinin receptors and endothelin receptors (Mantyh, 2014). Recent studies have demonstrated possibile roles of several receptors in CIBP, including receptors like chemokine receptors, purinergic receptors, adenosine receptors and protease activated receptors (Shenoy et al., 2016).

1.8. Involvement of central signalling

Excitatory synaptic transmission between primary afferents and neurons of the spinal cord is fundamentally mediated by glutamate, along with other co-transmitters like SP, CGRP and brain-derived growth factor (BDNF) (Gangadharan and Kuner, 2013). Ionotropic as well as metabotropic glutamatergic receptors critically contribute towards the determination of the strength of synaptic transmission and alterations in the spinal cord as a response to the continuing nociceptive activity (Gangadharan and Kuner, 2013). Activity-dependent modulation in spinal function includes long-term potentiation of individual synapses along with an enhancement of neuronal and non-neuronal (facilitated by glial cells) spinal excitation in the dorsal horn, causing enhanced pain sensitivity, which is termed ‘central sensitisation’ (Ji et al., 2003, Sandkuhler, 2009). An important trigger for both of these changes is the activation of spinal postsynaptic NMDARs as a response to continuing

nociceptive activity (Woolf and Salter, 2000). The resultant increase in the intracellular Ca^{2+} activates protein kinases like CaMKIIα, which leads to a greater number of AMPA-type glutamate receptors in postsynaptic membranes by recruiting AMPAR interacting proteins such as GRIP1 (Kuner, 2010). This increases postsynaptic excitation as well as causes further influx of Ca^{2+} by recruiting Ca^{2+}-permeable AMPAR (Galan et al., 2004, Hartmann et al., 2004, Park et al., 2009). More Ca^{2+}- dependent enzymes like cyclooxygenases (COX-2) (Zhou et al., 2014) and nitric oxide synthases (NOS) (Fleming et al., 1997) are also activated, to generate PGE2 and nitric oxide, respectively. Such molecules are considered to act as retrograde messengers, which facilitate release of neurotransmitter from primary afferent terminals in the spinal dorsal horn. Several synaptic-interacting proteins significantly contribute to the optimal arrangement of NMDAR and AMPAR channels in the postsynaptic membrane (Kuner, 2010). The persistent nociceptive activity also employs synaptic proteins which inhibit central sensitisation. This inhibition takes place either by inhibiting important enzymes or by disassembling the complexes of metabotropic glutamate receptors 1 and 5 (mGluR1,5) along with inositol triphosphate receptors (IP3R) (physical tether linking mGLuR with IP3R formed by protein like Homer) which are coupled to intracellular Ca^{2+} stores (Gangadharan and Kuner, 2013, Tu et al., 1998). Downstream of glutamatergic ion channels and GPCRs, the MAPKs, ERK1 and ERK2, are activated. The MAPKs then directly govern the excitability of neurons in the spinal cord by regulating the Kv4.2 channel, that generates A-type K^+ currents which regulate neuronal excitability (Gangadharan and Kuner, 2013). The ERK1/2 mediated phosphorylation of the Kv4.2 channel reduces A-type currents and enhances excitability of the superficial neurons of the spinal dorsal horn (Hu et al., 2006). Moreover, ERK1 and ERK2 increase AMPAR- and NMDAR-mediated currents in neurons of the dorsal horn of the spinal cord (Kohno et al., 2008).

Despite the fact that the majority of work on spinal mechanisms involved in chronic pain are based on postsynaptic targets, presynaptic involvement is increasingly recognised as being important. For instance, long term potentiation at synapses between nociceptors and neurons of the spinal cord that project to the periaqueductal gray matter needs activation of postsynaptic NMDAR for induction (Ikeda et al., 2006), but also employs a cGMP-regulated enhancement in the release of presynaptic neurotransmitter (Luo et al., 2012). The step occurs by activation of protein kinase G1 at the presynaptic level, which leads to phosphorylation of presynaptic IP3Rs along with myosin light chain subunits, leading to a Ca^{2+}-triggered enhancement in actin-myosin coupling and employment of synaptic vesicles. Also, nerve injury by itself is linked to an enhancement of neurotransmitter release from nociceptors (Inquimbert et al., 2012).

One of the most important concerns in pain research currently is the process leading to conversion of acute to chronic pain (Mifflin and Kerr, 2014). Activation and mediation of genomic changes is considered an important contributing mechanism in the development of pathological pain (Buchheit et al., 2012). In this regard, ERK1, ERK2, cAMP (cyclic adenosine monophosphate) and CaMKIV (calcium/calmodulin- dependant protein kinase type IV) act as communicators between synapse and nucleus to initiate the cAMP response element-binding protein (CREB) activation that regulates the expression of several proteins related to pain hypersensitivities like COX-2, TRPV1 and Ca^{2+} channels (Kawasaki et al., 2004). Ca^{2+} ions are transported into nuclei of excitatory neurons of the spinal cord in a manner dependent on nociceptive activity, thereby regulating a set of unique genomic changes which govern the functional and structural plasticity involved in inflammatory pain (Simonetti et al., 2013). The transcription of genes in neurons of the spinal cord is also governed by expression of transcriptional repressors like MeCP2 (Methyl-CpG-binding protein 2), that regulates inflammatory pain states (Geranton et al., 2007), and DREAM (downstream regulatory element antagonistic modulator), which functions to inhibit the expression of prodynorphin in the neurons of spinal cord, thereby producing hyperalgesia (Cheng et al., 2002).

Continuing nociceptive activity-evoked pronociceptive actions and central sensitisation are kept in control by spinal inhibitory mechanisms consisting of GABAergic and glycinergic neurotransmission (Ben-Ari et al., 2007, Legendre, 2001). Cannabinoids, opioids and adenosine released endogenously also exhibit an inhibitory function (Freund et al., Homayounfar et al., 2005). Local enkephalins that are secreted by enkephalinergic neurons lead to the inhibition of release of neurotransmitters and supress excitation at the postsynaptic level by inhibiting voltage-gated Ca^{2+} channels and activating GIRK channels respectively. Such inhibition based enkephalinergic processes are employed in the spinal cord by descending serotonergic and noradrenergic pathways, forming brainstem control of central sensitisation (Gangadharan and Kuner, 2013). There are also various molecular signalling events that are linked with disinhibition following nerve injury. PGE2, as an example, induces phosphorylation of the glycine receptor α3 subunit, which in turn counteracts glycinergic inhibition and hence underlies central inflammatory pain sensitisation (Harvey et al., 2004). Collapse of the chloride (Cl^-) gradient after nerve injury, caused by loss of the postsynaptic potassium chloride (K^+ Cl^-) exporter KCC2 (K-Cl (Potassium Chloride) Cotransporter 2) to decrease GABA-mediated inhibitory currents at the postsynaptic level is also another mechanism for disinhibition of neurons of the spinal cord (Beggs et al., 2012, Coull et al., 2003).

Along these lines, c-FOS and dynorphin expression levels are increased in the deeper laminae of the spinal cord in CIBP state (Falk and Dickenson, 2014, Peters et al., 2005). c-FOS and dynorphin

levels were also found to be changed in other inflammatory and neuropathic pain models, implying some mechanistic resemblances with parts of CIBP state (Abbadie and Besson, 1992, Wagner et al., 1993). Similar to the observations in inflammatory and neuropathic pain states, spinal cord neurons exhibit hyper-responsiveness towards evoked stimuli in CIBP (Urch et al., 2003, Donovan-Rodriguez et al., 2004). CIBP animals were found to exhibit increased number of wide dynamic range neurons in the superficial dorsal horn, resulting in hyper-responsiveness to peripheral stimuli of low thresholds (Donovan-Rodriguez et al., 2005). Descending controls from brain to spinal cord and periphery might also play crucial role in manifestations of CIBP (Falk and Dickenson, 2014).

1.9. Role of neuro-glia

Recently, signalling mechanisms that regulate interactions between neurons of the spinal cord and various glial cell types have become important targets in pain research. Purinergic signalling mechanisms consisting of P2X4 (Beggs et al., 2012), P2X7 (Clark et al., 2010a, Clark et al., 2010b) and P2Y12 (Tozaki-Saitoh et al., 2008) receptors contribute to recruitment and activation of microglia and are important regulators of central sensitisation (Gao and Ji, 2010a, McMahon and Malcangio, 2009). As a response to nerve injury, chemokines such as CX3CL1 (chemokine (C-X3-C motif) ligand 1), CCL2 (chemokine C-C motif ligand 2) and TNFα are released from primary afferent terminals, as well as ATP to activate their receptors CX3CR1 (chemokine (C-X3-C motif) receptor 1), CCR2 (chemokine C-C motif receptor 2), TNFR, P2X and P2Y on microglia (Beggs et al., 2012, Clark et al., 2010a, Gao and Ji, 2010a). These receptors being activated cause induction of p38 MAPK signalling in microglia, which contributes towards the synthesis and release of several molecular players like BDNF, TNFα, IL-1β, IL-6 and cathepsin S, which modulate the functions of neurons (Clark et al., 2009, Kawasaki et al., 2008). The released BDNF from microglia acts on tyrosine kinase B (TrkB) receptors in neurons at the postsynaptic level, causing downregulation of potassium chloride co-transporter KCC2 expression in the adjacent neurons, hence making them more susceptible to excitation (Coull et al., 2003). The TNFα secreted from microglia activates the Jun N-terminal Kinase (JNK) signalling in astrocytes, causing release of IL-1β, CCL2 and MMP (matrix metalloproteinase)-2, which alter the central sensitisation (Gangadharan and Kuner, 2013). TNFα also activates TNFR on presynaptic endings, causing glutamate release and enhanced excitatory postsynaptic potential (EPSP) by the activation of TRPV1 (Park et al., 2011). CCL2 and IL-1β that are released from astrocytes bind on their respective receptors (CCR2 and ILR) at presynaptic and postsynaptic locations, causing increased release of neurotransmitters and activation of NMDAR and AMPAR (Gao and Ji, 2010b). MMP-9 and MMP-2 are responsible for cleaving and activating the IL-1β, subsequently activating the microglia and astrocytes, hence playing an important role in developing and maintaining the neuropathic pain state (Gangadharan

and Kuner, 2013). Cathepsin S that is released from the microglia, mediates the cleavage of a transmembrane protein, fractalkine (FKN), which is expressed in neurons of the spinal cord and releases soluble FKN (s-FKN) which binds to its receptor, CX3CR1, present on microglia (Clark and Malcangio, 2012). This subsequently activates the p38 MAPK signalling process in microglia, thereby developing positive feed-forward and feed-back modulatory cycles, which possibly contribute to maintaining the chronic pain even long after the occurrence of an initial injury (Clark et al., 2007). In states of chronic pain, astrocyte activation causes negative and positive modulation of excitatory amino-acid transporter (EAAT) and GABA transporters, respectively (Gangadharan and Kuner, 2013). This increases the availability of excitatory amino acids like glutamate and decreases the availability of the major inhibitory amino acid neurotransmitter GABA, the net result of which is increased synaptic transmission (Gangadharan and Kuner, 2013). On similar grounds, massive astrocyte hypertrophy in the spinal cord has been observed in CIBP, suggesting the importance of glia in maintaining this pain state (Honore et al., 2000). Other studies have also reported microglial activation and involvement of mediators like MAPK family members in spinal cord, in facilitation of CIBP state (Hu et al., 2012a).

1.10. Analgesic drugs

Based on the above-described mechanisms, a range of approaches have been utilised to treat pain. Morphine, an agonist predominantly at the μ-opioid (MOP) receptor, is one of the most important members of the strong opioid analgesic class (Cao et al., 2010). All four opioid receptor types i.e. μ type, δ type, κ type and opioid receptor-like 1 / ORL1 type, belong to the superfamily of G_i /G_o -protein-coupled receptors (McDonald and Lambert, 2005). Opioid agonists enhance the opening of GIRK channel and also inhibit the opening of voltage-gated calcium channels (McDonald and Lambert, 2005, Connor et al., 2004). GIRK channels in neurons are key determinants of spinal analgesia (Tsantoulas and McMahon, 2014). These membrane changes decrease neuronal excitability as the increased K^+ conductance leads to hyperpolarisation of the membrane thereby causing the cell to be less likely to fire action potentials (McDonald and Lambert, 2005). Opioid receptors mediate presynaptic inhibition of calcium channels and inhibition of neurotransmitter release (Henderson, 2015). Drugs like morphine are well known to inhibit adenylyl cyclase (Connor et al., 2004). The net effect is inhibition of nociception (Rosenblum et al., 2008). Gabapentin is one of the drugs used in both epilepsy and neuropathic pain (Sills, 2006). It inhibits calcium currents via high-voltage-activated channels containing the $\alpha_2\delta$-1 subunit, that in turn decrease neurotransmitter release and to reduce postsynaptic excitability (Sills, 2006). Other mechanisms have also been proposed like modest actions on voltage gated potassium channels (Sills, 2006). NSAIDs (Non-steroidal anti-inflammatory drugs) like meloxicam inhibit COX, the enzyme responsible for the

conversion of arachidonic acid into prostaglandin H_2, which is the first step in the synthesis of PGE2 (mediators of inflammation) (Ricciotti and FitzGerald, 2011). Meloxicam, especially at therapeutic doses, has modest selectivity for inhibition of COX-2 over COX-1 (Noble and Balfour, 1996). Bisphosphonates like ibandronate are able to effectively improve the basic pathogenesis of bone disorders by reducing bone resorption (Ringe and Body, 2007). Hence they are considered to be an important part of palliative care in bone malignancy related pain especially that due to breast cancer metastasis (Ringe and Body, 2007). Tricyclic antidepressant drugs such as amitriptyline are also used as analgesic adjuvant drugs, which augment descending noradrenergic inhibition and are utilised for the management of neuropathic pain conditions (Tura and Tura, 1990). Drugs like gabapentin and amitriptyline are called adjuvant analgesics because they are the drugs with a primary indication other than pain; gabapentin being used as an anticonvulsant drug and amitriptyline being used as an antidepressant drug (Lussier et al., 2004, Mitra and Jones, 2012). Besides the conventionally used analgesic drugs like these, used for treatment of different pain conditions, several new drug candidates are being researched for their analgesic efficasy. For example, some of the key GPCR ligands in the preclinical or clinical phase of development include MS-Contin (extended release opioids), CR845 (peripherally restricted κ-opioid agonist), EMA401 (angiotensin type 2 receptor blocker), tizanidine (α2a adrenergic agonist) and AZD2423 (chemokine receptor 2 antagonist) (Yekkirala et al., 2017). Some of the new ligands targeting ion channels involved in pain transduction include JNJ-38893777 (TRPV1), Z944 (calcium channels), TV-45070 ($Na_v1.7$) and PF-04531083 ($Na_v1.8$) (Yekkirala et al., 2017). Some of the novel ligands targeting different enzymes modulating the pain processes include 2-MPPA (glutamate carboxypeptidase II), SUN (D-Amino acid oxidase) and Sivelestat (leukocyte elastase) (Yekkirala et al., 2017). In CIBP state, the most common treatment options used to alleviate bone pain are such analgesic drugs, bisphosphonates, radiopharmaceuticals, as well as the commonly used radiotherapy (Rades et al., 2010). Commonly used opioids in CIBP include morphine, codeine, oxycodone, hydromorphone, methadone, oxymorphone, levorphanol, fentanyl and meperidine (Rades et al., 2010).

1.11. The Walker 256 breast cancer cell-induced bone pain model in rats

1.11.1. Rat as the species of choice

Rats and mice are the most commonly used animal species for pain research (Walker et al., 1999), with rats being superior to mice in many practical respects (Mogil, 2009, Wilson and Mogil, 2001). The advantage of mouse pain models is the availability of transgenic mice for dissecting pathophysiological mechanisms (Mogil and Grisel, 1998) and mouse models of breast cancer might recapitulate key aspects of human breast cancer including poor immunogenicity and high metastatic

potential (Hahn et al., 2006). However, the main disadvantage of mice is their small size, making direct injection of tumor cells into the bone technically challenging (Pacharinsak and Beitz, 2008). By contrast, rat models are considered very suitable for efficacy assessment of therapeutic interventions for the treatment of breast CIBP (Medhurst et al., 2002). Walker 256 cell induced bone pain model is extensively induced in "rat" as the experimental species (Shenoy et al., 2016). This is mainly because the Walker 256 cell line is derived from rat breast tumour, and hence is syngeneic to the species of "rat" (*Rattus norvegicus*). There are hardly any studies that induced this model in other species. In one report, for example, Walker 256 cell-induced bone pain model was induced in mouse as the experimental species (Ji et al., 2017). The number of genes encoded by the rat genome is about same as the human genome (Gibbs et al., 2004). Importantly, almost all the human genes that are known to be associated with disease states have their orthologues in the rat genome, that have been highly conserved through the process of mammalian evolution (Gibbs et al., 2004). With such close mechanistic resemblance of physiological and pathophysiological processing in rats and humans, rat is an indispensable model to mimic human diseases and to study the efficacy and toxicity of novel drug moieties (Mullins and Mullins, 2004). The model using Walker 256 cells can be induced in both sexes of rats (Liu et al., 2010, Liu et al., 2011) and different rat strains are compatible with these cells (Earle, 1935, Jensen and Muntzing, 1970). Stage of the estrous cycle in female rats does not alter the development of CIBP (Zhu et al., 2014b).

1.11.2. Suitability of Walker 256 cells

The Walker tumor was first discovered in the breast of a pregnant albino rat (*Rattus norvegicus*) in 1928 by Dr. George Walker in Baltimore and it is regarded as a carcinosarcoma (Simpkins et al., 1991, McEuen and Thomson, 1933). It is one of the most widely used transplantable tumors in experimental research (Brigatte et al., 2007, Justice, 1985, Sroka et al., 2016, Wu et al., 2016b, Gambeta et al., 2016, Fan et al., 2016, Gao et al., 2016). Indeed, these cells are one of the most preferred cell lines because of the ease with which they can be standardized, maintained and propagated *in vitro*, as well as their extensive use *in vivo* since 1937 (Michaelson and Orcutt, 1957, Pigatto et al., 2016, Brigatte et al., 2016, Galuppo et al., 2016, Yalovenko et al., 2016, Trashkov et al., 2016).

Walker 256 cells cause significant bone resorption and increase skeletal fragility at the site of implantation in rats (Kurth et al., 2000), consistent with the phenotype observed in breast cancer patients with bone metastasis (Shih et al., 2004). In addition to being a reproducible method for inducing skeletal metastasis (Blouin et al., 2005, Mao-Ying et al., 2006, Badraoui et al., 2009), this model mimics key features of human breast CIBP, including pharmacological profile (Mao-Ying et

al., 2012, Mao-Ying et al., 2006, Cao et al., 2010). Walker 256 cells can be used in a variety of rat strains (Lu et al., 2015, Hang et al., 2015b) because these cells produce uniformly rapid growth, show very little regression, and are readily adaptable (Lewis et al., 2013, Oliveira and Gomes-Marcondes, 2016).

Growth of Walker 256 cells in the form of tumor is generally considered to be independent of the age and weight of the animals at the time of their inoculation (Walpole, 1951), however osteolysis and tumor growth might be greater in the bones of younger animals (Bassani et al., 1990). Another advantage is that after unilateral intra-tibial injection (ITI), tumor cells do not metastasize to the contralateral tibia during the experimental period and they only cause structural degradation of bones in the ipsilateral limb but not the contralateral limb (Kurth et al., 2002, Kurth et al., 2001). They also generally do not metastasize to highly perfused organs such as the lungs (Brigatte et al., 2007), in contrast to other cell lines such as the 13762 rat mammary carcinoma cell line or the c-SST2 rat mammary carcinoma cell line, which spontaneously metastasize (Blouin et al., 2005).

Although many scientists tend to presume that tumor cell lines behave indefinitely in a uniform manner (Lewis et al., 2013), changes may be induced by factors such as extended *in vitro* growth time, high passage number and cross contamination with other cell lines (Sacchi et al., 1984, Chang-Liu and Woloschak, 1997, Buehring et al., 2004, Liscovitch and Ravid, 2007). Immortalized cancer cell lines may also evolve *in vivo* over time in the animal models in which cancer is induced (Poste et al., 1982b). Various heterogeneous subpopulations of tumor cells within a tumor mass possess diverse metastatic potential and different propensities for metastasis to various organs (Poste et al., 1982a, Fidler, 1978). Similarly, immortalized Walker 256 cancer cell lines from different cell banks may possess diverse characteristics and behavior *in vivo* despite the fact that these cell lines are from rat origin and are without contamination (Lewis et al., 2013). In general, cell lines may be authenticated by short tandem repeat (STR) profiling of the microsatellite regions of DNA (Nims et al., 2010). However, as there is no reference DNA profile of the Walker 256 cell line (Lewis et al., 2013), researchers typically procure cells of a defined passage number from reputable cell banks. To minimize within- and between- laboratory variability in the use of these cells *in vivo*, it is important that cultured cells are banked and frozen at early passages, and that culture conditions including growth media, temperature, humidity and exposure to drugs are standardized (Marx, 2014).

1.11.3. General methodology

Although there are minor between-laboratory variations, the general method for induction of breast CIBP in rats has several aspects in common. The procedure generally involves making an incision to the skin and muscle around the knee joint of the anesthetized rat and injecting cancer cells into the tibial bone, followed by sealing of the drilled hole with bone wax, suturing of the wound and close monitoring of animals during post-surgical recovery (Mao-Ying et al., 2006). Cells can also be injected in the femur (Gui et al., 2013, Gui et al., 2015). Small differences in the number of injected Walker 256 cancer cells due to experimental errors typically have a minimal effect on the study outcome (Kurth et al., 2001). The physical process for injection of Walker 256 cells into the medullary canal of the bone does not impact the study outcome adversely as emphasized by the normal fibroblastic healing response around the drilled hole of injected bone (Kurth et al., 2002, Mao-Ying et al., 2006). Although outflow of cells during the injection process can be a common occurrence associated with the model, the syringe can be left in place inside the medullary canal of the bone for an additional one or two minutes to avoid leakage of cells along the injection track (Mao-Ying et al., 2006, Yu et al., 2009, Miao et al., 2010, Dong et al., 2011, Hu et al., 2012c).

1.11.4. Time frame for development of pain behaviors and analgesic efficacy testing

One of the most important and critical factors in the study of pain behavior and extent of bone destruction in this model is the timing of observations post-surgery (Qiu et al., 2012). Large tumors can develop in just a few days (Justice, 1985). However, the time period for development of pain behaviors may vary between studies based upon factors such as cell invasiveness and sex of the experimental animals (Wang et al., 2011b). Pain behavior due to the surgical process may be evoked in the ipsilateral (injected) hind paws if the animals are tested immediately after the inoculation surgery (Lan et al., 2010, Dong et al., 2011). Hence a recovery period of two to three days post-surgery must be provided for the animals (Wang et al., 2011b). For the purposes of studying different mechanisms of breast CIBP and for efficacy profiling of molecules with potential to be developed as novel analgesic agents, it is best to avoid extending the model beyond 20 to 25 days post-surgery (Hang et al., 2014, Yu et al., 2009, Mao-Ying et al., 2006, Tong et al., 2010a, Cao et al., 2010) due to overall poor animal health and ethical concerns (Kurth et al., 2001). In particular, prolonged observation times may be associated with more complex pathophysiology arising from systemic metastasis due to severe osteolysis (Qiu et al., 2012). Hence, the period between days 6 and 18 post-ITI is typically chosen for investigation of breast CIBP mechanisms and the efficacy testing of novel compounds with potential as analgesic agents (Wang et al., 2011b, Hu et al., 2012a, Wang et al., 2012c).

1.11.5. Nature of pain manifestation

In Walker 256 cell-CIBP, up-regulated expression and release of pro-inflammatory mediators including prostaglandin E2 (PGE2), nerve growth factor (NGF) and proinflammatory cytokines including interleukin (IL)-1β, IL-6 and tumor necrosis factor-α (TNF-α) in the spinal cord and dorsal root ganglia contributes to the pathogenesis of bone pain in rats (Cao et al., 2010, Liu et al., 2010, Lan et al., 2010, Mao-Ying et al., 2012, Dong et al., 2011, Yao et al., 2016, Zhu et al., 2016). Hence, neuroinflammation is an important pathogenic characteristic of this model (Hu et al., 2012c, Song et al., 2015).

Similar to the clinical situation, Walker 256 cell-CIBP manifests as spontaneous pain, hyperalgesia, allodynia as well as ambulatory pain, the severity of which largely depends upon the number of inoculated cells, but can also be affected by other experimental factors including cell origin as well as strain or sex of the animals used (Liu et al., 2010, Mao-Ying et al., 2006). Similarly, hind paw hypersensitivity induced by ITI with Walker 256 cells may be either unilateral (Wang et al., 2012c, Tong et al., 2010a, Liu et al., 2010, Wang et al., 2012a, Dong et al., 2011) or bilateral (Li et al., 2014a, Zhao et al., 2013, Mao-Ying et al., 2006, Mao-Ying et al., 2012). Peripheral mechanisms including circulating factors and transmedian sprouting, or central mechanisms such as signalling via commissural interneurons in the spinal cord and brain stem may underpin unilateral injury-induced contralateral mirror effects (Koltzenburg et al., 1999). This mirror image effect may also be correlated with spinal glia cell activation, proinflammatory cytokine production, and morphological changes within the local nerve, suggesting the involvement of glia (Chacur et al., 2001). The mirror image pain behavior induced in the contralateral hind paw in this model may be observed when the tumors are in the advanced stage (Miao et al., 2010, Zhao et al., 2013, Li et al., 2014a) Typically though, contralateral pain behaviors are of reduced intensity compared with the ipsilateral hind paw (Miao et al., 2010).

Thermal and mechanical pain behaviors are underpinned by different mechanisms (Paqueron et al., 2003, Wang et al., 2012a). Cutaneous nociceptors are particularly sensitized by thermal stimuli and nociceptors present in deep somatic tissues such as joints and muscle exhibit pronounced sensitization to mechanical stimuli (Schaible, 2007). Although thermal hyperalgesia has been reported in this model (Wang et al., 2012a, Duan et al., 2012, Liu et al., 2011), there are several studies in which hindpaw hypersensitivity to an applied noxious heat stimulus is not observed in rats following a unilateral ITI of Walker 256 cells (Wang et al., 2011b, Mao-Ying et al., 2006, Mao-Ying et al., 2012, Miao et al., 2010, Yao et al., 2008). Again, these differences may be attributed to various factors including between-vendor differences in animals and cancer cell-related factors. For

this reason, thermal hyperalgesia is not typically used as a pain behavioral endpoint in this model (Yu et al., 2009, Tong et al., 2010a, Zhao et al., 2010, Cao et al., 2010, Dong et al., 2011). A between-study comparison of Walker 256 cell- CIBP rat model is presented in Table 1.1.

Table 1.1. Comparative summary of previous work by others using the Walker 256 cell-CIBP model in rats.

Number of cells injected	**Rat Sex, Strain- (Number of studies)**	**Time frame of hindpaw hypersensitivity post- ITI (Days)**	**Nature of pain behavioral responses in the hind paw**				**Reference/s**
			MA	**MH**	**TH**	**S/MEP**	
$4x10^3$	F, W- (1)	14-19	+	NA	NA	+	(Cao et al., 2010)
$5x10^3$	F, SD- (1)	6-14	+	NA	NA	NA	(Zhao et al., 2013)
$1x10^4$	F, W- (1)	9-21	+	NA	NA	+	(Ke et al., 2013)
$1x10^4$	F, SD- (1)	7-18	+	NA	+	+	(Yao et al., 2016)
$3x10^4$	F, SD- (1)	Tested day 10	+	NA	NA	NA	(Liu et al., 2012)
$4x10^4$	F, W- (3) F, SD- (2)	3-16	+	NA	NA	NA	(Dong et al., 2011, Xia et al., 2014, Bu et al., 2014, Ye et al., 2014a, Guan et al., 2015)
$5x10^4$	F, SD- (2)	7-18	+	NA	+	NA	(Wang et al., 2016b, Qiu et al., 2014)
$5x10^4$	F, SD- (1)	5-14	NA	+	+	NA	(Qiu et al., 2012)
$1x10^5$	F, W- (2)	12-24	+	NA	+	+	(Bao et al., 2014b, Bao et al., 2015c)
$1x10^5$	M&F, SD- (4) M&F, W- (3)	5-28	+	NA	+	NA	(Liu et al., 2011, Jiang et al., 2014, Bao et al., 2015a, Fan et al., 2015, Jiang et al., 2015, Jiang et al., 2016, Ren et al., 2015)
$1x10^5$	F, SD- (8)	6-21	+	NA	NA	+	(Liu et al., 2010, Lan et al., 2010, Chen et al., 2012b, Wang et

							al., 2012c, Hang et al., 2012, Bian et al., 2016, Jin et al., 2014, Wang et al., 2012b)
$1x10^5$	F, SD- (8) F, W- (1)	5-21	+	NA	NA	NA	(Wang et al., 2011b, Hu et al., 2012a, Hu et al., 2012b, Hu et al., 2013, Hang et al., 2013c, Hang et al., 2013b, Hang et al., 2015b, Zhu et al., 2015a, Hang et al., 2015a)
$1x10^5$	F, SD- (1)	6-15	NA	+	NA	+	(Hang et al., 2014)
$1x10^5$	F, SD- (1)	6-15	NA	+	NA	NA	(Hang et al., 2013a)
$1x10^5$	F, W- (1)	Tested day 14	NA	NA	NA	+	(Bao et al., 2015b)
$2x10^5$	F, SD- (2) F, W- (1)	3-21	+	NA	NA	NA	(Huang et al., 2014, Pan et al., 2015, Jin et al., 2015, Wu et al., 2016a)
$2x10^5$	F, W- (1)	7-21	NA	+	-	+	(Miao et al., 2010)
$2x10^5$	F, SD- (1)	7-25	NA	+	-	NA	(Li et al., 2014a)
$2x10^5$	F, W- (1)	7-21	NA	+	+	+	(Wu et al., 2012b)
$3.5x10^5$	F, SD- (2)	5-21	+	NA	+	NA	(Wang et al., 2012a, Wang et al., 2015)
$4x10^5$	F, SD- (1)	5-21	+	NA	-	+	(Yin et al., 2010)
$4x10^5$	F, SD- (1) F, W- (1)	4-32	+	NA	-	NA	(Mao-Ying et al., 2012, Huang et al., 2012)
$4x10^5$	F, W- (2) F, SD- (1)	7-21	+	NA	+	+	(Duan et al., 2012, Yang et al., 2015, Zhou et al., 2015)
$4x10^5$	SD- (1)	3-21	+	NA	NA	+	(Cheng et al., 2014)

$4x10^5$	M&F, W- (10) F, SD- (2)	3-21	+	NA	NA	NA	(Yu et al., 2009, Tong et al., 2010a, Wang et al., 2012d, Wang et al., 2012e, Hu et al., 2012c, Zhang et al., 2013, Li et al., 2013, Gong et al., 2014, Zhu et al., 2014a, Hu et al., 2015a, Song et al., 2016, Li et al., 2016)
$4x10^5$	F, W- (1)	6-20	NA	NA	+	NA	(Xu et al., 2013)
$5x10^5$	F, SD- (1)	7-21	+	NA	+	+	(Liu et al., 2013b)
$5x10^5$	F, SD- (5) F, W- (1)	5-21	+	NA	+	NA	(Shen et al., 2014, Bao et al., 2014a, Liu et al., 2014b, Hu et al., 2015b, Zhu et al., 2016, Zhang et al., 2015)
$5x10^5$	F, SD- (1)	7-10	+	NA	NA	+	(Lu et al., 2015)
$5x10^5$	F, SD- (3)	9-21	+	NA	NA	NA	(Chen et al., 2013a, Chen et al., 2015, Song et al., 2015)
$5x10^5$	F, SD- (1)	7-10	NA	+	NA	+	(Lu et al., 2016)
$5x10^5$	M, SD- (1)	5-14	NA	+	NA	NA	(Xu et al., 2015)
$1x10^8$	F, SD- (1)	7-25	+	NA	NA	NA	(Zhao et al., 2010)

+, observed; -, not observed; F, female; M, male; MA, mechanical allodynia; MH, mechanical hyperalgesia; NA, not assessed; SD, Sprague Dawley; S/MEP, spontaneous or movement- evoked pain; TH, thermal hyperalgesia; W, Wistar

1.11.6. Regression of tumor and resolution of pain

Similar to the well-known human scenario of breast cancer regression (Barry, 2009, Hutter, 1982, Lewison, 1976, Onuigbo, 2012, Burnside et al., 2006), Walker 256 breast cancer cells may also potentially transform into a regressive variant *in vivo* (Guimarães et al., 2010) resulting in complete regression if the study is prolonged (Cavalcanti et al., 2003, Schanoski et al., 2004, Jensen and Muntzing, 1970). The mechanisms underlying spontaneous regression are not entirely clear but may involve development of an adaptive immune response (Pardoll and Topalian, 1998, Rees and Mian, 1999), differential propagation of tumor sub-clones in their microenvironment (Khong and Restifo, 2002) and consequent elimination by immune cells, antibodies, cytokines and chemokines (Dunn et al., 2002, Dunn et al., 2006, Bui and Schreiber, 2007, Jaganjac et al., 2008). Physical activity of the animals, exercise (Hoffman et al., 1962, Deminice et al., 2016b), dietary factors (Kwong et al., 1984, Bekesi and Winzler, 1970, Luty et al., 2016, DeWys et al., 1970) or hormonal levels (Khegay and Ivanova, 2015, Khegai, 2013) may influence the regression of these cells or inhibit the activities driven by these cells (Cruz et al., 2016, Deminice et al., 2016a, Fracaro et al., 2016, Campos-Ferraz et al., 2016, Toneto et al., 2016). In most studies, tumor regression is generally overlooked as the tumor-bearing rats are sacrificed before regression is evident (Guimarães et al., 2010). Thus, the verification of tibial tumor burden post-mortem is very important. However, the beginning of pain behavior resolution at 20-25 days post-surgery is typically not due to tumor regression, but may involve neurogenic and immunity-based factors (Zhao et al., 2010, Xu et al., 2013, Huang et al., 2014). In previous work by others using different cancer cell lines, upregulation of the endogenous opioid system is implicated in spontaneous pain behavior resolution (Muralidharan et al., 2013). Similarly, the endogenous opioid system could also have a role in Walker 256 cell-CIBP model (Li et al., 2016). In addition, lipoxins and endogenous lipoxygenase-derived eicosanoids, which represent a unique class of lipid mediators, have a broad spectrum of anti-inflammatory and antinociceptive activities. These are known to suppress the expression of spinal pro-inflammatory cytokines and might also contribute to spontaneous resolution of Walker 256 cell-CIBP in rats (Hu et al., 2012c). Inflammation, which is an important component of cancer pain (Falk and Dickenson, 2014) mostly involves active endogenous processes targeted at protecting the host, and is generally self-limiting and self-resolving (Chiang et al., 2005, Serhan and Savill, 2005, Schwab and Serhan, 2006).

1.11.7. Targets for novel analgesic drug discovery

The pathobiology of Walker 256 cell-CIBP in rats is complex involving inflammatory, neuropathic and tumorigenic components (Cao et al., 2010). Following injection, these cells cause osteolysis and bone resorption (Kurth et al., 2000, Kurth et al., 2001, Yu et al., 2009) and increase oxidative

stress and impair the antioxidant system in the bone microenvironment (Badraoui et al., 2009). They cause enhanced synthesis of IL-1β and TNF-α at the mRNA or protein level along with nuclear factor kappa-light-chain-enhancer of activated B cells (NF-κB), which indicates that increased neuroimmune responses is one of the important factors responsible for pain in this model (Cao et al., 2010, Song et al., 2016). Injection of these cells in the bones sequentially activates the extracellular signal-regulated protein kinase (ERK) / mitogen-activated protein kinase (MAPK) pathway in various cell types in the spinal cord of rats (Wang et al., 2011b, Wang et al., 2012e, Bian et al., 2016). A study has shown that the expression of sodium channels $Na_v1.8$ and $Na_v1.9$ is increased within the DRGs of rats in this model (Qiu et al., 2012). Similarly, A-type K^+ channels in the DRG are also involved in neuropathy in this model and the functions of these ion channels in the DRG neurons were found to change dynamically (Duan et al., 2012). By using whole patch clamp recordings from DRG neurons, a study has shown that the sensitivity of TRPV1 channels was significantly increased in this model (Xu et al., 2013). Spinal expression of K_{ATP} channels was reduced in this model and activation of these channels reduced associated pain hypersensitivities (Xia et al., 2014). In another study, the protein expression levels and mRNA levels of acid-sensing ion channel 3 were upregulated in the DRGs of rats in this model (Qiu et al., 2014). Hence, these ion channels may be important determinants of enhanced neuronal excitability in this breast CIBP model in rats.

Pain behavior and its relief in Walker 256 cell-CIBP in rats is mediated by the endogenous effectors of several targets interacting with their cognate receptors as summarized in Table 1.2. These include important targets like opioid receptors, toll like receptors, chemokine receptors and purinergic receptors. Some of the targets listed in this table might need further studies (e.g. use of antagonists) to confirm the pharmacological role of these receptors in the modulation of pain hypersensitivities in this model. Nevertheless, they provide important preliminary information on possible involvement of these targets.

Table 1.2. Role of endogenous effectors interacting with their cognate targets that mediate pain and analgesia in the Walker 256 cell- CIBP model in rats.

Receptor	**Ligand**	**Downstream molecule / effector**	***In vivo* pharmacological modulator used**	**Anatomical location of the receptor**	**Outcome of receptor activation**	**Reference/s**
Toll like receptor 4 (TLR4)	Lipopolysaccharide (Saitoh et al., 2004)	TNF- α, IL-1β; IL-6; p38MAPK	Inducible Lentivirus-Mediated small interfering RNA (siRNA) against TLR4; p38MAPK inhibitor- SB203580; TLR4 blocker- lipopolysaccharide Rhodobacter sphaeroides (LPSRS)	Spinal cord	Hypersensitivity	(Pan et al., 2015, Liu et al., 2010, Lan et al., 2010, Mao-Ying et al., 2012, Li et al., 2013, Liu et al., 2013b)
Lysophosphatidic acid 1 (LPA1) receptor	Lysophosphatidic acid	Ras homolog gene family (Rho), Rho Kinase (ROCK)	LPA1 receptor blocker- VPC32183; Rho inhibitor- BoTXC3; ROCK inhibitor- Y27632	DRGs, spinal cord	Hypersensitivity	(Zhao et al., 2010, Wu et al., 2016a)
Erythropoietin-producing human	EphrinB1, EphrinB2	IL-1, IL-6 and TNF-α; Matrix	EphB1 receptor blocker- EphB1-Fc;	Spinal cord	Hypersensitivity	(Dong et al., 2011, Liu et al., 2011)

hepatocellular carcinoma receptor B1 (EphB1)		metalloproteinase (MMP)-2/9	EphB1 receptor blocker- EphB2-Fc			
Epidermal growth factor-like receptor ErbB2	Neuregulin 1 (NRG1)	Akt-1, p38MAPK	ErbB2 inhibitor	Spinal cord	Hypersensitivity	(Jiang et al., 2014)
CX3C chemokine receptor 1 (CX3CR1)	Fractalkine	p38MAPK	Anti-CX3CR1 antibody	Spinal cord	Hypersensitivity	(Hu et al., 2012a, Yin et al., 2010, Cheng et al., 2014)
CC chemokine receptor-2 (CCR2)	Chemokine monocyte chemoattractant protein-1 (MCP-1)	phosphatidylinositol 3-kinase (PI3K), Akt	Anti-MCP-1 antibody; PI3K inhibitor LY294002; exogenous recombinant MCP-1; CCR2 antagonist RS102895	Spinal cord	Hypersensitivity	(Jin et al., 2015, Hu et al., 2012b, Hu et al., 2013, Ren et al., 2015)
Chemokine (C-X-C motif) receptor CXCR3	CXCL9, CXCL10, CXCL11	Akt, ERK 1/2	Recombinant CXCL10 protein, anti-CXCL10 antibody, CXCR3 antagonist	Spinal cord	Hypersensitivity	(Bu et al., 2014, Guan et al., 2015)
CXC motif receptor 4	CXCL12	TNF-α, NF-κB, IL-6 and MAPKs	Anti-CXCL12 neutralizing	Spinal cord	Hypersensitivity	(Shen et al., 2014, Hu et al., 2015b)

(CXCR4)			Antibody, CXCR4 inhibitor- AMD3100, Jun N-terminal Kinase (JNK) inhibitor SP600125, MAPK inhibitor U0126, p38 inhibitor SB503580			
Purinergic P2Y1 receptor (P2Y1R)	Extracellular Adenosine triphosphate (ATP) (Webb et al., 1994)	ERK1/2	P2Y1R antagonist MRS2179	DRGs, spinal cord	Hypersensitivity	(Chen et al., 2012b)
Purinergic P2X3 receptor (P2X3R)	Extracellular ATP	NF-κB	P2X3 receptor antagonist- A-317491	DRGs	Hypersensitivity	(Wu et al., 2012b, Zhou et al., 2015)
Purinergic P2X4 receptor (P2X4R)	Extracellular ATP (North, 2002)	p38MAPK	P2X4R siRNA	Spinal cord	Hypersensitivity	(Jin et al., 2014)
Purinergic P2X7 receptor (P2X7R)	ATP	IL-18, phosphorylated p38	inhibitor of P2X7R- Brilliant Blue G (BBG); RNA interference targeting the P2X7R	Spinal cord	Hypersensitivity	(Huang et al., 2014, Yang et al., 2015)
a3 glycine receptors	Glycine	None	siRNA targeting a3 GlyR, glycine receptor	Spinal cord	Alleviated hypersensitivity	(Zhang et al., 2013)

			antagonist- strychnine			
Adenosine A1 receptor	Adenosine	None	Adenosine A1 receptor antagonist- DPCPX	Spinal cord	Alleviated hypersensitivity	(Chen et al., 2013a)
Protease-activated receptor 2 (PAR2)	Trypsin and trypsin-like proteinases	NF-κB	PAR2 antagonist- FSLLRY-NH2	DRGs, Spinal cord	Hypersensitivity	(Bao et al., 2014a, Bao et al., 2014b)
Protease-activated receptor 4 (PAR4)	Thrombin	None	None	DRGs	Hypersensitivity	(Bao et al., 2015c)
Glucagon like peptide-1 receptor (GLP-1R)	Glucagon like peptide-1 (GLP-1)	Cyclic adenosine monophosphate (cAMP), protein kinase A (PKA)	GLP-1R agonists GLP-1(7–36)	Spinal cord	Alleviated hypersensitivity	(Gong et al., 2014)
Cannabinoid receptor type 2 (CB2)	2-arachidonoylglycerol (Basu et al., 2011)	IL-1β, IL-6, IL-18, TNF-α	CB2-selective antagonist- AM630; CB2-selective agonist- JWH-015	Spinal cord	Alleviated hypersensitivity	(Lu et al., 2015, Lu et al., 2016)
Prokineticin receptor 2 (PKR2)	Bv8 (prokineticin 2)	TNF- α	Bv8 neutralizing antibody	Spinal cord	Hypersensitivity	(Hang et al., 2015b)
Corticotropin-releasing factor (CRF) receptor	Corticotropin-releasing factor (CRF)	None	CRF receptor antagonist (α-helical-CRF)	Spinal cord	Hypersensitivity	(Fan et al., 2015)
μ-opioid receptor	Endomorphin-2	PI3K, PKA	MOR antagonist- β-	Spinal cord	Alleviated	(Chen et al., 2015,

(MOR)			funaltrexamine (β-FNA)		hypersensitivity	Jiang et al., 2016, Yao et al., 2016)
Sigma-1 Receptor	Tryptaminergic trace amines, as well as neuroactive steroids such as dehydroepiandrosterone (DHEA) and pregnenolone (Fontanilla et al., 2009)	Inositol trisphosphate (IP3)	Sigma-1 receptor antagonist -BD1047	Spinal cord	Hypersensitivity	(Zhu et al., 2015a)
N-Methyl-D-Aspartate (NMDA) Receptor	Glutamate, glycine or D-serine (Hogan-Cann and Anderson, 2016)	None	None	DRGs, spinal cord	Hypersensitivity	(Wang et al., 2012b)

1.11.8. Limitations and potential improvement of the model

Like many other preclinical models, this model has short-comings which might hinder translation of promising preclinical data into successful clinical outcomes. There exist at least subtle mechanistic differences in the processing of pain pathways between humans and rodents, which hinders translation of findings in rodents to the humans (Low, 2013). Additionally, there are significant differences in behavioural outcomes and measures of pain in experimental animals and humans (Deuis et al., 2017). Mostly, efficacy profiling in preclinical pain models is driven by a desire to reduce the intensity of pain behavioral readouts. However, a reduction in pain intensity is not always a good measure of the success of a pain treatment (Ballantyne and Sullivan, 2015). Pain is a subjective emotional experience and clinically, a powerful analgesic response can be elicited by placebo treatment (Tuttle et al., 2015, Kaptchuk and Miller, 2015). Hence, responses in experimental animals may not necessarily correlate with the responses expected from humans in the clinical setting. It is also necessary to remember that animals at different ages may process nociception differently (McKelvey et al., 2015) and hence, selection of the correct age of animals that suits the experimental goals may be critical.

Important factors that significantly affect pain research outcomes, such as the sex of the researchers interacting with the animals (Sorge et al., 2014) should not be overlooked in preclinical studies. Sex of the experimental animals or human subjects is a key source of variation in pro-nociceptive signalling (Wiesenfeld-Hallin, 2005, Sorge et al., 2015). In a recent large-scale gene regulatory study (Qu et al., 2015), the main findings were that men and women may require different strategies for treatment of pain, and so sex differences in pain research should not be ignored (Cahill and Aswad, 2015, Brings and Zylka, 2015, Ferrarelli, 2015, Vacca et al., 2016, Vacca et al., 2014, Murphy et al., 2009).

There are many types of breast cancer in the clinical setting (Sharma et al., 2010) with the potential to cause pain, and the extent to which this model provides insights into these various subtypes is currently unclear. It is also important to have standardized protocols when using such preclinical models in order to minimize between-investigator and between-laboratory differences in implementation (Freedman and Gibson, 2015).

1.11.9. Conclusion

Cancer-associated pain, especially intractable bone pain, is very debilitating (Kane et al., 2015). Although this model involving ITI of Walker 256 cells in rats might not exactly mimic the metastatic spread of breast cancer to the axial skeleton in humans (Kurth et al., 2002, Kurth et al.,

2001), it provides insights into the pathobiology and mechanisms of breast CIBP and is hence used widely in experimental research (Liu et al., 2015, Du et al., 2015, Hu et al., 2015a, Lu et al., 2015, Hang et al., 2015b). It might be considered to be a suitable preclinical model for efficacy assessment of novel compounds from discovery programs aimed at identifying drugs with potential to alleviate breast CIBP in humans.

1.12. Summary

It is apparent from the literature that pain can manifest via various mechanisms. Specifically, pain hypersensitivities developed by metastases of breast cancer cells to the axial skeleton is highly complex. Walker 256 breast cancer cell induced bone pain in rats is a useful preclinical tool, however, its efficient usage in research warrants further detailed characterization by various methods including transcriptomic approaches. A better understanding of this model may assist in identifying new mechanisms of pain hypersensitivities associated with breast cancer metastases to the axial skeleton and also in discovery of novel analgesic agents targeted against the complex pathobiology of breast cancer induced bone pain. While several pharmacological targets have been assessed in Walker 256 cell induced bone pain model, novel analgesic drug targets like somatostatin receptor type 4 yet remain unexplored, and it will be interesting to assess the potential of such novel targets in alleviating pain hypersensitivities in this cancer induced bone pain model.

1.13. Hypotheses and Aims

1.13.1. Hypotheses

1.13.1.1. The Walker 256 breast cancer cell induced bone pain model in rats closely mimics the pathophysiology of breast cancer induced bone pain in patients and is well suited for probing the mechanisms of action and assessing new analgesic drug candidates for alleviating this condition.

1.13.1.2. Induction of Walker 256 breast cancer cell induced bone pain in rats is associated with differential expression of genes that underpin the pathophysiology of pain, relative to sham-rats.

1.13.1.3. The somatostatin receptor – 4 is a novel pharmacological target mediating analgesia in a rat model of Walker 256 breast cancer cell induced bone pain.

1.13.2. Aims

1.13.2.1. To establish, optimize and characterize the Walker 256 breast cancer cell induced bone pain model in rats using behavioral, radiological, histological, immunohistochemical and pharmacological methods.

1.13.2.2. To perform transcriptomic characterization of the Walker 256 breast cancer cell induced bone pain model in rats.

1.13.2.3. To assess the analgesic efficacy of J-2156, a somatostatin receptor– 4 agonist, in a rat model of Walker 256 breast cancer cell induced bone pain.

Chapter 2

Optimization and *in vivo* profiling of a refined rat model of Walker 256 breast cancer cell-induced bone pain using behavioral, radiological, histological, immunohistochemical and pharmacological methods

2.1. Foreword

As described in Chapter 1, there are several factors like animal-based, cancer cell-based, etcetera that can affect the nature of pain hypersensitivities developed in the Walker 256 breast cancer cell-induced bone pain model in rats. Hence, I thoroughly optimized, validated and characterized this model using various techniques. I am thankful to Dr John Mackie (Specialist Veterinary Pathologist, Brisbane, Australia) and Dr Karine Mardon (NIF Facility Fellow and Molecular Imaging Facility Manager, The Centre for Advanced Imaging, The University of Queensland, Brisbane, Australia) for their expert assistance in histopathological analysis and radiological analysis of tibiae, respectively.

This chapter has been adopted with permission from a previously published research article that arose from this thesis (Shenoy et al., 2017), published by Frontiers in Pharmacology (http://journal.frontiersin.org/article/10.3389/fphar.2017.00442/full)

2.2. Introduction

Unrelenting pain in patients with advanced cancer significantly reduces quality of life (Bu et al., 2014). Metastases of cancer cells to the skeleton often causes pain in breast cancer patients (Bu et al., 2014) with over 70% of patients with terminal breast cancer having bony metastases (Coleman, 2006, Currie et al., 2013, Cleeland et al., 2016). Bony metastases are often asymptomatic initially and are usually diagnosed following the occurrence of bone pain or skeletal complications involving damage to the bone structure (Cleeland et al., 2016). In the later stages of metastatic breast cancer, bone pain can become excruciating making it very difficult to treat (Kane et al., 2015). Knowledge on the precise mechanisms by which breast and other cancers metastasize to bone and produce pain is incomplete (Zhu et al., 2015b). Primary breast tumours at the original site causes less or no pain, yet once these cells have metastasized to bone, patients may suffer excruciating pain (Lozano-Ondoua et al., 2013b). In the clinical setting, non-steroidal anti-inflammatory drugs (NSAIDs), strong opioids, medications that inhibit the activity of osteoclasts

like bisphosphonates, bone targeted monoclonal antibodies, radiation therapy and surgical management are the mainstay of pharmacotherapeutic treatment of breast cancer-induced bone pain (BCIBP) (Kane et al., 2015, Milgrom et al., 2017). A major challenge involved in understanding the interplay of mechanisms underpinning the pathobiology of BCIBP is establishment of a suitable rodent model which exhibits characteristics similar to those of BCIBP in humans (Slosky et al., 2015). Until the late twentieth century, cancer-induced bone pain (CIBP) models in animals were initiated by systemically injecting the cancer cells, causing poor animal health due to tumour in the liver and lungs as well as random and multi-sited bone deposits (Urch, 2004). Subsequently, models involving local injection of breast cancer cells within a single bone have proven successful, avoiding the spread of tumours systemically to the highly perfused organs or neighbouring soft tissue (Schwei et al., 1999).

The unique contribution of our study described herein is establishment of a clinically relevant, optimised Wistar Han female rat model of BCIBP that we have extensively characterised using behavioural, pharmacological, radiological (micro-computed tomography (µCT)), histological and immunohistochemical methods. Our findings show for the first time, that the severity and nature of mechanical pain hypersensitivity behaviours developed in the hindpaws of female Wistar Han rats depends on the initial number of Walker 256 (W256) cells given by unilateral intra-tibial injection (ITI). Additionally, we have thoroughly assessed and documented general animal health in a temporal manner in the same animals for up to 66 days post-ITI. A role for opioid-sensitive mechanisms in the spontaneous resolution of pain hypersensitivities observed at later stages of the model in the continued presence of bone cancer disease was investigated for the first time in this model. To the best of our knowledge, our pharmacological data are the first 'back translation' profiling of this rat model of BCIBP, showing analgesic efficacy of single bolus doses of clinically available analgesic drugs (morphine, meloxicam) and adjuvant agents (gabapentin, amitriptyline) used to treat various types of chronic pain.

2.3. Material and Methods

2.3.1. Drugs, chemicals and reagents

Morphine (DBL^{TM} morphine sulfate injection BP- 30 mg in 1mL) was procured from Hospira Pty Ltd (Melbourne, Australia). Gabapentin was kindly provided by Dr Ben Ross, School of Pharmacy, The University of Queensland (Brisbane, Australia). Amitriptyline (amitriptyline hydrochloride), meloxicam (meloxicam sodium salt hydrate), naloxone (naloxone hydrochloride dihydrate), Triton^{TM} X-100, Tween 20, paraformaldehyde (PFA) and bovine serum albumin (BSA) were

procured from Sigma-Aldrich® (NSW, Australia). Isoflurane (IsoFlo™) was procured from Abbott Australasia Pty Ltd (NSW, Australia). Medical oxygen and medical carbon dioxide were procured from Coregas Pty Ltd (NSW, Australia). Triple antibiotic powder (Tricin®) was procured from Jurox Pty Ltd (NSW, Australia). Benzylpenicillin (BenPen™, benzylpenicillin sodium for injection) was procured from CSL Ltd (VIC, Australia). Pentobarbitone (Lethabarb®, pentobarbitone sodium) was procured from Virbac (Australia) Pty Ltd (NSW, Australia). Eye ointment (Refresh Night Time®) was purchased from Allergan Australia Pty Ltd (NSW, Australia). Ethylenediaminetetraacetic Acid, disodium salt, dihydrate (UltraPure™ EDTA), 4',6-diamidino-2-phenylindole, dihydrochloride (DAPI), Prolong® Gold antifade reagent, phosphate-buffered saline (PBS), medium 199 (1X), horse serum, Dulbecco's phosphate-buffered saline (DPBS, 1X) and 0.25% trypsin-EDTA (1X) were purchased from Thermo Fisher Scientific Australia Pty Ltd (VIC, Australia). Normal goat serum (NGS) was purchased from Cell Signaling Technology® (MA, USA). Tissue-Tek® O.C.T. Compound was procured from ProSciTech Pty Ltd (QLD, Australia). Water for injection BP was purchased from Pfizer Australia Pty Ltd (NSW, Australia). 10 % neutral-buffered formalin (NBF) was purchased from Australian Chemical Reagents (QLD, Australia). Methanol and acetone were purchased from EMD Millipore Corporation (MA, USA).

2.3.2. Cell culture

W256 breast cancer cells [LLC-WRC 256 (ATCC® CCL-38™)] at passage number 290 were procured from the American Type Culture Collection (ATCC; VA, USA). The cells were cultured and passaged following the ATCC guidelines. Cells within passage number 292-319 were used in the present study. To summarize, the cells were thawed from the frozen stocks and cultured in 75cm^2 Cellstar® flasks (Greiner bio-one) at 37 ºC (5% CO_2: 95% atmospheric air) in 20 mL of Medium 199 (1X) supplemented with 5% horse serum. For detachment of cells, they were initially rinsed gently with 3 mL of DPBS (1X), followed by trypsinization using 2 mL of 0.25% trypsin-EDTA (1X). The cells thus detached were collected by centrifugation with 8 mL of medium for 4 min at 200 ×g. The resultant supernatant was discarded, the pellet was re-suspended in 3 mL of DPBS and cell counting was performed using a hemocytometer. After re-centrifuging the pellet for 4 min at 200 ×g, the cells obtained were suspended in DPBS in the required concentration (4×10^3, 1.5×10^4, 4×10^4, 1.5×10^5 and 4×10^5 cells/10 µL DPBS). Heat-killed (HK) W256 cells were prepared in the same way as the live cells but with an additional step involving heating for 15 min at 90 °C.

2.3.3. Animals

Female Wistar Han (HsdBrlHan) rats used in these experiments were procured from the Herston Medical Research Centre (Brisbane, Australia) of The University of Queensland. On arrival at our

facility, rats were approximately 3-4 weeks of age with a body weight in the range of ~50-70 g. Rats were caged in groups of two to three in a room with controlled temperature (23 °C ± 2 °C) and a 12 h/12 h light–dark cycle. Standard rodent chow (Specialty Feeds, Western Australia, Australia) and tap water were available to the rats *ad libitum*. Kimwipes (Kimberly-Clark Professional, New South Wales, Australia) and Rat Chewsticks (Able Scientific, Western Australia, Australia) were provided as environmental enrichment. Rats were subject to acclimatization for at least 3 days prior to initiating experimentation. All the experiments herein were performed in the light phase. Approval of experimental procedures was obtained from the Animal Ethics Committee of The University of Queensland (QLD, Australia). The experiments were undertaken in accordance with the requirements of the Australia Code of Practice for the Care and Use of Animals for Scientific Purposes (8th edition, 2013).

2.3.4. Surgical procedure

Unilateral intra-tibial injections were performed in a manner similar to that described by others (Mao-Ying et al., 2006, Muralidharan et al., 2013) but with some modifications. Briefly, rats (~80–120 g) were anesthetized deeply with 3% isoflurane delivered in oxygen. Eye ointment was used to avoid drying of eyes during the surgical procedure. Benzylpenicillin injection was subcutaneously administered at a dose of 60 mg per rat. A unilateral rostro-caudal incision of approximately 1 cm in length was created on the upper medial half of the lower left hind limb. After the exposure of the tibia, using a 23-gauge needle, the bone was pierced medial to the tibial tuberosity below the knee joint. A 10 µL injection containing W256 cells in the required number, or HK cells (sham-rats) or DPBS (control rats) was administered into the bone cavity with a Hamilton® syringe (80508:705SN 50 µL SYR SPECIAL (22 /2″/4), NV, USA). In all of the experiments (except experiment 4), at least one rat received an ITI of HK cells as a control for lack of pain hypersensitivity, including the experiments designed for pharmacological testing (Supplementary Table 2.1). The bone was immediately sealed using Ethicon^{TM} W810 bone wax (Johnson-Johnson International, Diegem, Belgium). The muscles and the skin were stitched in place with non-absorbable USP 5/0 sutures Dysilk® suture (Dynek Pty Ltd, SA, Australia). Topical antibiotic powder was then dusted on the wound. The hindpaw of the injected limb is termed as the ‘ipsilateral’ hindpaw, while that of the non-injected limb is termed as the ‘contralateral’ hindpaw. After the surgery, rats were closely monitored. The general animal health and their body weights were regularly assessed throughout the experimental period.

2.3.5. Animal groups and experimental timelines

The number of animals involved in individual groups along with the details of each of the experiments performed together with their corresponding durations are shown in Figure 2.1. For the ease of editing and typesetting the figure, clinical observations have not been denoted for experiments 2 to 16 in Figure 2.1, although they were performed. Baseline pain behavioural tests prior to surgeries / ITI (referred as day 0) were performed on rats from all the experiments (Supplementary Table 2.2). To comprehensively characterise the model, one group of rats received an ITI of DPBS and another group (naïve) of animals did not undergo surgery or ITI (experiment 4).

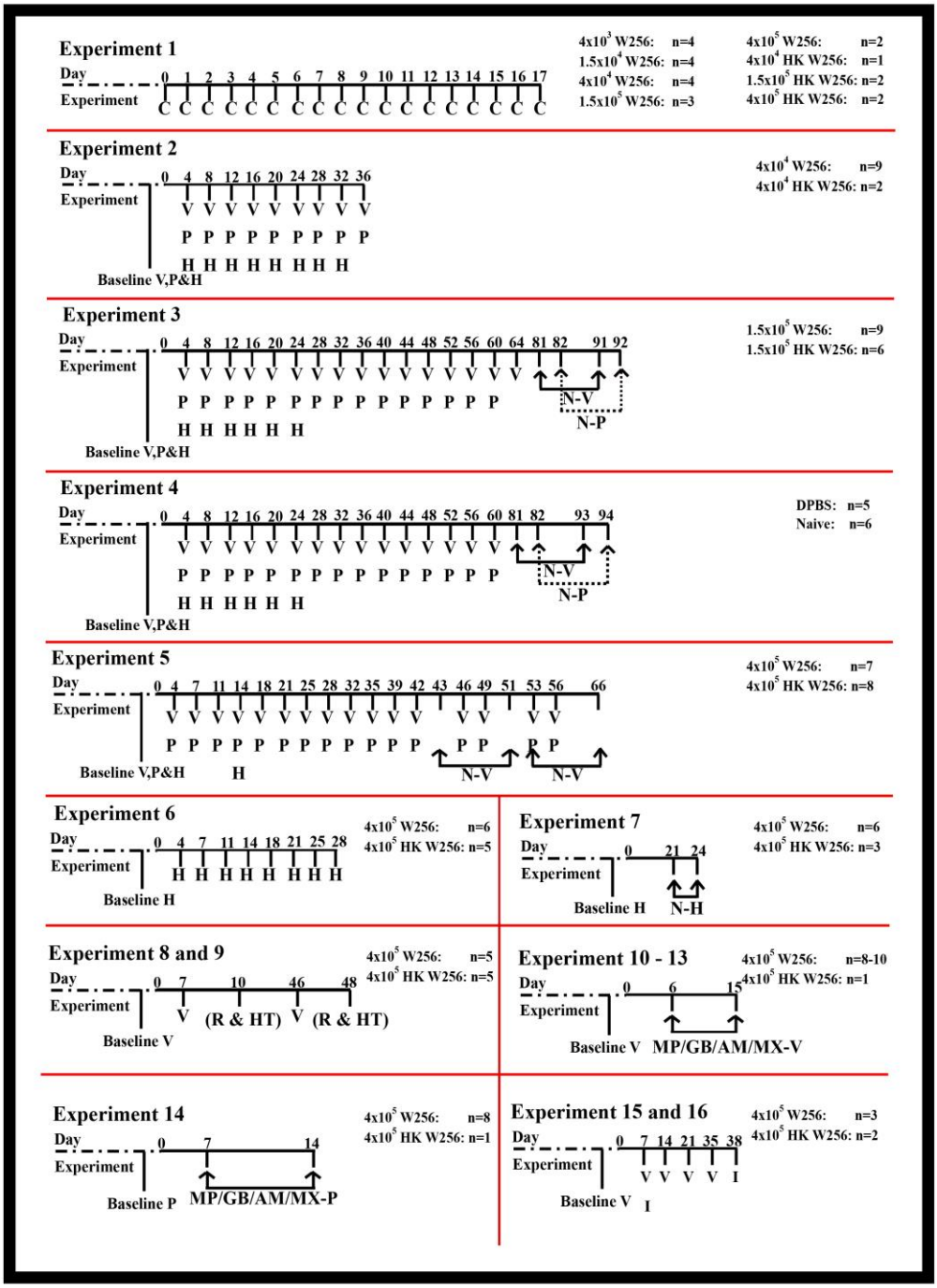

Figure 2.1. Timeline of assessments performed in individual experiments. AM, amitriptyline; C, clinical observations; GB, gabapentin; H, Hargreaves testing; HK, heat-killed; HT, histological assessment; I, immunohistochemical assessment; MP, morphine; MX, meloxicam; MP/GB/AM/MX-P, paw pressure testing after drug injection; MP/GB/AM/MX-V, von Frey testing after drug injection; N-H, Hargreaves testing after naloxone injection; N-P, paw pressure testing after naloxone injection; N-V, von Frey testing after naloxone injection; P, paw pressure testing; R, radiological assessment; V, von Frey testing; W256, Walker 256 cells.

2.3.6. General Health Characteristics

The primary aim of Experiment 1 was to perform clinical observations and document temporal changes in general health along with body weights for the study duration. Animal welfare checks for mortality, morbidity and food and water levels were performed twice daily until the study completion. Body weights and clinical observations (general health parameters) were generally monitored at least once per week until the study completion in all the experiments. The observation method and the clinical parameters / symptoms were obtained and modified from the previously established standard methods (Moser and MacPhail, 1990, Haggerty, 1991) and Guidance Document on the Recognition, Assessment, and Use of Clinical Signs as Humane Endpoints for Experimental Animals Used in Safety Evaluation (OECD Environmental Health and Safety Publications Series on Testing and Assessment No. 19, 2000). Briefly, each rat in the study was carefully examined for their appearance, clonic movements, tonic movements, gait, stereotypy and bizarre behaviour, if any. Assessment of appearance included parameters such as diarrhoea, piloerection, salivation, palpebral closure, lacrimation, lack of grooming, bleeding from orifices and moribundity. Assessment of clonic movements included parameters such as wet dog shakes, clonic convulsions, myoclonic jerks, severe or whole body tremors, mild tremors, quivers of limbs, skin, ears or head, repetitive movements of jaws and mouth. Assessment of tonic movements included severe clonic and / or tonic convulsions causing dyspnoea, postictal depression or death, jumps with all feet leaving the surface, rigid forward extension of head and body, head and body rigidly arched backward and contraction of extensors. Assessment of gait included lameness, body drags, tiptoe walk, dragging or extension of forelimbs or inability to support weight, feet markedly point outward from the body, exaggerated or over-compensated movements of hind limbs, excessive sway, rocks or lurches and ataxia. Assessment of stereotypy involved repetitive sniffing, pacing, stereotypic grooming and circling. Assessment of bizarre behaviour involved writhing or flopping, retropulsion, straub tail, self-mutilation and head weaving amongst others. The form used for recording clinical observations in experimental rats is shown in Supplementary Figure 2.1.

2.3.7. Pain behavioral studies

2.3.7.1. Assessment of mechanical allodynia in the hindpaws

Assessment of development of mechanical allodynia (hypersensitivity to applied non-noxious mechanical stimuli) in both hindpaws was performed using calibrated von Frey filaments (Stoelting Co., Wood Dale, IL, USA) by determining the lowest mechanical threshold that elicits a paw withdrawal response (Ren, 1999). Rats were individually positioned into wire mesh cages and they were acclimatized for around 15 to 30 min before von Frey testing. Until the filaments buckled

slightly, they were physically applied on the plantar surface of the hindpaws. Absence of a response after 3 s suggested the use of a higher filament in the ascending order (2, 4, 6, 8, 10, 12, 14, 16, 18, and 20 g) until the response was observed. By contrast, a withdrawal response observed within 3 s suggested the use of a filament evoking a lower force than before. Testing was initiated with a 6 g filament, and the filaments were subsequently changed to obtain an increased or decreased force based upon the earlier response. The baseline paw withdrawal thresholds (PWTs) for individual hindpaws were the mean of three observed readings with an interval of 5 min between two successive readings. For pharmacological testing of compounds at regular intervals over a 3-h post-dosing period, the starting filament at each time point was dependent upon the previous reading. Rats with PWTs $\leq$ 6 g in the ipsilateral hindpaw were defined as having fully developed mechanical allodynia. All of the von Frey assessments were performed in a blinded manner.

2.3.7.2. Assessment of mechanical hyperalgesia in the hindpaws

Temporal development of mechanical hyperalgesia (hypersensitivity to applied noxious mechanical stimuli) in the bilateral hindpaws was determined using an Analgesy-meter (Ugo Basile, Italy). The mechanical force required to elicit withdrawal of each of the hindpaws (paw pressure thresholds (PPTs)) of the animal was measured (Randall et al., 1957). Specifically, each hindpaw was positioned on a small plinth under a rounded cone-shaped pusher which avoids tissue damage. Depressing the pedal-switch started the mechanism of exertion of force. As soon as the rat struggled, the pedal was immediately released and the applied force was recorded. A cut-off of 200 g maximum was used to avoid hindpaw injury. Baseline PPTs were the mean of three observations for a hindpaw with at interval of at least 5-min between consecutive assessments. Rats with ipsilateral PPTs $\leq$ 80 g were considered to have fully developed mechanical hyperalgesia. All of the PPT assessments were performed in a blinded manner.

2.3.7.3. Assessment of thermal hyperalgesia in the hindpaws

Development of thermal hyperalgesia (hypersensitivity to applied noxious heat stimuli) in the hindpaws was studied using the plantar test / Hargreaves apparatus (Ugo Basile, Italy) to assess the time required to elicit a withdraw response (paw thermal thresholds (PTTs)) to an applied noxious heat stimulus (Hargreaves et al., 1988). Rats were individually positioned in Perspex chambers having a glass floor and acclimatized for at least 30 min before performing the test. A noxious heat stimulus (infrared (IR) intensity value-30; 135 mW/cm^2) was radiated to the plantar surface of the hindpaws and the PTT values were noted. A cut-off time of a maximum of 30 s was used to avoid damage to the tissue. Baseline PTTs were the mean of three observations for a hindpaw with an

interval of 5-min between consecutive tests. All of the PTT assessments were performed in a blinded manner.

2.3.7.4. Test compound administration

Animals were dosed by the first person and assessments were performed by the second person to ensure that study blinding was not compromised. Each rat received a maximum of five intraperitoneal (i.p.) or subcutaneous (s.c.) doses of test compounds or vehicle with at least 2 days of 'washout' between consecutive doses. Test compound dosing solutions in the present work were prepared using Water for injection BP as the vehicle. Doses of all test compounds are expressed in terms of their water-soluble salts similar to previous studies from our laboratory (Varamini et al., 2012, Han et al., 2014a, Kuo et al., 2015, Smith et al., 2013, South et al., 2009) and by others (Maguire et al., 2013, Samal et al., 2015, Negus et al., 2012).

2.3.7.4.1. Effect of naloxone on pain phenotypes

Rats from experiments 3, 4, 5 and 7 were given single bolus doses of naloxone (15 mg/kg s.c.) or vehicle after the apparent hypersensitivity of the hindpaws to applied mechanical stimuli had resolved. After injecting naloxone or vehicle, PWTs, PPTs or PTTs were assessed in the hindpaws at pre-defined intervals during a 3 hour period post-dosing.

2.3.7.4.2. Anti-allodynic effect of morphine, gabapentin, amitriptyline and meloxicam

Rats having fully developed mechanical allodynia in their ipsilateral hindpaws were administered single bolus doses of morphine (0.3, 1 and 3 mg/kg s.c.), gabapentin (30, 70 and 100 mg/kg i.p.), amitriptyline (3, 10 and 30 mg/kg i.p.) and meloxicam (2.5, 5.0 and 7.5 mg/kg i.p.) or vehicle. PWTs were measured in both hindpaws immediately pre-dose and at 0.25, 0.5, 0.75, 1.0, 1.25, 1.5, 2 and 3 h post-dosing.

2.3.7.4.3. Anti-hyperalgesic effect of morphine, gabapentin, amitriptyline and meloxicam

PPTs were measured in both hindpaws of rats with fully developed mechanical hyperalgesia following administration of single bolus doses of morphine (3 mg/kg s.c.), gabapentin (100 mg/kg i.p.), amitriptyline (30 mg/kg i.p.), meloxicam (7.5 mg/kg i.p.) or vehicle. PPTs were assessed immediately before dosing and at 0.25, 0.5, 0.75, 1.0, 1.25, 1.5, 2 and 3 h post-dosing.

2.3.8. Tibial bone µCT scan

Rats (ITI of 4 x 10^5 W256 cells, n=3; ITI of 4 x 10^5 HK W256 cells, n=3) from Experiments 8 and 9 were euthanized on day 10 and day 48 with an overdose of pentobarbitone sodium (1 mL/kg of

325.73 g/L; Lethabarb®). The tibiae were collected and fixed in 10 % NBF for at least 2 days. Micro-CT scanning was conducted using a preclinical Inveon Multimodality PET/CT Scanner (Siemens Medical Soln., TN, USA) at the Centre for Advanced Imaging (CAI) at The University of Queensland. The μ-CT images were obtained using Inveon Acquisition Workstation software (IAW version 2.0, Siemens). The X-ray source voltage was set to 80 kV and the current to 250 μA. The scans were conducted using 360° rotation with 360 rotation steps using a medium–high magnification and with a binning factor of 2. The exposure time was 2300 ms and the CT scanning process totally took approximately 60 min. The μ-CT images were reconstructed using a Feldkamp reconstruction software (Siemens) resulting in an isotropic voxel dimension of 27.9 μm. The CT data were calibrated in Hounsfield units (HU) defined such that the water and air have 0 and 1000 HU values, respectively. The images were analysed using Inveon Research Workstation software (IRW version 4.1, Siemens) to measure the bone volume / total volume (BV/TV ratio), trabecular thickness ($T_b.T_h$), trabecular spacing ($T_b.S_p$) and trabecular number ($T_b.N$) in the proximal diaphyseal regions of the ipsilateral tibial bones, as described previously (Muralidharan et al., 2013).

2.3.9. Tibial bone histology

Rats (ITI of 4 x 10^5 W256 cells, n=3; ITI of 4 x 10^5 HK W256 cells, n=3) from Experiments 8 and 9 were euthanized on day 10 and day 48 with pentobarbitone sodium (1 mL/kg of 325.73 g/L; Lethabarb®). Tibiae were harvested and fixed by immersing in 10 % neutral-buffered formalin (Liu et al., 2016, Jin et al., 2016) for at least 2 days. These tibiae were then immersed in 15 % w/v solution of UltraPure™ EDTA in phosphate buffer for at least 4 weeks, with the EDTA solution being changed twice per week (Hald et al., 2009). The soft decalcified bones were then rinsed, and after dehydration they were embedded in paraffin and cut into 4 μm cross-sections with a RM2235 rotary microtome (Leica Microsystems, Wetzlar, Germany) at the QIMR Berghofer Medical Research Institute, Brisbane, Australia. Sections of proximal diaphyseal regions of ipsilateral tibiae were mounted on Uber slides (InstrumeC Pty Ltd, Vic, Australia) and stained using hematoxylin and eosin (H&E) (Mao-Ying et al., 2006) to assess histological changes in the tibial structure.

2.3.10. Immunocytochemistry of W256 cells: Cytokeratin 18

W256 cells were seeded onto sterile coverslips in 24 well-plates. Once the cells were 80-90 % confluent, the culture medium was aspirated and the cells were briefly rinsed using PBS. The cells were fixed with ice-cold methanol (4 min at -20 °C). The fixing agent was aspirated and the cells were washed with 0.2 % Tween 20 and 0.1 % Triton™ X-100 in PBS for 10 min. The fixed cells were subsequently blocked for 30 min with 1 % BSA in PBS at 23 °C ± 2 °C. Anti-Cytokeratin 18

antibody [C04] (Alexa Fluor® 488) ab187573 (1:20 dilution, Abcam, VIC, Australia), prepared in 1 % BSA in PBS, was added to the wells containing the coverslips and the plate was incubated at 37 ^{o}C for 3 hours in the dark (~0.002 lux). The antibody solution in the wells was then aspirated and the cells were rinsed with PBS thrice for 5 minutes each. A 0.5 µg/mL solution of DAPI was added and the cells were incubated for 5-10 min. The DAPI solution was then aspirated and the cells were washed with PBS. Next, the processed cells on coverslips were mounted on Superfrost® Plus slides (Lomb Scientific Pty Ltd., NSW, Australia) using Prolong® Gold antifade reagent. The mounted slides were allowed to dry and stabilise in the dark at 4-8 ^{o}C overnight, prior to image capture using a fluorescence microscope as mentioned in section 2.3.12.

To validate the above results of immunocytochemical staining, anti-Cytokeratin 18 antibody [C-04] ab668 (1:100 dilution, Abcam, VIC, Australia), which was used in both immunocytochemistry and immunohistochemistry applications in other works (Leong et al., 2008, Wang et al., 2009b), was used as a second confirmatory antibody. The procedure for staining of cells with the second antibody was similar to that of the previous antibody as described above. However, after the primary antibody treatment, the cells were incubated with Goat anti-Mouse IgG (H+L) Secondary Antibody, Alexa Fluor 546 A-11030 (1:500 dilution, Thermo Fisher Scientific, IL, USA) in PBS with 0.1 % Tween 20 (PBST) for around 2 hours in the dark (~0.002 lux) at 23 °C ± 2 °C, followed by 2 × 5 min washes with PBST and 1 x 5 min wash with PBS before treatment with DAPI.

2.3.11. Tibial bone immunohistochemistry

Rats (ITI of 4 x 10^5 W256 cells, n=3; ITI of 4 x 10^5 HK W256 cells, n=2) from experiment 15 and 16 were euthanized on days 7 and 38 with an overdose of pentobarbitone and then perfusion-fixed using 4% PFA. The tibiae were collected and further post-fixed with 4 % PFA. The tibiae were stored in 10 % NBF for 2 days at 4-8 ^{o}C. These tibiae were then decalcified in a manner similar to that described in section 2.3.9. The decalcified bones were allowed to post-fix for 2 h in 4% PFA solution (4-8 °C), cryoprotected successively in 15% sucrose/PBS and 30% sucrose/PBS at 4-8 °C and subsequently placed in a 1:1 mixture of OCT:30% sucrose/PBS at 4-8 °C, after which they were freeze-mounted in Tissue-Tek® O.C.T. Compound. Frozen tibial longitudinal sections (7 µm thick) were cut using a Cryostar NX70, (Thermo Fisher Scientific, Waltham, USA) and mounted on Uber Plus charged slides (InstrumeC, Vic, Australia). In order to identify the tumor infiltration by using immunohistochemistry, tibial sections were washed with a 1X PBS (pH 7.4) solution (3 × 5 min), followed by blocking with 10% NGS containing 0.3 % Triton™ X-100 in PBS for 1-2 hour at room temperature. The sections were allowed to incubate with anti-Cytokeratin 18 antibody [C04] (Alexa Fluor® 488) ab187573 (1:20 dilution) diluted in 2 % NGS in PBST overnight at 4-8 °C.

This was followed by 2 × 5 min washes using PBST and 1 x 5 min wash with PBS. The sections were allowed to incubate with DAPI for 5-10 min and subsequently washed with PBS (2 x 5 min) and the cover-slips were placed along with Prolong® Gold antifade reagent.

Similar to the procedure outlined in section 2.3.10, anti-Cytokeratin 18 antibody [C-04] ab668 (1:100 dilution) was also used to validate the results of immunohistochemical staining. The procedure for staining of tibial sections with the second antibody was similar to that of the previous antibody described above. However, the sections were allowed to incubate with primary antibody overnight at 23 °C ± 2 °C, and then incubated with Goat anti-Mouse IgG (H+L) Secondary Antibody, Alexa Fluor 546 A-11030 (1:600 dilution) in PBST for 2 hours in the dark (~0.002 lux) at 23 °C ± 2 °C. This was followed by 2 × 5 min washes using PBST and 1 x 5 min wash with PBS and the sections were subsequently treated with DAPI and mounted as described above.

2.3.12. Image acquisition

For the histology experiments, images were captured with an Aperio ScanScope XT system (Leica Biosystems, Nussloch, Germany) located at the School of Biomedical Sciences, The University of Queensland and processed using Aperio ImageScope v12.3.0.5056 software (Leica Biosystems). Images from immunocytochemistry and immunohistochemistry experiments were captured with an Axioskop 40 microscope (Carl Zeiss, Göttingen, Germany) attached to an Axiocam MRm camera (Carl Zeiss) and processed using AxioVision Rel. v4.8 software (Carl Zeiss). For the immunocytochemistry and immunohistochemistry experiments, images were acquired at a fixed exposure time, optimised using auto-exposure settings of AxioVision Rel. v4.8 software and by using filters suitable for the fluorophore of the secondary antibody. Immunohistochemistry based images from at least 3-4 non-adjacent sections per rat were acquired randomly.

2.3.13. Data analysis

All the values have been expressed as mean $\pm$ standard error of the mean (SEM). For treatments having $n \leq 2$, the values are expressed as mean or absolute value, without calculating the error. Generation of graphs and data processing were done using the GraphPad Prism™ (v7.00) software package. The PWT values of rats administered single bolus doses of test compound or vehicle were normalized by subtracting the pre-dosing baseline values so as to obtain ΔPWT values as follows:

$$\Delta\text{PWT value} = (\text{postdosing PWT}) - (\text{Average predosing baseline PWT})$$

Area under the curve (AUC) for ΔPWT versus time curves (ΔPWT AUC values) were calculated using trapezoidal integration to determine the extent and duration of action of test compounds for

relief of allodynia. ΔPWT AUC values were then converted into a percentage of the maximum possible ΔPWT AUC (% MAX ΔPWT AUC) with the following formula:

$$\%\text{MAX } \Delta\text{PWT AUC} = \frac{\Delta\text{PWT AUC}}{\text{Maximum } \Delta\text{PWT AUC}} \text{ x } 100$$

Dose–response curves were generated by plotting mean (±SEM) % MAX ΔPWT AUC values versus log dose of each of the test compounds. The PPT data and the naloxone data were processed in a similar way as described above. Non-linear regression (GraphPad Prism™ v7.00) was used to determine the ED_{50} values for each drug treatment against mechanical allodynia in the ipsilateral as well as the contralateral hindpaws.

2.3.14. Statistical analysis

Statistical analyses were performed using the GraphPad Prism™ v7.00 software package. The criterion of statistical significance was $p \leq 0.05$. Two-way analysis of variance (ANOVA) followed by the Bonferroni test was used to analyse between-group differences in body weights, behavioural data, pharmacological data and tibial bone morphometric changes. The Mann-Whitney test was used to assess between group body weight differences with missing intermediate values and to compare differences in ΔPPT AUC values for each test compound- and vehicle-treated group. One-way ANOVA followed by the Dunnett's test was used in order to compare differences in ΔPWT AUC values for each test compound- and vehicle-treated groups. The unpaired t test was used in order to compare the extent and duration of naloxone induced rescue of the pain phenotype. For statistical comparisons using ANOVA, F values were reported along with their associated degrees of freedom (treatment, time, interaction and residual). For two-way ANOVA, F values were expressed as F(df of treatment, time, interaction/residual). Whereas, for one-way ANOVA, F values were expressed as F(df of treatment, residual).

2.4. Results

2.4.1. General Health Characteristics

In terms of body weight, there were no significant differences between animals given an ITI of W256 and HK W256 cells in experiment 1 ($F_{(7, 17, 119/238)} = 1.2, 1125, 1.5$; $p > 0.05$), experiment 2 ($F_{(1, 43, 43/387)} = 2.2, 619.7, 0.9$; $p > 0.05$) (Figure 2.2A), experiment 3 ($p > 0.05$) (Figure 2.2B), experiment 5 ($p > 0.05$) (Figure 2.2C), experiment 7 ($F_{(1, 14, 14/98)} = 0.7, 766.6, 1.3$; $p > 0.05$), experiment 8 ($F_{(1, 8, 18/64)} = 0.4, 400.8, 2.7$; $p > 0.05$), experiment 9 ($F_{(1, 11, 11/88)} = 1.1, 364, 0.05$; $p > 0.05$), experiment 10 ($F_{(1, 8, 8/64)} = 0.3, 180.6, 2.8$; $p > 0.05$), experiment 11 ($F_{(1, 8, 8/64)} = 1.0, 314.8,$

1.6; $p > 0.05$), experiment 12 ($F_{(1, 7, 7/63)} = 0.5, 66.0, 0.2$; $p > 0.05$), experiment 13 ($F_{(1, 7, 7/49)} = 1.1, 195.4, 0.8$; $p > 0.05$) and experiment 14 ($F_{(1, 9, 9/63)} = 0.7, 141.5, 1.6$; $p > 0.05$). Additionally, there were no significant differences in between body weights of animals given an ITI of DPBS and age-matched control female Wistar Han rats in experiment 4 ($p > 0.05$). Although there were slight differences between body weights of rats administered W256 and HK W256 cells in experiment 6 ($F_{(1, 12, 12/108)} = 8.9, 508.1, 3.1$; $p \leq 0.05$), experiment 15 ($F_{(1, 6, 6/18)} = 11.9, 84.1, 1.3$; $p \leq 0.05$) and experiment 16 ($F_{(1, 11, 11/33)} = 62.6, 314.2, 0.6$; $p \leq 0.05$) at some time points, these were either due to differences in initial body weights or due to non-cancer factors. Importantly, there were consistent gains in the body weights of all animals throughout the experiments (Supplementary Figure 2.2).

A total of 173 rats were used in this study, out of which 9 rats (5%) were found to have health-related issues and of these 3 (1.7%) were euthanized for ethical reasons as outlined below. One rat from experiment 1 given an ITI of 4×10^3 W256 cells had a slight tumour like appearance in the bone near the injection site. Nevertheless, the overall health of the animal was satisfactory and no other complications were observed. Another rat from experiment 1 given an ITI of 1.5×10^5 W256 cells had a mild infection at the sight of surgery with visible pus exudate. Under anaesthesia, the infected site was cleaned and topical antibiotic powder was applied, followed by a subcutaneous injection of benzylpenicillin at a dose of 60 mg. Subsequently, the infection resolved. One rat given an ITI of 4×10^3 W256 cells, two rats given an ITI of 1.5×10^5 W256 cells and one rat given an ITI of 4×10^5 HK W256 cells from experiment 1 had mild swelling at the injection site, which resolved spontaneously. One rat from experiment 4 given an ITI of DPBS was excluded from the study and euthanized due to lack of normal body weight gain due to a crooked incisor. One rat given an ITI of 4×10^5 W256 cells from experiment 5 was excluded and euthanized due to the presence of a large external tumour growth on the injected tibia. One rat from experiment 6 given an ITI of 4×10^5 W256 cells was excluded and euthanized due to lethargic behaviour and low body weight; upon post-mortem investigation, a large metastatic lesion was observed on the intestine.

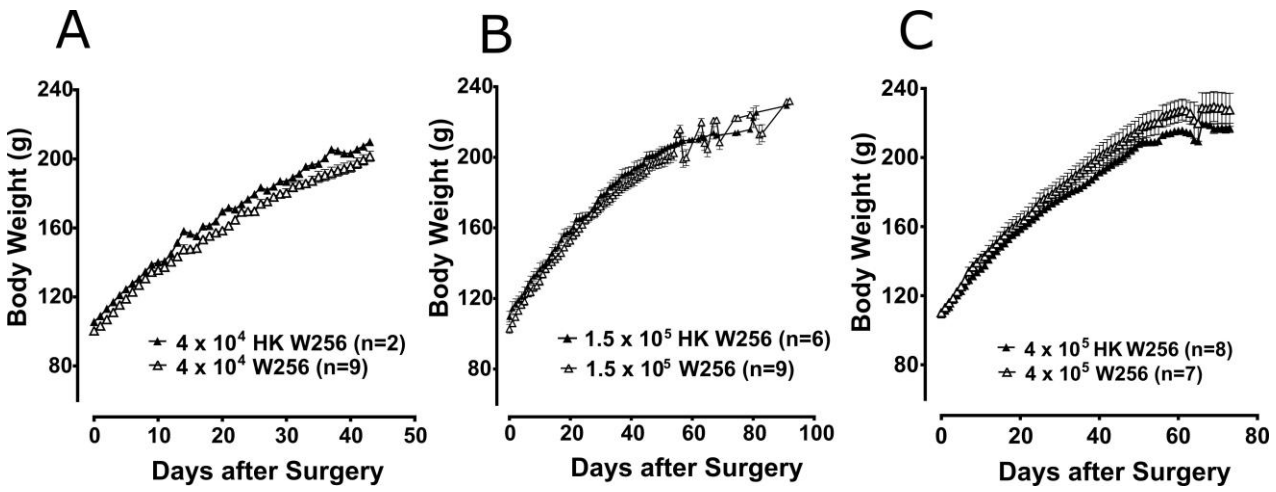

Figure 2.2. Body weight of rats from individual experiments. Panels in the figure show mean (±SEM) body weight of rats from (A) experiment 2, (B) experiment 3 and (C) experiment 5. HK, heat-killed; W256, Walker 256 cells. There were no statistically significant differences in body weight between any treatment groups ($p>0.05$; experiment 2, Two-way ANOVA, *posthoc* Bonferroni test; experiment 3 and 5, Mann-Whitney test).

2.4.2. Assessment of mechanical allodynia in the hindpaws

The aim of these experiments was to assess the development of mechanical allodynia in the BCIBP rats after inoculation of W256 cells. ITI of lower number of W256 cells in BCIBP rats produced unilateral mechanical allodynia, whereas increasing the number of inoculated cells produced hypersensitivities in the bilateral hindpaws. The magnitude of hypersensitivities also depended on the number of cells inoculated. The hypersensitivities spontaneously resolved after around 3-4 weeks.

2.4.2.1. Experiment 2

Unilateral ITI of 4 x 10^4 W256 cells in rats did not significantly reduce PWTs in either the ipsilateral ($F_{(1, 9, 9/81)} = 0.8, 2.1, 1.3$; $p > 0.05$) or the contralateral ($F_{(1, 9, 9/81)} = 4.2, 2.9, 1.2$; $p > 0.05$) hindpaws throughout the experiment *c.f.* rats administered a unilateral ITI of 4 x 10^4 HK W256 cells (Figure 2.3A).

2.4.2.2. Experiment 3

Unilateral ITI of 1.5 x 10^5 W256 cells in rats significantly reduced the PWTs in the ipsilateral ($F_{(1, 16, 16/208)} = 66.9, 13.4, 8.6$; $p \leq 0.05$) hindpaw between days 4 and 20 after surgery and in the contralateral ($F_{(1, 16, 16/208)} = 14.7, 3.3, 2.4$; $p \leq 0.05$) hindpaws between days 16 and 20 after surgery *c.f.* rats given an ITI of 1.5 x 10^5 HK W256 cells, with a maximum reduction of 50.6 % and 23.0 % in the ipsilateral and contralateral PWTs relative to the corresponding baseline PWTs, respectively (Figure 2.3B).

2.4.2.3. Experiment 4

Unilateral ITI of DPBS in rats did not significantly reduce PWTs in either the ipsilateral ($F_{(1, 15, 15/135)}$ = 0.4, 1.9, 1.2; $p > 0.05$) or the contralateral ($F_{(1, 15, 15/135)}$ = 0.4, 1.6, 1.1; $p > 0.05$) hindpaws throughout the experiment *c.f.* age-matched control (naïve) rats (Supplementary Figure 2.3A).

2.4.2.4. Experiment 5

Unilateral ITI of 4 x 10^5 W256 cells in rats significantly reduced the PWTs in both the ipsilateral ($F_{(1, 16, 16/208)}$ = 228.0, 35.5, 25.8; $p \leq 0.05$) and contralateral ($F_{(1, 16, 16/208)}$ = 154.4, 28.0, 20.5; $p \leq 0.05$) hindpaws between days 7 and 25 after surgery *c.f.* rats given an ITI of 4 x 10^5 HK W256 cells, with a maximum reduction of 58.9 % and 42.3 % in the ipsilateral and contralateral PWTs relative to the corresponding baseline PWTs, respectively (Figure 2.3C).

2.4.2.5. Experiment 8

Unilateral ITI of 4 x 10^5 W256 cells in rats significantly reduced the PWTs in both the ipsilateral ($F_{(1, 1, 1/8)}$ = 81.6, 140.5, 45.5; $p \leq 0.05$) and contralateral ($F_{(1, 1, 1/8)}$ = 39.6, 103.7, 55.8; $p \leq 0.05$) hindpaws at day 7 after surgery *c.f.* rats given a unilateral ITI of 4 x 10^5 HK W256 cells, with an observed decrease of 58.8 % and 51.3 % in the ipsilateral and contralateral PWTs relative to the corresponding baseline PWTs, respectively (Supplementary Figure 2.3B).

2.4.2.6. Experiment 9

Unilateral ITI of 4 x 10^5 W256 cells in rats significantly reduced the PWTs in both the ipsilateral ($F_{(1, 2, 2/16)}$ = 26.1, 79.3, 41.9; $p \leq 0.05$) and contralateral ($F_{(1, 2, 2/16)}$ = 25.2, 47.9, 26.6; $p \leq 0.05$) hindpaws at day 7 after surgery *c.f.* rats administered a unilateral ITI of 4 x 10^5 HK W256 cells, with a reduction of 58.6 % and 52 % in the ipsilateral and contralateral PWTs respectively. At day 46 after surgery there was no significant difference between PWTs of both ipsilateral ($F_{(1, 2, 2/16)}$ = 26.1, 79.3, 41.9; $p > 0.05$) and contralateral ($F_{(1, 2, 2/16)}$ = 25.2, 47.9, 26.6; $p > 0.05$) hindpaws *c.f.* rats administered a unilateral ITI of 4 x 10^5 HK W256 cells (Supplementary Figure 2.3C).

2.4.2.7. Experiment 15

Unilateral ITI of 4 x 10^5 W256 cells in rats significantly reduced the PWTs in both the ipsilateral ($F_{(1, 1, 1/3)}$ = 171.6, 25.4, 15.0; $p \leq 0.05$) and contralateral ($F_{(1, 1, 1/3)}$ = 95.3, 28.9, 28.9; $p \leq 0.05$) hindpaws at day 7 after surgery *c.f.* rats administered a unilateral ITI of 4 x 10^5 HK W256 cells, with a reduction of 52.2 % and 27.9 % in the ipsilateral and contralateral PWTs respectively (Supplementary Figure 2.3D).

2.4.2.8. Experiment 16

Unilateral ITI of 4 x 10^5 W256 cells in rats significantly reduced the PWTs in both the ipsilateral ($F_{(1, 4, 4/12)}$ = 98.7, 13.2, 12.7; $p \leq 0.05$) and contralateral ($F_{(1, 4, 4/12)}$ = 67.6, 6.0, 5.1; $p \leq 0.05$) hindpaws between days 7 and 21 after surgery *c.f.* rats administered a unilateral ITI of 4 x 10^5 HK

W256 cells, with a maximum reduction of 55.6 % and 33.3 % in the ipsilateral and contralateral PWTs relative to the corresponding baseline PWTs, respectively (Supplementary Figure 2.3E).

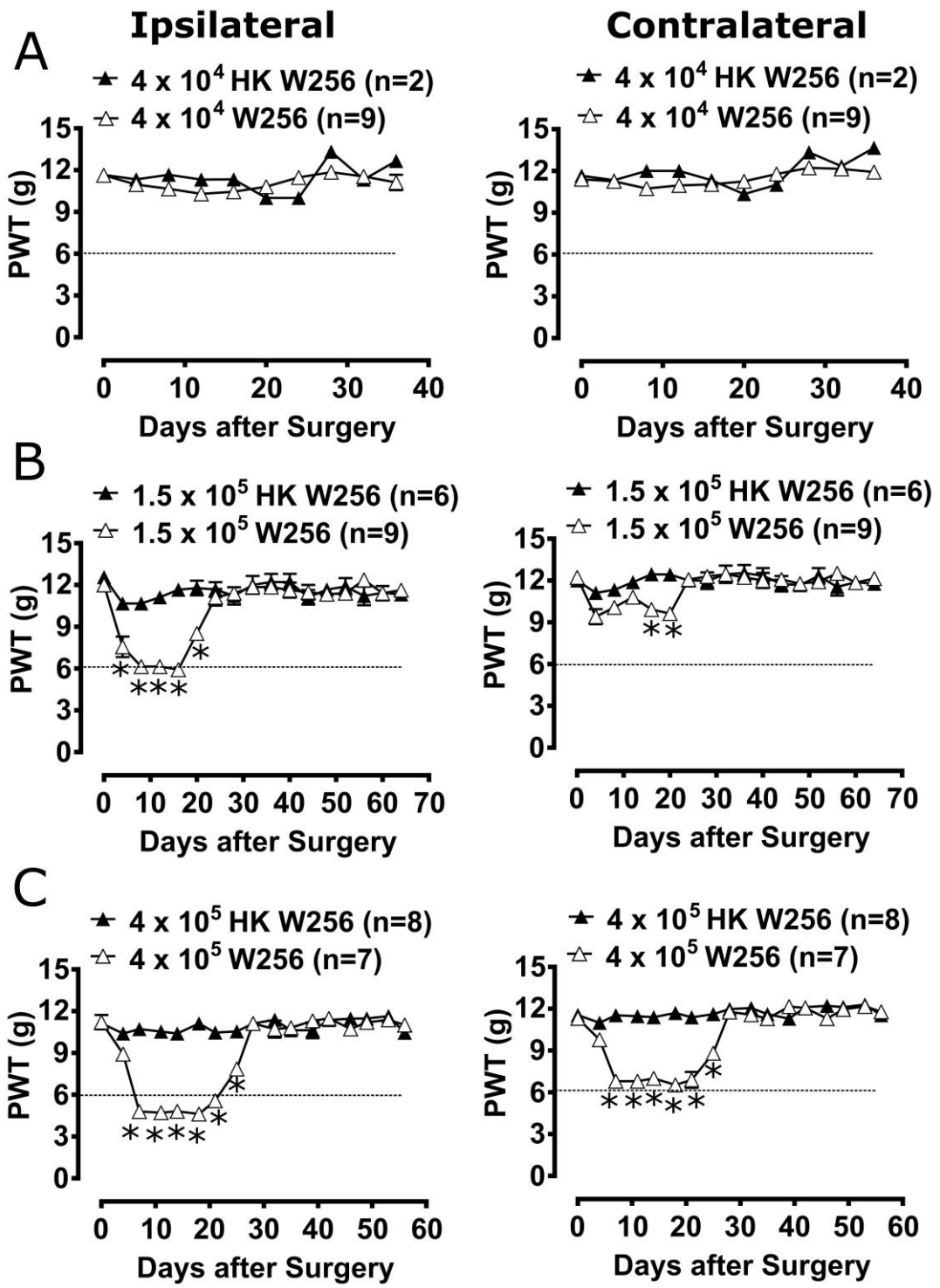

Figure 2.3. Paw withdrawal thresholds (PWTs) of ipsilateral and contralateral hindpaws of rats. Panels in the figure show mean (±SEM) PWTs of rats from (A) experiment 2, (B) experiment 3 and (C) experiment 5. Rats with PWTs $\leq$ 6 g in the ipsilateral hindpaw were considered to have fully developed mechanical allodynia as indicated by the dotted line. HK, heat-killed; W256,

Walker 256 cells. *p<0.05 (Two-way ANOVA, *posthoc* Bonferroni test) *c.f.* rats given an ITI of HK W256 cells.

2.4.3. Assessment of mechanical hyperalgesia in the hindpaws

The aim of these experiments was to assess the development of mechanical hyperalgesia in the BCIBP rats after inoculation of W256 cells. ITI of lower number of W256 cells in BCIBP rats produced unilateral mechanical hyperalgesia, whereas increasing the number of inoculated cells produced hypersensitivities in the bilateral hindpaws. The magnitude of hypersensitivities also depended on the number of cells inoculated. The hypersensitivities spontaneously resolved after around 3-4 weeks.

2.4.3.1. Experiment 2

Unilateral ITI of 4 x 10^4 W256 cells in rats did not significantly reduce PPTs in either the ipsilateral ($F_{(1, 9, 9/81)}$ = 0.1, 0.5, 0.7; $p > 0.05$) or the contralateral ($F_{(1, 9, 9/81)}$ = 0.1, 1.5, 0.5; $p > 0.05$) hindpaws throughout the experiment *c.f.* rats administered a unilateral ITI of 4 x 10^4 HK W256 cells (Figure 2.4A).

2.4.3.2. Experiment 3

Unilateral ITI of 1.5 x 10^5 W256 cells in rats significantly reduced the PPTs in the ipsilateral ($F_{(1, 15, 15/195)}$ = 185.4, 22.0, 20.4; $p \leq 0.05$) hindpaws between days 4 and 20 after surgery and in the contralateral ($F_{(1, 15, 15/195)}$ = 68.0, 7.5, 2.6; $p \leq 0.05$) hindpaws between days 4 and 16 after surgery *c.f.* rats administered a unilateral ITI of 1.5 x 10^5 HK W256 cells, with a maximum reduction of 50 % and 12.7 % respectively in the ipsilateral and the contralateral PPTs relative to corresponding baseline PPTs (Figure 2.4B).

2.4.3.3. Experiment 4

Unilateral ITI of DPBS in rats did not significantly reduce PPTs in either the ipsilateral ($F_{(1, 15, 15/135)}$ = 0.001, 2.3, 1.6; $p > 0.05$) or the contralateral ($F_{(1, 15, 15/135)}$ = 1.3, 3.1, 1.3; $p > 0.05$) hindpaws throughout the experiment *c.f.* naïve non-injected rats (Supplementary Figure 2.4).

2.4.3.4. Experiment 5

Unilateral ITI of 4 x 10^5 W256 cells in rats significantly reduced the PPTs in the ipsilateral ($F_{(1, 16, 16/208)}$ = 1262, 137.6, 91.8; $p \leq 0.05$) hindpaws between days 4 and 25 after surgery and in the contralateral ($F_{(1, 16, 16/208)}$ = 203.7, 55.4, 37.1; $p \leq 0.05$) hindpaws between days 7 and 25 *c.f.* rats administered a unilateral ITI of 4 x 10^5 HK W256 cells, with a maximum reduction of 52.1 % and 44.1 % in the ipsilateral and the contralateral PPTs relative to the corresponding baseline PPTs, respectively (Figure 2.4C).

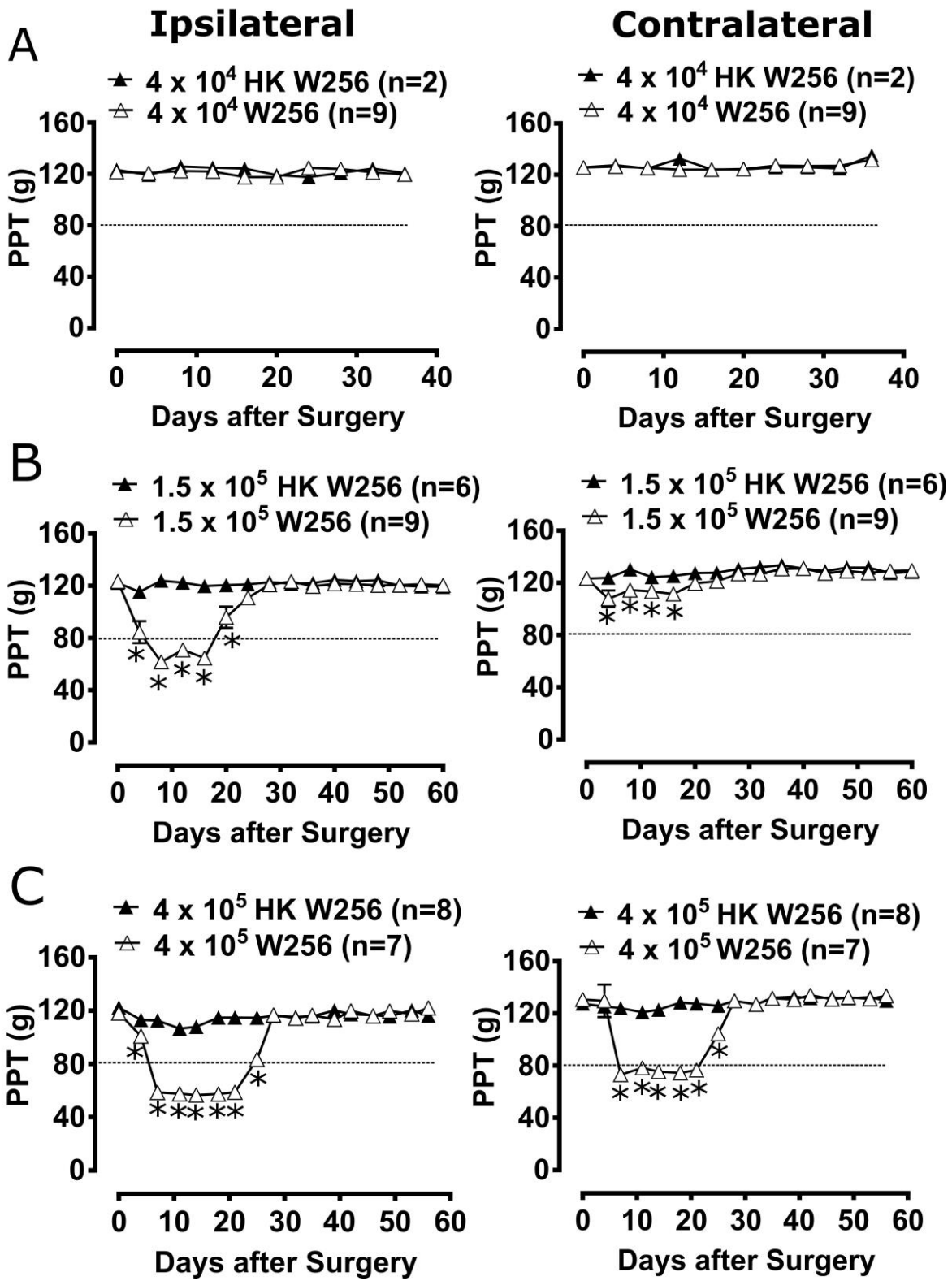

Figure 2.4. Paw pressure thresholds (PPTs) of ipsilateral and contralateral hindpaws of rats. Panels in the figure show mean (±SEM) PPTs of rats from (A) experiment 2, (B) experiment 3 and (C) experiment 5. Rats with PPTs $\leq$ 80 g in the ipsilateral hindpaw were considered to have fully developed mechanical hyperalgesia as indicated by the dotted line. HK, heat-killed; W256, Walker

256 cells. *p<0.05 (Two-way ANOVA, *posthoc* Bonferroni test) *c.f.* rats given an ITI of HK W256 cells.

2.4.4. Assessment of thermal hyperalgesia in the hindpaws

The aim of these experiments was to assess the development of thermal hyperalgesia in the BCIBP rats after inoculation of W256 cells. ITI of W256 cells in BCIBP rats did not produce thermal hyperalgesia.

2.4.4.1. Experiment 2

Unilateral ITI of 4 x 10^4 W256 cells in rats did not significantly reduce PTTs in either the ipsilateral ($F_{(1, 8, 8/72)}$ = 2.7, 0.5, 1.1; p > 0.05) or the contralateral ($F_{(1, 8, 8/72)}$ = 0.3, 1.1, 0.6; p > 0.05) hindpaws throughout the experiment *c.f.* rats administered a unilateral ITI of 4 x 10^4 HK W256 cells (Figure 2.5A).

2.4.4.2. Experiment 3

Unilateral ITI of 1.5 x 10^5 W256 cells in rats did not significantly reduce PTTs in either the ipsilateral ($F_{(1, 6, 6/78)}$ = 0.4, 1.5, 1.8; p > 0.05) or the contralateral ($F_{(1, 6, 6/78)}$ = 6.1, 0.9, 1.1; p > 0.05) hindpaws throughout the experiment *c.f.* rats administered a unilateral ITI of 1.5 x 10^5 HK W256 cells (Figure 2.5B).

2.4.4.3. Experiment 4

Unilateral ITI of DPBS in rats did not significantly reduce PTTs in either the ipsilateral ($F_{(1, 6, 6/54)}$ = 0.1, 1.3, 2.5; p > 0.05) or the contralateral ($F_{(1, 6, 6/54)}$ = 1.9, 0.6, 1.0; p > 0.05) hindpaws throughout the experiment *c.f.* naïve non-injected rats (Supplementary Figure 2.5A).

2.4.4.4. Experiment 5

Unilateral ITI of 4 x 10^5 W256 cells in rats did not significantly reduce PTTs in either the ipsilateral ($F_{(1, 1, 1/13)}$ = 0.0002, 0.1, 0.2; p > 0.05) or the contralateral ($F_{(1, 1, 1/13)}$ = 1.1, 0.7, 0.7; p > 0.05) hindpaws at day 14 after surgery *c.f.* rats administered a unilateral ITI of 4 x 10^5 HK W256 cells (Supplementary Figure 2.5B).

2.4.4.5. Experiment 6

Unilateral ITI of 4 x 10^5 W256 cells in rats did not significantly reduce PTTs in either the ipsilateral ($F_{(1, 8, 8/72)}$ = 1.0, 3.1, 0.7; p > 0.05) or the contralateral ($F_{(1, 8, 8/72)}$ = 0.8, 6.7, 0.3; p > 0.05) hindpaws throughout the experiment *c.f.* rats administered a unilateral ITI of 4 x 10^5 HK W256 cells (Figure 2.5C).

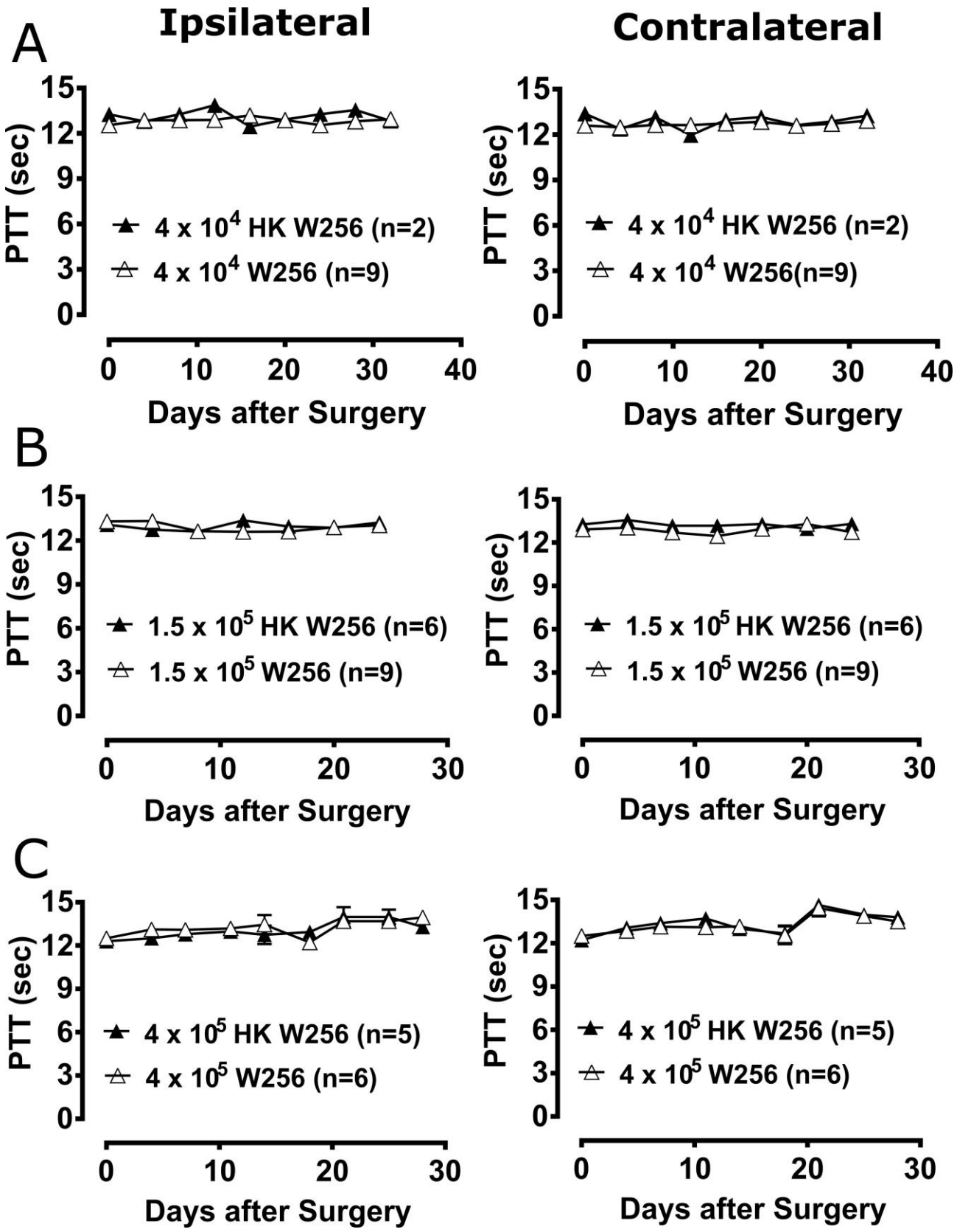

Figure 2.5. Paw thermal thresholds (PTTs) of ipsilateral and contralateral hindpaws of rats. Panels in the figure show mean (±SEM) PTTs of rats from (A) experiment 2, (B) experiment 3 and (C) experiment 6. HK, heat-killed; W256, Walker 256 cells. There were no statistically significant differences in PTTs between the treatment groups in any of these experiments ($p>0.05$; Two-way ANOVA, *posthoc* Bonferroni test).

Based upon the cell number-dependent experimental results in female Wistar Han rats administered with a unilateral ITI of W256 cells, 400,000 cells/10 μL DPBS was found to be the optimum cell number as it produced distinct bilateral hindpaw hypersensitivity whilst maintaining satisfactory animal health throughout the study (Table 2.1).

Table 2.1. Summary of W256 cell number-dependent variations in the experimental outcomes in female Wistar Han rats administered a unilateral ITI of these cells.

Number of cells injected	**Gain in body weight**	**Animal health**	**Mechanical allodynia**						**Mechanical hyperalgesia**						**Thermal hyperalgesia**	
			Ipsi			**Contra**			**Ipsi**			**Contra**			**Ipsi**	**Contra**
			Obs.	Dur. (days)	Ext. (%)	Obs.	Dur. (days)	Ext. (%)	Obs.	Dur. (days)	Ext. (%)	Obs.	Dur. (days)	Ext. (%)		
40,000	✓	✓	-	N/A	N/A	-	N/A	N/A	-	N/A	N/A	-	N/A	N/A	-	-
150,000	✓	✓	+	4-20	50.6	+	16-20	23.0	+	4-20	49.9	+	4-16	12.7	-	-
400,000	✓	✓	+	7-25	58.8	+	7-25	42.2	+	4-25	52.1	+	7-25	44.0	-	-

✓, satisfactory; +, observed; -, not observed; Contra., contralateral hindpaws; Dur., duration in days post-ITI; Ext., extent of percentage reduction in PWTs / PPTs; Ipsi., ipsilateral hindpaws; N/A, not applicable; Obs., observation

2.4.5. Test compound administration

The aim of these experiments was to chatacterise the model by pharmacological testing of various drugs in the BCIBP rats. Administration of naloxone to the BCIBP rats in the resolved-pain state rescued the pain phenotype. Standard analgesic drugs morphine, gabapentin, amitriptyline and meloxicam alleviated the mechanical allodynia in a dose-dependant manner. Similarly, these standard analgesic drugs also alleviated the mechanical hyperalgesia in the BCIBP rats at the doses tested in the study.

2.4.5.1. Effect of naloxone (s.c.) on pain behavioural phenotypes

2.4.5.1.1. Experiment 3

Administration of naloxone in the time interval, day 81-day 91, to a group of rats administered a unilateral ITI of 1.5 x 10^5 W256 cells significantly reduced the PWTs from 0.25 to 0.75 h after injection in both the ipsilateral ($F_{(1, 8, 8/104)}$ = 12.8, 5.3, 1.1; $p \leq 0.05$) and contralateral ($F_{(1, 8, 8/104)}$ = 9.6, 5.2, 2.8; $p \leq 0.05$) hindpaws *c.f.* rats administered a unilateral ITI of 1.5 x 10^5 HK W256 cells, with a maximum reduction of 24 % and 26.4 % in the ipsilateral and contralateral PWTs relative to the corresponding baseline PWTs, respectively (Supplementary Figure 2.6A). Administration of naloxone to these rats in the interval, day 82-day 92, significantly ($F_{(1, 8, 8/104)}$ = 3.1, 1.4, 4.3; $p \leq 0.05$) reduced the PPTs from 0.75 to 1 h after injection in the ipsilateral hindpaw and significantly ($F_{(1, 8, 8/104)}$ = 3.7, 1.9, 2.3; $p \leq 0.05$) reduced the PPTs at 0.75 h after injection in the contralateral hindpaw *c.f.* rats injected with the corresponding number of HK W256 cells, with a maximum reduction of 15.2 % and 10.5 % in the ipsilateral and the contralateral PPTs relative to the corresponding baseline PPTs, respectively (Supplementary Figure 2.6B).

2.4.5.1.2. Experiment 4

Administration of naloxone to group of rats given an ITI of DPBS or naïve control rats did not significantly alter PWTs in either the ipsilateral ($F_{(1, 8, 8/72)}$ = 0.2, 0.5, 0.9; $p > 0.05$) or the contralateral ($F_{(1, 8, 8/72)}$ = 0.01, 0.1, 0.9; $p > 0.05$) PWTs (Supplementary Figure 2.6C). Similarly, naloxone did not significantly alter the ipsilateral ($F_{(1, 8, 8/72)}$ = 0.3, 1.2, 0.9; $p > 0.05$) or contralateral ($F_{(1, 8, 8/72)}$ = 1.3, 1.8, 0.5; $p > 0.05$) PPTs throughout the testing period in the same animals (Supplementary Figure 2.6D).

2.4.5.1.3. Experiment 5

Administration of naloxone to group of rats administered a unilateral ITI of 4 x 10^5 W256 cells in the time interval, day 43-day 51, post-ITI significantly ($F_{(1, 8, 8/104)}$ = 173.7, 33.8, 22.5; $p \leq 0.05$) reduced the PWTs from 0.25 to 1.25 h after naloxone injection in the ipsilateral hindpaw. Similarly, there was a significant ($F_{(1, 8, 8/104)}$ = 130.9, 27.5, 17.9; $p \leq 0.05$) reduction in PWTs from 0.25 to 1 h after injection, in the contralateral hindpaws *c.f.* rats injected with 4 x 10^5 HK W256 cells. The

maximum decreases were 60.7 % and 51.1 % in the ipsilateral and contralateral PWTs relative to the corresponding baseline PWTs, respectively (Figure 2.6A). Administration of naloxone to these rats in the interval, day 53-day 66 post-ITI significantly ($F_{(3,\ 8,\ 24/208)}$ = 7.3, 9.8, 1.9; $p \leq 0.05$) reduced the PWTs from 0.25 to 0.75 h in the ipsilateral hindpaws and significantly ($F_{(3,\ 8,\ 24/208)}$ = 6.5, 7.5, 1.8; $p \leq 0.05$) reduced PWTs from 0.5 to 0.75 h in the contralateral hindpaws. The maximum PWT decreases were 35.8 % and 20.4 % in the ipsilateral and contralateral hindpaws relative to the corresponding baseline PWTs, respectively (Figure 2.6B).These findings were in contrast to the lack of effect observed in naloxone injected rats administered a unilateral ITI of 4 x 10^5 HK W256 cells or vehicle injected rats administered a unilateral ITI of 4 x 10^5 W256 cells and 4 x 10^5 HK W256 cells.

2.4.5.1.4. Experiment 7

Administration of naloxone to rats administered a unilateral ITI of 4 x 10^5 W256 cells did not significantly reduce the PTTs in either the ipsilateral ($F_{(3,\ 8,\ 24/112)}$ = 2.7, 0.9, 0.8; $p > 0.05$) or the contralateral ($F_{(3,\ 8,\ 24/112)}$ = 0.2, 0.3, 1.1; $p > 0.05$) hindpaws throughout the testing (Supplementary Figure 2.6E).

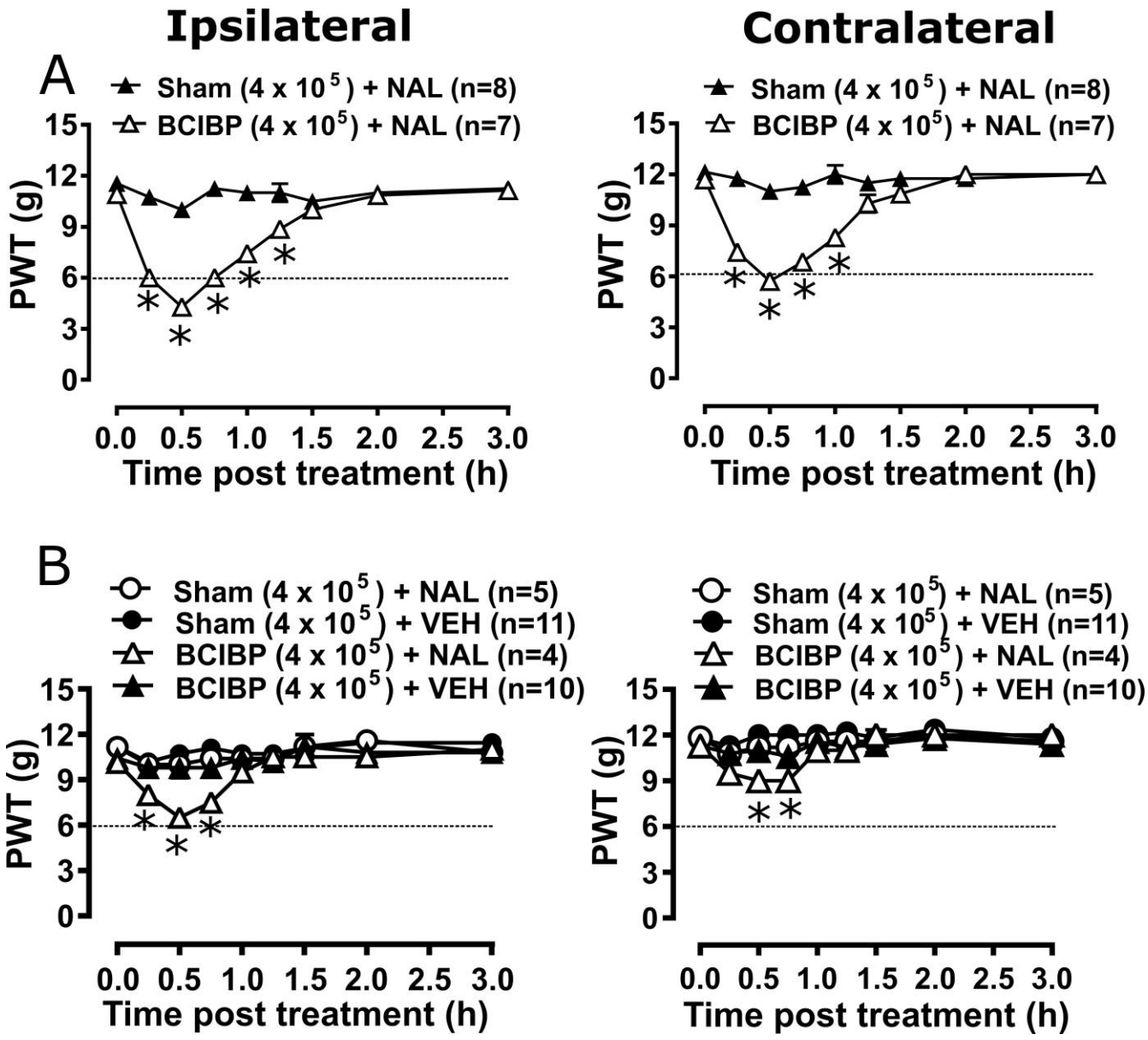

Figure 2.6. Effect of naloxone on ipsilateral and contralateral paw withdrawal thresholds (PWTs) of rats. Panels in the figure show mean (±SEM) PWT versus time curves from experiment 5 following naloxone or vehicle injection between (A) day 43-51 post-ITI and (B) day 53-66 post-ITI. The dotted line indicates the threshold PWT value at / below which the rats were considered to have fully developed mechanical allodynia. BCIBP (4 x 10^5), group of rats given an ITI of 4 x 10^5 W256 cells; HK, heat-killed; NAL, naloxone (15 mg/kg s.c.); Sham (4 x 10^5), group of rats given an ITI of 4 x 10^5 HK W256 cells; VEH, vehicle; W256, Walker 256 cells. *$p<0.05$ (Two-way ANOVA, *posthoc* Bonferroni test) *c.f.* rats given an ITI of HK W256 cells.

The extent and duration of naloxone induced rescue of the pain phenotype in rats from these experiments are tabulated in Table 2.2.

Table 2.2. Extent and duration of naloxone induced rescue of pain phenotype.

Exp. No.	Days post ITI	ITI	Drug treatment	ΔPWT AUC (g.h)		ΔPPT AUC (g.h)		ΔPTT AUC (sec.h)		Time (h)	
				Ipsi	Contra	Ipsi	Contra	Ipsi	Contra	Peak effect	~Duration of action
3	82-92	1.5 x 10^5 W256	Naloxone	-	-	22.2 (± 4.76)	14.8 (± 3.91)	-	-	0.75	1
		1.5 x 10^5 HK W256	Naloxone	-	-	9.3 (± 4.44)	4.2 (± 2.13)	-	-	NE	NE
3	81-91	1.5 x 10^5 W256	Naloxone	4.1 (± 1.18)	4.4 (± 1.13)	-	-	-	-	0.5	1
		1.5 x 10^5 HK W256	Naloxone	1.8 (± 0.50)	1.5 (± 0.25)	-	-	-	-	NE	NE
4	82-94	DPBS	Naloxone	-	-	7.2 (± 2.30)	10.7 (± 5.75)	-	-	NE	NE
		Naïve	Naloxone	-	-	5.3 (± 1.75)	13.2 (± 5.41)	-	-	NE	NE
4	81-93	DPBS	Naloxone	0.9 (±	0.7 (±	-	-	-	-	NE	NE

				0.35)	0.33)						
		Naïve	Naloxone	0.9 (± 0.56)	1.3 (± 0.72)	-	-	-	-	NE	NE
5	43-51	4 x 10^5 W256	Naloxone	6.2 (± 0.75)*	5.5 (± 0.70)*	-	-	-	-	0.5	1.5
		4 x 10^5 HK W256	Naloxone	2.5 (± 0.55)	1.7 (± 0.39)	-	-	-	-	NE	NE
5	53-66	4 x 10^5 W256	Naloxone	2.5 (± 0.35)	1.8 (± 0.57)	-	-	-	-	0.5-0.75	1.25
		4 x 10^5 W256	Vehicle	1.1 (± 0.74)	1.1 (± 0.50)	-	-	-	-	NE	NE
		4 x 10^5 HK W256	Naloxone	1.9 (± 0.38)	1.6 (± 0.44)	-	-	-	-	NE	NE
		4 x 10^5 HK W256	Vehicle	1.7 (± 0.48)	0.6 (± 0.18)	-	-	-	-	NE	NE
7	21-24	4 x 10^5 W256	Naloxone	-	-	-	-	2.2 (± 1.06)	3.3 (± 1.06)	NE	NE

								3.1 (± 0.77)			
		4 x 10^5 W256	Vehicle	-	-	-	-	2.1 (± 1.33)	1.4 (± 0.59)	NE	NE
		4 x 10^5 HK W256	Naloxone	-	-	-	-	0.7 (± 0.33)	2.1 (± 1.31)	NE	NE
		4 x 10^5 HK W256	Vehicle	-	-	-	-		0.9 (± 0.16)	NE	NE

Contra, contralateral hindpaws; Ipsi, ipsilateral hindpaws; NE, no drug effect; -, not assessed. *p≤0.05 (Unpaired t test) *c.f.* rats administered a unilateral ITI of 4 x 10^5 HK W256 cells that received single bolus dose of naloxone

2.4.5.2. Anti-allodynic effect of morphine (s.c.), gabapentin (i.p.), amitriptyline (i.p.) and meloxicam (i.p.)

BCIBP-rats having fully developed mechanical allodynia (PWTs ≤ 6g) in the ipsilateral hindpaws and administered single bolus doses of the clinically available analgesic drugs (morphine and meloxicam) or the adjuvant agents (gabapentin and amitriptyline), evoked unique pharmacological profiles consistent with their distinct modes of action. Anti-allodynia was produced in a dose-dependent manner by each of these drugs in both the ipsilateral (Figure 2.7A-D) and the contralateral hindpaws (Supplementary Figure 2.7A-D). Extent and duration of anti-allodynia (ΔPWT AUC) and ED_{50s} of each of the test compounds against mechanical allodynia in the ipsilateral and contralateral hindpaws, is summarized in Table 2.3. The dose response curves of morphine and gabapentin in BCIBP rats have been shown in Figure 2.8, and those of amitriptyline and meloxicam have been shown in Figure 2.9. Some of the effects of these pharmacological characterization experiments were modest, in alignment with the variable potencies of different drugs to alleviate cancer pain hypersensitivities in clinic.

2.4.5.2.1. Experiment 10

Administration of 0.3 mg/kg morphine did not produce significant ($F_{(3, 8, 24/160)}$ = 35.3, 18.1, 5.7; $p > 0.05$) anti-allodynia in the ipsilateral hindpaw throughout the testing, while it produced significant ($F_{(3, 8, 24/160)}$ = 44.8, 17.6, 4.8; $p \leq 0.05$) anti-allodynia between 0.5 and 0.75 h after injection in the contralateral hindpaw *c.f.* rats injected with vehicle. Administration of 1 mg/kg morphine produced significant ($F_{(3, 8, 24/160)}$ = 35.3, 18.1, 5.7; $p \leq 0.05$) anti-allodynia between 0.25 and 1.25 h after injection in the ipsilateral hindpaw, while it produced significant ($F_{(3, 8, 24/160)}$ = 44.8, 17.6, 4.8; $p \leq 0.05$) anti-allodynia between 0.25 and 1 h after injection in the contralateral hindpaw *c.f.* rats injected with vehicle. Administration of 3 mg/kg morphine produced significant anti-allodynia between 0.25 and 1.5 h after injection in both ipsilateral ($F_{(3, 8, 24/160)}$ = 35.3, 18.1, 5.7; $p \leq 0.05$) and contralateral ($F_{(3, 8, 24/160)}$ = 44.8, 17.6, 4.8; $p \leq 0.05$) hindpaws *c.f.* rats injected with vehicle.

2.4.5.2.2. Experiments 11 and 12

Gabapentin induced anti-allodynia was characterised by an onset of action which was delayed in nature. Administration of 30 mg/kg gabapentin produced significant ($F_{(3, 8, 24/160)}$ = 32.2, 7.9, 1.0; $p \leq 0.05$) anti-allodynia in the ipsilateral hindpaw at 1.25 h after injection, while it did not produce significant ($F_{(3, 8, 24/160)}$ = 25.0, 7.0, 1.0; $p > 0.05$) anti-allodynia in the contralateral hindpaw throughout the testing *c.f.* rats injected with vehicle. Administration of 70 mg/kg gabapentin produced significant anti-allodynia between 1.25 and 1.5 h after injection in both ipsilateral ($F_{(3, 8, 24/160)}$ = 32.2, 7.9, 1.0; $p \leq 0.05$) and contralateral ($F_{(3, 8, 24/160)}$ = 25.0, 7.0, 1.0; $p \leq 0.05$) hindpaws *c.f.* rats injected with vehicle. Administration of 100 mg/kg gabapentin produced significant ($F_{(3, 8, 24/160)}$ = 32.2, 7.9, 1.0; $p \leq 0.05$) anti-allodynia in the ipsilateral hindpaw from 0.75 h to at least 3 h after

injection, and it produced significant ($F_{(3, 8, 24/160)}$ = 25.0, 7.0, 1.0; $p \leq 0.05$) anti-allodynia in the contralateral hindpaw from 1 h to at least 3 h after injection *c.f.* rats injected with vehicle. Administration of 3 mg/kg amitriptyline did not produce significant ($F_{(3, 8, 24/160)}$ = 15.3, 8.4, 2.0; $p > 0.05$) anti-allodynia in the ipsilateral hindpaw throughout the testing, whereas it produced significant ($F_{(3, 8, 24/160)}$ = 17.7, 9.2, 2.9; $p \leq 0.05$) anti-allodynia at 0.75 h after injection in the contralateral hindpaw *c.f.* rats injected with vehicle. Administration of 10 mg/kg amitriptyline produced significant anti-allodynia between 0.5 and 1 h after injection in both ipsilateral ($F_{(3, 8, 24/160)}$ = 15.3, 8.4, 2.0; $p \leq 0.05$) and contralateral ($F_{(3, 8, 24/160)}$ = 17.7, 9.2, 2.9; $p \leq 0.05$) hindpaws *c.f.* rats injected with vehicle. Administration of 30 mg/kg amitriptyline produced significant anti-allodynia between 0.5 and 1.5 h after injection in both ipsilateral ($F_{(3, 8, 24/160)}$ = 15.3, 8.4, 2.0; $p \leq 0.05$) and contralateral ($F_{(3, 8, 24/160)}$ = 17.7, 9.2, 2.9; $p \leq 0.05$) hindpaws *c.f.* rats injected with vehicle.

2.4.5.2.3. Experiment 13

Meloxicam induced anti-allodynia was characterised by an onset of action which was delayed in nature. Administration of 2.5 mg/kg meloxicam produced significant ($F_{(3, 8, 24/160)}$ = 54.1, 11.2, 2.3; $p \leq 0.05$) anti-allodynia in the ipsilateral hindpaw at 1.25 h after injection, whereas it did not produce significant ($F_{(3, 8, 24/160)}$ = 50.6, 12.3, 2.0; $p > 0.05$) anti-allodynia in the contralateral hindpaw *c.f.* rats injected with vehicle. Administration of 5 mg/kg meloxicam produced significant anti-allodynia between 1 and 2 h after injection in both the ipsilateral ($F_{(3, 8, 24/160)}$ = 54.1, 11.2, 2.3; $p \leq 0.05$) and contralateral ($F_{(3, 8, 24/160)}$ = 50.6, 12.3, 2.0; $p \leq 0.05$) hindpaws *c.f.* rats injected with vehicle. Administration of 7.5 mg/kg meloxicam produced significant anti-allodynia between 0.75 to at least 3 h after injection in both the ipsilateral ($F_{(3, 8, 24/160)}$ = 54.1, 11.2, 2.3; $p \leq 0.05$) and contralateral ($F_{(3, 8, 24/160)}$ = 50.6, 12.3, 2.0; $p \leq 0.05$) hindpaws *c.f.* rats injected with vehicle.

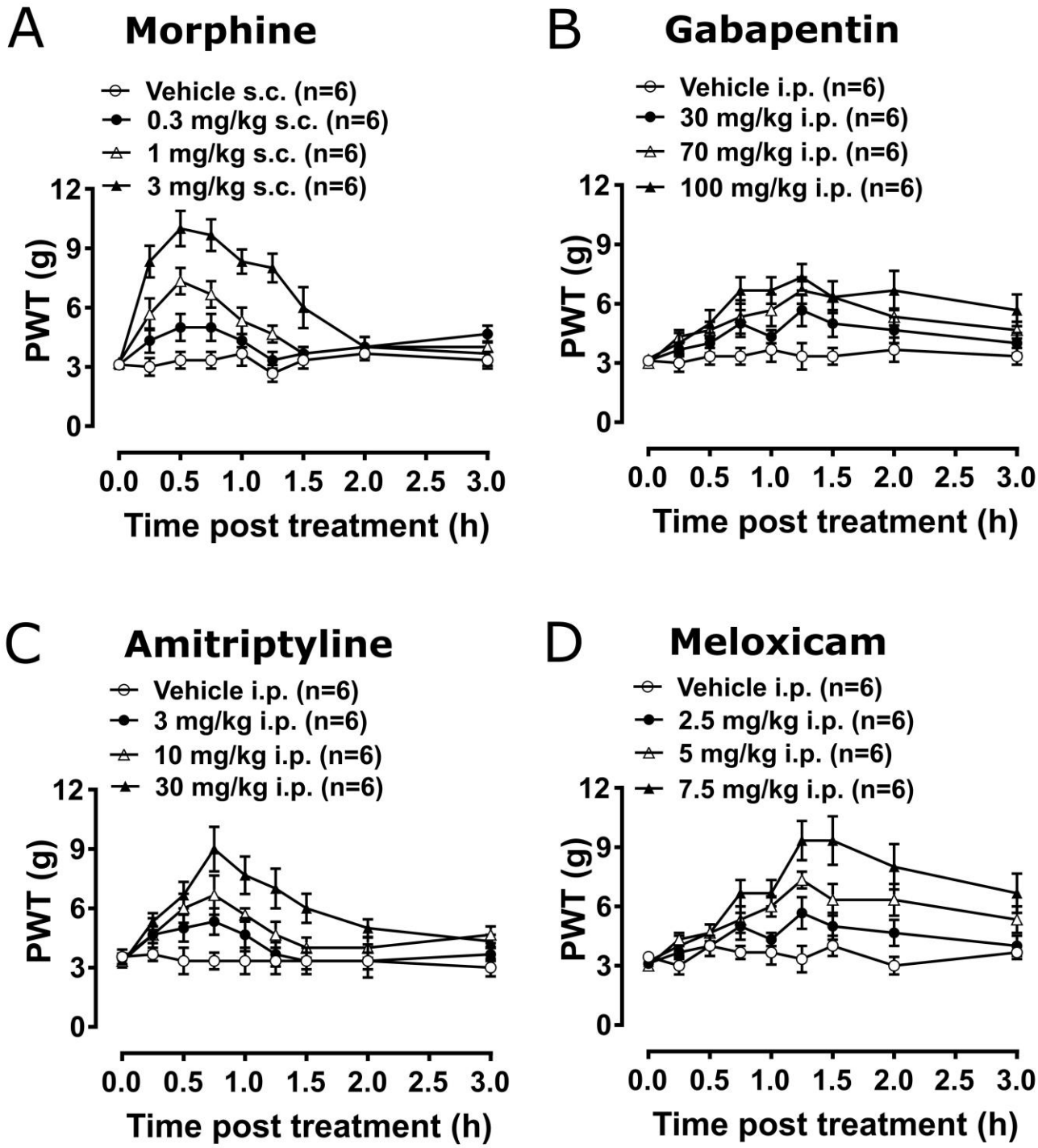

Figure 2.7. Temporal changes in the paw withdrawal thresholds (PWTs) of BCIBP rats in the ipsilateral hindpaws following the administration of single bolus doses of analgesic and adjuvant drugs. Panels in the figure show temporal changes in mean (±SEM) PWT versus time curves following injection of (A) morphine, (B) gabapentin, (C) amitriptyline and (D) meloxicam.

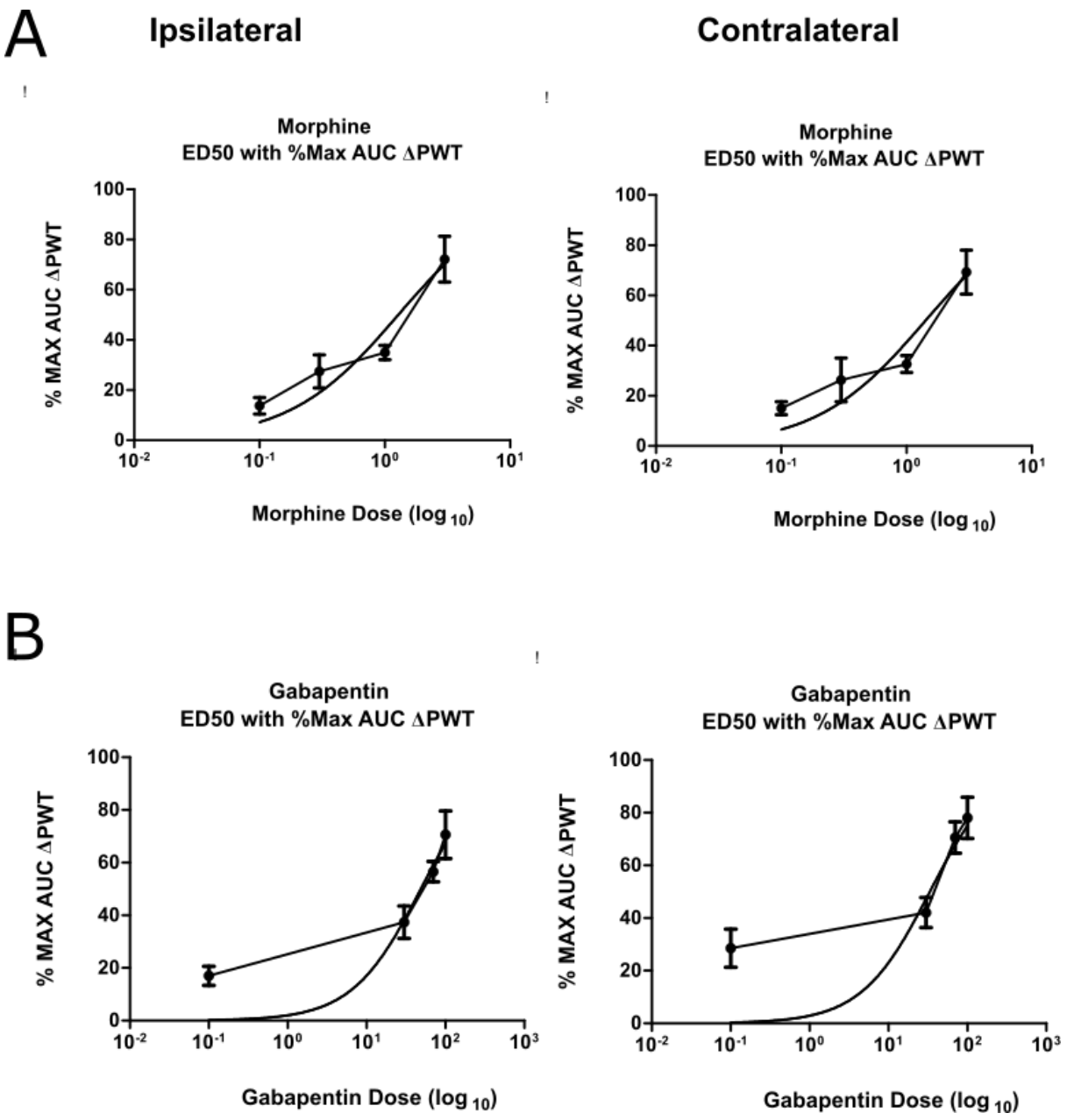

Figure 2.8. Dose response curves of morphine and gabapentin in BCIBP rats. Panels in the figure show % MAX AUC ΔPWT (representative of response) versus $\log_{10}$ dose (representative of dose) curves of (A) morphine and (B) gabapentin in the ipsilateral and contralateral hindpaws. $ED_{50\text{-IPSI}}$ and $ED_{50\text{-CONTRA}}$ values for morphine were found to be 1.3 and 1.4 mg/kg, respectively, and for gabapentin were found to be 47.1 and 30.8 mg/kg, respectively.

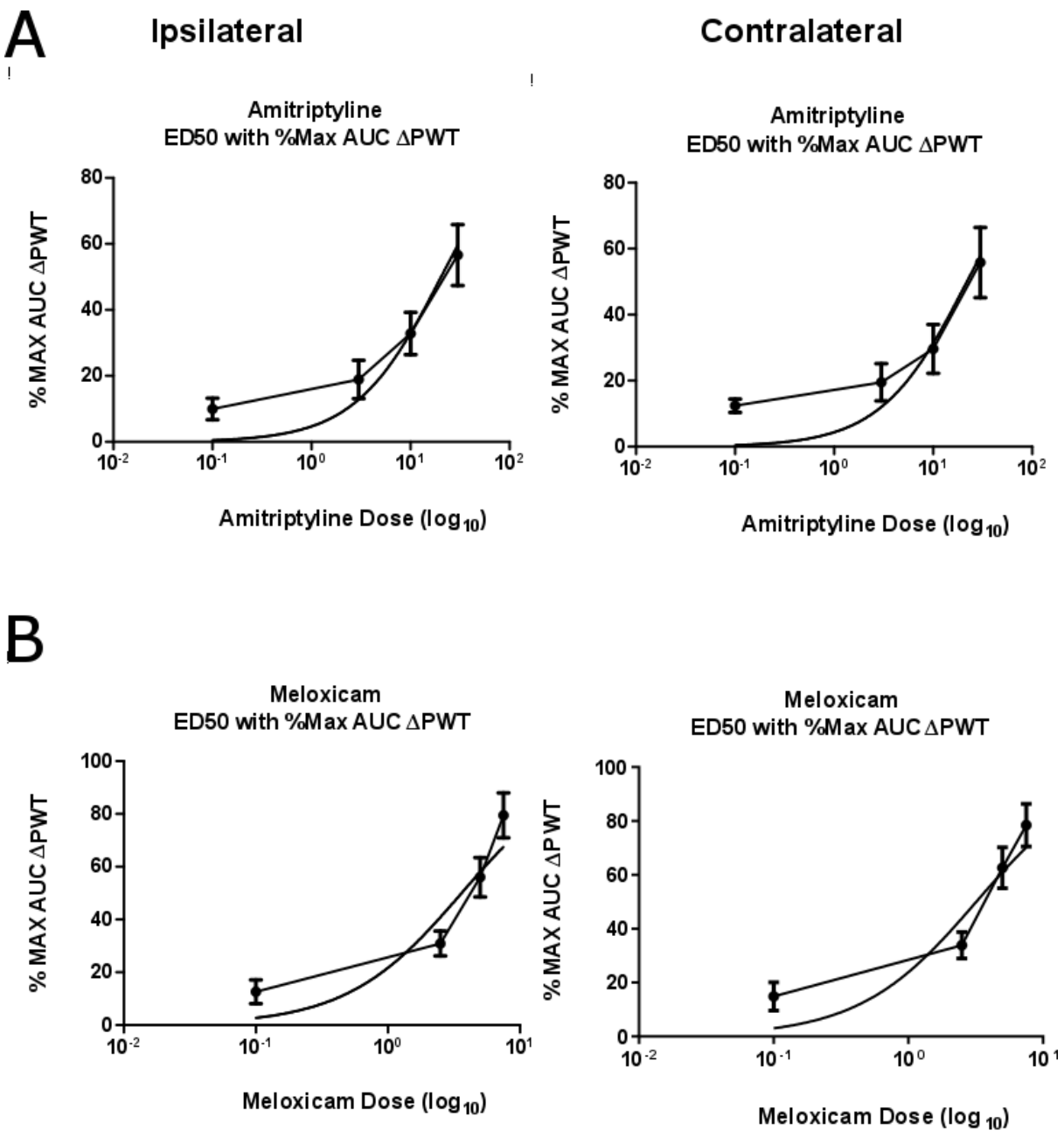

Figure 2.9. Dose response curves of amitriptyline and meloxicam in BCIBP rats. Panels in the figure show % MAX AUC ΔPWT (representative of response) versus $\log_{10}$ dose (representative of dose) curves of (A) amitriptyline and (B) meloxicam in the ipsilateral and contralateral hindpaws. $ED_{50\text{-IPSI}}$ and $ED_{50\text{-CONTRA}}$ values for amitriptyline were found to be 20.1 and 21.4 mg/kg, respectively, and for meloxicam were found to be 3.9 and 3.5 mg/kg, respectively.

Table 2.3. Extent and duration of anti-allodynia (ΔPWT AUC) and potencies of test compounds.

Test compound and route of administration	**Time (h)**		**Mean ΔPWT at peak effect (g)**		**ΔPWT AUC (g.h)**		**ED_{50} for the alleviation of mechanical allodynia in the bilateral hindpaws (mg/kg)**			
	Peak effect	**~Duration of action**					**Ipsilateral**		**Contralateral**	
			Ipsi	**Contra**	**Ipsi**	**Contra**	**Mean**	**95% CI**	**Mean**	**95% CI**
Morphine (s.c.)										
0.3 mg/kg	0.5 – 0.75	2	1.9 (± 0.76)	2.2 (± 1.07)	3.7 (± 0.88)	3.9 (± 1.28)	1.3	0.90 - 1.83	1.4	0.98 – 2.08
1 mg/kg			4.1 (± 0.70)	4.2 (± 0.72)	4.7 (± 0.38)*	4.8 (± 0.49)*				
3 mg/kg			6.9 (± 1.00)	6.2 (± 0.72)	9.6 (± 1.22)*	10.2 (± 1.28)*				
Vehicle			NA	NA	1.8 (± 0.44)	2.2 (± 0.38)				
Gabapentin (i.p.)										
30 mg/kg	1.25 - 1.5	>3	2.6 (± 0.83)	2.4 (± 0.78)	4.5 (± 0.73)	4.5 (± 0.61)	47.1	35.25 – 63.04	30.8	21.9 – 43.2
70 mg/kg			3.7 (± 0.61)	3.7 (± 0.68)	6.8 (± 0.46)*	7.5 (± 0.63)*				
100 mg/kg			4.1 (± 0.70)	4.1 (± 0.58)	8.4 (± 1.08)*	8.3 (± 0.83)*				

Vehicle			NA	NA	2.0 (± 0.43)	3.0 (± 0.76)				
Amitriptyline (i.p.)	0.75 – 1.25	2					20.1	13.82 – 29.11	21.4	14.27 – 32.19
3 mg/kg			2 (± 0.81)	2.1 (± 0.78)	2.6 (± 0.80)	2.6 (± 0.75)				
10 mg/kg			3.3 (± 0.99)	2.8 (± 0.78)	4.5 (± 0.89)	4.0 (± 0.99)				
30 mg/kg			5.8 (± 1.15)	4.9 (± 0.89)	7.8 (± 1.28)*	7.4 (± 1.42)*				
Vehicle			NA	NA	1.4 (± 0.45)	1.7 (± 0.27)				
Meloxicam (i.p.)	1.25 – 1.5	>3					3.9	2.79 – 5.43	3.5	2.51 – 4.79
2.5 mg/kg			2.6 (± 0.83)	2.2 (± 0.66)	4.5 (± 0.67)*	4.5 (± 0.65)*				
5 mg/kg			4.3 (± 0.45)	4.3 (± 0.45)	8.1 (± 1.07)*	8.2 (± 1.00)*				
7.5 mg/kg			6.1 (± 0.96)	5.3 (± 0.62)	11.5 (± 1.22)*	10.3 (± 1.04)*				
Vehicle			NA	NA	1.8 (± 0.64)	2.0 (± 0.68)				

CI, confidence interval; Contra., contralateral hindpaws; Ipsi., ipsilateral hindpaws; NA, not applicable; *p<0.05 (One-way ANOVA, *posthoc* Dunnett's multiple comparisons test) *c.f.* rats that received single bolus doses of vehicle

2.4.5.3. Anti-hyperalgesic effect of morphine (s.c.), gabapentin (i.p.), amitriptyline (i.p.) and meloxicam (i.p.)

BCIBP-rats having fully developed mechanical hyperalgesia (PPTs ≤ 80g) in the ipsilateral hindpaws and administered single bolus doses of the clinically available analgesic drugs (morphine and meloxicam) or the adjuvant agents (gabapentin and amitriptyline), evoked anti-hyperalgesia in both the ipsilateral (Figure 2.10A-D) and the contralateral hindpaws (Supplementary Figure 2.8A-D). Extent and duration of anti-hyperalgesia (ΔPPT AUC) of each of the test compounds in the ipsilateral and the contralateral hindpaws, is summarized in Table 2.4.

2.4.5.3.1. Experiment 14

Administration of 3 mg/kg morphine produced significant anti-hyperalgesia between 0.5 and 1 h in the ipsilateral hindpaw ($F_{(1,\ 8,\ 8/64)}$ = 5.5, 1.8, 2.7; $p \leq 0.05$) and between 0.5 and 0.75 h in the contralateral hindpaw ($F_{(1,\ 8,\ 8/64)}$ = 5.1, 1.7, 2.4; $p \leq 0.05$) *c.f.* rats injected with vehicle. Gabapentin induced anti-hyperalgesia was characterised by a delayed onset of action. Administration of 100 mg/kg gabapentin produced significant anti-hyperalgesia between 1 and 1.5 h in the ipsilateral hindpaw ($F_{(1,\ 8,\ 8/64)}$ = 9.8, 1.6, 1.2; $p \leq 0.05$) and between 1 and 1.25 h in contralateral hindpaw ($F_{(1,\ 8,\ 8/64)}$ = 11.6, 1.2, 1.7; $p \leq 0.05$) *c.f.* rats injected with vehicle. Administration of 30 mg/kg amitriptyline produced significant relief of hyperalgesia at 0.75 h in both the ipsilateral ($F_{(1,\ 8,\ 8/64)}$ = 5.1, 3.9, 2.3; $p \leq 0.05$) and contralateral ($F_{(1,\ 8,\ 8/64)}$ = 4.9, 3.9, 2.4; $p \leq 0.05$) hindpaws *c.f.* rats injected with vehicle. Meloxicam induced anti-hyperalgesia was characterised by a delayed onset of action. Administration of 7.5 mg/kg meloxicam did not produce anti-hyperalgesia in the ipsilateral hindpaws $F_{(1,\ 8,\ 8/64)}$ = 5.9, 3.0, 2.6; $p > 0.05$). By contrast, meloxicam at 7.5 mg/kg produced significant ($F_{(1,\ 8,\ 8/64)}$ = 7.1, 2.7, 3.4; $p \leq 0.05$) anti-hyperalgesia from 1.25 to at least until 3 h in the contralateral hindpaws *c.f.* rats injected with vehicle.

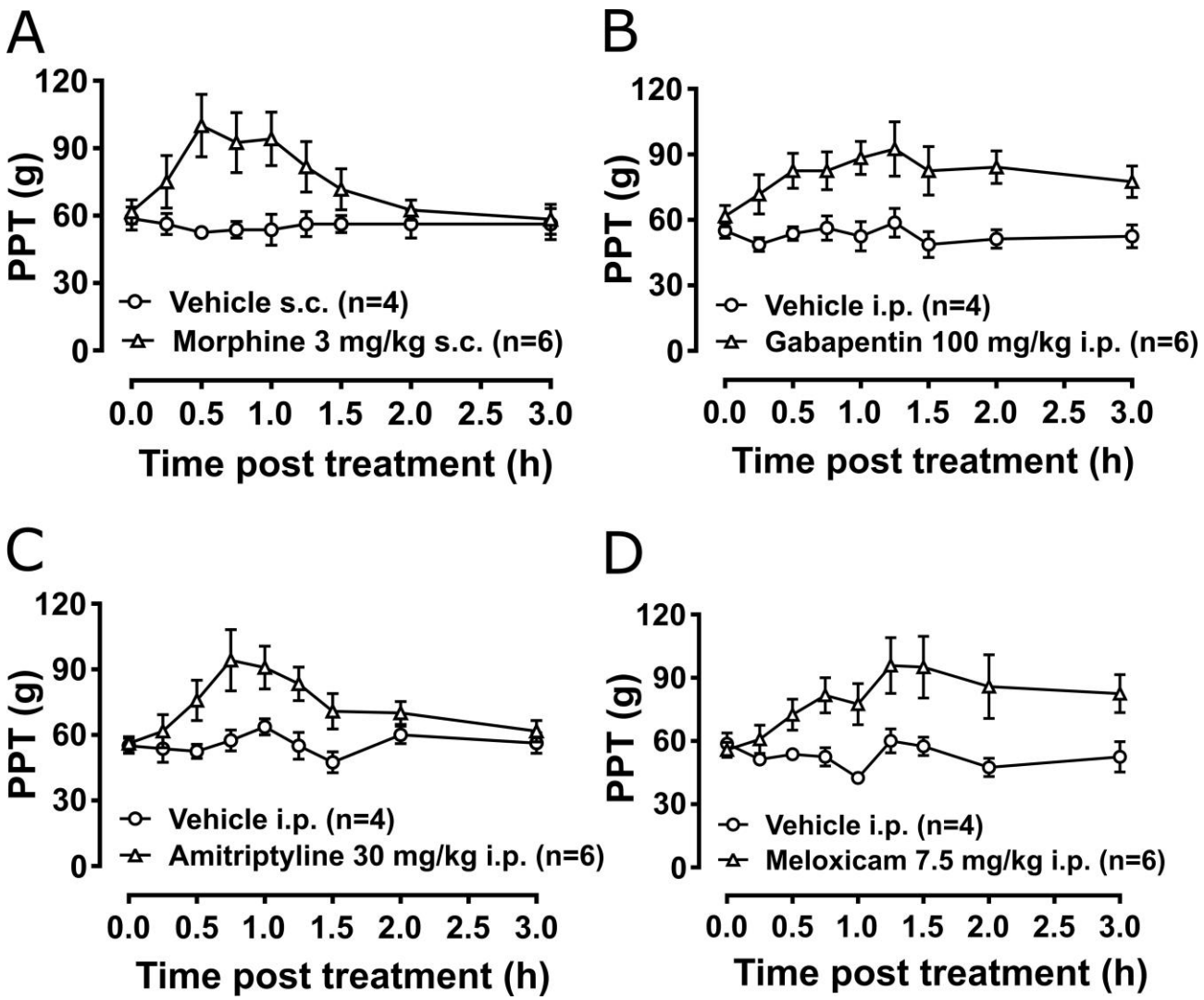

Figure 2.10. Temporal changes in the paw pressure thresholds (PPTs) of BCIBP rats in the ipsilateral hindpaws following administration of single bolus doses of analgesic and adjuvant drugs. Panels in the figure show temporal changes in mean (±SEM) PPT versus time curves following injection of (A) morphine, (B) gabapentin, (C) amitriptyline and (D) meloxicam.

Table 2.4. Extent and duration of anti-hyperalgesia (ΔPPT AUC).

Test compound and route of administration	**Time (h)**		**Mean ΔPPT at peak effect (g)**		**ΔPPT AUC (g.h)**	
	Peak effect	**~Duration of action**	**Ipsilateral**	**Contralateral**	**Ipsilateral**	**Contralateral**
Morphine (s.c.)						
3 mg/kg			40 (± 11.62)	36.7 (± 10.88)	49.5 (± 17.28)*	46.7 (± 17.21)*
Vehicle	0.5	2	NA	NA	10.0 (± 4.18)	9.2 (± 4.85)
Gabapentin (i.p.)						
100 mg/kg			32.5 (± 10.7)	30.8 (± 10.60)	64.2 (± 19.79)	61.8 (± 18.71)
Vehicle	1.25	>3	NA	NA	9.7 (± 3.48)	5.4 (± 3.35)
Amitriptyline (i.p.)						
30 mg/kg			38.9 (± 14.55)	36.7 (± 13.42)	54.7 (± 17.69)	53.3 (± 17.30)
Vehicle	0.75	2	NA	NA	11.6 (± 2.36)	10.5 (± 3.69)
Meloxicam (i.p.)						
7.5 mg/kg			41.7 (± 14.64)	38.6 (± 13.22)	85.0 (± 33.62)	82.0 (± 32.52)
Vehicle	1.25 – 1.5	>3	NA	NA	8.1 (± 4.69)	4.1 (± 4.06)

NA, not applicable; *p<0.05 (Mann-Whitney test) *c.f.* rats that received single bolus doses of vehicle

2.4.6. Tibial bone µCT scan

The aim of these experiments was to assess the effect of inoculation of W256 cells in the tibiae of BCIBP rats, compared to the corresponding sham rats. Significant decreases in the BV/TV ratio and in $T_b.N$, coupled with an increase in the $T_b.S_p$ were indicative of tumour induced osteolysis in the W256 cell injected tibiae.

2.4.6.1. Experiments 8 and 9

The 3D- µCT radiological images and 2D-trabecular bone images of rats were obtained at day 10 post-ITI (Figure 2.11A-D) and day 48 post-ITI (Figure 2.11I-L).

2.4.6.1.1. Bone volume / total volume (BV/TV ratio)

The BV/TV ratios for the proximal diaphyseal regions of tibiae from rats given an ITI of 4 x 10^5 W256 cells and euthanized on day 10 (Figure 2.11E) ($F_{(1, 1, 1/4)} = 11.0, 0.03, 0.2$; $p \leq 0.05$) and day 48 (Figure 2.11M) ($F_{(1, 1, 1/4)} = 11.0, 0.03, 0.2$; $p \leq 0.05$) post-ITI, were significantly lower *c.f.* rats given an ITI of 4 x 10^5 HK W256 cells and euthanized at the respective time points.

2.4.6.1.2. Trabecular thickness ($T_b.T_h$)

The $T_b.T_h$ of the proximal diaphyseal regions of tibiae from rats given an ITI of 4 x 10^5 W256 cells and euthanized at day 10 (Figure 2.11F) ($F_{(1, 1, 1/4)} = 2.1, 167.9, 230.2$; $p > 0.05$) or day 48 (Figure 2.11N) ($F_{(1, 1, 1/4)} = 2.1, 167.9, 230.2$; $p > 0.05$) post-ITI did not significantly change *c.f.* rats given an ITI of 4 x 10^5 HK W256 cells and euthanized at the respective time points.

2.4.6.1.3. Trabecular spacing ($T_b.S_p$)

The $T_b.S_p$ of the proximal diaphyseal regions of tibiae of rats given an ITI of 4 x 10^5 W256 cells and euthanized at day 10 (Figure 2.11G) ($F_{(1, 1, 1/4)} = 21.1, 4.9, 0.1$; $p \leq 0.05$) and day 48 (Figure 2.11O) ($F_{(1, 1, 1/4)} = 21.1, 4.9, 0.1$; $p \leq 0.05$) post-ITI was significantly higher *c.f.* rats given an ITI of 4 x 10^5 HK W256 cells and euthanized at the respective time points.

2.4.6.1.4. Trabecular number ($T_b.N$)

The $T_b.N$ ratio of the proximal diaphyseal regions of tibiae of rats given an ITI of 4 x 10^5 W256 cells and euthanized at day 48 (Figure 2.11P) post-ITI was significantly ($F_{(1, 1, 1/4)} = 9.0, 0.6, 0.007$; $p \leq 0.05$) lower than that for rats given an ITI of 4 x 10^5 HK W256 cells on day 48 post-ITI. By contrast, for rats euthanized on day 10 (Figure 2.11H) post-ITI, the ratio was not significantly different ($F_{(1, 1, 1/4)} = 9.0, 0.6, 0.007$; $p > 0.05$) from that of rats given an ITI of 4 x 10^5 HK W256 cells and euthanized at day 10 post-ITI.

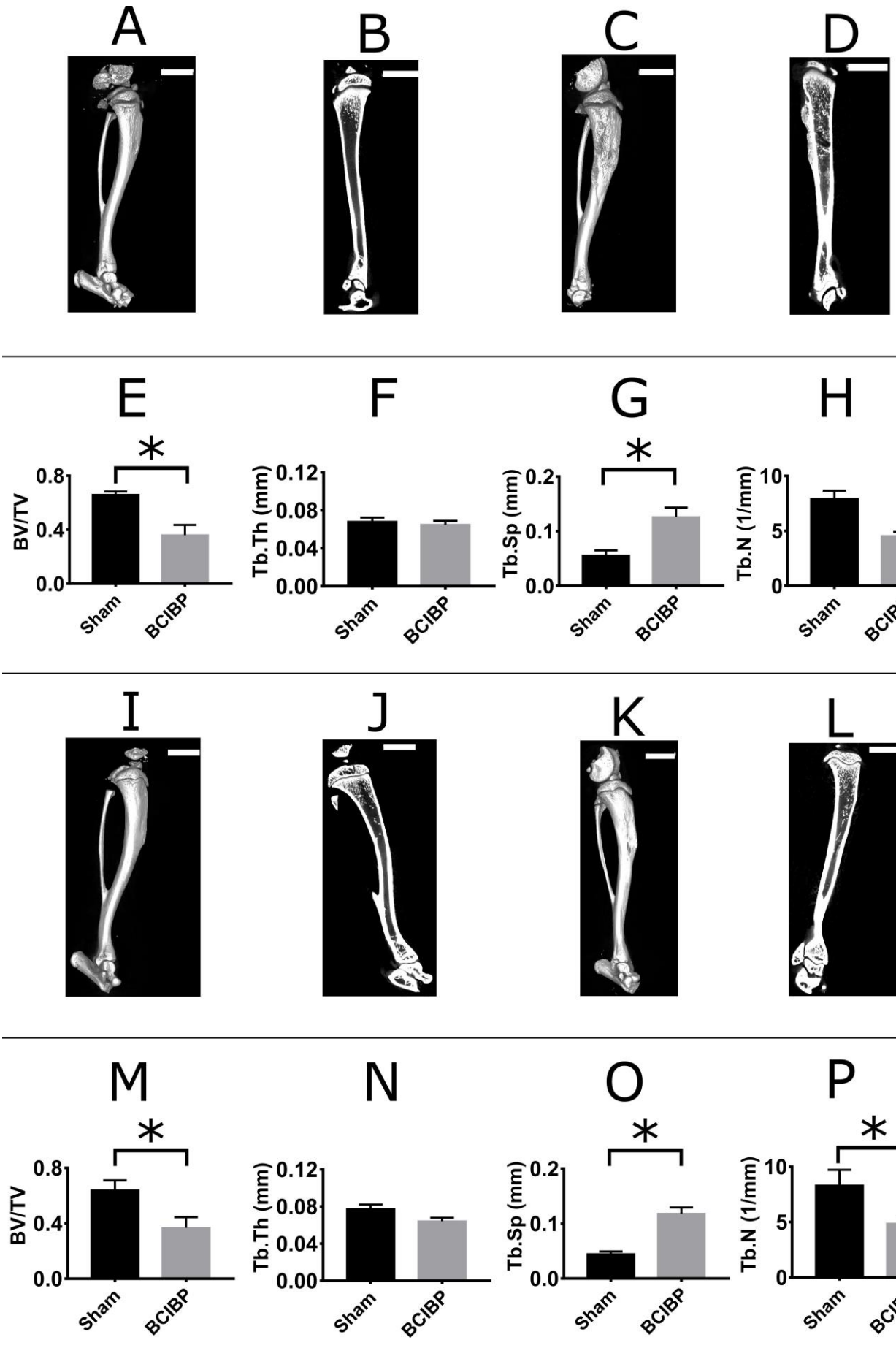
A
B
C
D
E
F
G
H
*
BV/TV
0.8
0.4
0.0
Tb.Th (mm)
0.12
0.08
0.04
0.00
Tb.Sp (mm)
0.2
0.1
0.0
Tb.N (1/mm)
10
5
0
Sham
BCIBP
I
J
K
L
M
N
O
P

Figure 2.11. Radiological assessment of tibiae from BCIBP rats and the corresponding sham rats. Panels in the figure show (A) 3D-µCT radiological image of a sham rat's tibia at day 10 post-ITI, (B) trabecular bone of a sham rat's tibia at day 10 post-ITI, (C) 3D-µCT radiological image of a BCIBP rat's tibia at day 10 post-ITI, (D) trabecular bone of a BCIBP rat's tibia at day 10 post-ITI, (E-H) morphometric changes in BCIBP rats' tibiae relative to sham rats' tibiae at day 10 post-ITI, (I) 3D-µCT radiological image of a sham rat's tibia at day 48 post-ITI, (J) trabecular bone of a sham rat's tibia at day 48 post-ITI, (K) 3D-µCT radiological image of a BCIBP rat's tibia at day 48 post-ITI, (L) trabecular bone of a BCIBP rat's tibia at day 48 post-ITI, (M-P) morphometric changes in BCIBP rats' tibiae relative to sham rats' tibiae at day 48 post-ITI. *$p<0.05$ (Two-way ANOVA, *posthoc* Bonferroni test). Scale bar – 5 mm.

2.4.7. Tibial bone histology

2.4.7.1. Experiments 8 and 9

Histological assessment of H&E stained sections showed marked osteolytic lesions due to bone destruction and immature *de novo* formation of bone in the proximal diaphyseal regions of the ipsilateral tibiae from groups of rats that had received a unilateral ITI of 4 x 10^5 W256 cells at both day 10 (Figure 2.12B) and day 48 (Figure 2.12D) post-ITI. There were no such changes evident in the tibiae of sham-rats that had received a unilateral ITI of 4 x 10^5 HK W256 cells and euthanized at the respective time points (Figure 2.12A and 2.12C).

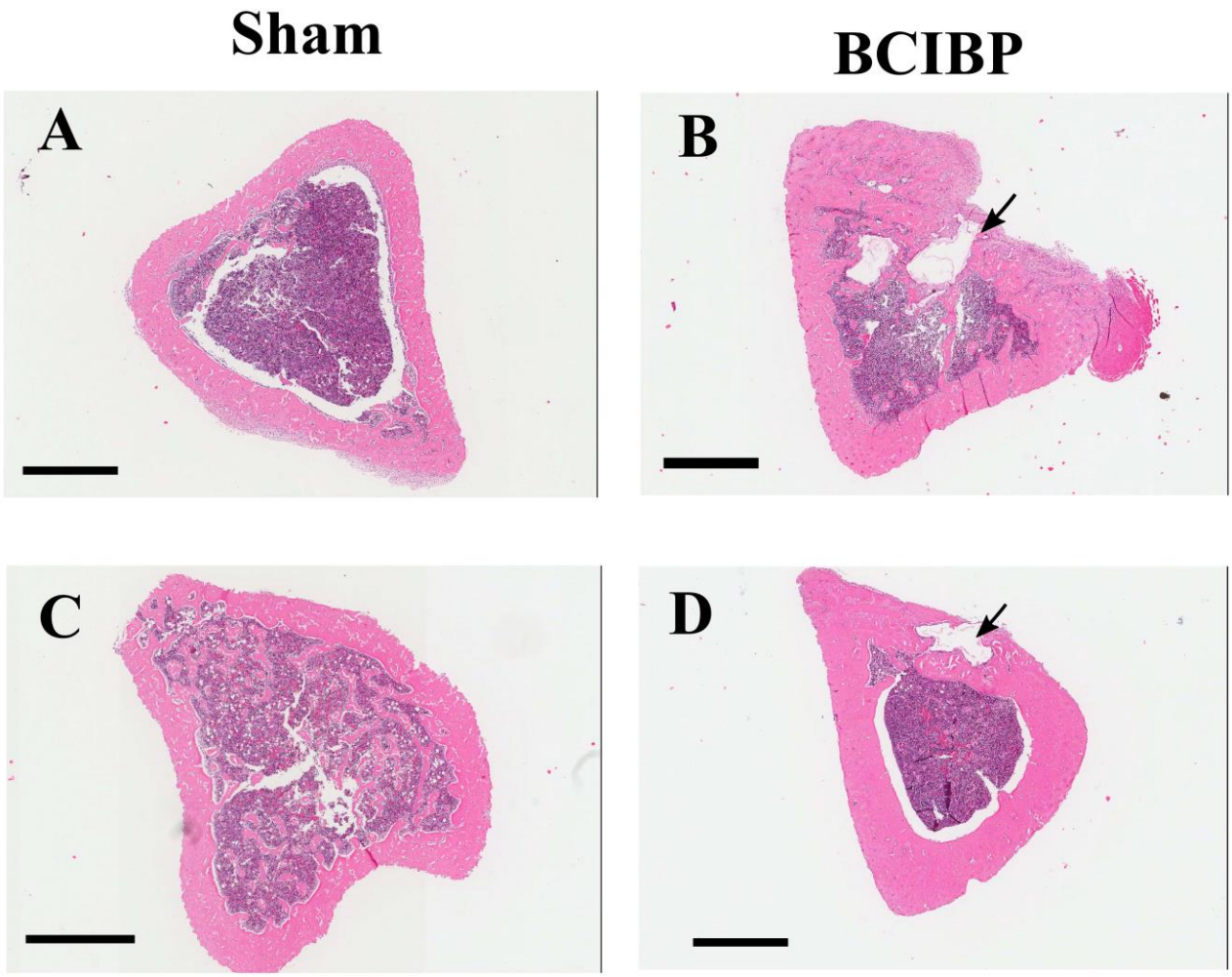

Figure 2.12. Histological assessment of tibiae from BCIBP rats and corresponding sham rats. Panels in the figure show representative images of H&E staining of tibial sections of (A) sham rat at day 10 post-ITI, (B) BCIBP rat at day 10 post-ITI, (C) sham rat at day 48 post-ITI and (D) BCIBP rat at day 48 post-ITI. Black arrowheads show destruction of cortical bone of tibiae. Scale bar – 1 mm.

2.4.8. Immunocytochemistry of W256 cells: Cytokeratin 18

Using the anti-Cytokeratin 18 antibody [C04] (Alexa Fluor® 488) ab187573 (Abcam), cultured and fixed W256 cells showed immunofluorescent staining (Figure 2.13) which was in accord with Cytokeratin 18 expression in ATCC W256 cells reported by others (Lewis et al., 2013). Similar results were obtained with anti-Cytokeratin 18 antibody [C-04] ab668 (Abcam) which was used as a second confirmatory antibody (Supplementary Figure 2.9).

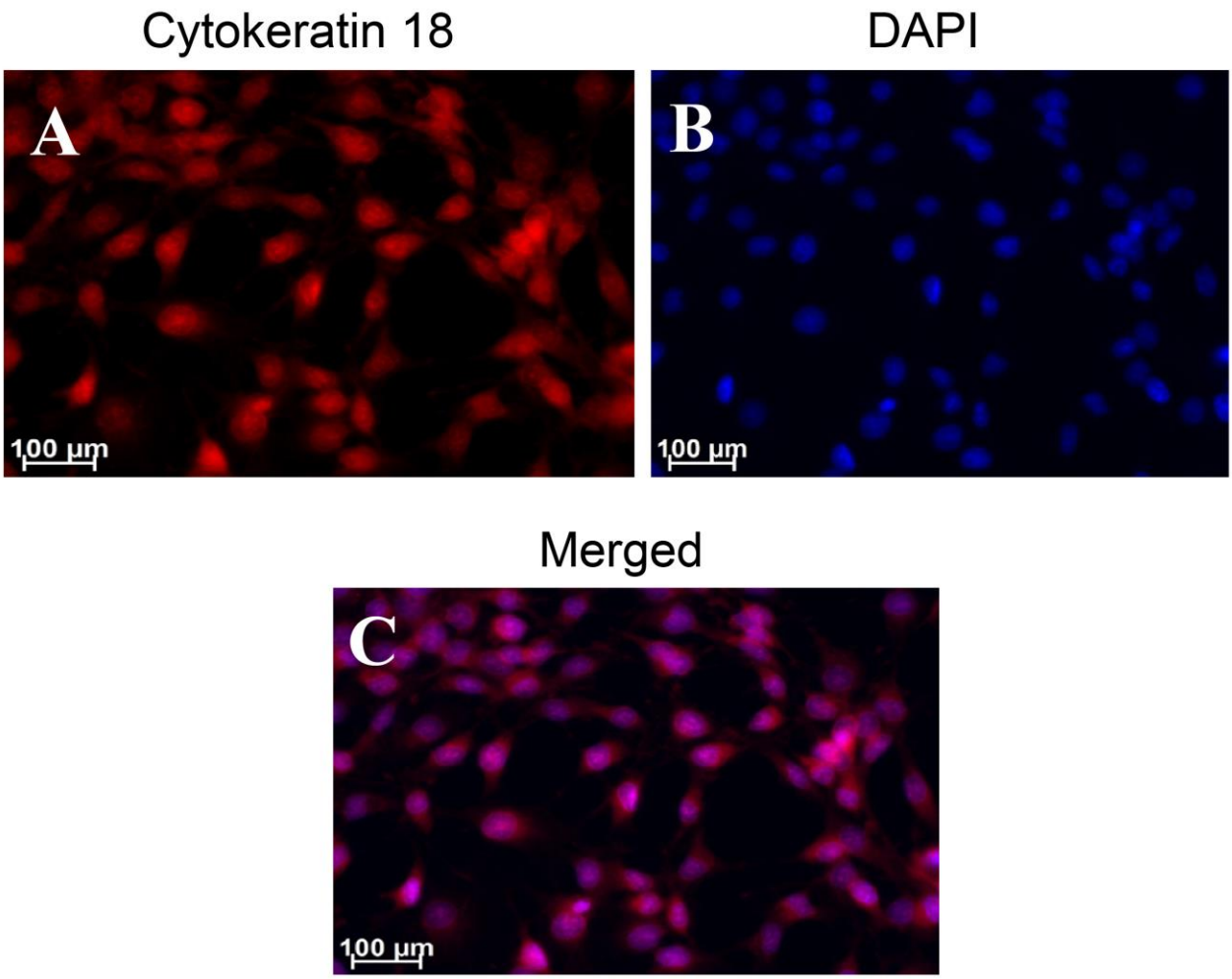

Figure 2.13. Immunocytochemical staining of the Walker 256 cell line for Cytokeratin 18 using the ab187573 (Abcam) antibody. Panels in the figure show (A) cytokeratin 18 (B) DAPI and (C) A and B merged.

2.4.9. Tibial bone immunohistochemistry

2.4.9.1. Experiment 15 and 16

The presence of W256 cancer cells in longitudinal sections of the ipsilateral tibiae from rats given these cells by unilateral ITI was confirmed by immunohistochemical staining using the anti-Cytokeratin 18 antibody [C04] (Alexa Fluor® 488) ab187573 (Abcam). Cytokeratin 18 immunofluorescence was observed in sections from BCIBP-rats' tibiae collected on both day 7 (Figure 2.14B) and day 38 (Figure 2.14D) after unilateral ITI of 4 x 10^5 W256 cells. Importantly, in the corresponding tibial sections from sham-rats administered a unilateral ITI of 4 x 10^5 HK W256 cells, specific immunofluorescence for Cytokeratin 18 was absent at both time points (Figure 2.14A and 14C). Similar results were obtained with another anti-Cytokeratin 18 antibody ([C-04] ab668 (Abcam)) in the experiment that was used as a confirmatory step (Supplementary Figure 2.10).

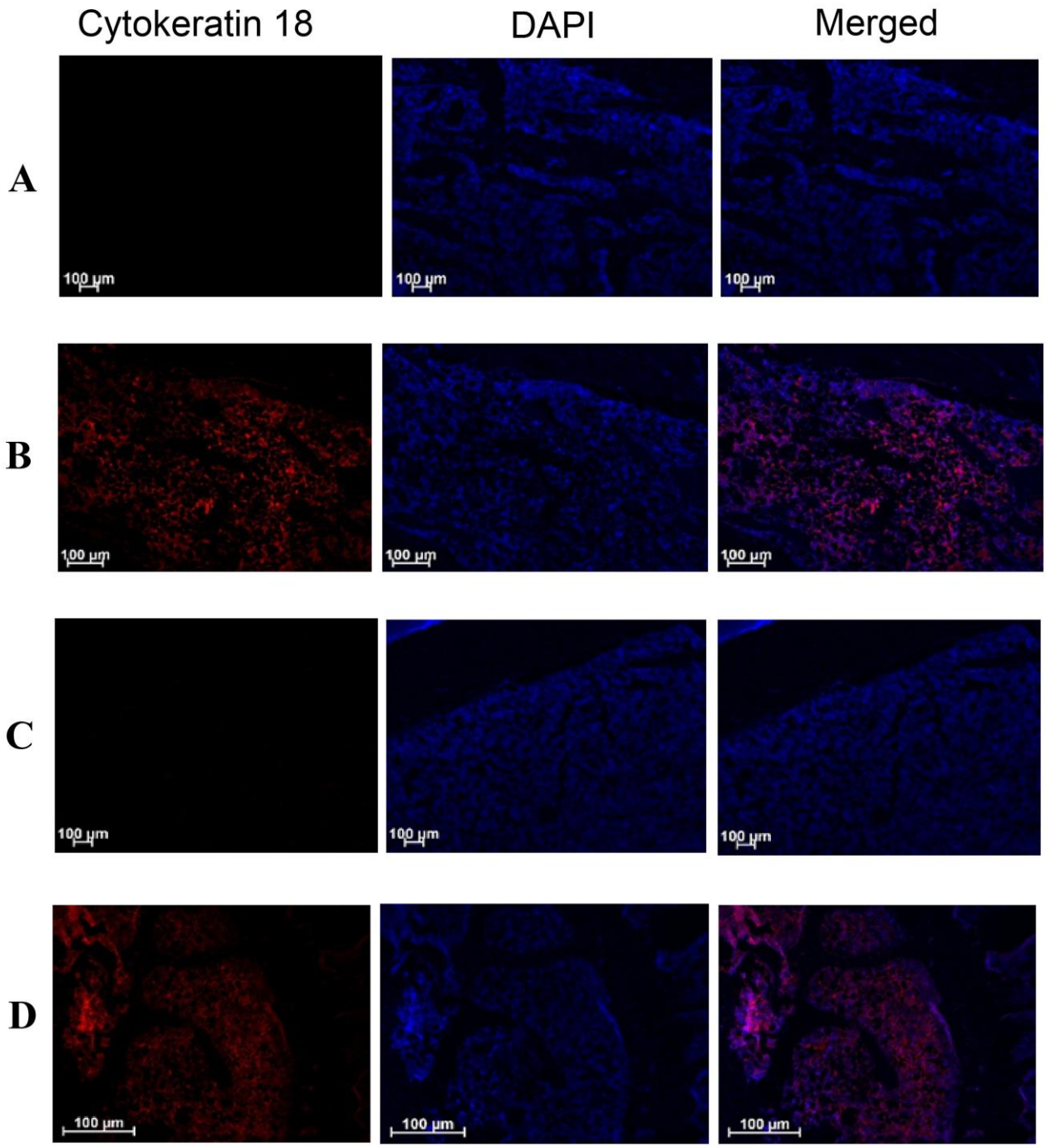

Figure 2.14. Immunohistochemical staining of Cytokeratin 18 in tibial sections of BCIBP rats and the corresponding sections from sham rats using the ab187573 (Abcam) antibody. Panels in the figure show immunofluorescence imaging of tibial sections of (A) sham rat at day 7 post-ITI, (B) BCIBP rat at day 7 post-ITI, (C) sham rat at day 38 post-ITI and (D) BCIBP rat at day 38 post-ITI.

2.5. Discussion

In the present study, we have established an optimized model of breast cancer-induced bone pain in rats successfully and have comprehensively characterized the model using behavioural, radiological, pharmacological, histological and immunohistochemical methods. Our optimised model successfully addresses the issue of poor general animal health that is a major limitation of previously described models. Using female Wistar Han rats, we are the first to show that the severity (magnitude/extent) of Walker 256 cell-induced mechanical allodynia and mechanical hyperalgesia, is directly correlated with the initial number of cancer cells inoculated in the tibiae. Following unilateral ITI of W256 cells, rats in the present study developed bilateral mechanical allodynia and mechanical hyperalgesia, which is the most common manifestation in CIBP (Paley et al., 2011). Cancer-induced bone destruction was observed in the tibiae of rats using both radiological and histological assessments, in concordance with osteolytic changes seen in patients with breast cancer metastases to the skeleton (O'Sullivan et al., 2015, Woolf et al., 2015). The model was also found to be suitable for screening of analgesic drugs with diverse mechanisms of action.

Animal models involving injection of cancer cells in bone are commonly used in experimental research to study pathophysiological mechanisms of pain hypersensitivities and disease progression (Kaan et al., 2010, Liu et al., 2016, Taipaleenmäki et al., 2015, Torrano et al., 2016, Graham et al., 2014). Using mice and rats of different ages, weight ranges, sexes, strains and various breeding and housing conditions, CIBP studies employ a wide variety of cultured cancer cell lines including lung cancer (e.g. Lewis Lung), prostate cancer (e.g. PC3N, ACE-1, AT-3), breast cancer (e.g. 66.1, 4T1, MDA-MB-231, MDA-MB-231-TXSA, MRMT1), colon cancer (e.g. Colon-26), osteosarcoma (NCTC 2472) and fibrosarcoma (e.g. MC57G) (Slosky et al., 2015, Pacharinsak and Beitz, 2008, Falk and Dickenson, 2014, Lozano-Ondoua et al., 2013b, Currie et al., 2013, Currie et al., 2014). These cell lines which are injected into the tibia, humerus, femur and calcaneus in various CIBP studies (Falk and Dickenson, 2014) can give rise to distinct pain behaviours and neurochemical changes (Sabino et al., 2003). The features of any given animal model of CIBP thus require characterisation using standardised protocols to reduce the number of variables affecting the experiments to enhance experimental reproducibility. In the present work, W256 cells were selected as they are widely used in research (Brigatte et al., 2007, Justice, 1985) and because of the ease with which they can be cultured, standardised and reproduced (McEuen and Thomson, 1933, Hang et al., 2015b). A comparative summary of previous studies using the W256 cell-induced bone pain model in rats, has been comprehensively provided in a recent review (Shenoy et al., 2016).

Until recently, the animal models of CIBP involved injection of cancer cells systemically, which resulted in deterioration of the overall animal health due to metastases to vital organs like the lungs, liver, brain and throughout the skeleton (Urch, 2004, Simmons et al., 2015). In CIBP models based upon the ITI of cancer cells, distant metastases can occur due to the cells escaping from the drilled hole or due to osteolysis of the bones, leading to severe degradation of the animal health and loss of body weight (Muralidharan et al., 2013). Hence, it is very important that all of the animals involved in the CIBP studies are closely monitored throughout the experimental period. Our work herein is the first to systematically assess and document clinical health parameters in animals following ITI of W256 cells. We carefully monitored all animals and found that the number with deteriorated health was very low. Such animals were immediately excluded from the experiments and were humanely euthanized for ethical reasons.

We used changes in threshold values (PPTs) as indicative of mechanical hyperalgesia. Going by the technical definition of hyperalgesia, there might be a component of allodynia in the PPT response, unless the stimulus is painful from the get-go. One of the possible reasons why researchers commonly use this 'threshold' method for hyperalgesia assessment could be that it is ethically not quite acceptable to burden the hindpaws of the rat (already in pain) with a noxious stimulus from the get-go. While slowly ascending the force on the hindpaws of the animal gives that animal the freedom to voluntarily withdraw the paw as soon as the pain becomes unbearable or the operator can intervene and unload the paw as soon as the animal shows signs of struggle. Hence, assessement of mechanical allodynia (Ke et al., 2013, Dong et al., 2011, Bu et al., 2014, Xia et al., 2014, Bao et al., 2014a) and mechanical hyperalgesia (Al-Rejaie et al., 2015, Whiteside et al., 2004, Ferrari et al., 2017, Zambelli et al., 2017, Griggs et al., 2016) in terms of changes in threshold values (PWTs and PPTs) is a well established and common practice in the preclinical pain research field. Interestingly, mechanical hypersensitivity also developed in the contralateral hindpaws of rats given a unilateral ITI of W256 cells, although it was less intense than that evoked in the ipsilateral hindpaws. We are the first to show that the number of Walker 256 cells injected in the tibiae is an important experimental manipulation influencing the nature of pain hypersensitivities developed. With lower number of cells inoculated, the pain hypersensitivities developed are unilateral in nature (developed in ipsilateral hindpaws). By increasing the number of cells, pain hypersensitivities become bilateral in nature (in both ipsilateral and contralateral hindpaws). Peripherally acting mechanisms like the involvement of circulating factors and transmedian sprouting, or centrally acting mechanisms like signalling through the commissural interneurons of the spinal cord could be the cause of contralateral mirror effects associated with unilateral injury (Koltzenburg et al., 1999). These contralateral effects could also be associated with activation of spinal glial cells and

proinflammatory cytokine secretion, as well as morphological changes in the local tibial nerves, similar to effects that have been reported in a model of sciatic inflammatory neuritis (Chacur et al., 2001). Inoculation of breast cancer cells in bones is known to produce massive sprouting of sensory nerve fibres of the periosteum in rodent models of CIBP (Bloom et al., 2011). Noxious inputs persistently coming from the periphery can affect the pain circuitry causing bilateral hypersensitivity via the descending pain control system (Ikeda et al., 2007, Meeus and Nijs, 2007). Thermal hyperalgesia did not develop in rats given a unilateral ITI of W256 cells. The absence of thermal hyperalgesia is in contrast to pain behaviours observed after ITI of AT3B prostate cancer cells (Muralidharan et al., 2013), suggesting that tumour-specific interactions with the bone environment and/or peripheral nerves innervating the bone contribute to this difference. Thermal and mechanical pain behaviours are known to be underpinned by diverse mechanisms (Paqueron et al., 2003, Wang et al., 2012a). Nociceptors present in the skin are sensitized by thermal stimuli, while the nociceptors which are deeply situated in the somatic tissues like joints and muscle are highly sensitive to mechanical stimuli (Schaible, 2007).

After approximately three weeks post-surgery, the mechanical allodynia and mechanical hyperalgesia in the hindpaws of rats administered a unilateral ITI of W256 cells spontaneously resolved and this state was maintained until the end of the study. While all the existing studies using this model typically assess the pain behaviors only until around 20-25 days after injection of cancer cells, our findings are the first to successfully investigate the model for up to 66 days and to show that W256 cell-induced bone pain can apparently resolve spontaneously at later stages despite the ongoing presence of cancer cells, similar to the clinical situation in humans. The beginning of resolution of pain hypersensitivity behaviour around 20–25 days after surgery in this model has been observed in other studies, although these studies only assessed pain behaviors until 20-25 days (Zhao et al., 2010, Xu et al., 2013, Huang et al., 2014). A similar spontaneous reversal of mechanical hypersensitivity has been reported in rats administered a unilateral ITI of MRMT-1 cells in a BCIBP model (Falk et al., 2015b). Cancer metastases to bones without clinical pain or other symptoms is not uncommon (Phanphaisarn et al., 2016, Costelloe et al., 2009). In a recent retrospective patient record study involving 1105 women with breast cancer skeletal metastases, it was found that the burden of symptoms including pain decreased after the diagnosis of bone metastases, although there was no substantial increase in use of analgesic medication after the diagnosis of bone metastases compared to the scenario before the diagnosis (Cleeland et al., 2016). In this study, only a small proportion of patients (~ 16 %) were newly introduced to analgesic medications or had the dose of their existing medications increased after the diagnosis of bone metastases. These observations are consistent with the notion that the human body has endogenous

pain-relieving mechanisms in place to attenuate pain due to progression of metastatic disease and so limit the presentation of symptoms.

The work presented herein is the first to use histology, radiology and immunohistochemistry to provide evidence that the cancer disease remains persistent in the rat tibiae, despite apparent resolution of pain hypersensitivities at later stages of this model. We chose immunohistochemistry as a technique to stain tibial sections, because it provides direct evidence of the presence of cancer cells (Slade and Coombes, 2007). The presence of cancer cells in the tibiae during both the pain state and the resolved-pain state was confirmed with immunohistochemical staining of Cytokeratin 18. Endogenous opioids potentially play a very important role in cancer pain attenuation (Zhao et al., 2016, Lesniak et al., 2016, Roques et al., 2012). We administered naloxone, which is a non-selective antagonist of opioid receptor (van Dorp et al., 2007), to assess whether similar mechanisms might contribute in the present model and we are the first to show that naloxone rescued the pain phenotype. The observed re-emergence of pain behaviours after naloxone administration not only further supports the continued presence of tumour cells in bone, but also supports the hypothesis that the endogenous opioid system could be at least partially responsible for the spontaneous resolution of pain hypersensitivity. A CIBP model involving an ITI of prostate cancer cells in rats showed similar spontaneous resolution of pain due to endogenous opioid-sensitive mechanisms (Muralidharan et al., 2013). Studies in mice using osteosarcoma-induced bone pain model also showed such a spontaneous resolution of hypersensitivity in the hindpaws that was unmasked by administration of naloxone to reverse the analgesia produced by endogenous opioids (Baamonde et al., 2006, Menendez et al., 2003). Similarly, several other studies have found that the endogenous opioid system might play a key role in resolution of cancer pain hypersensitivities (Menendez et al., 2008, Sevcik et al., 2006). While endogenous opioid-sensitive mechanisms have been implicated in the resolution of cancer pain in a number of studies (Li et al., 2016), involvement of other complex neuroimmune mechanisms is also possible. For instance, lipoxins and endogenous lipoxygenase-derived eicosanoids – members of the lipid mediators class with a wide spectrum of effects against inflammation and nociception– suppress the spinal expression of pro-inflammatory cytokines and might also be partially responsible for spontaneous resolution of W256 cell-CIBP in this model (Hu et al., 2012c).

One of the reasons for resolution of pain hypersensitivities in this model could be phenotypic changes in the cancer cells growing in the bone marrow. Remodeling of bone (Bloom et al., 2011), physical outgrowth of tumor and interaction with the nerves (Schmidt, 2014), along with the production of algogenic substances secreted by cancer cells colonized in the bone (Tong et al.,

2010b) can contribute to the pain hypersensitivities. The resolution of hypersensitivities could be a consequence of endogenous counteraction at any of these mechanistic levels. To test whether cancer cells have changed their phenotype, a comparative proteomic assessment of cancer cells grown in *in vitro* culture with the cells colonizing the bone at the resolved pain-state would need to be performed. While the continued presence of tumour load was confirmed by immunohistochemical analysis at a state when the pain hypersensitivity was resolved in this model, elimination of cancer cells could also contribute to the observed resolution of pain behaviours. The phenomenon of breast cancer regression is well-known in humans (Lewison, 1976, Hutter, 1982, Burnside et al., 2006, Barry, 2009, Onuigbo, 2012). Similarly, W256 breast cancer cells also have the potential to transform into a variant known for its regression *in vivo* (Guimarães et al., 2010), causing cancer regression with the prolonged duration of the study (Jensen and Muntzing, 1970, Cavalcanti et al., 2003, Schanoski et al., 2004).

Our present work is the first to pharmacologically characterize the W256 cell-induced bone pain model in rats and to show that the model is responsive to clinically used analgesic drugs that have different mechanisms of action. Morphine, gabapentin, amitriptyline and meloxicam are important drugs representing diverse analgesic drug classes used in treating cancer pain (Mantyh et al., 2002). Morphine, an agonist predominantly at the μ-opioid (MOP) receptor, is one of the most important members of the strong opioid analgesic class (Cao et al., 2010). All three major opioid receptor types (μ, δ, κ) belong to the superfamily of G_i /G_o -protein-coupled receptors (McDonald and Lambert, 2005). Opioid agonists enhance the opening of GIRK channels (Ikeda et al., 2000); inhibit the opening of voltage-gated calcium channels, and inhibit cAMP production by adenylate cyclase. The net effect is inhibition of nociception (Rosenblum et al., 2008). The $ED_{50\text{-Ipsilateral}}$ of morphine in this model (1.3 mg/kg) was found to be higher than that in a cisplatin induced peripheral neuropathy model (0.8 mg/kg; s.c.) (Han et al., 2014a), similar to that in a neuropathic pain model of spared nerve injury (1.2 mg/kg; s.c.) (Zhao et al., 2004), but lower than that in nociceptive paw pressure test (2.8 mg/kg; s.c.) (Morgan et al., 2006) in rats. Our findings are aligned with others who showed that morphine is effective in alleviating pain hypersensitivities in this model (Guo et al., 2017, Liu et al., 2017a). In other studies, mRNA and protein levels of μ-opioid receptors in the spinal dorsal horn and dorsal root ganglia of rats were reduced following unilateral ITI of W256 cells in this model (Yao et al., 2016, Hou et al., 2017). Gabapentin is used in both epilepsy and neuropathic pain. It inhibits calcium currents via high-voltage-activated channels containing the $\alpha_2\delta$-1 subunit, and decreases the excitatory neurotransmitter glutamate and increases the inhibitory neurotransmitter GABA, thereby reducing the excitability (Sills, 2006). Other mechanisms have also been proposed including modest actions on voltage gated potassium channels (Sills, 2006). The $ED_{50\text{-Ipsilateral}}$ of

gabapentin in this model (47.1 mg/kg) was higher than that reported in a neuropathic pain model of spinal nerve ligation (34 mg/kg; i.p.) in rats (Hunter et al., 1997). Tricyclic antidepressant drugs such as amitriptyline are also used as analgesic adjuvant drugs, which augment descending noradrenergic inhibition and are utilised for the management of neuropathic pain conditions (Tura and Tura, 1990). NSAIDs (Non-steroidal anti-inflammatory drugs) such as meloxicam inhibit COX, the enzyme responsible for the conversion of arachidonic acid into prostaglandin H_2, which is an initial step in the synthesis of PGE2, a mediator of inflammation. At therapeutic doses, meloxicam has modest selectivity for inhibition of COX-2 over COX-1 (Noble and Balfour, 1996). The $ED_{50\text{-}Ipsilateral}$ of morphine and gabapentin in our optimized model (1.3 and 47.1 mg/kg, respectively) were lower than that reported in prostate CIBP model (1.9 and 78.0 mg/kg, respectively), whereas the $ED_{50\text{-}Ipsilateral}$ of amitriptyline and meloxicam (20.1 and 3.9 mg/kg, respectively) were higher than that determined in the prostate CIBP model (14.9 and 2.6 mg/kg, respectively) in rats (Muralidharan et al., 2013). Morphine, gabapentin, amitriptyline and meloxicam produced dose-dependent analgesia in our optimized rat model of BCIBP, with each of the drugs having a unique pharmacological profile in terms of extent and duration of action and time of peak effect. Considering the ED_{50} doses (mg/kg), the potency rank order was: morphine > meloxicam > amitriptyline > gabapentin. Hence, our model was found to be suitable for assessing the pain-relieving effects of compounds from diverse pharmacological drug classes that are used clinically to alleviate CIBP. It is worth mentioning that molecular assessments were not performed to confirm that the analgesic effects produced by these standard drugs in this model were mediated by their putative modes of action. Only morphine, gabapentin, amitriptyline and meloxicam- the drugs which are well-known to produce analgesia in humans with cancer pain, were tested in this work. However, further validation of the model could be performed by testing of drugs not effective in relieving pain in humans, so as to estimate the false positive rate. Nevertheless, anti-hypersensitivity effects were not observed in any of the vehicle control groups that were included in each of these experiments.

Pain is one of the major problems in cancer patients having metastases to their bones (Tsuzuki et al., 2016). CIBP is a complex pathological manifestation of inflammatory, neuropathic and cancer-specific or tumorigenic components (Cao et al., 2010). Efficient preclinical models of cancer-induced bone pain are essential to understand the underlying complexities and to assist in the drug discovery processes aimed at identifying novel compounds for relieving the debilitating pain (Blouin et al., 2005). In the present work, we systematically injected a number of different concentrations of W256 cells in a rat model and assessed the health characteristics of the animals. The development of pain hypersensitivity depended upon the initial number of cells inoculated,

while excellent animal health was maintained at all cell numbers assessed. Analogous to clinical practice, we used radiological and histological techniques to evaluate cancer-induced bone changes (Mertens et al., 1998, Menezes and Ahmed, 2014, Heck et al., 2006) and found profound osteolysis. This observation is in contrast to prostate cancer metastases to bones, in which mixed osteolytic-osteogenic bone lesions are formed with osteosclerotic effects predominating in both the clinic and the animal models (Muralidharan and Smith, 2013, Ibrahim et al., 2010). Although the cancer cells were still present in the tibiae of animals herein, the hindpaw hypersensitivity of rats resolved at later stages of the model and the endogenous opioid system was at least partially responsible for this spontaneous pain resolution. We performed detailed pharmacological profiling using standard analgesic drugs used to treat CIBP in the clinical setting and found that this model could be useful to assess novel analgesic compounds with diverse mode of actions.

Supplementary Table 2.1. Mean (±SEM) values of behavioural tests of rats given an ITI of HK cells as a control for lack of pain hypersensitivity.

Experiment no.	Day post-ITI	Mean PWT (g)		Mean PPT (g)		Mean PTT (sec)	
		Ipsi	Contra	Ipsi	Contra	Ipsi	Contra
7	21	-	-	-	-	13.3 (± 0.25)	13.5 (± 0.49)
10	8 13	10 11.3	11.3 12	-	-	-	-
11	8 10 15	10.7 10.7 10	11.3 10.7 10.7	-	-	-	-
12	7 9 11 14	11.3 11.3 12 12	12 10.7 12.7 12.7	-	-	-	-
13	7 9 12	10.7 11.3 10.7	12 12 12	-	-	-	-
14	7 10 12 14	-	-	115 111.7 116.7 110	125 116.7 123.3 116.7	-	-

Contra, contralateral hindpaws; Ipsi, ipsilateral hindpaws; -, not assessed

Supplementary Table 2.2. Mean (±SEM) values of baseline behavioural tests of rats prior to surgeries / ITI.

Experiment no.	**Mean pre-surgery baseline PWT (g)**				**Behavioural test value; unit**
	W256 cells' group		**HK cells' group**		
	Ipsi	**Contra**	**Ipsi**	**Contra**	
7	12.9 (± 0.65)	13.1 (± 0.79)	10.8 (± 0.51)	11.7 (± 0.16)	PTT; sec
10	10.1 (± 0.28)	10.5 (± 0.24)	9.3	10	PWT; g
11	10.2 (± 0.25)	10.7 (± 0.23)	9.3	10	PWT; g
12	10.6 (± 0.31)	10.7 (± 0.40)	10.7	11.3	PWT; g
13	10.5 (± 0.37)	10.3 (± 0.38)	11.3	10.7	PWT; g
14	102.1 (± 2.41)	104.8 (± 2.55)	105	108.3	PPT; g

Contra, contralateral hindpaws; Ipsi, ipsilateral hindpaws

CD-FM-AN30 Clinical Observation Record

Study No.:_____ Animal Chip No.:_____ Cage No.: _____ Week:_____

Observation	Date/Study Day						
Operator							
Animal Weight (g)							
Mortality							
Moribund							
No abnormalities detected (NAD) (animal is well and healthy)	❐	❐	❐	❐	❐	❐	❐
Grading of Observations: M = Mild; Mo = Moderate; S = Severe							
Skin and Fur							
piloerection							
lack of grooming							
fur loss							
irritation or sores							
Eyes & mucus membranes							
palpebral closure							
eyes cloudy							
ocular or nasal discharge (including chromodacryorrhea)							
excessive salivation							
diarrhoea							
bleeding from orifice							
Respiratory & circulatory function							
increased respiratory rate							
decreased respiratory rate							
gasping							
blueness of extremities							
Gait & posture							
hunched posture or gait							
ataxia							
excessive sway, rocks or lurches							
hind limbs show exaggerated or overcompensated movements, drag or are splayed							
feet point markedly outward from body							
forelimbs drag, are extended or unable to support weight							
walks on tiptoe							
lameness							
Behaviour							
reduced activity levels							
increased activity levels							
circling							
stereotypic grooming							
pacing							
repetitive sniffing							
head weaving							
writhing or flopping							
retropulsion							
straub tail							
self-mutilation / autotomy							
Clonic Tremors or Convulsions							
repetitive movements of mouth and jaws							
quivers of limbs, ears, head or skin							
tremors (mild, moderate or severe)							
myoclonic jerks							
clonic convulsions							
wet dog shakes							
Tonic Tremors or Convulsions							
contraction of extensors							
head and body rigidly arched							
jumps with all feed leaving surface							
severe clonic and /or tonic							
convulsions resulting in dyspnoea, postictal depression or death							
Comments							

Any of the following unexpected observations noted below will be considered as potential humane endpoints for the animal, whereby staff and students must notify the CI/Study Director and the OIC immediately. In the event that the CI/Study Director or the OIC is not immediately contactable, staff and students will euthanize the animal.

(1) Animal is moribund (2) Weight loss > 10% overnight or >20% over 3 consecutive days (3) Two or more "severe" scores are noted in the Clinical Observations

Supplementary Figure 2.1. Form used to record clinical observations in rats.

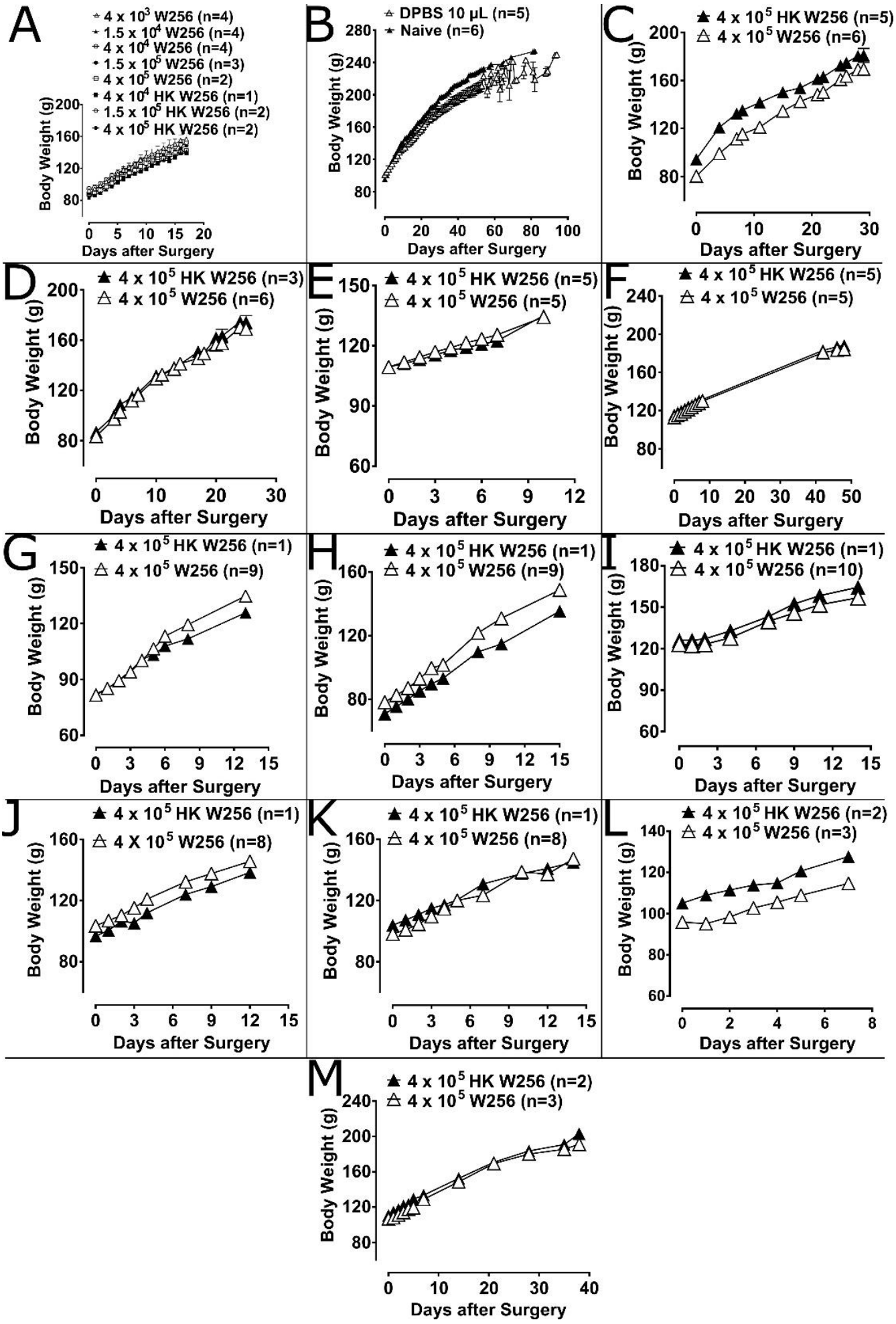
A
4 x 10^3 W256 (n=4)
1.5 x 10^4 W256 (n=4)
4 x 10^4 W256 (n=4)
1.5 x 10^5 W256 (n=3)
4 x 10^5 W256 (n=2)
4 x 10^4 HK W256 (n=1)
1.5 x 10^5 HK W256 (n=2)
4 x 10^5 HK W256 (n=2)
Body Weight (g)
Days after Surgery
B
DPBS 10 µL (n=5)
Naive (n=6)
Body Weight (g)
Days after Surgery
C
4 x 10^5 HK W256 (n=5)
4 x 10^5 W256 (n=6)
Body Weight (g)
Days after Surgery
D
4 x 10^5 HK W256 (n=3)
4 x 10^5 W256 (n=6)
Body Weight (g)
Days after Surgery
E
4 x 10^5 HK W256 (n=5)
4 x 10^5 W256 (n=5)
Body Weight (g)
Days after Surgery
F
4 x 10^5 HK W256 (n=5)
4 x 10^5 W256 (n=5)
Body Weight (g)
Days after Surgery
G
4 x 10^5 HK W256 (n=1)
4 x 10^5 W256 (n=9)
Body Weight (g)
Days after Surgery
H
4 x 10^5 HK W256 (n=1)
4 x 10^5 W256 (n=9)
Body Weight (g)
Days after Surgery
I
4 x 10^5 HK W256 (n=1)
4 x 10^5 W256 (n=10)
Body Weight (g)
Days after Surgery
J
4 x 10^5 HK W256 (n=1)
4 X 10^5 W256 (n=8)
Body Weight (g)
Days after Surgery
K
4 x 10^5 HK W256 (n=1)
4 x 10^5 W256 (n=8)
Body Weight (g)
Days after Surgery
L
4 x 10^5 HK W256 (n=2)
4 x 10^5 W256 (n=3)
Body Weight (g)
Days after Surgery
M
4 x 10^5 HK W256 (n=2)
4 x 10^5 W256 (n=3)
Body Weight (g)
Days after Surgery

Supplementary Figure 2.2. Body weight of rats from various experiments. Panels in the figure show mean (±SEM) body weight of rats from (A) experiment 1, (B) experiment 4, (C) experiment 6, (D) experiment 7, (E) experiment 8, (F) experiment 9, (G) experiment 10, (H) experiment 11, (I) experiment 12, (J) experiment 13, (K) experiment 14, (L) experiment 15 and (M) experiment 16. HK, heat-killed; W256, Walker 256 cells.

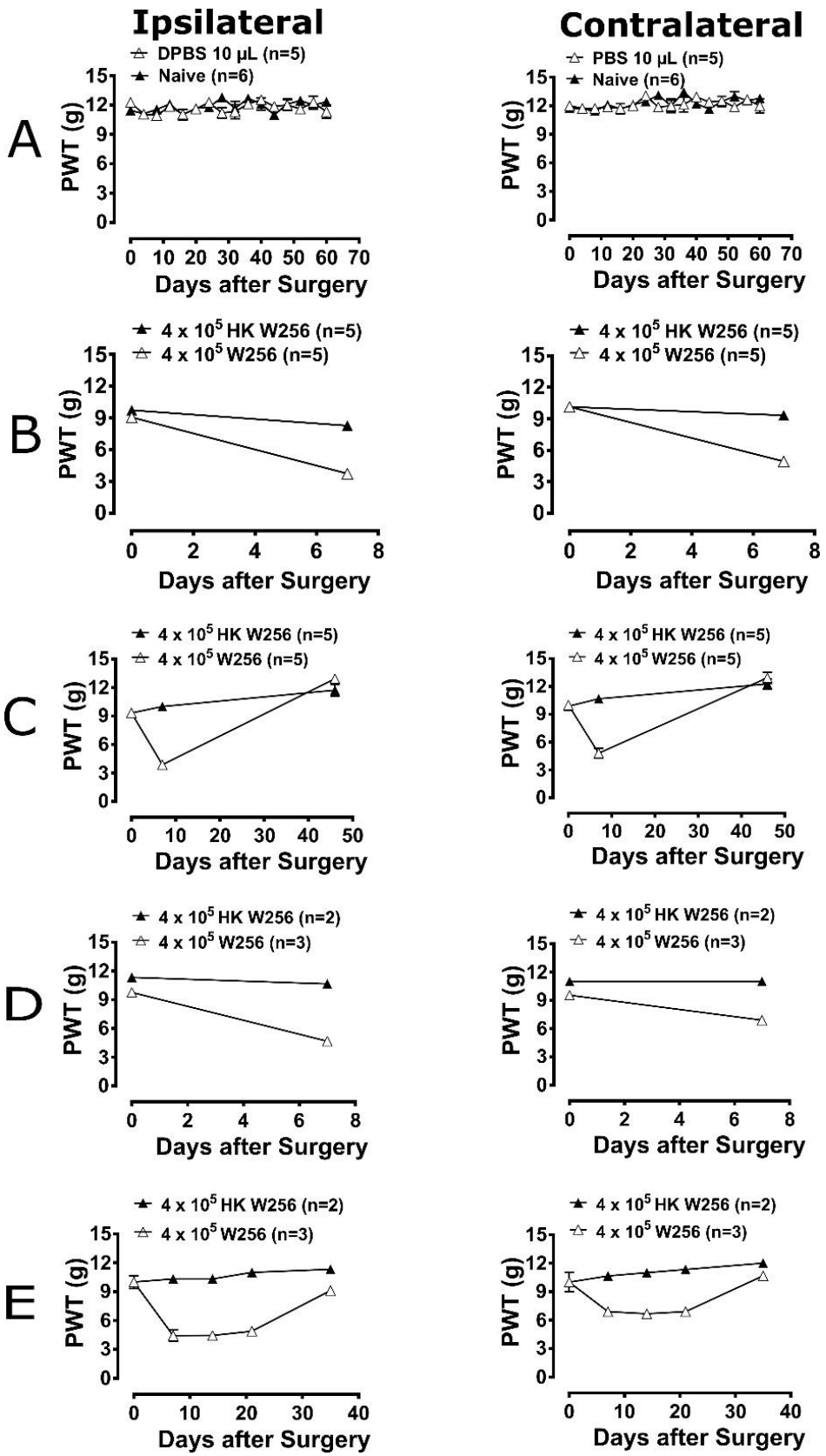

Supplementary Figure 2.3. Paw withdrawal thresholds (PWTs) of ipsilateral and contralateral hindpaws of rats. Panels in the figure show mean (±SEM) PWTs of rats from (A) experiment 4, (B) experiment 8, (C) experiment 9, (D) experiment 15 and (E) experiment 16. HK, heat-killed; W256, Walker 256 cells.

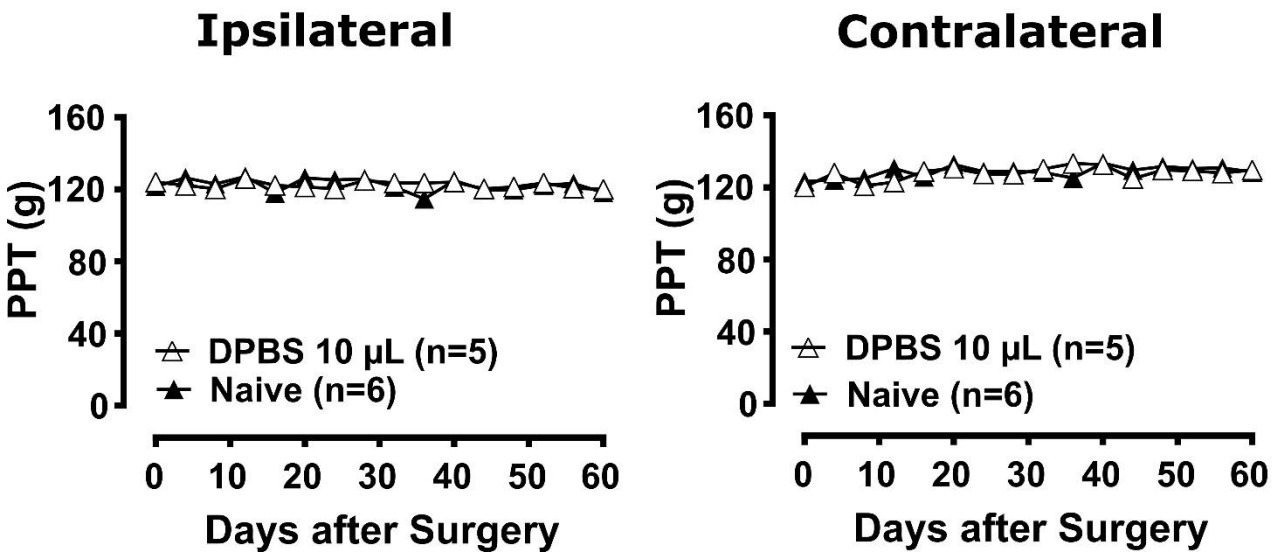

Supplementary Figure 2.4. Paw pressure thresholds (PPTs) of the ipsilateral and contralateral hindpaws of rats from experiment 4.

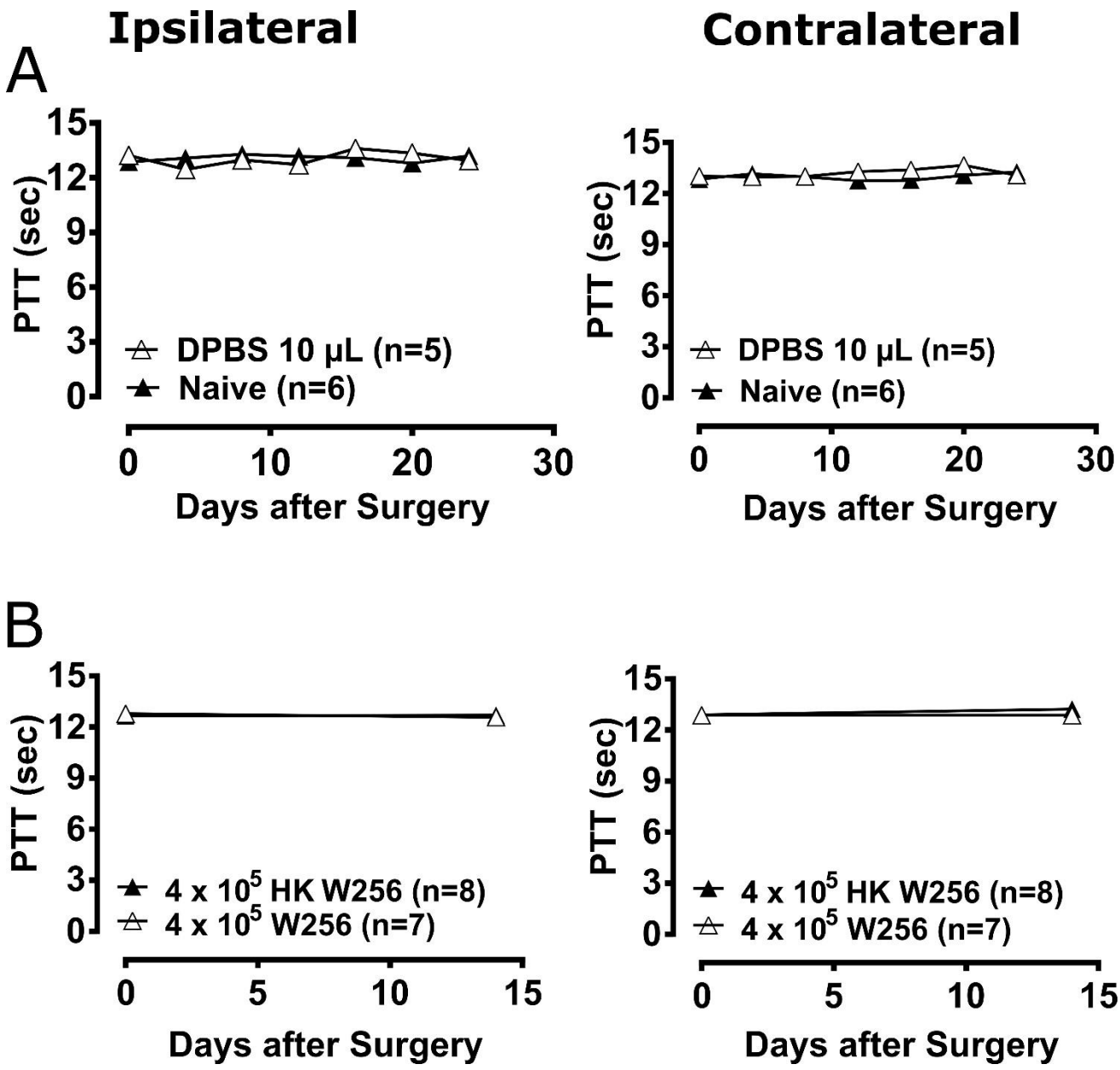

Supplementary Figure 2.5. Paw thermal thresholds (PTTs) of the ipsilateral and contralateral hindpaws of rats. Panels in the figure show mean (±SEM) PTTs of rats from (A) experiment 4 and (B) experiment 5. HK, heat-killed; W256, Walker 256 cells.

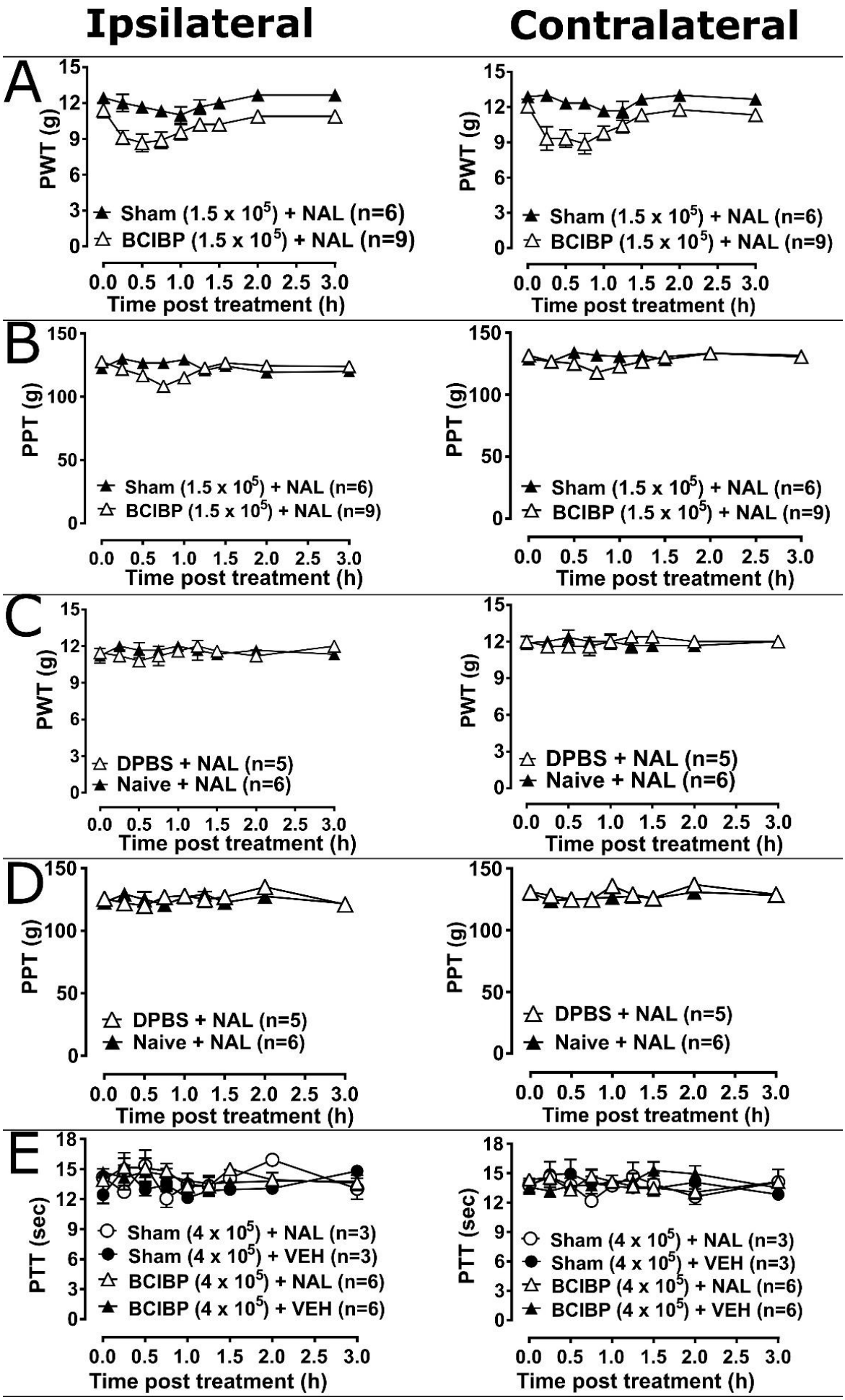
Ipsilateral
Contralateral
A
PWT (g)
Sham (1.5 x 10^5) + NAL (n=6)
BCIBP (1.5 x 10^5) + NAL (n=9)
Time post treatment (h)
B
PPT (g)
Sham (1.5 x 10^5) + NAL (n=6)
BCIBP (1.5 x 10^5) + NAL (n=9)
Time post treatment (h)
C
PWT (g)
DPBS + NAL (n=5)
Naive + NAL (n=6)
Time post treatment (h)
D
PPT (g)
DPBS + NAL (n=5)
Naive + NAL (n=6)
Time post treatment (h)
E
PTT (sec)
Sham (4 x 10^5) + NAL (n=3)
Sham (4 x 10^5) + VEH (n=3)
BCIBP (4 x 10^5) + NAL (n=6)
BCIBP (4 x 10^5) + VEH (n=6)
Time post treatment (h)

Supplementary Figure 2.6. Effect of naloxone on ipsilateral and contralateral PWT / PPT / PTT values of rats. Panels in the figure show changes in mean (±SEM) (A) PWTs in experiment 3 following naloxone injection between day 81-91 post-ITI, (B) PPTs in experiment 3 following naloxone injection between day 82-92 post-ITI, (C) PWTs in experiment 4 following naloxone injection between days 81-93 post-ITI, (D) PPTs in experiment 4 following naloxone injection between days 82-94 post-ITI and (E) PTTs in experiment 7 following naloxone injection between days 21-24 post-ITI. BCIBP (1.5×10^5), group of rats given an ITI of 1.5×10^5 W256 cells; BCIBP (4×10^5), group of rats given an ITI of 4×10^5 W256 cells; DPBS, group of rats given an ITI of 10 µL DPBS; HK, heat-killed; NAL, naloxone (15 mg/kg s.c.); Sham (1.5×10^5), group of rats given an ITI of 1.5×10^5 HK W256 cells; Sham (4×10^5), group of rats given an ITI of 4×10^5 HK W256 cells; VEH, vehicle; W256, Walker 256.

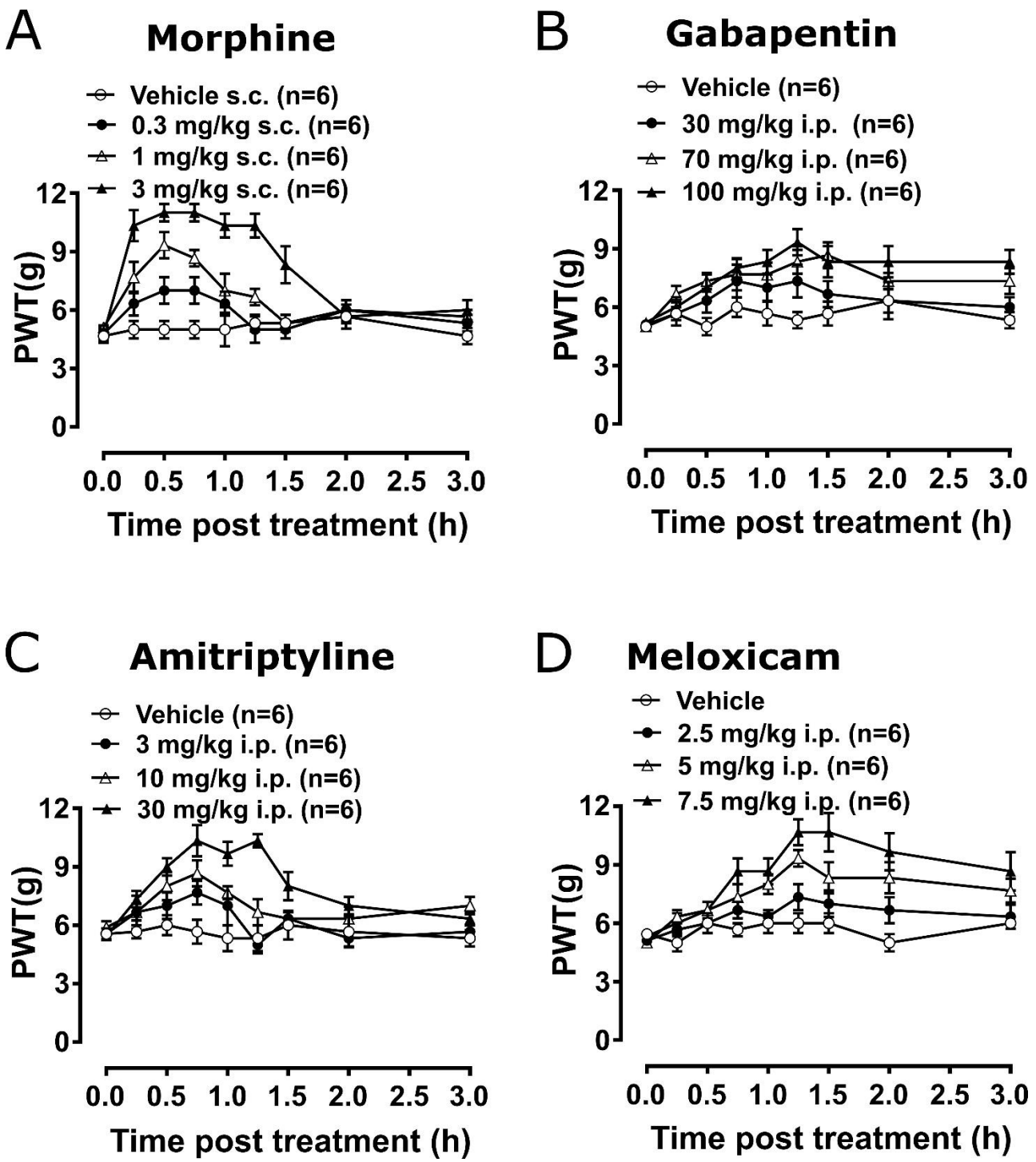

Supplementary Figure 2.7. Temporal changes in the paw withdrawal thresholds (PWTs) of the contralateral hindpaws for BCIBP rats following administration of single bolus doses of analgesic and adjuvant drugs. Panels in the figure show temporal changes in mean (±SEM) PWTs versus time curves following injection of (A) morphine, (B) gabapentin, (C) amitriptyline and (D) meloxicam.

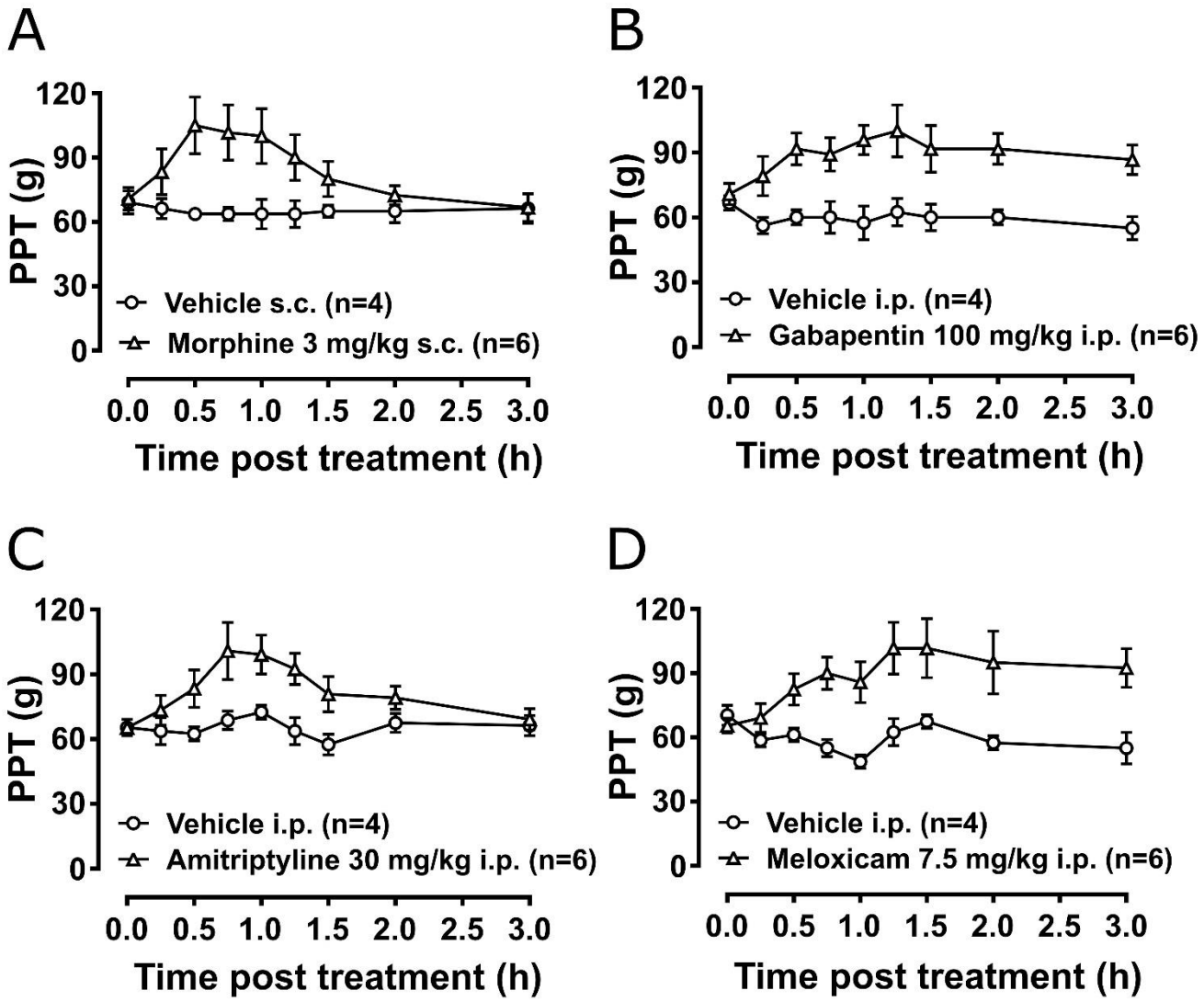

Supplementary Figure 2.8. Temporal changes in the paw pressure thresholds (PPTs) of the contralateral hindpaws for BCIBP rats following administration of single bolus doses of analgesic and adjuvant drugs. Panels in the figure show temporal changes in mean (±SEM) PPTs versus time curves following injection of (A) morphine, (B) gabapentin, (C) amitriptyline and (D) meloxicam.

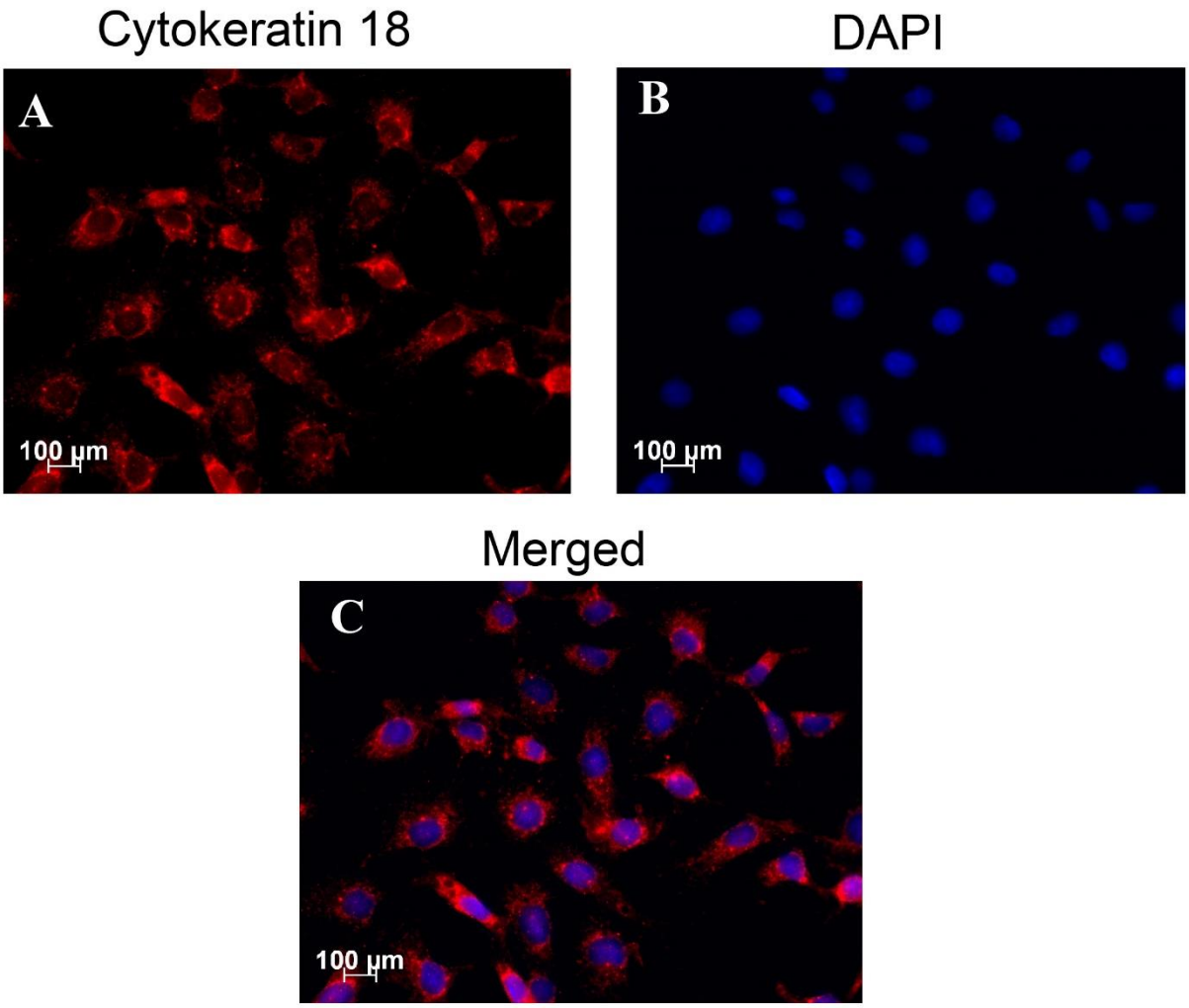

Supplementary Figure 2.9. Immunocytochemical staining of the Walker 256 cell line for Cytokeratin 18 using the ab668 (Abcam) antibody. Panels in the figure show (A) cytokeratin 18 (B) DAPI and (C) A and B merged.

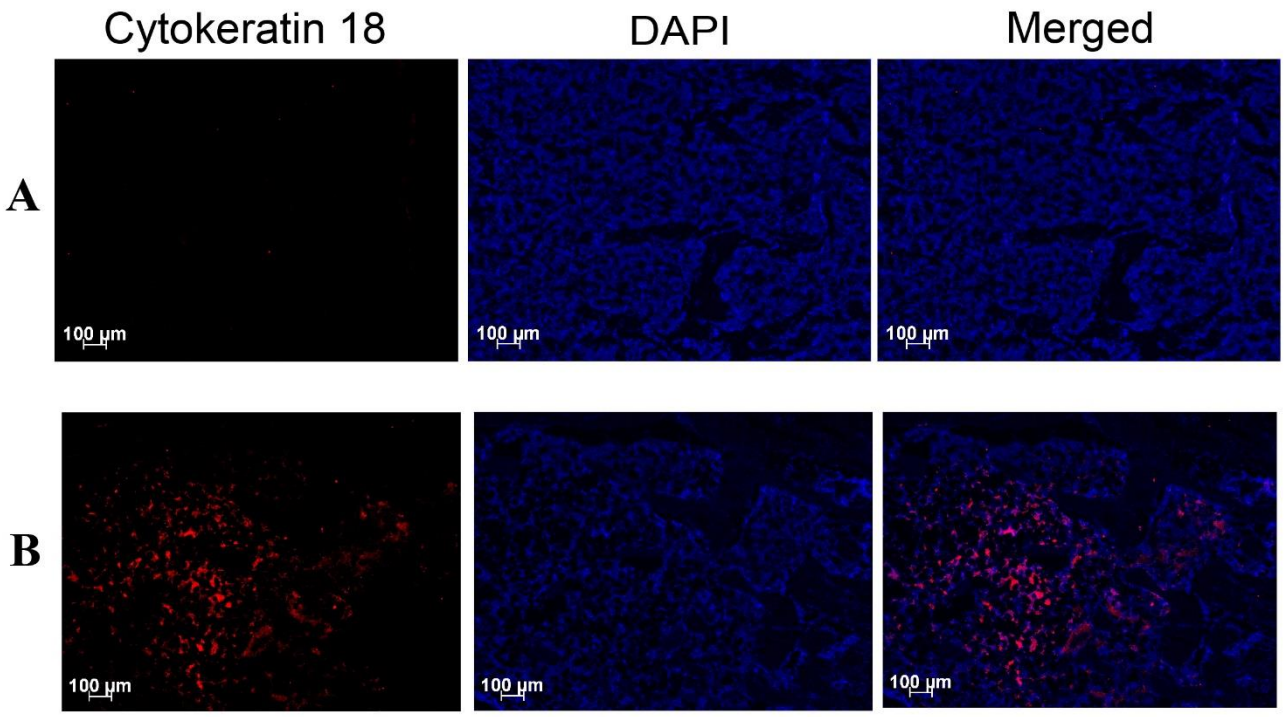

Supplementary Figure 2.10. Immunohistochemical staining of Cytokeratin 18 in tibial sections from BCIBP rats and the corresponding sections from sham rats using the ab668 (Abcam) antibody. Panels in the figure show immunofluorescence imaging of tibial sections from (A) sham and (B) BCIBP rats at day 7 post-ITI.

Chapter 3

Transcriptomic characterisation of the optimised rat model of Walker 256 breast cancer cell-induced bone pain

3.1. Foreword

As described in Chapter 2, the Walker 256 cell-induced bone pain model was validated and characterised showing that this preclinical model has several similarities in common with breast cancer-induced bone pain in humans. Mechanism-based studies are very important to seek new analgesic drugs for the treatment of breast cancer induced bone pain. Hence, it is necessary to understand the gene-level changes that occur in the pathophysiology of the preclinical model used in the drug discovery process. Hence, I performed a transcriptomic characterisation of the Walker 256 cell-induced bone pain model using the neural tissues, which are known to be key players of pain processing pathways. Additionally, I also performed the transcriptomic characterization of the Walker 256 cell line cultured *in vitro* so as to predict the molecular genetic profile of this cell line and to be able to comment on the nature of breast cancer disease produced *in vivo* by this cell line. I am thankful to the Institute for Molecular Bioscience Sequencing Facility (The University of Queensland, QLD, Australia; mainly Dr Gregory Baillie) and the Boehringer Ingelheim Pharma GmbH & Co. KG (Biberach, BW, Germany; mainly Dr German Leparc) for their assistance with RNA-seq procedures and bioinformatics analysis of the Walker 256 cell line and rat neural tissues, respectively.

3.2. Introduction

Breast cancer induced bone pain (BCIBIP) is a significant problem in clinic (Kane et al., 2015). BCIBP can manifest as neuropathic pain, inflammatory pain as well as mixed hypersensitivity and also involves tumour-specific components (Cao et al., 2010). The existing analgesic drug regimens used to treat BCIBP are often insufficient to mitigate the associated pain and may also exhibit severe side effects particularly in high doses (Bloom et al., 2011). Hence, it is very important to seek novel analgesics with reduced side effect profiles to treat BCIBP. One of the key aspects of the analgesic drug discovery process is employing preclinical models that aptly mimic the human pathophysiology of BCIBP (Slosky et al., 2015). The Walker 256 breast cancer cell-induced bone pain model in rats is a useful research tool that mimics key features of the human BCIBP condition (Shenoy et al., 2016).

The Walker 256 cell line is one of the most common cell lines used in experimental research (Justice, 1985, Brigatte et al., 2007, Sroka et al., 2016). However, the molecular genetic profile of this cell line is not yet established. It is not even known whether the Walker 256 cell line expresses common breast cancer marker genes such as the estrogen receptor, progesterone receptor, androgen receptor and Her2. It is important to understand the genetic composition of the Walker 256 cell line used in the experimental model of BCIBP, so as to predict the resemblances of the skeletal metastases produced in this model to the clinical features of the human cancer disease. In the process of seeking new analgesic drugs for treating BCIBP, it is also very important that mechanisms of pain hypersensitivities are elucidated (Mantyh, 2014). However, there is insufficient information on global gene expression changes at the level of dorsal root ganglia (DRGs) and the spinal cord, occurring in the pathophysiology of BCIBP. Similar to the clinical situation, the pain hypersensitivities in the Walker 256 BCIBP model resolves at later stages. However, the genetic changes in DRGs that underpin the self-resolving nature of pain hypersensitivities in this model have not been elucidated before.

To address these gaps in the scientific literature, we have performed RNA-seq analysis of the Walker 256 cell line cultured *in vitro*. We have also performed the RNA-seq analysis of the ipsilateral lumbar L4-6 DRGs and lumbar spinal cord tissues of rats from our optimised BCIBP model. This chapter describes the molecular genetic profile of the Walker 256 cell line and also provides transcriptomic insights into the changes occurring in the neural tissues of rats in the pathophysiological state of BCIBP.

3.3. Material and methods

3.3.1. Drugs, Chemicals and reagents

The details of drugs, chemicals and regents used have been covered in section 2.3.1 of chapter 2.

3.3.2. Cell culture

The details of the cell culture procedure used has been described in section 2.3.2 of chapter 2.

3.3.3. Animals, surgical procedure, assessment of health characteristics and measurement of mechanical allodynia

The details of animals, surgical procedure, assessment of health characteristics and measurement of mechanical allodynia were as described in sections 2.3.3, 2.3.4, 2.3.6 and 2.3.7.1 of Chapter 2, respectively.

3.3.4. RNA-Seq and bioinformatics analysis

The Walker 256 cells were cultured and harvested by using the procedure described in section 2.3.2 of Chapter 2. The RNA was extracted from the cells using Absolutely RNA Miniprep Kit (Agilent Technologies, VIC, Australia) following the manufacturer's instructions. Library construction and the bioinformatics analysis were conducted by the Institute for Molecular Bioscience Sequencing Facility (The University of Queensland, QLD, Australia). RNA-Seq was conducted on an Illumina NextSeq 500 platform as 75-nucleotide single-end runs and libraries were prepared using TruSeq stranded total RNA library preparation. The reads were mapped using STAR aligner (version star/2.3.0e) and samtools. The reads were mapped to the Ensembl/Rnor_6.0. Count tables were generated using HTSeq_count from HTSeq package (Yin et al., 2016c). Genes were considered to be above the noise level if the read count was $\geq$10. For sequencing of RNA from neural tissues, on day-10 and 48 following intra-tibial injection (ITI) of Walker 256 cells, the rats were euthanized with pentobarbitone injection followed by decapitation, and the lumbar L4-L6 DRGs and lumbar L4-L6 spinal cord segments were harvested. Three biological replicates (n=3) were used in each of the groups. The tissues were treated with RNA*later*™ stabilization solution (Thermo Fisher Scientific, VIC, Australia). Total RNAs were individually extracted using the Ambion Magmax™-96 total RNA isolation kit (Life Sciences) according to the manufacturer's instructions. Briefly, 5 mg of tissue was placed in the lysis solution and homogenised in Qiagen Tissuelyzer™ for a period of 30 sec. Nucleic acids were captured onto magnetic beads, washed and treated with DNase. Total RNA was then eluted in 50 µl elution buffer. RNA quality and concentration was measured using an RNA Pico chip on an Agilent Bioanalyzer. Library construction and bioinformatics analysis were performed by the Boehringer Ingelheim Pharma GmbH & Co. KG (Biberach, BW, Germany). The sequencing library preparation was done using 200 ng of total RNA input with the TruSeq RNA Sample Prep Kit v2-Set B (RS-122-2002, Illumina Inc, San Diego, CA) producing a 275bp Fragment including Adapters in average size. In the final step before sequencing, 8 individual libraries were normalized and pooled together using the adapter indices supplied by the manufacturer. Pooled libraries were then clustered on the cBot Instrument form Illumina using the TruSeq SR Cluster Kit v3 - cBot - HS(GD-401-3001, Illumina Inc, San Diego, CA). Sequencing was then performed as 86 bp, single reads and 7 bases index read on an Illumina HiSeq3000 instrument using the TruSeq SBS Kit HS- v3 (FC-401-3002, Illumina Inc, San Diego, CA). RNA-Seq reads were aligned to the rat genome using the STAR Aligner v2.5.2a with the corresponding Ensembl 70 reference genome (http://www.ensembl.org). Sequenced read quality was checked with FastQC v0.11.2 (http://www.bioinformatics.babraham.ac.uk/projects/fastqc/) and alignment quality

metrics were calculated using the RNASeQC v1.18. Following read alignment, duplication rates of the RNA-Seq samples were computed with bamUtil v1.0.11 to mark duplicate reads and the dupRadar v1.4 Bioconductor R package for assessment. The gene expression profiles were quantified using Cufflinks software version 2.2.1 to get the Reads Per Kilobase of transcript per Million mapped reads (RPKM) as well as read counts. Differential gene expression (DGE) analysis was performed with the uniquely mapping read counts as input for the Bioconductor LIMMA analysis R package with normalization factors calculated using trimmed mean of M-values (TMM) and subsequently voom normalized. The list of top differentially expressed genes were filtered for significant differential expression using an adjusted P-value threshold at 0.05 (after Benjamini–Hochberg multiple testing correction) and a log2 fold change threshold of >= |0.5|. The comparisons of groups made to obtain differentially expressed genes have been tabulated in Table 3.1. Day 10 post-ITI was chosen as the timepoint at which rats displayed pain behavioural hypersensitivities. Day 48 post-ITI was chosen as the timepoint at which the pain hypersensitivities were resolved. Three types of comparisions were made as shown in the Table 3.1. Firstly, we compared the DRGs of the animals in pain state with the sham control animals that received heat-killed cancer cells. Secondly, we compared the changes in gene expression in DRGs during pain state, with respect to the animals in resolved-pain state. Lastly, we compared the gene expression in spinal cord tissues of animals in pain state with the sham control animals that received heat-killed cancer cells. The ontology analyses of genes expressed in the Walker 256 cell line and the differentially expressed genes in rat neural tissues were performed using the PANTHER database by following previously published protocols (Mi et al., 2013a, Mi et al., 2013b). The Kyoto Encyclopedia of Genes and Genomes (KEGG) pathway analysis was performed using the web-based platform, KOBAS 3.0 server (Wu et al., 2006, Xie et al., 2011, Zhang et al., 2017, Shi et al., 2017). STRING network analysis diagrams were generated using STRING v10.5 (Szklarczyk et al., 2015).

Table 3.1. Schematic of group comparisons of neural tissues in BCIBP rats to obtain differentially expressed genes.

Comparison	**Group A**	**Group B**
1	Ipsilateral lumbar L4-6 DRGs, Heat-Killed cells' group, Day 10 post-ITI	Ipsilateral lumbar L4-6 DRGs, Live cells group, Day 10 post-ITI
2	Ipsilateral lumbar L4-6 DRGs, Live cells group, Day 48 post-ITI	Ipsilateral lumbar L4-6 DRGs, Live cells group, Day 10 post-ITI

3	Lumbar L4-6 Spinal cord, Heat-Killed cells group, Day 10 post-ITI	Lumbar L4-6 Spinal cord, Live cells group, Day 10 post-ITI

3.4. Results

A total of 216233726 reads were generated from all Walker 256 cell line samples (no feature- 23764566; ambiguous- 292378; alignment not unique- 106349779). In neural tissue samples, all the samples had around 90% of reads uniquely mapped to the rat genome (Appendix-1). The principal component analysis using the read counts for all genes showed clear clustering and segregation of populations in the two dimensional representations (Appendix-2), suggesting that obvious differences existed in the RNA expression between different groups, and not as variations within groups (Chung et al., 2016).

3.4.1. Presence of genes with breast cancer implications in Walker 256 cell line

The twenty most abundant genes present in the Walker 256 cell line and their roles in breast cancer have been summarised in Table 3.2. These included genes important genes like Nedd4, Fn1, Ctsb and Ahnak.

Table 3.2. 20 most abundant genes in Walker 256 cell line and their role in breast cancer.

Gene Abbreviation	Gene name	Reads	Possible implication	Reference
RNaseP_nuc	Nuclear RNase P	191160	-	-
RNase_MRP	RNase mitochondrial RNA processing	182336	Proliferative functions of breast cancer	(Park and Jeong, 2015)
Actb	Actin Beta	179217	Proliferation and tumour aggressiveness of breast cancer	(Guo et al., 2013)
7SK	RNA, 7SK small nuclear	156254	-	-
AY172581.24		122538	-	-
Nedd4	Neural Precursor Cell Expressed, Developmentally Down-Regulated 4, E3 Ubiquitin Protein Ligase	111755	Oncogenic function in breast cancer	(Jung et al., 2013, Ye et al., 2014b)

Fn1	Fibronectin 1	97292	Aggressive behaviour of breast cancer	(Yang et al., 2014)
Ctsb	Cathepsin B	96231	High invasiveness, tumour growth and metastasis of breast cancer	(Kallunki et al., 2013, Bengsch et al., 2014)
Ahnak	AHNAK nucleoprotein, Neuroblast differentiation-associated protein AHNAK	93214	Migration and metastasis of breast cancer	(Sudo et al., 2014, Shankar et al., 2010)
Mt-co1	Mitochondrially Encoded Cytochrome C Oxidase I	92829	Mutation of this gene is implicated in breast cancer	(Gallardo et al., 2006)
Rplp0	Ribosomal Protein Lateral Stalk Subunit P0	83214	-	-
Eef1a1	Eukaryotic Translation Elongation Factor 1 Alpha 1	76805	Formation, progression and metastasis of breast cancer	(Edmonds et al., 1996, Al-Maghrebi et al., 2005)
Vim	Vimentin	73350	Invasiveness and metastasis of breast cancer	(Hendrix et al., 1997, Domagala et al., 1994)

Eef2	Eukaryotic Translation Elongation Factor 2	70931	Oncogenic function in breast cancer cell growth	(Oji et al., 2014)
Flna	Filamin A	67368	Development and progression of breast cancer	(Tian et al., 2013)
Vcan	Versican	66480	Formation of suitable tumour microenvironment in breast cancer	(Kischel et al., 2010)
S100a6	S100 Calcium Binding Protein A6	59680	Progression of breast cancer	(McKiernan et al., 2011)
Fstl1	Follistatin Like 1	56282	Promotion of bone metastasis of breast cancer by causing induction of immune dysfunction	(Kudo-Saito, 2013, Kudo-Saito et al., 2013)
Thbs2	Thrombospondin 2	56189	Oncogenic function in breast cancer	(Weng et al., 2016)
Pdia3	Protein Disulfide Isomerase Family A Member 3	56172	Carcinogenic process and aggressiveness of breast cancer	(Ramos et al., 2015)

-, not applicable

3.4.2. Genes marking the mammary origin of the Walker 256 cell line

Several genes that are the markers of mammary origin (Zaha, 2014) were present in the Walker 256 cell line, while some were absent (Figure 3.1).

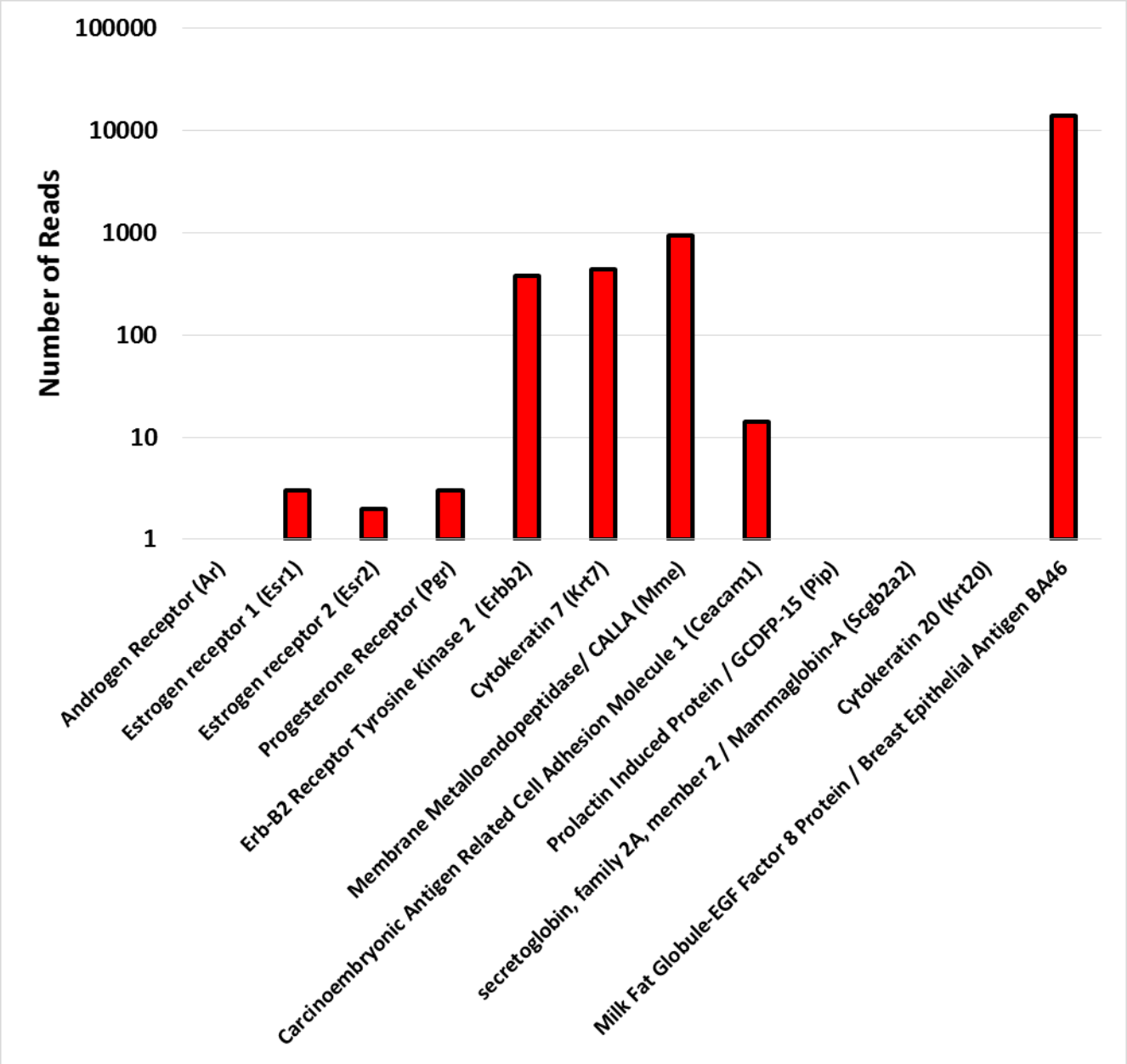

Figure 3.1. Genes indicating the mammary origin of the Walker 256 cell line.

3.4.3. Molecular classification of Walker 256 cell line

Gene expression profile of Walker 256 cell line, when compared to human breast cancer cell lines (Kao et al., 2009, Neve et al., 2006), revealed that this cell line resembles basal-B subtype of cell lines (Figure 3.2).

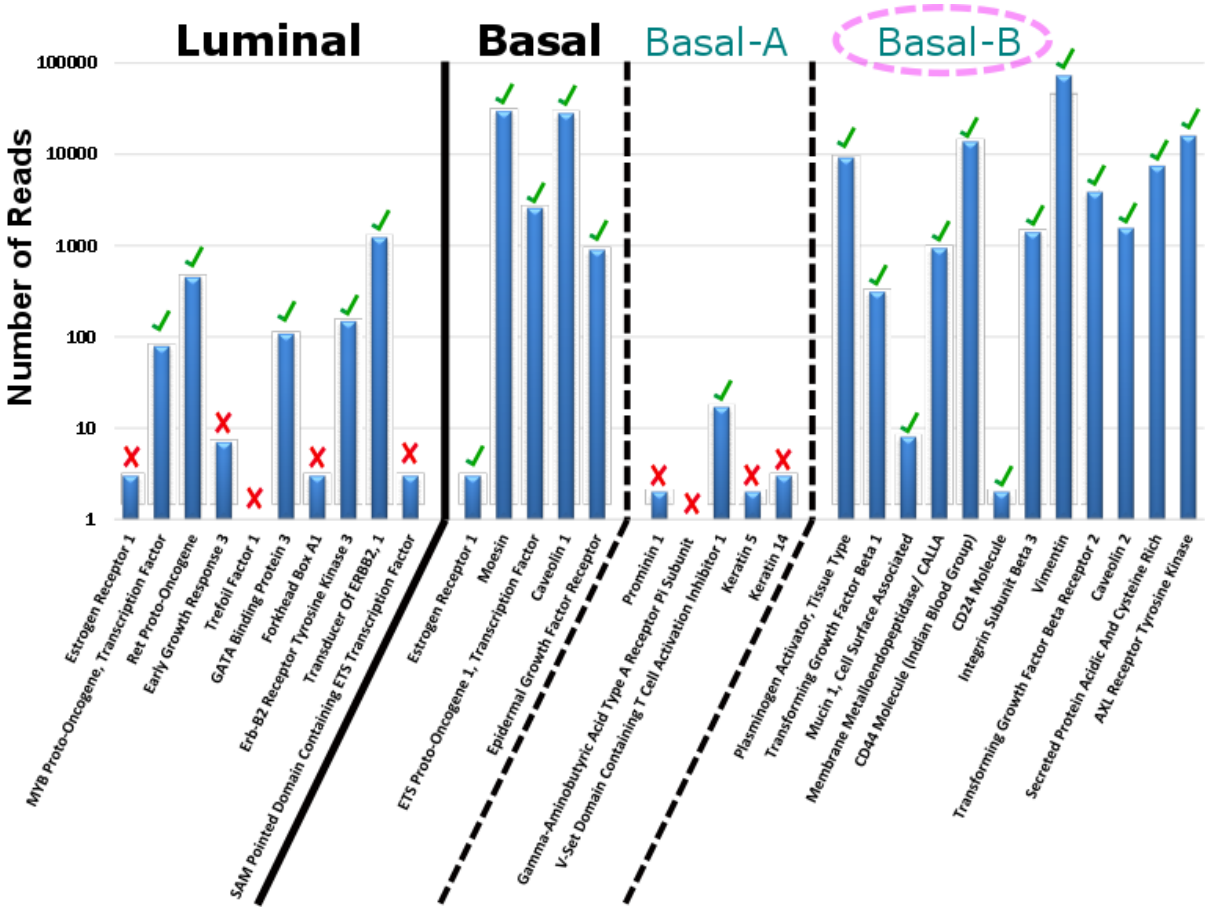

Figure 3.2. Molecular classification of the Walker 256 cell line. Green tick mark, meets the gene expression requirement of the given cell line subtype; Red cross mark, does not meet the gene expression requirement of the given cell line subtype.

3.4.4. Genes of prognostic / therapeutic / invasiveness markers of breast cancer in the Walker 256 cell line

Similar to clinical scenario of breast tumours, Walker 256 cell line expressed genes of several prognostic / therapeutic / invasiveness markers of breast cancer (Aleskandarany et al., 2015, Zaha, 2014), while some of the common genes were absent (genes were considered to be above the noise level only if the read count was ≥10; so gene count <10 might be considered to be noise, and hence the corresponding gene is considered to be absent) (Figure 3.3).

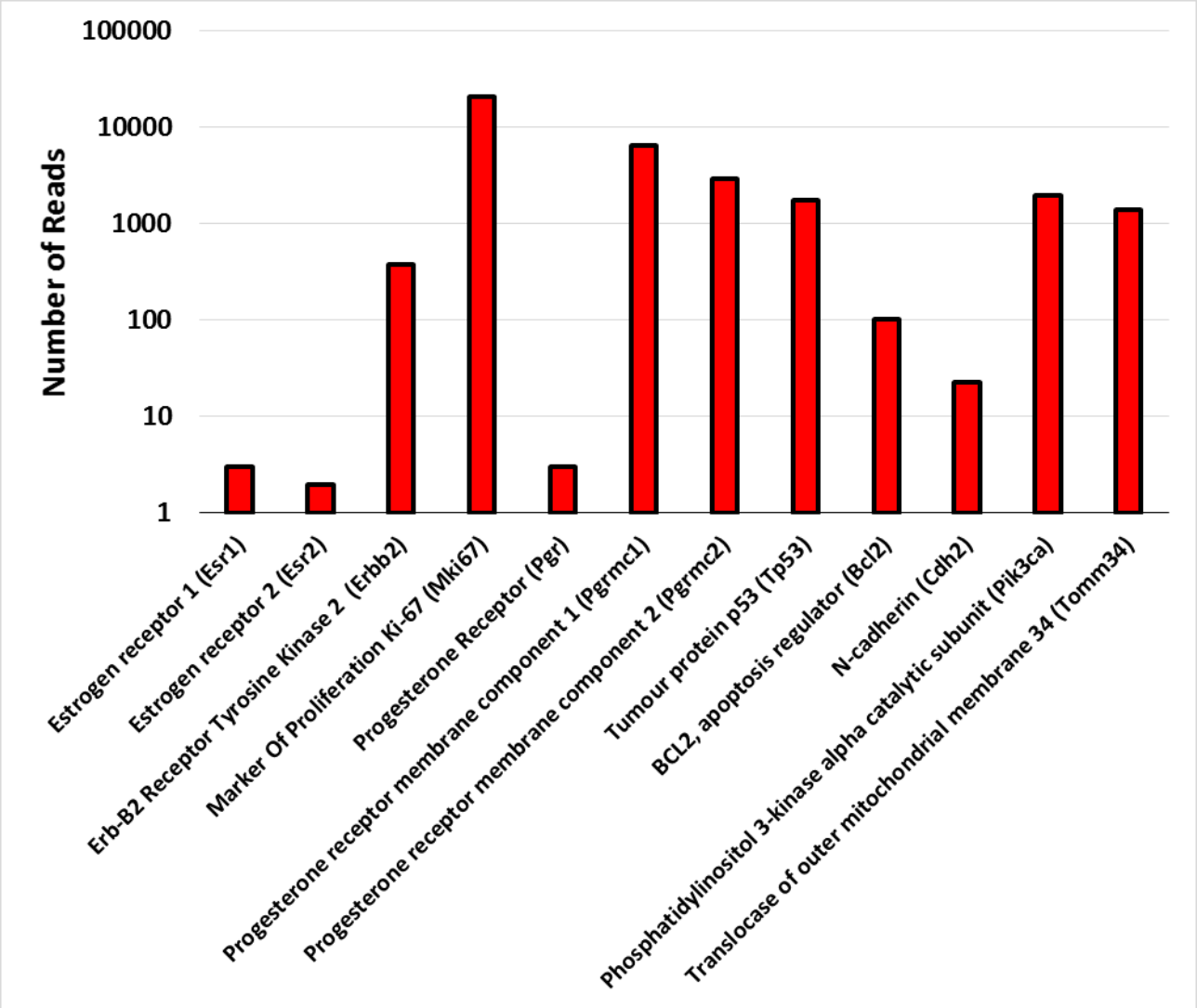

Figure 3.3. Genes of common prognostic / therapeutic / invasiveness markers of breast cancer in the Walker 256 cell line.

3.4.5. Gene ontology analysis on the Walker 256 cell line RNA sample: Biological Process

The results of Biological Process ontology analysis of the Walker 256 cell line have been provided in Table 3.3.

Table 3.3. Percentage of the number of genes in Walker 256 cell line classified into subcategories of the Biological Process ontology.

Functional Category	**Percentage (%) of number of genes classified to the Category over the total number of genes**
cellular component organization or biogenesis	9.1
cellular process	41.3
localization	10.6
reproduction	1.7
biological regulation	9.8
response to stimulus	11
developmental process	9.3
multicellular organismal process	7.3
locomotion	0.7
biological adhesion	2.5
metabolic process	35.4
immune system process	5.2
cell killing	0.1

3.4.6. Gene expression changes in BCIBP rats' ipsilateral lumbar L4-6 DRGs during the pain-state

No significant changes were found at the mRNA level in the DRGs of BCIBP rats in pain–state compared to rats at day 10 post- ITI after an ITI of heat-killed cells.

3.4.7. Gene expression changes in BCIBP rats' lumbar L4-6 spinal cord during the pain-state

294 genes were differentially expressed in the lumbar L4-6 spinal cords of BCIBP rats in pain-state compared to rats at day 10 post-ITI after an ITI of heat-killed cells, including several upregulated genes like Erb-B2 Receptor Tyrosine Kinase 4 (Erbb4), Transforming growth factor-β receptor 1 (*Tgfbr1*), Solute Carrier Family 12 Member 2 (Slc12a2 / NKCC1) and Myristoylated Alanine-Rich C-Kinase Substrate (Marcks). Downregulated genes included SLC9A3 Regulator 2 (Slc9a3r2), Annexin A2 (Anxa2), Cysteine-rich protein 2 (Crip2), RET Receptor Tyrosine Kinase (RET), Neuregulin 1 (Nrg1), Potassium Two Pore Domain Channel Subfamily K Member 4 (Kcnk4) and Nuclear Receptor Subfamily 2 Group F Member 6 (Nr2f6 / Ear2). These genes are known to have roles in the pain processing pathway. The list of all the upregulated and the downregulated genes in

lumbar L4-6 spinal cord of BCIBP rats during the pain state is shown in Appendix-3 and Appendix-4, respectively.

3.4.8. Gene expression changes in BCIBP rats' ipsilateral lumbar L4-6 DRGs at the resolved pain-state

25 genes were differentially expressed in the ipsilateral lumbar DRGs of BCIBP rats at the resolved-pain state (day 48 post-ITI) compared to BCIBP rats during the pain state (day 10 post-ITI), including several downregulated genes like Cell Adhesion Molecule 4 (Cadm4), Matrix Metalloproteinase-14 (Mmp14), Sphingosine-1-Phosphate Receptor 3 (S1pr3), Glutathione Peroxidase 7 (Gpx7) and CD93 Molecule (CD93 / C1qR) known to have roles in the pain processing pathway. The list of all the upregulated and the downregulated genes in the ipsilateral lumbar L4-6 DRGs of BCIBP rats in the resolved pain state is shown in Appendix-5 and Appendix-6, respectively.

3.4.9. Gene ontology analysis on differentially expressed genes in the lumbar spinal cord during the pain state- Biological Process

The results of the Biological Process ontology analysis on differentially expressed genes in the lumbar spinal cord of BCIBP rats at day 10 post-ITI, compared to rats at day 10 post-ITI after an ITI of heat-killed cells, are shown in Table 3.4-3.6.

Table 3.4. Percentage of the number of genes classified into subcategories of the Biological Process ontology of differentially expressed genes in spinal cord of BCIBP rats at day 10 post-ITI, compared to rats at day 10 post-ITI after an ITI of heat-killed cells.

Functional Category	**Percentage of number of genes classified to the Category over the total number of genes**
cellular component organization or biogenesis (GO:0071840)	10.40%
cellular process (GO:0009987)	45.40%
localization (GO:0051179)	9.60%
reproduction (GO:0000003)	1.80%
biological regulation (GO:0065007)	16.10%
response to stimulus (GO:0050896)	8.90%
developmental process (GO:0032502)	11.80%
multicellular organismal process (GO:0032501)	8.20%

biological adhesion (GO:0022610)	2.90%
locomotion (GO:0040011)	1.10%
metabolic process (GO:0008152)	31.10%
immune system process (GO:0002376)	3.20%

Table 3.5. Percentage of the number of genes classified into subcategories of the Biological Process ontology of upregulated genes in the lumbar spinal cord of BCIBP rats at day 10 post-ITI, compared to rats at day 10 post-ITI after an ITI of heat-killed cells.

Functional Category	**Percentage of number of genes classified to the Category over the total number of genes**
cellular component organization or biogenesis (GO:0071840)	8.50%
cellular process (GO:0009987)	46.30%
localization (GO:0051179)	12.20%
reproduction (GO:0000003)	2.40%
biological regulation (GO:0065007)	13.40%
response to stimulus (GO:0050896)	8.50%
developmental process (GO:0032502)	9.80%
multicellular organismal process (GO:0032501)	2.40%
biological adhesion (GO:0022610)	2.40%
locomotion (GO:0040011)	2.40%
metabolic process (GO:0008152)	32.90%

Table 3.6. Percentage of the number of genes classified into subcategories of the Biological Process ontology of downregulated genes in the lumbar spinal cord of BCIBP rats at day 10 post-ITI, compared to rats at day 10 post-ITI after an ITI of heat-killed cells.

Functional Category	**Percentage of number of genes classified to the Category over the total number of genes**
cellular component organization or biogenesis (GO:0071840)	11.10%
cellular process (GO:0009987)	44.90%
localization (GO:0051179)	8.60%
reproduction (GO:0000003)	1.50%
biological regulation (GO:0065007)	17.20%

response to stimulus (GO:0050896)	9.10%
developmental process (GO:0032502)	12.60%
multicellular organismal process (GO:0032501)	10.60%
biological adhesion (GO:0022610)	3.00%
locomotion (GO:0040011)	0.50%
metabolic process (GO:0008152)	30.30%
immune system process (GO:0002376)	4.50%

3.4.10. Gene ontology analysis on differentially expressed genes in the lumbar spinal cord during the pain state- Cellular Component

The results of Cellular Component ontology analysis on differentially expressed genes in the lumbar spinal cord of BCIBP rats at day 10 post-ITI, compared to rats at day 10 post-ITI after an ITI of heat-killed cells, are shown in Table 3.7-3.9.

Table 3.7. Percentage of the number of genes classified into subcategories of the Cellular Component ontology of differentially expressed genes in the lumbar spinal cord of BCIBP rats at day 10 post-ITI, compared to rats at day 10 post-ITI after an ITI of heat-killed cells.

Functional Category	**Percentage of number of genes classified to the Category over the total number of genes**
synapse (GO:0045202)	0.40%
cell junction (GO:0030054)	0.40%
membrane (GO:0016020)	8.60%
macromolecular complex (GO:0032991)	8.60%
extracellular matrix (GO:0031012)	1.80%
cell part (GO:0044464)	28.60%
organelle (GO:0043226)	11.80%
extracellular region (GO:0005576)	4.60%

Table 3.8. Percentage of the number of genes classified into subcategories of the Cellular Component ontology of upregulated genes in the lumbar spinal cord of BCIBP rats at day 10 post-ITI, compared to rats at day 10 post-ITI after an ITI of heat-killed cells.

Functional Category	**Percentage of number of genes classified to the Category over the total number of genes**
synapse (GO:0045202)	1.20%

membrane (GO:0016020)	9.80%
macromolecular complex (GO:0032991)	9.80%
extracellular matrix (GO:0031012)	2.40%
cell part (GO:0044464)	28.00%
organelle (GO:0043226)	9.80%
extracellular region (GO:0005576)	7.30%

Table 3.9. Percentage of the number of genes classified into subcategories of the Cellular Component ontology of downregulated genes in the lumbar spinal cord of BCIBP rats at day 10 post-ITI, compared to rats at day 10 post-ITI after an ITI of heat-killed cells.

Functional Category	**Percentage of number of genes classified to the Category over the total number of genes**
cell junction (GO:0030054)	0.50%
membrane (GO:0016020)	8.10%
macromolecular complex (GO:0032991)	8.10%
extracellular matrix (GO:0031012)	1.50%
cell part (GO:0044464)	28.80%
organelle (GO:0043226)	12.60%
extracellular region (GO:0005576)	3.50%

3.4.11. Gene ontology analysis on differentially expressed genes in the lumbar spinal cord during the pain state- Molecular Function

The results of Molecular Function ontology analysis on differentially expressed genes in the lumbar spinal cord of BCIBP rats at day 10 post-ITI, compared to rats at day 10 post-ITI after an ITI of heat-killed cells, are shown in Table 3.10-3.12.

Table 3.10. Percentage of the number of genes classified into subcategories of the Molecular Function ontology of differentially expressed genes in the lumbar spinal cord of BCIBP rats at day 10 post-ITI, compared to rats at day 10 post-ITI after an ITI of heat-killed cells.

Functional Category	**Percentage of number of genes classified to the Category over the total number of genes**
binding (GO:0005488)	22.50%
receptor activity (GO:0004872)	3.20%
structural molecule activity (GO:0005198)	6.10%

signal transducer activity (GO:0004871)	0.70%
channel regulator activity (GO:0016247)	0.40%
catalytic activity (GO:0003824)	25.70%
transporter activity (GO:0005215)	7.50%

Table 3.11. Percentage of the number of genes classified into subcategories of the Molecular Function ontology of upregulated genes in the lumbar spinal cord of BCIBP rats at day 10 post-ITI, compared to rats at day 10 post-ITI after an ITI of heat-killed cells.

Functional Category	**Percentage of number of genes classified to the Category over the total number of genes**
binding (GO:0005488)	23.20%
receptor activity (GO:0004872)	4.90%
structural molecule activity (GO:0005198)	2.40%
signal transducer activity (GO:0004871)	1.20%
catalytic activity (GO:0003824)	34.10%
transporter activity (GO:0005215)	7.30%

Table 3.12. Percentage of the number of genes classified into subcategories of the Molecular Function ontology of downregulated genes in the lumbar spinal cord of BCIBP rats at day 10 post-ITI, compared to rats at day 10 post-ITI after an ITI of heat-killed cells.

Functional Category	**Percentage of number of genes classified to the Category over the total number of genes**
binding (GO:0005488)	22.20%
receptor activity (GO:0004872)	2.50%
structural molecule activity (GO:0005198)	7.60%
signal transducer activity (GO:0004871)	0.50%
channel regulator activity (GO:0016247)	0.50%
catalytic activity (GO:0003824)	22.20%
transporter activity (GO:0005215)	7.60%

3.4.12. Kyoto Encyclopedia of Genes and Genomes (KEGG) pathway analysis on differentially expressed genes in the lumbar spinal cord during the pain state

The results of KEGG analysis on differentially expressed genes in the lumbar spinal cord of BCIBP rats at day 10 post-ITI, compared to rats at day 10 post-ITI after an ITI of heat-killed cells, are shown in Table 3.13-3.15.

Table 3.13. KEGG pathway analysis of differentially expressed genes in the lumbar spinal cord of BCIBP rats at day 10 post-ITI, compared to rats at day 10 post-ITI after an ITI of heat-killed cells.

Term	ID	Input number	P-Value
Focal adhesion	rno04510	8	0.003732282
Pathways in cancer	rno05200	12	0.00411679
Small cell lung cancer	rno05222	5	0.004922272
Alzheimer's disease	rno05010	7	0.0055924
Protein digestion and absorption	rno04974	5	0.0067878
Amoebiasis	rno05146	5	0.008740098
Apoptosis - multiple species	rno04215	3	0.009372294
Chronic myeloid leukemia	rno05220	4	0.016462193
ECM-receptor interaction	rno04512	4	0.017174889
Aldosterone-regulated sodium reabsorption	rno04960	3	0.017475233
Notch signaling pathway	rno04330	3	0.020822029
Oxidative phosphorylation	rno00190	5	0.021025461
Ovarian steroidogenesis	rno04913	3	0.027126126
Parkinson's disease	rno05012	5	0.027311263
Apoptosis	rno04210	5	0.028075749
Amyotrophic lateral sclerosis (ALS)	rno05014	3	0.029901391
Endocrine resistance	rno01522	4	0.033359803
AGE-RAGE signaling pathway in diabetic complications	rno04933	4	0.043920525
Glioma	rno05214	3	0.044156646
Butanoate metabolism	rno00650	2	0.044401295
Non-alcoholic fatty liver disease (NAFLD)	rno04932	5	0.045217888
Proteoglycans in cancer	rno05205	6	0.045885549
Pancreatic cancer	rno05212	3	0.049536447

Table 3.14. KEGG pathway analysis of upregulated genes in the lumbar spinal cord of BCIBP rats at day 10 post-ITI, compared to rats at day 10 post-ITI after an ITI of heat-killed cells.

Term	**ID**	**Input number**	**P-Value**
Ovarian steroidogenesis	rno04913	3	0.000796151
Hepatitis B	rno05161	4	0.001459407
Pancreatic cancer	rno05212	3	0.00159203
Hippo signaling pathway	rno04390	4	0.001879169
Pathways in cancer	rno05200	6	0.002330001
Chronic myeloid leukemia	rno05220	3	0.002476312
Small cell lung cancer	rno05222	3	0.003387932
Prostate cancer	rno05215	3	0.003731631
Proteoglycans in cancer	rno05205	4	0.005744101
Cell cycle	rno04110	3	0.009551574
FoxO signaling pathway	rno04068	3	0.010186125
HTLV-I infection	rno05166	4	0.01507905
Glioma	rno05214	2	0.019849557
Colorectal cancer	rno05210	2	0.021067562
p53 signaling pathway	rno04115	2	0.022951502
Melanoma	rno05218	2	0.024902353
Adherens junction	rno04520	2	0.026239322
Focal adhesion	rno04510	3	0.030805205
Hypertrophic cardiomyopathy (HCM)	rno05410	2	0.033344055
TGF-beta signaling pathway	rno04350	2	0.034845888
Dilated cardiomyopathy	rno05414	2	0.036373673
Peroxisome	rno04146	2	0.037926988
Endocrine resistance	rno01522	2	0.043558632

Table 3.15. KEGG pathway analysis of downregulated genes in the lumbar spinal cord of BCIBP rats at day 10 post-ITI, compared to rats at day 10 post-ITI after an ITI of heat-killed cells.

Term	ID	Input number	P-Value
Alzheimer's disease	rno05010	7	0.000926013
Protein digestion and absorption	rno04974	5	0.001729715
ECM-receptor interaction	rno04512	4	0.005765665
Oxidative phosphorylation	rno00190	5	0.005828677
Parkinson's disease	rno05012	5	0.007756017
Notch signaling pathway	rno04330	3	0.008843486
Amyotrophic lateral sclerosis (ALS)	rno05014	3	0.012919977
Amoebiasis	rno05146	4	0.013005997
Non-alcoholic fatty liver disease (NAFLD)	rno04932	5	0.013540325
Butanoate metabolism	rno00650	2	0.024679577
Huntington's disease	rno05016	5	0.027866895
Focal adhesion	rno04510	5	0.033778547
Apoptosis	rno04210	4	0.034497932
Apoptosis - multiple species	rno04215	2	0.037858087

3.4.13. STRING network analysis on differentially expressed genes in the lumbar spinal cord during the pain state

STRING network analysis of differentially expressed genes in the lumbar spinal cord of BCIBP rats at day 10 post-ITI, compared to rats at day 10 post-ITI after an ITI of heat-killed cells, is shown in Figure 3.4-3.6. The STRING network images show the clusters of functionally related genes based on the associated evidence available in the database.

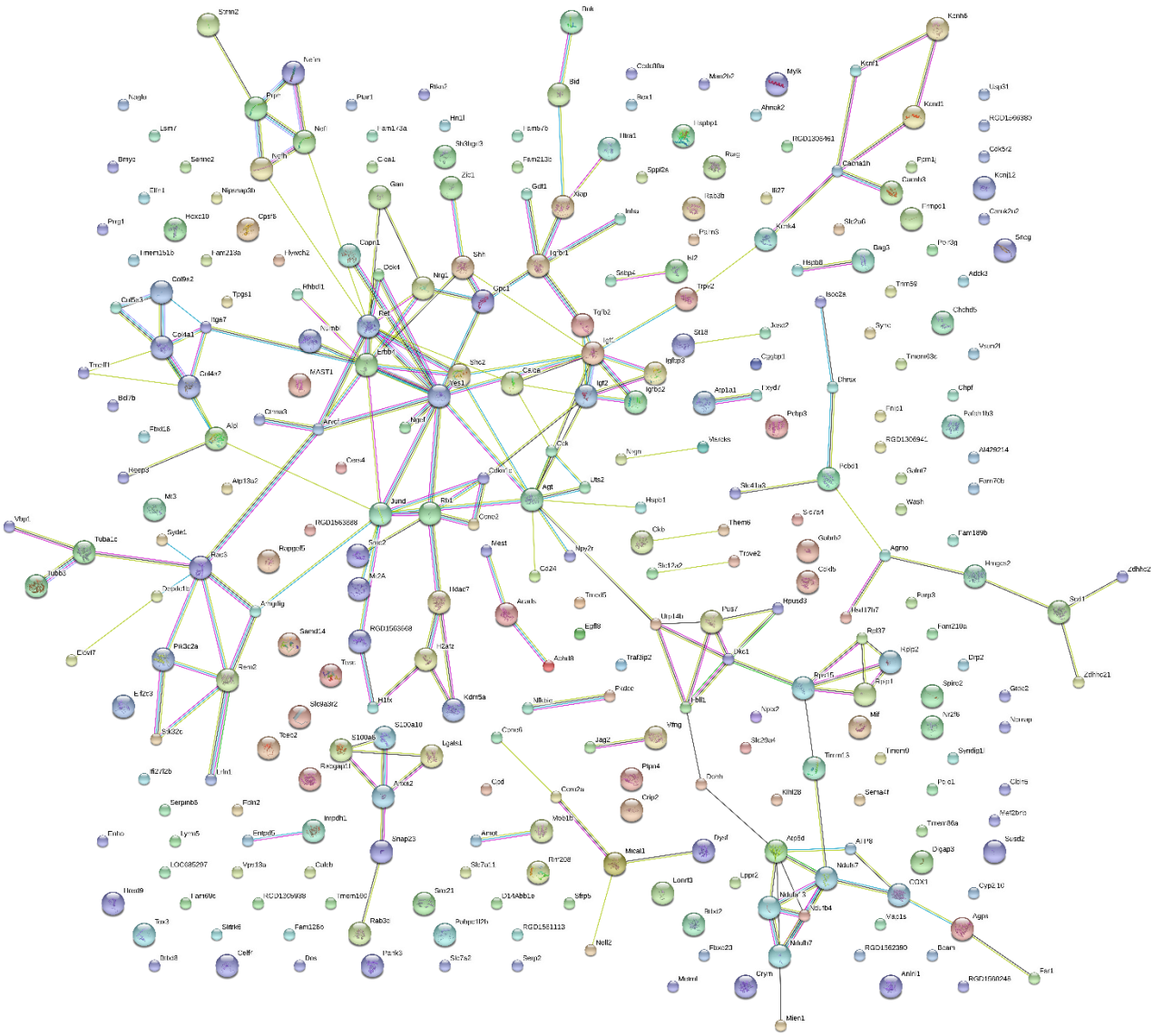

Figure 3.4. STRING network analysis of differentially expressed genes in the lumbar spinal cord of BCIBP rats at day 10 post-ITI, compared to sham rats at day 10 post-ITI after an ITI of heat-killed cells.

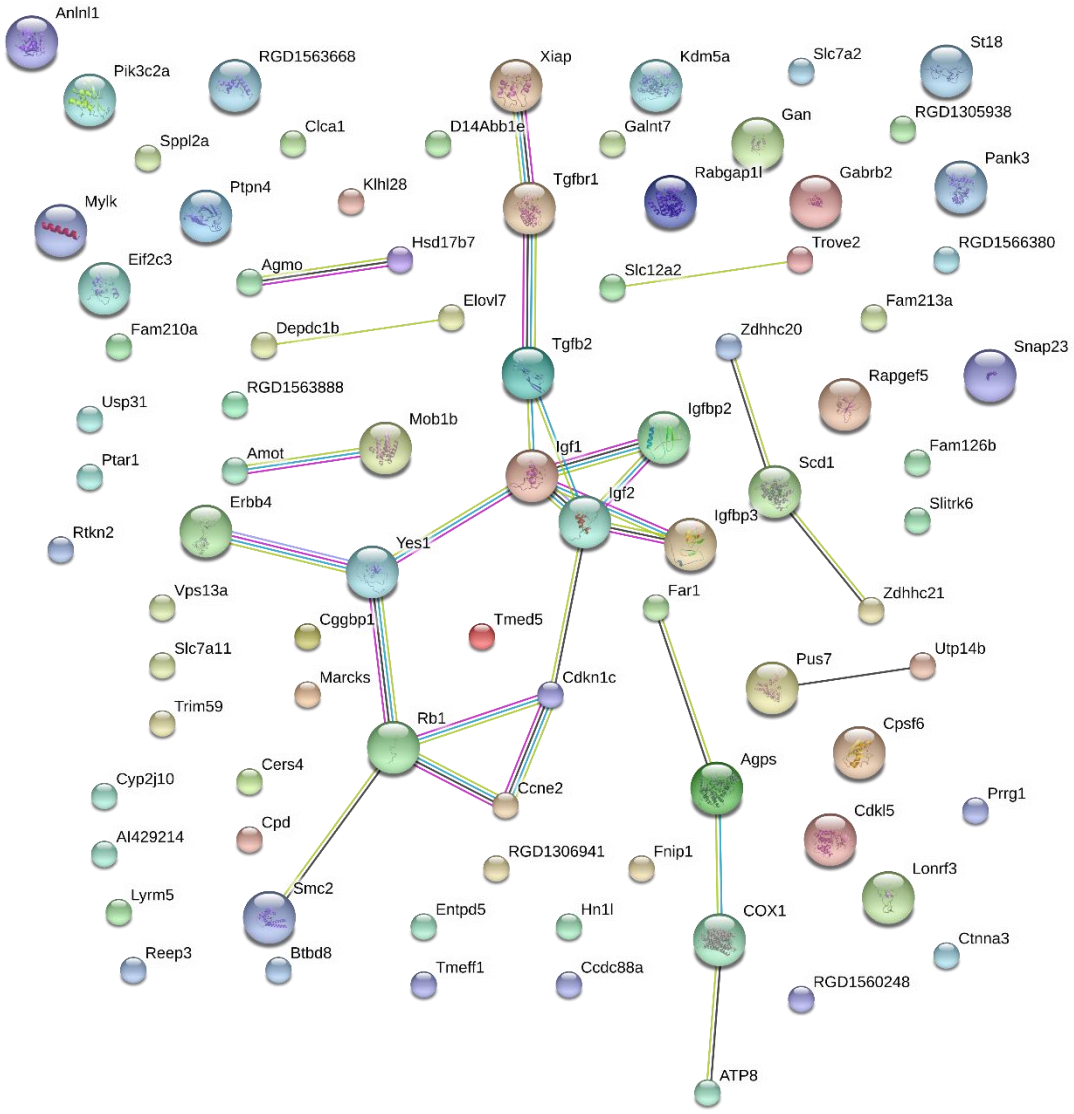

Figure 3.5. STRING network analysis of upregulated genes in the lumbar spinal cord of BCIBP rats at day 10 post-ITI, compared to sham rats at day 10 post-ITI after an ITI of heat-killed cells.

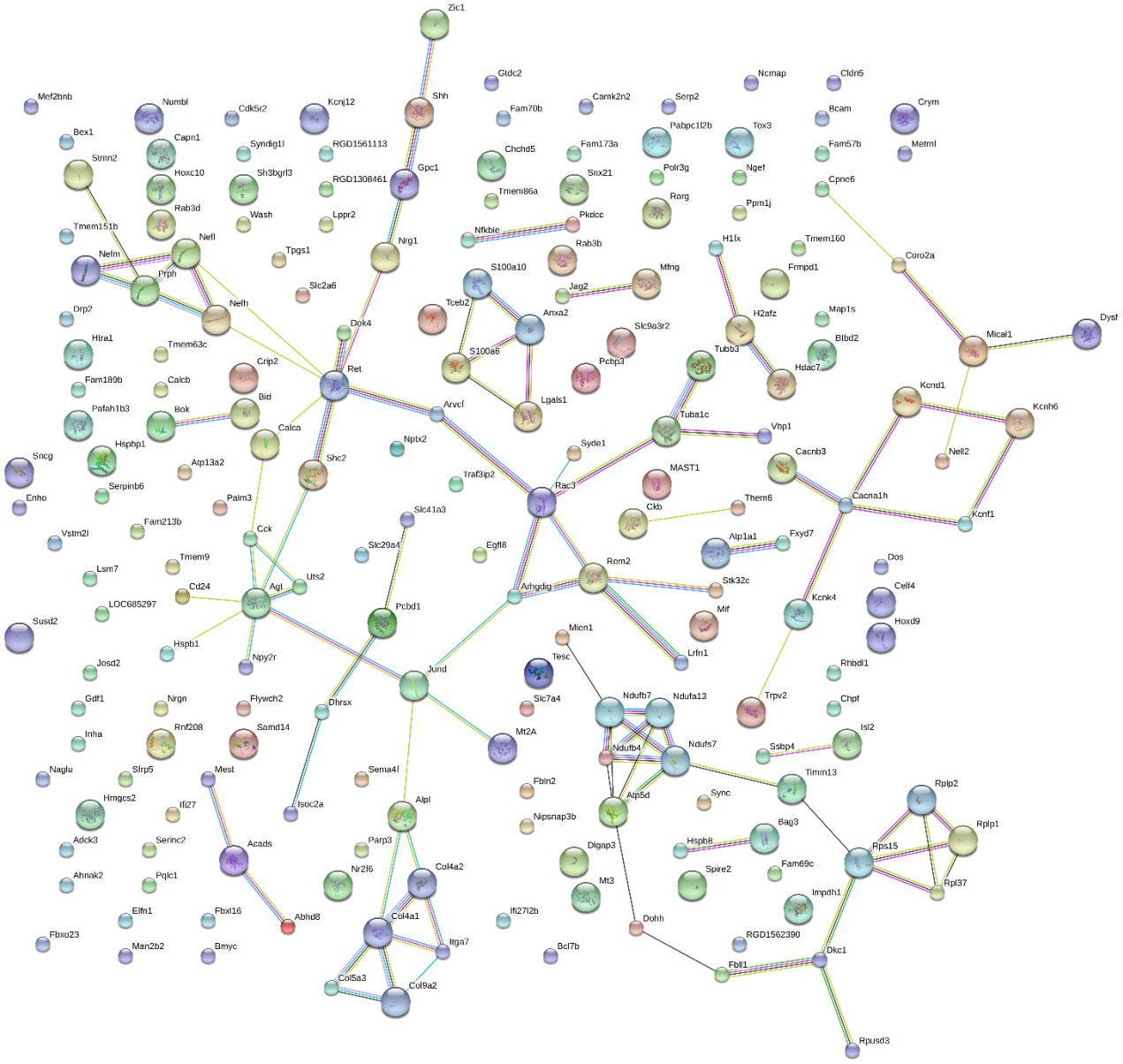

Figure 3.6. STRING network analysis of downregulated genes in the lumbar spinal cord of BCIBP rats at day 10 post-ITI, compared to sham rats at day 10 post-ITI after an ITI of heat-killed cells.

3.5. Discussion

The Walker 256 cell line is one of the most commonly used cell lines in breast cancer research, however its molecular genetic profile is still unknown. Hence, we used RNA-seq which is a powerful tool for gene expression analysis (Yin et al., 2016b). Human breast cancers are quite heterogeneous in nature and there are several schemes to classify breast cancers like histological, functional and molecular classifications (Malhotra et al., 2010). The most important classification system of breast cancer is based on molecular subtypes, because the pharmacotherapeutic treatment thereof depends on the molecular subtypes (Kimbung et al., 2015). Clinically, there are five molecular subtypes of breast cancer tumours: luminal-A, luminal-B, Erbb2, basal-like and normal-like; while there are three molecular subtypes of human breast cancer cell lines: luminal, basal-A and basal-B (Kao et al., 2009, Neve et al., 2006, Yersal and Barutca, 2014, Cianfrocca and Gradishar, 2009). Luminal cell lines resemble either luminal-A or B tumours in the clinical setting, whereas basal-A cell lines resemble basal-like tumours (Kao et al., 2009). The work presented in this chapter is the first to report that the Walker 256 cell line resembles the basal-B molecular subtype of breast cancer cell lines. Basal-B type cell lines represent an uncommon tumour subtype which is not yet well-characterised and might resemble basal-like / triple-negative tumors or Erbb2 tumours or might also display a stem cell like expression profile (Neve et al., 2006, Kao et al., 2009). These cell lines are typically highly invasive in nature, when compared to basal-A and luminal cell lines (Neve et al., 2006). We found that the Walker 256 cell line is estrogen / androgen / progesterone receptor negative and Her2 positive in nature. It is not known in detail whether the breast cancer pain phenotype differs between cancer subtypes. Several important genes like Mki67 and Tp53 known for aggressiveness of breast cancers were expressed in the Walker 256 cell line. Overall, several different genes pertaining to progression of breast cancer were identified to be present in the Walker 256 cell line. Importantly, the work presented in this chapter is the first to report the ontological analysis of genes expressed by the Walker 256 cell line, using the ontological classification type- Biological Process.

In the transcriptomic characterization of neural tissues from BCIBP rats herein, the ontological analysis and KEGG pathway analysis of differentially expressed genes provided valuable insights into different pathological pathways involved in this model. The gene ontology analysis of differentially expressed genes in spinal cord tissues of rats in pain-state, identified important biological processes (e.g. biological adhesion) and cellular components (e.g. synapse, cell junction, extracellular matrix, extracellular region) that are known to be associated with pain (Jamieson et al., 2014). Similarly, using KEGG pathways enrichment analysis of differentially expressed genes in spinal cord of rats in pain-state, we found that KEGG pathways like focal adhesion, pathways in

cancer, proteoglycans in cancer, and HTLV-I infection, known to be involved in chronic neuropathic pain (Zhang and Yang, 2017), were significantly enriched. STRING network analysis provided insights into the interactions between differentially expressed genes.

There were no changes observed in the ipsilateral lumbar DRGs at the mRNA level at day 10 post-ITI of Walker 256 cells. This is an intriguing finding, in view of the fact that tumour cells grow in vicinity of the peripheral nerves within the bone. However, a wide range of possible mechanistic changes could underpin the pathophysiology of this model, which has not been studied in this thesis. It is possible that mRNA levels of targets change at a different time point (for example, after day 15 following cancer inoculation), and RNA-seq analysis at various time points within the pain-state window might further help to identify the gene level changes contributing to the pathophysiology of this model. A significant discordance between genes and protein expression in the tissues is also not unexpected, at a given timepoint (Kosti et al., 2016). Additionally, it is noteworthy that gross changes in proteins are not always essential in driving the process of nociception, as variety of factors like structural changes in target receptors, modulation of signals emanating from these targets converging on other targets / ion channels, etc. might contribute in the process. Importantly, during the pain state, significant changes in the mRNA levels of several genes were clearly evident in the spinal cord, as per the data provided in this thesis. This strongly suggests of the spinal mediation in the pain pathophysiology of this model. Additionally, the changes could also occur in the brain, which has not been assessed in this study. Changes in protein levels of different targets in DRGs, spinal cord or brain might underpin the pathophysiology in this model. For example, important proteins like nerve growth factor (NGF) could be responsible at the protein level for inducing peripheral sensitization (Jankowski and Koerber, 2010). A variety of mechanistic changes could be occurring in different neuronal and non-neuronal tissues, including structural / conformational changes as well as modulation of the functions of the receptors, ion channels and enzymes involved in pain processing pathways, and alterations in the binding / functional abilities of their endogenous ligands, substrates or downstream effectors, as well as altered trafficking of various targets.

It is well known that peripheral nerve sensitisation can induce changes in the dorsal horn of the spinal cord (Gao and Ji, 2009). Spinal cord is considered to be an important target in gene expression studies involving animal models of pain hypersensitivities (Rodriguez Parkitna et al., 2006, Rojewska et al., 2014). The gene-level changes observed in the spinal cord are in alignment to the well-established fact that chronic pain associated with malignant cancer induced bone disease is significantly manifested due to the spinal sensitisation and synaptic plasticity in the spinal cord,

that is responsible for amplification of the nociceptive signals and transmission of impulses to the higher centres (Delaney et al., 2008). Several important proalgesic genes were upregulated in the pain state in BCIBP rats' lumbar spinal cord at day 10 post-ITI, compared to sham rats given an ITI of heat-killed cancer cells at day 10 post-ITI. Many genes known to mediate analgesic activity were also found to be downregulated in the spinal cord of rats during the pain state. Erbb4 gene was upregulated in BCIBP rats' lumbar spinal cord during the pain state. This could be a result of peripheral nerve damage due to cancer growth and osteolysis, as the Erbb4 gene was upregulated in the spinal cord of female rats following nerve root injury (LaCroix-Fralish et al., 2006). The transforming growth factor-β receptor 1 (*Tgfbr1*) gene was upregulated in the lumbar spinal cord of BCIBP rats during the pain state. Tgfbr1 is known to be an important gene implicated in pain processing pathways as the conditional knockout of this gene in trigeminal ganglia and DRGs of mice has been shown to attenuate hyperalgesia (Utreras et al., 2012). The solute Carrier Family 12 Member 2 (Slc12a2 / NKCC1) gene was upregulated in the lumbar spinal cord during the pain state. A role of NKCC1, a protein encoded by the Slc12a2 gene, in nociception is well established (Gagnon and Delpire, 2013). Myristoylated Alanine-Rich C-Kinase Substrate (Marcks) was upregulated in the spinal cord during the pain state in BCIBP rats herein. The phosphorylation of Marcks in the lumbar spinal cord is involved in inflammatory pain and the maintenance of neuropathic pain (Tatsumi et al., 2005).

The SLC9A3 Regulator 2 (Slc9a3r2) gene was downregulated in BCIBP rat spinal cord during the pain state. In work by others, Slc9a3r2 was downregulated in spinal cord, following traumatic spinal cord injury in rats (Yang et al., 2017). Another important gene known to mediate analgesic activity was downregulated in the lumbar spinal cord during the pain state herein was Annexin A2 (Anxa2). Anxa2 reduces the availability of TRPA1 channels in sensory neurons and thereby inhibits nociceptive signalling (Avenali et al., 2014). However, whether Anxa2 plays any role in modulating nociception at the spinal level warrants further investigation. During the pain state in BCIBP rats, the gene encoding the protein Cysteine-rich protein 2 (Crip2), which participates in spinal nociceptive processing and inhibits the generation of inflammatory pain (Schmidtko et al., 2008), was downregulated in the lumbar spinal cord. Endogenous GDNF family ligands/ RET Receptor Tyrosine Kinase (Ret) signalling is known to attenuate hypersensitivities associated with neuropathic and inflammatory pain (Golden et al., 2010). During the pain state of BCIBP rats, the RET gene was downregulated in the lumbar spinal cord, and hence further assessment of the effects of downregulation of this gene in facilitating pain hypersensitivities, would be interesting. An isoform of Neuregulin 1 (Nrg1) has been shown to decrease in DRGs of rats following spinal nerve ligation (Kanzaki et al., 2012). In the present study, Nrg1 was downregulated in BCIBP rats'

lumbar spinal cord during the pain state, suggesting a possible role of Nrg1 gene in nerve injury, regeneration and neuropathic pain in this cancer pain model. Potassium Two Pore Domain Channel Subfamily K Member 4 (Kcnk4) has an inhibitory role on pain hypersensitivities (Danser and Anand, 2014, Schneider et al., 2014). Kcnk4 was downregulated in the spinal cord of BCIBP rats during the pain state, which could be one of the factors responsible for enhanced hypersensitivities in this model. Another important gene mediating analgesic activity that was downregulated in spinal cord during the pain state was Nuclear Receptor Subfamily 2 Group F Member 6 (Nr2f6 / Ear2). It has been shown that Ear2 (Nr2f6) knockout mice exhibit increased nociception (Warnecke et al., 2005). Additionally, the transient receptor potential vanilloid type 2 (Trpv2) gene, known to be involved in pain transduction (Mercado et al., 2010), was downregulated in BCIBP rats' lumbar spinal cord during the pain state. This could be a consequence of body's endogenous repair processes to combat the pain hypersensitivities.

In BCIBP rats' ipsilateral lumbar DRGs at day-48 post-ITI (resolved pain state), several proalgesic genes were found to be downregulated, compared to the BCIBP rats' ipsilateral lumbar DRGs at day-10 post-ITI (pain state). Matrix Metalloproteinase-14 (Mmp14) was one of the genes downregulated. Mmp-14 is an activator of Matrix Metalloproteinase-2 (Mmp-2), which is implicated in neuropathic pain development in the late phase (Ji et al., 2009b). Sphingosine-1-Phosphate Receptor 3 (S1pr3) gene was also downregulated in the ipsilateral lumbar DRGs of BCIBP rats during the resolved pain state. S1pr3 receptors, which are present on most DRG neurons, are known to mediate nociceptor excitation and ongoing pain behaviour in mice and humans (Camprubi-Robles et al., 2013). CD93 Molecule (CD93 / C1qR) is another proalgesic gene that was downregulated in the ipsilateral lumbar DRGs of rats during the resolved pain state. Inhibiting C1qR is suggested to have potential in treating neuropathic pain (Chen et al., 2013b). Additionally, two other genes that were downregulated in the ipsilateral lumbar DRGs of rats during the resolved pain state were Cell Adhesion Molecule 4 (Cadm4) and Glutathione Peroxidase 7 (Gpx7). Gene deletion of Cadm4 causes myelin abnormalities that resemble a neuropathic condition (Golan et al., 2013). Gpx7 is upregulated in the axonal compartment of rat DRGs in a neuropathic pain model of sciatic nerve entrapment (Hirai et al., 2017). Although genes encoding components of the opioid system were not changed at the mRNA level in the ipsilateral lumbar DRGs of BCIBP rats during the resolved pain state, the fact remains that the resolved pain hypersensitivities are reversed by administration of naloxone. This emphasizes that the endogenous opioid-sensitive mechanisms could underpin the resolution of pain hypersensitivities at the protein level. Also, endogenous opioid-sensitive mechanisms might possibly contribute towards the pain resolution at the spinal cord or brain levels, which remains to be investigated in the future. This is

the first report of ontological characterisation of differentially expressed genes in neural tissues of Walker 256 cell induced BCIBP in rats and it provides important insights.

Total mRNA based gene expression patterns of breast cancer tissues cannot be assumed to be the features of breast cancer cells alone, because breast cancer tumours also consist of additional components including other types of epithelial cells, adipose cells, stromal cells, components of the immune system and vasculature as well as endothelial cells (Perou et al., 1999). So the system used to classify breast cancer tumours cannot be accurately extrapolated to classify the breast cancer cell lines, and vice versa. The work presented in this chapter was intended to identify the molecular subtype of the Walker 256 breast cancer cell line. However, the subtype of breast cancer tumour produced by Walker 256 cells *in vivo* cannot be defined using the present data, and hence is out of the scope of present work.

The work presented in this chapter is a pioneering attempt to perform transcriptomic characterization of not only the neural tissues of the BCIBP rat model, but also the Walker 256 breast cancer cell line used to induce this model. It is noteworthy that the application of RNA-seq procedures can have some drawbacks like any other scientific technique. For example, the sequencing depths can affect the detection of transcripts and the identification of differential expression. This increases the number of false positives with an increase in the total number of read counts (Tarazona et al., 2011). Improvements in the RNA-seq protocol can be made by altering the library preparation methods. Additionally, improving the sequencing accuracy and mapping pecision can help in reducing the noise levels and thereby improves the differential expression analysis (Tarazona et al., 2011). RNA-seq quantification can also underestimate the expression of several genes. Two / multiple stage analysis of RNA-seq data might help in uniquely assigning multi-mapped or ambiguous reads to group of genes (Robert and Watson, 2015). In such complex exploratory studies, it is hard to attribute a pathological role to a gene, without further assessments. To follow up a ‘hit’ identified in such RNA-seq studies, we would need further detailed validations using functional and pharmacological assays, as well as studies in knockout animals. However, RNA-seq method is a very useful technique in gene-based studies, because RNA-seq analysis of cancers has potential to be clinically translated into patient care (Roychowdhury and Chinnaiyan, 2016). It is well known that there can be significant differences in the genetic expression profile of a cancer cell line cultured *in vitro* and the tumour cells growing *in vivo*. So the future approach could be to isolate tumour cells from rat tibial bone marrow and perform transcriptomic analysis to study the genetic expression profile of the actual tumour. The knowledge of differentially expressed genes in neural tissues of BCIBP rats has the potential to direct studies aimed at investigating the

mechanisms underpinning pain hypersensitivities and also may provide insights into potential therapeutic interventions in the management of BCIBP. The neural tissues used for RNA-seq analysis in the present study were whole ipsilateral lumbar DRGs and lumbar spinal cord tissues, which contain multiple types of neurons, glial cells and other components like vasculature. The future approach could be to focus specifically on neuronal subtypes in the DRGs and spinal cord of BCIBP rats.

Chapter 4

Analgesic efficacy of J-2156, a somatostatin receptor– 4 agonist, in a rat model of breast cancer induced bone pain

4.1. Foreword:

In the previous two chapters, I have reported a thorough characterization of Walker 256 cell induced rat model of bone cancer pain using behavioural, pharmacological, radiological, histological, immunohistochemical and transcriptomic approaches. Hence, the last part of my research project was to characterize and validate the suitability of this model in assessing novel analgesic compounds. Somatostatin receptor 4 (SST4 receptor) is an interesting pharmacological target mediating pain pathobiology and analgesia. J-2156, an SST4 receptor agonist, is a novel compound known to be effective in alleviating pain hypersensitivities in animal models of neuropathic and inflammatory pain. Hence, I performed pharmacological and *ex vivo* characterization of the Walker 256 cell induced bone pain model to assess whether the SST4 receptor is able to mediate analgesia in a preclinical model of cancer induced bone pain which involves both neuropathic and inflammatory pain components, along with unique tumour-specific factors. I am thankful to Dr Louise CJ Gorham, Dr Janet Nicholson and Dr Laura Corradini (Boehringer Ingelheim Pharma GmbH & Co. KG, Biberach, BW, Germany) for supplying the data on *in vitro* binding affinity/potency of J-2156.

This chapter has been adopted from a research manuscript that arose from this thesis, under review for publication by the journal Frontiers in Pharmacology.

4.2. Introduction

Breast cancer is the most frequent type of cancer diagnosed in women and the major cause of cancer-associated mortalities in the world (DeSantis et al., 2015). Metastasis of breast cancer cells to the skeleton is a significant problem as it may cause excruciating pain (Bu et al., 2014). Bone metastases lead to destruction of bones due to increased activity of osteoclasts (Kane et al., 2015). Cancer cells in the bones locally stimulate as well as induce the release of inflammatory mediators (Kane et al., 2015, Lozano-Ondoua et al., 2013a, Esquivel-Velazquez et al., 2015). Sensory nerve fibres innervating tumour bearing bones, undergo pathological sprouting and reorganisation (Bloom et al., 2011). Hence, cancer-induced bone pain has a very complex pathophysiology as it is underpinned by both inflammatory and neuropathic components, along with an interplay of cancer-specific factors (Cao et al., 2010). It involves pathobiological alterations of peripheral tissues and

nerve fibres as well as characteristic neurochemical changes at the level of the spinal cord (Falk and Dickenson, 2014).

Presently, non-steroidal anti-inflammatory drugs (NSAIDs), strong opioid analgesics, bisphosphonates and monoclonal antibodies targeted to the inhibition of osteoclastic activity are the main drug treatments for breast cancer-induced bone pain (BCIBP) (Kane et al., 2015). However, these treatments may be inadequate and/or may evoke dose-limiting side effects (Shenoy et al., 2016). Hence, it is important to identify new targets for development of novel analgesic agents with improved efficacy and tolerability for alleviation of BCIBP. One such target is the somatostatin receptor type 4 (SST4 receptor) (Abdel-Magid, 2015, Crider and Witt, 2007, Somvanshi and Kumar, 2014). J-2156 [(1'S,2S)-4amino-N-(1'-carbamoyl-2'-phenylethyl)-2-(4"-methyl-1"-naphthalenesulfonylamino)butanamide] is an agonist that binds with nanomolar affinity to the human SST4 receptor and that has more than 400-fold selectivity compared with other somatostatin receptors (Engstrom et al., 2005). To complete the preclinical profile of J-2156, we tested its *in vitro* potency and selectivity towards human and rat SSTR4 receptor as well as a panel of 67 known pharmacological targets. Although there are several know ligands / agonists of the SST4 receptor (Crider and Witt, 2007, Erchegyi et al., 2003a, Erchegyi et al., 2003b, Grace et al., 2003), J-2156 has high potency and a low propensity to cause receptor desensitisation (Engström et al., 2006, Engstrom et al., 2005). Additionally, in work by others, J-2156 has been shown to induce pain relief in animal models of both inflammatory and neuropathic pain (Sándor et al., 2006, Schuelert et al., 2015).

However to date, the efficacy of J-2156 in BCIBP, has not been assessed preclinically. Hence this study was primarily designed to assess the efficacy of J-2156 to alleviate mechanical allodynia and hyperalgesia in a rat model of BCIBP previously validated in our laboratory (Shenoy et al., 2017). Due to limited permeability of the blood-brain barrier, at the doses tested, J-2156 is considered likely to act on peripheral SST4 receptors, although it is also capable of inhibiting spinal neurons (Schuelert et al., 2015). Peripheral small diameter peptidergic and non-peptidergic C-fibres as well as medium-large diameter fibres including A-δ and A-β fibres have key roles in the neural signalling of cancer pain (Colvin and Fallon, 2008, Ye et al., 2014c, Mantyh, 2006, Urch et al., 2003, Mao-Ying et al., 2006, Donovan-Rodriguez et al., 2005). Our work herein is the first to assess the distribution of the SST4 receptor in primary somatosensory neurons of the ipsilateral lumbar dorsal root ganglia (DRGs) of rats in the BCIBP model. In addition, in the same animal model, we have assessed the effect of J-2156 on lumbar spinal dorsal horn expression levels of phosphorylated

extracellular signal-regulated kinase (pERK), a protein implicated in the pathobiology of central sensitisation and persistent pain (Gao and Ji, 2009).

4.3. Material and methods

4.3.1. Drugs, chemicals and reagents

Triton™ X-100, Tween 20 and paraformaldehyde (PFA) were purchased from Sigma-Aldrich® (NSW, Australia). Isoflurane (IsoFlo™) was purchased from Abbott Australasia Pty Ltd (NSW, Australia). Medical oxygen was purchased from Coregas Pty Ltd (NSW, Australia). Triple antibiotic powder (Tricin®) was purchased from Jurox Pty Ltd (NSW, Australia). Benzylpenicillin (BenPen™, benzylpenicillin sodium for injection) was purchased from CSL Ltd (VIC, Australia). Pentobarbitone (Lethabarb®, pentobarbitone sodium) was purchased from Virbac (Australia) Pty Ltd (NSW, Australia). Eye ointment (Refresh Night Time®) was purchased from Allergan Australia Pty Ltd (NSW, Australia). 4',6-diamidino-2-phenylindole, dihydrochloride (DAPI), Prolong® Gold antifade reagent, phosphate-buffered saline (PBS), medium 199 (1X), horse serum, Dulbecco's phosphate-buffered saline (DPBS, 1X) and 0.25% trypsin-EDTA (1X) were purchased from Thermo Fisher Scientific Australia Pty Ltd (VIC, Australia). Normal goat serum (NGS) was purchased from Cell Signaling Technology® (MA, USA). Tissue-Tek® O.C.T. Compound was purchased from ProSciTech Pty Ltd (QLD, Australia). Sodium Chloride injection BP (British Pharmacopoeia) (0.9%) was purchased from Pfizer Australia Pty Ltd (NSW, Australia). J-2156 was obtained from Boehringer Ingelheim Pharma GmbH & Co. KG, (BW, Germany).

4.3.2. Radioligand binding assays

4.3.2.1. Assessment of reactivity of J-2156 to receptors of the somatostatin family

These binding studies were conducted in order to determine the selectivity and affinity of J-2156 to different human somatostatin receptors and to the rat SST4 subtype. Radioligand binding assays were performed in 96-well ELISA plates (NUNC, Denmark) using binding buffer (10 mM/L HEPES; 1 mM/L EDTA; 5 mM/L $MgCl_2x6H_20$) containing 30 µg/mL bacitracin (Sigma, Germany), and 5 mg/ml protease-free BSA fraction V (Sigma, Germany, A-3059). The pH was adjusted to 7.6 using 4 M NaOH. Selectivity of J-2156 was determined using membrane preparations from CHO-K1 cells stably-expressing human somatostatin receptor subtypes 1-5. J-2156 was tested in duplicates, over a range of concentrations from 10^{-12} M to 10^{-5} M and the endogenous ligands somatostatin 14 (BioTrend, Germany), somatostatin 28 and cortistatin 17 were run in parallel as positive controls. Binding curves were derived from competition binding experiments against 0.05 nM [125I]-Tyr3-somatostatin-(1-14) (ANAWA Trading SA, Switzerland).

The final activity of the label was 80.5 TBq/mM. The end volume was 250µl/well, where initially 25 µl of compound was added to each well, followed by 25 µl of radioligand and then finally 200 µl of cell suspension. Total-binding was defined using only the assay buffer and nonspecific binding was defined with 1 µM somatostatin 14. The initial incubation was carried out at room temperature (23-24 ^{o}C) for 3 hours with constant shaking. The reaction was then terminated by rapid filtration through a Packard harvester (Perkin Elmer, Waltham, MA) onto unifilter-96 GF/B filter plates (Perkin Elmer, Waltham, MA) which had been pre-soaked in 0.3% polyethyleneimine (Sigma, Germany). The plates were washed 3 times using ice-cold (4 ^{o}C) physiological (9 g/L) sodium chloride (NaCl) solution (Merck, USA) at an approximate volume of 300 µL/well. Following addition of 50 µL/well of scintillant (Microscint 20, Packard, USA), the plates were further incubated at room temperature (23-24 ^{o}C) for 1 hour in the dark. Analysis for radioactivity was conducted using the Top Count NXT^{TM} microplate scintillation counter (Packard, USA).

4.3.2.2. Assessment of cross-reactivity of J-2156 to other pharmacological targets

J-2156 was assessed in a lead profiling binding assay screen (Ricerca Biosciences LLC) consisting of 67 pharmacological targets, to identify the affinity of J-2156 for a range of receptors, ion channels, transporters, etc. by following standard radioligand binding assay protocols (Guerrero et al., 2010b, Guerrero et al., 2010a, Strøbæk et al., 2013). The significance level of inhibition or stimulation at 10 µM was predefined at ≥50 % for all the assays.

4.3.3. Potency of J-2156: cAMP inhibition

Total cAMP accumulation was measured using the LANCE cAMP detection kit (Perkin Elmer, Waltham, MA), in 384 optical assay plates. J-2156 was tested at concentrations ranging from 10^{-12} M to 10^{-5} M at a volume of 2 µL/well. All dilutions were prepared in stimulation buffer prepared from HBSS 1x solution (Gibco, UK), with an addition of 5 mM HEPES buffer (Gibco, UK), 0.1% BSA (Serva, Germany) and 500 mM isobutylmethylxanthine (IBMX, Sigma, Germany). IBMX, an inhibitor of cAMP phosphodiesterases, was added to prevent the enzymatic breakdown of the produced cAMP. Each concentration of standard or J-2156 was tested in duplicate or triplicate, respectively. The cAMP standard was prepared by diluting 8 µL of the 50 µM standard solution (provided by Perkin Elmer, Waltham) in 92 µL of stimulation buffer, to make a concentration of 1 µM. Serial dilutions were then prepared, using the stimulation buffer, from 1000 nM to 0.01 nM, of cAMP standard. Initially the compounds or standards were pipetted to each well, the plates were then centrifuged at a speed of 1000 revolutions per minute (rpm) to ensure that the solution was at the bottom of the well. Intact H4 cells expressing either human or rat SST4 receptors (Perkin Elmer, Waltham) were used at 1250 cells/well or 1000 cells/well respectively with a volume of 5 µl/well.

The cells were stored in frozen aliquots (1 ml) at – 80°C and defrosted on the day of use. The vial was suspended in 9 ml DPBS solution and the number of cells were counted using 0.4% trypan blue stain (Invitrogen, Life Technologies, Germany) and the countess automated cell counter (Invitrogen, Life Technologies, Germany). A pellet was formed by centrifuging the cell suspension at 1200 rpm for 5 minutes, the DPBS was aspirated off and the pellet was re-suspended in the calculated volume of assay stimulation buffer. To this, the supplied Alexa Fluor® antibody was added at a dilution of 1:100. Next, the cells were added to the plate to allow pre-treatment with the compounds for 10 minutes at room temperature (23-24 ^{o}C). Following the addition of cells, the plates were centrifuged at a speed of 1000 rpm. For the standard, 5 µL of the supplied Alexa Fluor® antibody was mixed with 495 µL of stimulation buffer and rather than adding cells, 5 µL of the antibody solution was added to the standard wells. After 10 minutes, stimulation was achieved by adding either 10 µM or 30 µM forskolin (Sigma, Germany) for human or rat receptors, respectively. The plates were again centrifuged at 1000 rpm. The final volume was 10 µL/well. Plates were incubated for 1 hour at room temperature (23-24 ^{o}C) with constant shaking. Finally, the detection buffer (Perkin Elmer, Waltham) was added (10 µL/well) and the plates were centrifuged at 1000 rpm. This was followed by a further incubation period of 1 hour at room temperature (23-24 ^{o}C) in the dark. Plates were read using an EnVision Xcite 2104 multilabel reader (Perkin Elmer, Waltham, MA) at 665 nm.

4.3.4. Cell culture

Walker 256 cells were used to induce BCIBP in rats as reported in the literature (Shenoy et al., 2016). The Walker 256 breast cancer cell line [LLC-WRC 256 (ATCC® CCL-38^{TM})] at passage number 290 was purchased from the American Type Culture Collection (ATCC; VA, USA). The cells were cultured and passaged following the ATCC guidelines. The cells were thawed from frozen stocks and cultured in 75cm^2 Cellstar® flasks (Greiner bio-one) at 37 ^{o}C (5% CO2: 95% atmospheric air) in 20 mL of Medium 199 (1X) with an additional supplementation of 5% horse serum. In order to detach the cells, they were gently rinsed with 3 mL of DPBS (1X), followed by treatment with 2 mL of 0.25% trypsin-EDTA (1X). The cells thus detached were harvested by centrifuging with 8 mL of medium for 4 min at 200 ×g. The supernatant thus obtained was discarded, the pellet re-suspended in 3 mL of DPBS and cell counting was performed with a hemocytometer. After again centrifuging the pellet for 4 min at 200 ×g, the cells were suspended in DPBS to obtain a final dilution of 4×10^5 cells/10 µL. Heat-killed Walker 256 cells were prepared similarly to the live cells, however, the cells were heated to 90 °C for 15 min.

4.3.5. Animals

Female Wistar Han (HsdBrlHan) rats were used in the experiments. Animals were purchased from the Herston Medical Research Centre (Brisbane, Australia) of The University of Queensland. At the time of arrival in our research facility, the rats were approximately 3-4 weeks old and their body weights were in the range ~50-70 g. Rats were housed in small groups of two to three in individually ventilated cages in a room having a controlled temperature (23 °C ± 2 °C) and a 12 h/12 h light–dark cycle. Standard rodent chow (Specialty Feeds, WA, Australia) and tap water were available to all rats *ad libitum*. Kimwipes (Kimberly-Clark Professional, NSW, Australia) and Rat Chewsticks (Able Scientific, WA, Australia) were provided in the individual cages as environmental enrichment. Rats were subject to acclimatization in the animal housing facility for at least 3 days prior to initiating experiments. The experiments on these rats were performed in the light phase. The procedures involving animal experimentation were approved by the Animal Ethics Committee of The University of Queensland (QLD, Australia). The experiments described herein were performed as per the requirements of the Australia Code of Practice for the Care and Use of Animals for Scientific Purposes (8th edition, 2013).

4.3.6. Surgical procedure

Unilateral intra-tibial injections (ITI) were performed in accordance with the procedures reported previously (Mao-Ying et al., 2006, Muralidharan et al., 2013), with some modifications. In brief, rats in the weight range ~80–120 g were anesthetized deeply using 3% isoflurane delivered in oxygen. To avoid drying of the eyes during the surgical procedure, eye ointment was applied. Benzylpenicillin (60 mg per rat) injection was subcutaneously administered. A rostro-caudal incision of approximately 1 cm was made on the upper medial half of the lower left hindlimb. Following exposure of the tibia, using a 23-gauge needle, a hole was drilled into the bone below the knee joint, medial to the tibial tuberosity. Either live (BCIBP group) or heat-killed (sham-injected group) Walker 256 cells (4×10^5 cells in 10 µL DPBS) were injected into the bone cavity with a Hamilton® syringe (80508:705SN 50 µL SYR SPECIAL (22 /2″/4), NV, USA). Subsequently, the drilled hole in the bone was sealed immediately with Ethicon™ W810 bone wax (Johnson-Johnson International, Diegem, Belgium). The muscles and the skin were subsequently sutured using non-absorbable USP 5/0 Dysilk® suture (Dynek Pty Ltd, SA, Australia). Finally, topical antibiotic powder was applied to the stitched wound. The hindlimb injected with cells is termed as the ‘ipsilateral’ hindlimb and the non-injected hindlimb is termed as the ‘contralateral’ hindlimb. Following completion of the surgical procedure, rats were closely monitored for recovery and their general health was routinely assessed at least once per week until the end of the study.

4.3.7. Behavioral studies

4.3.7.1. Assessment of mechanical allodynia in the hindpaws

Development of mechanical allodynia in the bilateral hindpaws was assessed using calibrated von Frey filaments (Stoelting Co., Wood Dale, IL, USA). The lowest mechanical threshold which elicited a paw withdrawal response was measured (Ren, 1999). Rats were individually placed in wire mesh cages and acclimatized for approximately 15 to 30 min before applying the von Frey filaments. The filaments were individually applied to the surface of the plantar region of each hindpaw until they were slightly buckled. If there was no response after 3 s of applying the filament, the next higher filament was used in the ascending order (2, 4, 6, 8, 10, 12, 14, 16, 18, and 20 g) until the response was observed. If the hindpaw withdrawal response was observed within 3 s the next filament evoking a lower force was used. Initiation of the testing was done using a 6 g filament, and the subsequent force was modified depending upon the previous response. The baseline paw withdrawal thresholds (PWTs) of the ipsilateral as well as the contralateral hindpaws were recorded thrice at an interval of 5 min each and the mean of these readings was calculated. For behavioural testing after administration of J-2156 at pre-defined intervals over a 3 h period, the starting filament depended on the previous response. Rats having ipsilateral PWTs $\leq$ 6 g were defined as having fully developed mechanical allodynia. All the assessments using von Frey filaments were performed by an investigator blinded to the treatment.

4.3.7.2. Assessment of mechanical hyperalgesia in the hindpaws

Development of mechanical hyperalgesia in the hindpaws was tested using an Analgesy-meter (Ugo Basile, Italy). The mechanical force required to produce a withdrawal response in each of the hindpaws (paw pressure thresholds (PPTs)) of each rat was assessed (Randall et al., 1957). Briefly, each hindpaw was individually placed on a small plinth beneath a cone-shaped pusher with a rounded tip so as to avoid damage to the hindpaw tissue. The mechanism of exerting the force was started by depressing the pedal-switch. The pedal was released immediately when the rat began to struggle and the applied force was subsequently noted. A maximum cut-off force of 200 g was used to prevent injury to the hindpaws. Three baseline readings for each of the hindpaws were recorded with an interval of 5 min between successive readings. The mean baseline PPTs were calculated for each hindpaw. For pharmacological assessment of the anti-hyperalgesic effect of J-2156, rats with an ipsilateral PPT $\leq$ 80 g were considered to have fully developed mechanical hyperalgesia. All the PPT assessments were performed by an investigator blinded to the treatment group.

4.3.8. Administration of J-2156 and behavioural testing

Dosing of animals was performed by one investigator while the behavioural assessments were subsequently performed by a second investigator blinded to the treatment groups to ensure that the investigator bias was minimal throughout the procedure. Each rat received up to four individual intraperitoneal (i.p.) doses of test compounds or vehicle with at least 2 days of 'washout' between successive doses. Sodium Chloride injection BP (0.9 %) was used as vehicle for preparing J-2156 dosing solutions. Rats with fully developed hindpaw hypersensitivity were administered a single bolus dose of J-2156 (1, 3 and 10 mg/kg, i.p.) or vehicle between day 7-14 post-ITI of Walker 256 cancer cells. PWTs or PPTs were assessed in both the hindpaws immediately before compound or vehicle i.p. administration and subsequently at 0.25, 0.5, 0.75, 1.0, 1.25, 1.5, 2 and 3 h post-dosing.

4.3.9. Immunohistochemistry

Rats were euthanized on day 7 post-ITI with an injection of pentobarbitone and immediately perfusion-fixed with ice-cold 4% PFA. The tissues (brain/liver/spinal cord/DRGs) were harvested and further post-fixed with 4 % PFA. The spinal cord tissues used to assess the effect of J-2156 on pERK levels, were collected from the rats at the time of peak effect of J-2156. The tissues were cryoprotected successively in 15% sucrose/PBS and 30% sucrose/PBS at 4-8 °C and then immersed in a 1:1 mixture of OCT:30% sucrose/PBS at 4-8 °C, followed by freeze-mounting in Tissue-Tek® O.C.T. Compound. Frozen coronal sections of brain and transverse sections of liver, spinal cord and ipsilateral lumbar DRGs (7 μm thick) were obtained using a Cryostar NX70, (Thermo Fisher Scientific, Waltham, USA) and mounted on Uber Plus charged slides (InstrumeC Pty Ltd, VIC, Australia). The sections were washed with PBS (pH 7.4) solution thrice for 5 min each, and blocked with 10% NGS in PBS containing 0.3 % Triton™ X-100 for 1-2 hour at 23 °C ± 2 °C. Further, these sections were incubated with the respective primary antibody, diluted in 2 % NGS in PBS containing 0.1 % Tween 20, overnight at 4-8 °C. The primary antibodies used in the present study were anti-SST4 receptor antibody PA3208 (1:250 dilution, Life Technologies Australia Pty Ltd, VIC, Australia), anti-somatostatin antibody ab183855 (1:500 dilution, Abcam, VIC, Australia), anti-substance P (SP) antibody ab14184 (1:25 dilution, Abcam, VIC, Australia), anti-neurofilament 200 kDa (NF200) antibody ab82259 (1:50 dilution, Abcam, VIC, Australia) and anti-pERK antibody 4370S (1:50 dilution, Cell Signaling Technology®, MA, USA). Isolectin B4 (IB4) L 2895 (1:100 dilution, Sigma-Aldrich®, NSW, Australia) was also used. We used SP, IB4 and NF200 as specific somatosensory cell markers for peptidergic C-fibres, non-peptidergic C-fibres and medium-large diameter fibres including A-δ and A-β fibres, respectively (Le Pichon and Chesler, 2014). The sections were then washed twice for 5 min each with PBS containing 0.1 % Tween 20 and once for 5 min with PBS. These sections were further incubated with the corresponding secondary antibody,

diluted in PBS containing 0.1 % Tween 20, for 2 h at 23 °C ± 2 °C in the dark (~0.002 lux). The secondary antibodies used in the present study were goat anti-mouse IgG (H+L), Alexa Fluor 546 A-11030 (1:600 dilution, invitrogen™, OR, USA), goat anti-mouse IgG (H+L), Alexa Fluor 488 A-11029 (1:500 dilution, invitrogen™, OR, USA), goat anti-rabbit IgG (H+L), Alexa Fluor 488 A-11034 (1:600 dilution, invitrogen™, OR, USA), goat anti-rabbit IgG (H+L), Alexa Fluor 546 A-11035 (1:1000 dilution, invitrogen™, OR, USA) and Cy™3 AffiniPure goat anti-rabbit IgG (H+L) 111-165-003 (1:600 dilution, Jackson ImmunoResearch Inc., PA, USA). For co-localisation experiments, a suitable combination of primary antibodies and a combination of secondary antibodies were used. The dilutions of the two different antibodies in the same solution were made such that the final concentration of each of the antibodies in the solution was achieved as required. The sections were then washed twice with PBS containing 0.1 % Tween 20 and once with PBS for 5 min each. The sections were subsequently incubated with DAPI (0.5 µg/mL solution) for around 5-10 min and finally washed with PBS twice for 5 min each. The cover-slips were mounted on the sections along with Prolong® Gold antifade reagent. The mounted slides thus obtained were set aside to dry and stabilise in the dark at 4-8 ^{o}C overnight. Finally, the images were captured with a fluorescence microscope and analysed.

4.3.10. Acquisition of images and analysis

Images of experiments from immunohistochemistry were captured with an Axioskop 40 microscope that was attached to an Axiocam MRm camera. The images were processed using AxioVision Rel. v4.8 software (imaging equipments and software were from Carl Zeiss, Göttingen, Germany). For each of the experiments, images were captured at a fixed exposure time, which was optimised using auto-exposure settings of AxioVision Rel. v4.8 software. The filters used in the microscope were chosen to suit the respective fluorophore of the secondary antibody used in each of the experiments. For multiple labelling in co-localisation experiments, suitable filters were manually chosen in the microscope, so as to suit multiple fluorophores, for snapping one at a time in each of the experiments. For quantitative analysis, at least 3-4 non-adjacent sections per animal from each of the groups (n=3-4/group) were randomly selected. Images were assigned codes by the first investigator and quantitative analysis was performed by the second investigator in a blinded manner. Densitometric counts were quantified using AxioVision Rel. v4.8 software and the data was expressed as fold-changes in fluorescence intensity according to the standard immunohistochemistry analysis protocol validated in our laboratory (Khan et al., 2014, Khan et al., 2015, Muralidharan et al., 2014).

4.3.11. Data analysis and statistical analysis

All values have been expressed as mean ± standard error of the mean (SEM). In the radioligand binding assays of J-2156 with somatostatin receptors, Ki denotes a dissociation / inhibition constant, and can be considered to be the reciprocal of the binding affinity (Cheng and Prusoff, 1973). Data were obtained by non-linear regression analysis of the concentration response curves. The Cheng-Prusoff equation was used to derive the Ki values (Cheng and Prusoff, 1973). This was calculated using GraphPad Prism™ (v6.00) software, using the setting of 'one site – Fit Ki'. The constraints applied were: both the concentration of radioligand in nM (HotNM = 0.05 nM) and the equilibrium dissociation constant (Kd) of the radioligand in nM (HotKdNM for somatostatin receptor 1 = 0.85 nM; somatostatin receptor 2 = 1.2 nM; somatostatin receptor 3 = 0.31 nM; SST4 receptor = 0.45 nM; somatostatin receptor 5 = 2.0 nM).

In the cAMP inhibition assays, the term IC_{50} denotes the concentration producing 50 % inhibition (Cheng and Prusoff, 1973). The IC_{50} values were reported as the concentration of J-2156 producing 50% inhibition of the forskolin-stimulated cAMP production. Data were obtained by non-linear regression analysis of the concentration-response curves. The IC_{50} values were calculated with the GraphPad Prism™ (v6.00) software using the equation 'log(inhibitor) vs. normalised response'. Constraints were applied to the bottom value, which was set to the maximal inhibition produced by somatostatin 14.

All other graphs were stored, represented and analyzed using the GraphPad Prism™ (v7.00) software. The PWT values of individual rats that received single bolus doses of either J-2156 or the vehicle were normalized by subtracting pre-dosing baseline values so as to obtain ΔPWT values as given below:

$$\Delta\text{PWT value} = (\text{post} - \text{dosing PWT}) - (\text{Average pre} - \text{dosing baseline PWT})$$

Area under the curve (AUC) of ΔPWT versus time graphs (ΔPWT AUC values) for rats was calculated using trapezoidal integration to find the extent and duration of the anti-allodynic effect of each dose of J-2156. Next, the ΔPWT AUC values were further converted to a percentage of the maximum possible ΔPWT AUC (% MAX ΔPWT AUC) by using the following formula:

$$\%\text{MAX } \Delta\text{PWT AUC} = \frac{\Delta\text{PWT AUC}}{\text{Maximum } \Delta\text{PWT AUC}} \text{ x } 100$$

Dose–response curves were produced by plotting mean (±SEM) % MAX ΔPWT AUC values versus log dose of J-2156. The PPT data were processed by using similar steps as described above for the PWT data. Non-linear regression (GraphPad Prism™ v7.00) was used to calculate the ED_{50}

values of J-2156 for the alleviation of mechanical allodynia and mechanical hyperalgesia in each of the hindpaws.

GraphPad Prism™ v7.00 software was used to perform statistical analyses. The criterion for statistical significance was $p \leq 0.05$. To assess the between-group differences of baseline PWT/PPT values and PWT/PPT or ΔPWT/ΔPPT values following J-2156 administration, two-way analysis of variance (ANOVA) followed by the Bonferroni test was used. To assess differences between protein (SST4 receptor, somatostatin and pERK) expression in neural tissues as well as the data from co-localisation experiments, the Mann-Whitney test was used. One-way ANOVA followed by the Dunnett's test was used to compare between-group differences in ΔPWT/ΔPPT AUC values and % MAX ΔPWT/ΔPPT AUC values. For statistical comparisons using ANOVA, the F values are reported along with their associated degrees of freedom (treatment, time, interaction and residual). For two-way ANOVA, F values are reported as F(df of treatment, time, interaction/residual). While, for one-way ANOVA, F values are reported as F(df of treatment, residual).

4.4. Results

4.4.1. Radioligand binding assays

4.4.1.1. Assessment of reactivity of J-2156 to receptors of the somatostatin family

The affinity and selectivity of various somatostatin agonists for the five human somatostatin receptors and the rat SST4 subtype were established using radioligand binding assays. The somatostatin receptor selective endogenous ligands, somatostatin 14 and somatostatin 28, as well as the non-selective endogenous ligand, cortistatin 17, were used as positive controls (data not shown). These showed nanomolar affinities for all subtypes, thereby indicating no selectivity for a specific receptor subtype, but consistently showed least affinity for the somatostatin receptor 2. The log Ki (mean ± SEM; n=4) values of J-2156 for human somatostatin receptors 1, 2, 3 and 5 were found to be -6.23 ± 0.18, -4.60 ± 0.37, -6.63 ± 0.18 and -6.33 ± 0.17, respectively. By comparison, the log Ki (mean ± SEM) values of J-2156 in human (n=4) and rat (n=3) SST4 receptors were found to be -9.25 ± 0.09 and -9.05 ± 0.40, respectively. The Ki values of J-2156, derived using the Cheng-Prusoff equation, were found to be 0.6 nM and 0.9 nM for human and rat SST4 receptors, respectively.

4.4.1.2. Assessment of cross-reactivity of J-2156 to other pharmacological targets

J-2156 (10 μM) did not significantly stimulate or inhibit any of the pharmacological targets from the panel of 67 standard targets at / above the predefined significance level of ≥50 %. The J-2156 mediated non-cognate stimulation or inhibition of a panel of 67 pharmacological targets including various receptors, ion channels, transporters, etc. is summarised in Supplementary Table 4.1. These data suggest that J-2156 does not display significant cross-reactivity to any of these known pharmacological targets.

4.4.2. Potency of J-2156: cAMP inhibition

Using cAMP assays, we found that J-2156 is potently efficacious at both human and rat SST4 receptors. The log IC_{50} values [mean ± S.E.M (nM; n=3)] of J-2156 for human and rat SST4 receptors were found to be -10.3 ± 0.2 and -10.1 ± 0.1, respectively. The results also confirmed that the SST4 receptor can functionally couple to the adenylyl cyclase pathway potently; the EC_{50} of J-2156 being 0.5 nM and 0.8 nM for the human and rat receptors, respectively.

4.4.3. Development of mechanical allodynia and mechanical hyperalgesia in the bilateral hindpaws

Unilateral ITI of Walker 256 cells induced temporal development of mechanical hypersensitivity in the bilateral hindpaws in rats, in agreement with our findings in chapter 2 as well as previous findings by others (Mao-Ying et al., 2006, Mao-Ying et al., 2012). The mean (±SEM) PWTs in the ipsilateral hindpaws of BCIBP-rats were significantly ($F(1, 5, 5/65) = 432.1, 34.8, 30.6$; $p \leq 0.05$) reduced from day 4 post-ITI *c.f.* sham rats (Figure 4.1A). The mean (±SEM) PWTs in the contralateral hindpaws of BCIBP-rats were significantly ($F(1, 5, 5/65) = 198.8, 17.6, 21.1$; $p \leq 0.05$) reduced from day 7 post-ITI *c.f.* sham rats (Figure 4.1B). The mean (±SEM) PPTs in the ipsilateral hindpaws of BCIBP-rats were significantly ($F(1, 5, 5/65) = 1532, 139.3, 75.2$; $p \leq 0.05$) reduced from day 4 post-ITI *c.f.* sham rats (Figure 4.1C). The mean (±SEM) PPTs in the contralateral hindpaws of BCIBP-rats were significantly ($F(1, 5, 5/65) = 146.3, 32.0, 27.4$; $p \leq 0.05$) reduced from day 7 post-ITI *c.f.* sham rats (Figure 4.1D).

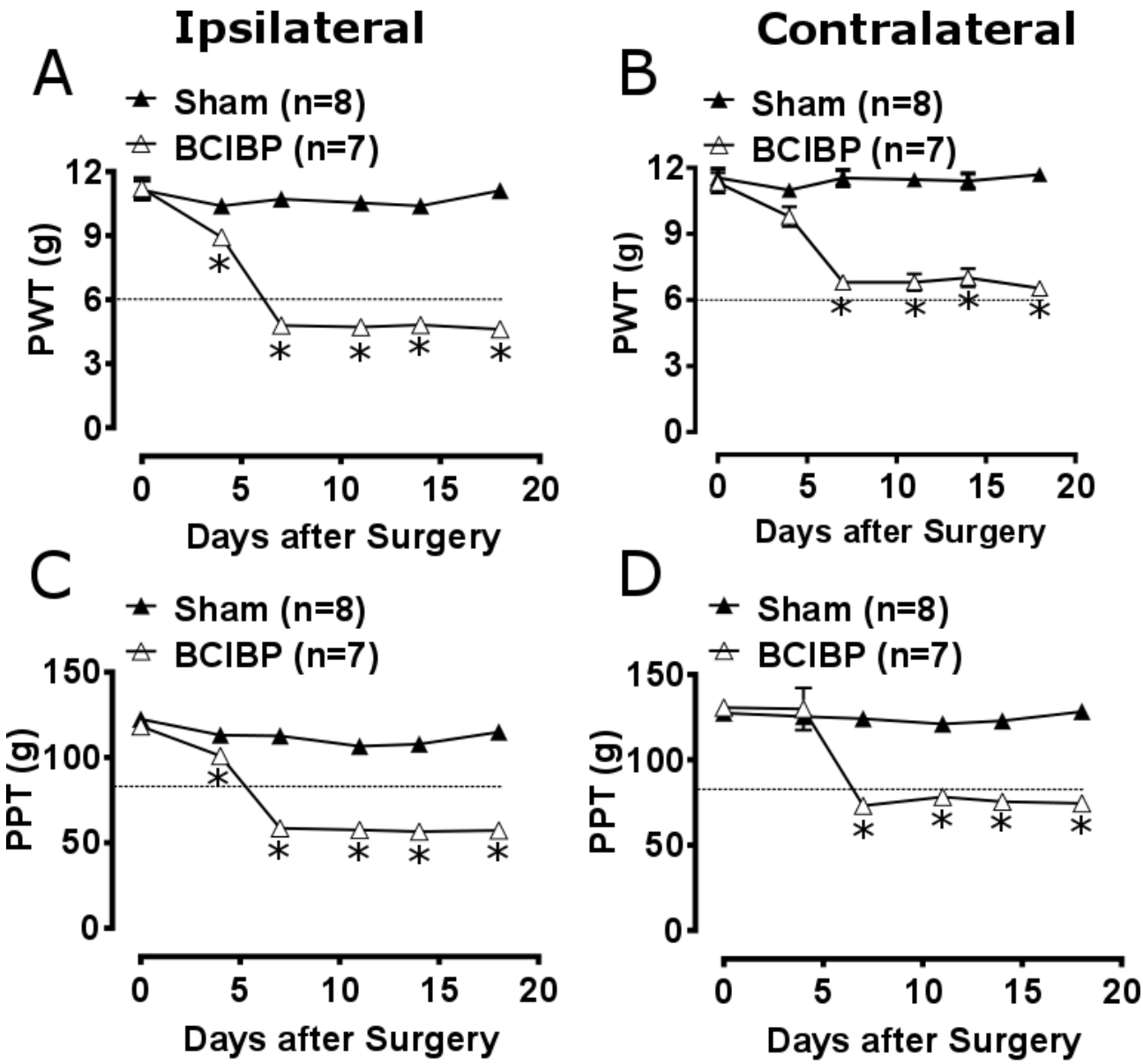

Figure 4.1. Temporal changes in mean (±SEM) paw withdrawal thresholds (PWTs) and paw pressure thresholds (PPTs) in the hindpaws of rats following a unilateral ITI of 4 x 10^5 Walker 256 cells (BCIBP group) and 4 x 10^5 heat-killed Walker 256 cells (sham group). Panels in the figure show (A) PWTs in the ipsilateral hindpaws, (B) PWTs in the contralateral hindpaws, (C) PPTs in the ipsilateral hindpaws and (D) PPTs in the contralateral hindpaws. The dotted line shows the threshold criterion for full development of mechanical allodynia (PWTs ≤ 6 g, panel A-B) and mechanical hyperalgesia (PPTs ≤ 80 g, panel C-D). *p≤0.05 (Two-way ANOVA, *posthoc* Bonferroni test) *c.f.* sham rats.

4.4.4. Anti-allodynic effect of J-2156 in BCIBP

Administration of J-2156 to BCIBP-rats produced dose dependent anti-allodynia in both the ipsilateral and the contralateral hindpaws (Figure 4.2). The $ED_{50\text{-Ipsilateral}}$ and $ED_{50\text{-Contralateral}}$ of J-

2156 against mechanical allodynia in the BCIBP-rats were found to be 3.7 mg/kg (95% confidence interval, 2.5-5.4) and 6.6 mg/kg (95% confidence interval, 4.2-10.5), respectively.

The extent and duration of efficacy (ΔPWT AUC) of J-2156 for the relief of mechanical allodynia in the bilateral hindpaws of rats in the BCIBP model are shown in Supplementary Table 4.2. The time courses of the anti-allodynic effect of J-2156 in BCIBP-rats at each of the doses tested have been summarised in Supplementary Table 4.3. Temporal changes in ΔPWT and the % MAX ΔPWT AUC values of the ipsilateral and contralateral hindpaws at each of the doses of J-2156 tested are shown in Supplementary Figure 4.1.

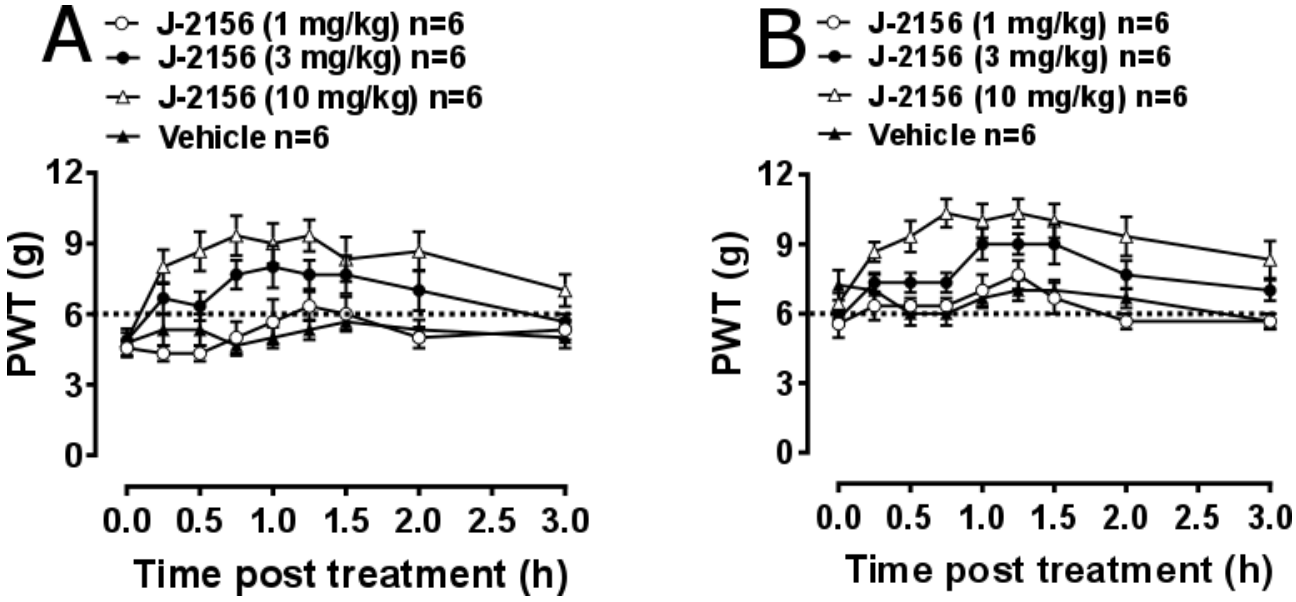

Figure 4.2. Anti-allodynic effect of single bolus doses (i.p.) of J-2156 on ipsilateral and contralateral hindpaw withdrawal thresholds (PWTs) in BCIBP-rats. Panels in the figure show mean (±SEM) (A) ipsilateral PWT versus time curves and (B) contralateral PWT versus time curves. The dotted line shows the threshold criterion of fully developed mechanical allodynia (≤ 6 g).

4.4.5. Anti-hyperalgesic effect of J-2156 in BCIBP

Administration of J-2156 to BCIBP-rats produced dose dependent anti-hyperalgesia in both the ipsilateral and the contralateral hindpaws (Figure 4.3). The $ED_{50\text{-Ipsilateral}}$ and $ED_{50\text{-Contralateral}}$ of J-2156 for relief of mechanical hyperalgesia in the BCIBP-rats were found to be 8.0 mg/kg (95% confidence interval, 5.3-12.2) and 5.0 mg/kg (95% confidence interval, 3.6-6.8), respectively.

The extent and duration of action (ΔPPT AUC values) of J-2156 for the relief of mechanical hyperalgesia in the bilateral hindpaws of BCIBP-rats is shown in Supplementary Table 4.4. The

time courses of the anti-hyperalgesic effect of J-2156 in BCIBP-rats at each of the doses tested are summarised in Supplementary Table 4.5. Temporal changes in the ΔPPT and the % MAX ΔPPT AUC values of the ipsilateral and contralateral hindpaws at each of the doses of J-2156 tested are shown in Supplementary Figure 4.2.

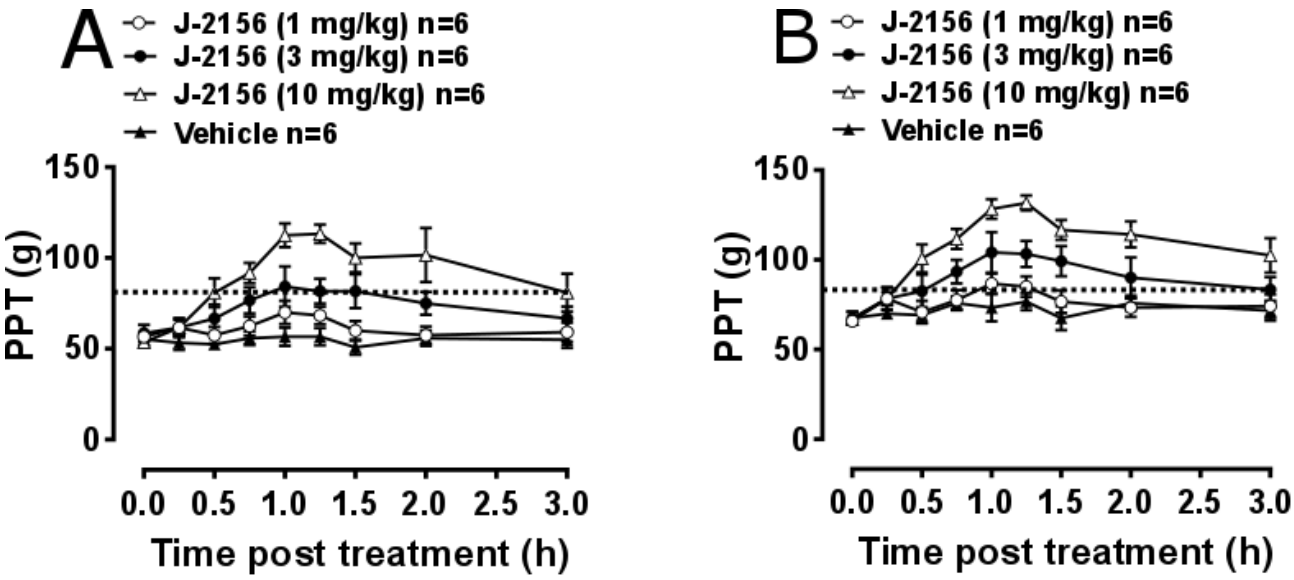

Figure 4.3. Anti-hyperalgesic effect of single bolus doses (i.p.) of J-2156 on ipsilateral and contralateral hindpaw pressure thresholds (PPTs) in BCIBP rats. Panels in the figure show mean (±SEM) (A) ipsilateral PPT versus time curves and (B) contralateral PPT versus time curves. The dotted line shows the threshold criterion of fully developed mechanical hyperalgesia (≤ 80 g).

4.4.6. Validation of the anti-SST4 receptor antibody

In the liver, somatostatin receptors type 1, 2, 3 and 5 are expressed, but expression levels of the SST4 receptor are negligible (Jung et al., 2006, Reynaert et al., 2004, Song et al., 2004, Murray et al., 2004). Conversely, the SST4 receptor is abundantly expressed in brain tissue (Selmer et al., 2000a, Selmer et al., 2000b). In coronal sections of rat brain used as a positive control, the SST4 receptor antibody produced immunofluorescence consistent with expectations. Importantly, in sections of rat liver that was used as a negative control, SST4 immunofluorescence was absent (Supplementary Figure 4.3). The immunofluorescence patterns of anti-SST4 receptor antibody using the afore-mentioned positive and negative control sections demonstrated its specificity for the SST4 receptor and absence of cross-reactivity with other somatostatin receptors, thereby validating the antibody.

4.4.7. Expression of SST4 receptor in DRGs and spinal cord in BCIBP

Expression levels of the SST4 receptor in sections of either the lumbar DRGs (Figure 4.4A, B and E) or the lumbar spinal dorsal horns (Figure 4.4C, D and F) of BCIBP-rats did not change significantly ($p > 0.05$) *c.f.* the corresponding sections from sham rats.

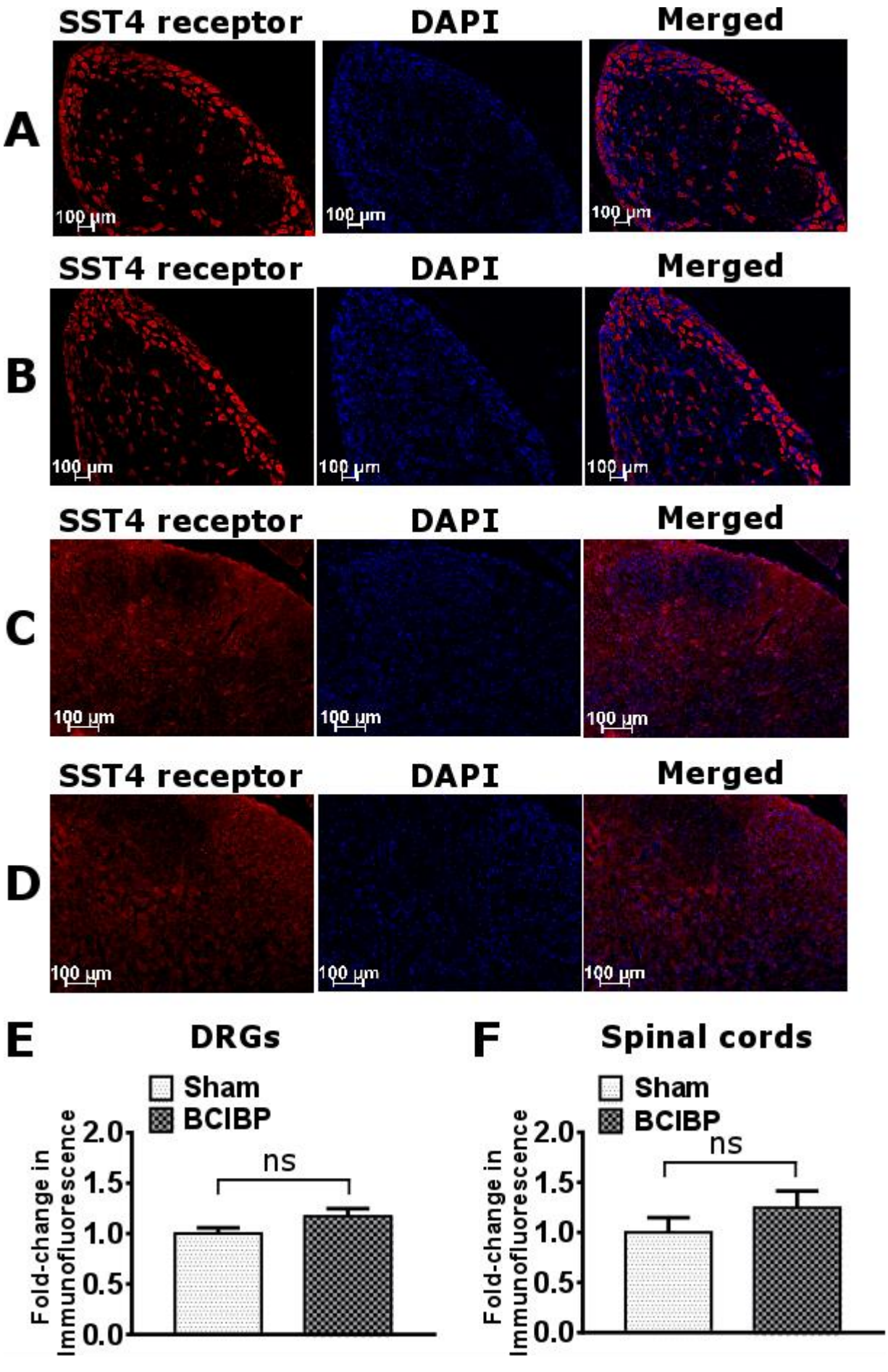
A
SST4 receptor
DAPI
Merged
100 µm
B
SST4 receptor
DAPI
Merged
100 µm
C
SST4 receptor
DAPI
Merged
100 µm
D
SST4 receptor
DAPI
Merged
100 µm
E
DRGs
Sham
BCIBP
ns
Fold-change in Immunofluorescence
2.0
1.5
1.0
0.5
0.0
F
Spinal cords
Sham
BCIBP
ns
Fold-change in Immunofluorescence
2.0
1.5
1.0
0.5
0.0

Figure 4.4. Expression levels of the SST4 receptor in sections of ipsilateral lumbar L4-L6 dorsal root ganglia (DRGs) and in sections of the lumbar spinal dorsal horns of BCIBP-rats and the corresponding sections from sham rats (n=3-4/group). Panels in the figure show representative sections of (A) DRG of a sham rat, (B) DRG of a BCIBP-rat, (C) spinal dorsal horn of a sham rat and (D) spinal dorsal horn of a BCIBP-rat. Panel (E) shows fold-change in immunofluorescence of ipsilateral lumbar DRG sections of the BCIBP group relative to the sham group and (F) shows fold-change in immunofluorescence of lumbar spinal cord sections of the BCIBP group relative to the sham group. ns, statistically not significant ($p>0.05$, Mann-Whitney test).

4.4.8. Expression of somatostatin in DRGs and spinal cord in BCIBP

Expression levels of somatostatin in sections of either the lumbar DRGs (Figure 4.5A, B and E) or the lumbar spinal dorsal horns (Figure 4.5C, D and F) of BCIBP-rats did not change significantly ($p > 0.05$) *c.f.* the corresponding sections from sham rats.

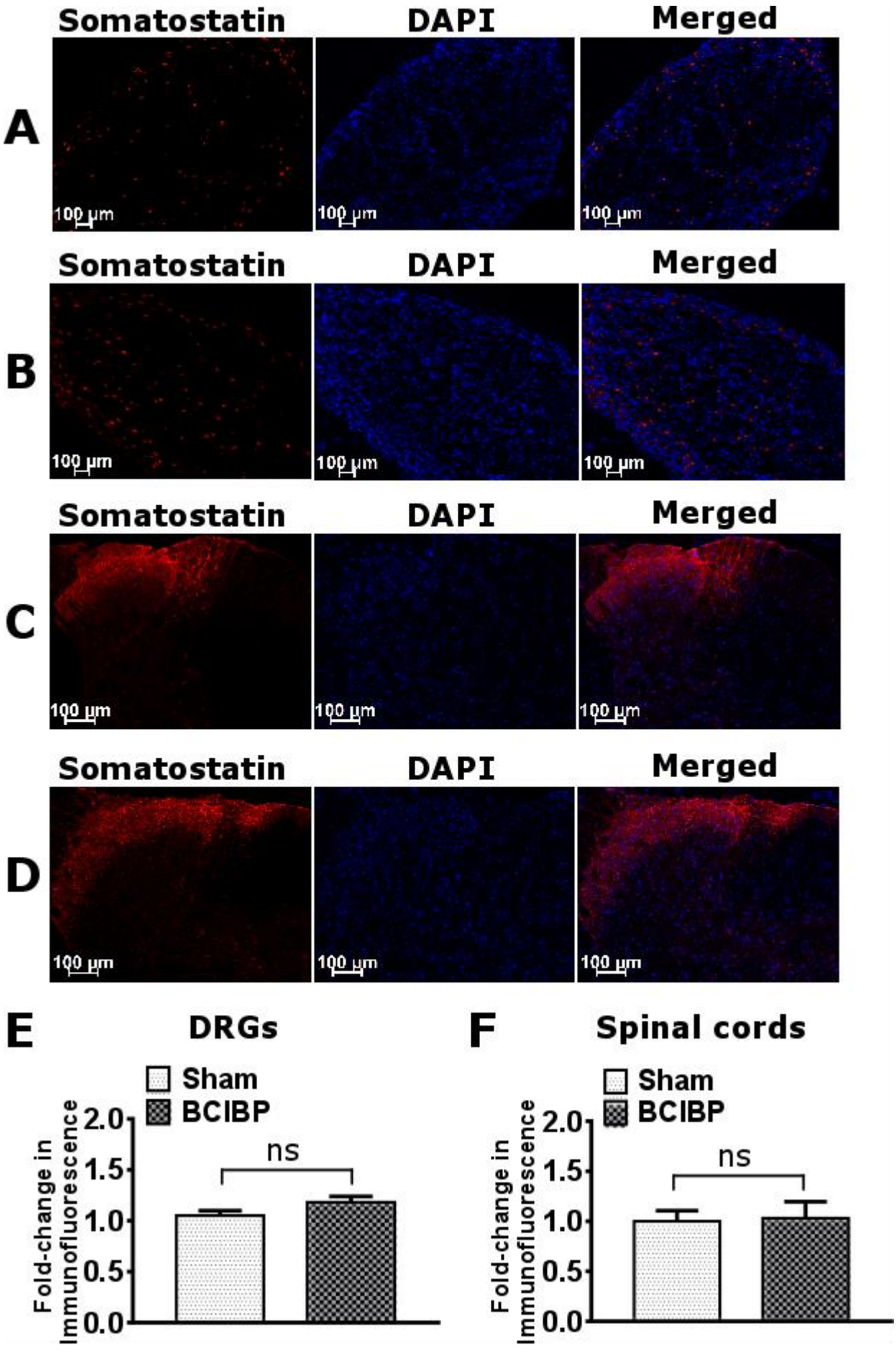
A
Somatostatin
DAPI
Merged
100 μm
B
Somatostatin
DAPI
Merged
100 μm
C
Somatostatin
DAPI
Merged
100 μm
D
Somatostatin
DAPI
Merged
100 μm
E
DRGs
Sham
BCIBP
ns
Fold-change in Immunofluorescence
2.0
1.5
1.0
0.5
0.0
F
Spinal cords
Sham
BCIBP
ns
Fold-change in Immunofluorescence
2.0
1.5
1.0
0.5
0.0

Figure 4.5. Expression levels of somatostatin in sections of ipsilateral lumbar L4-L6 dorsal root ganglia (DRGs) and spinal dorsal horns of BCIBP-rats and the corresponding sections from sham rats (n=3-4/group). Panels in the figure show representative sections of (A) a lumbar DRG from a sham rat, (B) a lumbar DRG from a BCIBP-rat, (C) a lumbar spinal dorsal horn from a sham rat and (D) a lumbar spinal dorsal horn from a BCIBP-rat. Panel (E) shows fold-change in immunofluorescence of ipsilateral lumbar DRG sections from the BCIBP group relative to the corresponding sections from the sham group and (F) shows the fold-change in immunofluorescence of lumbar spinal cord sections from the BCIBP group relative to the sham group. ns, statistically not significant ($p>0.05$, Mann-Whitney test).

4.4.9. Distribution of the SST4 receptor in the ipsilateral lumbar DRGs of BCIBP-rats

In BCIBP-rats, 77 % of SP-positive neurons, 86 % of IB4-positive neurons and 92 % of NF200-positive neurons expressed the SST4 receptor. By comparison, from total SST4 receptor-positive neurons, 28 %, 37 % and 20 % were positive for SP, IB4 and NF200, respectively (Figure 4.6). This distribution profile in BCIBP-rats did not differ significantly ($p > 0.05$) from that of the sham-rats. Although there was a statistically significant ($p \leq 0.05$) decrease in the percentage of SP-positive neurons expressing the SST4 receptor in BCIBP-rats *c.f.* sham rats, this change was only marginal (~ 5 %) and probably not physiologically relevant.

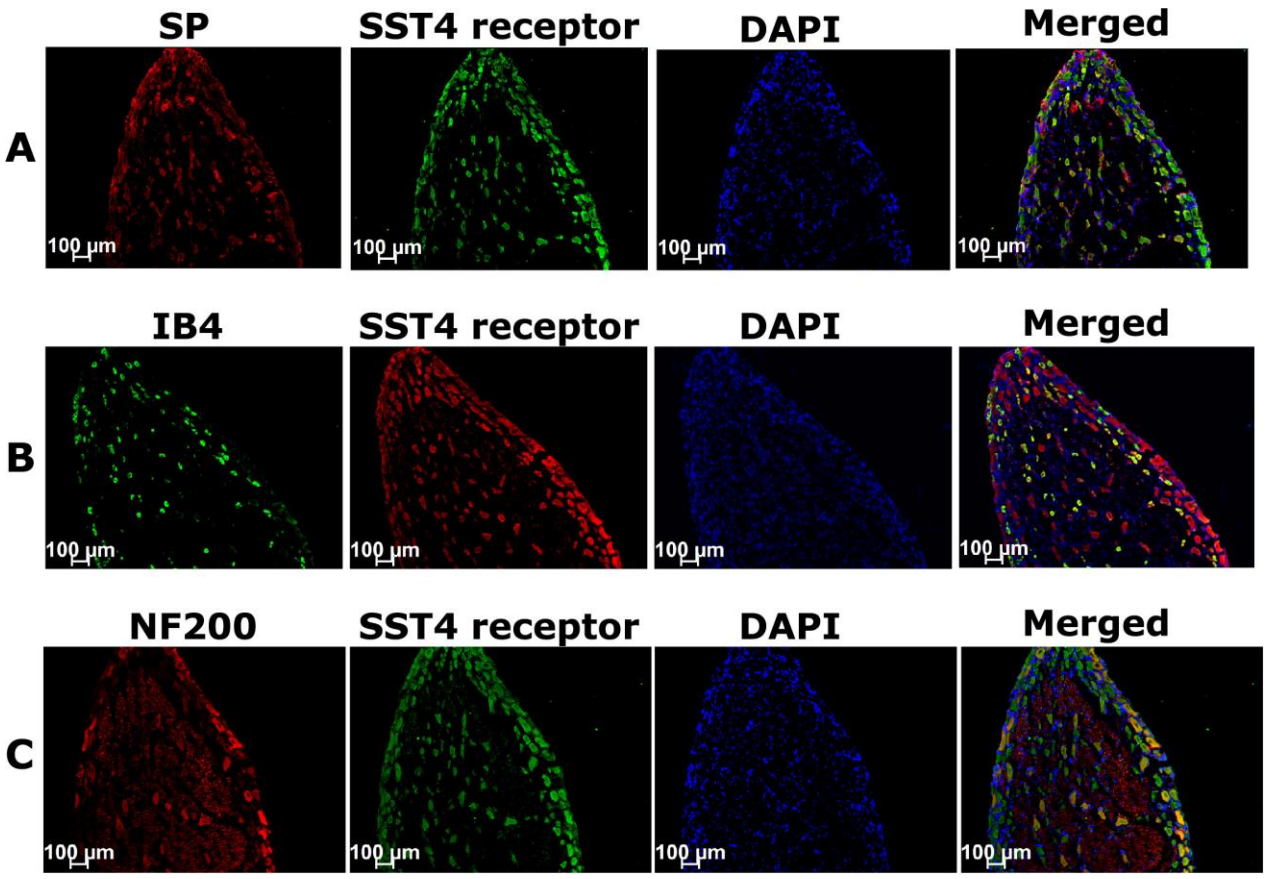

Figure 4.6. Immunostaining showing co-localization of the SST4 receptor with (A) substance P (SP), (B) isolectin B4 (IB4) and (C) neurofilament 200 kDa (NF200) in representative sections from ipsilateral lumbar L4-L6 dorsal root ganglia (DRGs) of BCIBP-rats (n=3-4/group).

4.4.10. Effect of J-2156 on pERK levels in the lumbar spinal cord of BCIBP-rats

Several studies have established that pERK expression levels are elevated in the lumbar spinal cord of rats that received a unilateral ITI of Walker 256 cells (Hu et al., 2015a, Wang et al., 2011b, Ding et al., 2017, Chen et al., 2012b, Sun et al., 2017a, Zhu et al., 2015a). In BCIBP-rats administered a bolus dose of J-2156 at 10 mg/kg i.p., p-ERK expression levels in the lumbar spinal dorsal horns at the time of peak effect of anti-hypersensitivity were significantly ($p \leq 0.05$) decreased *c.f.* the corresponding sections from drug-naïve BCIBP-rats (Figure 4.7).

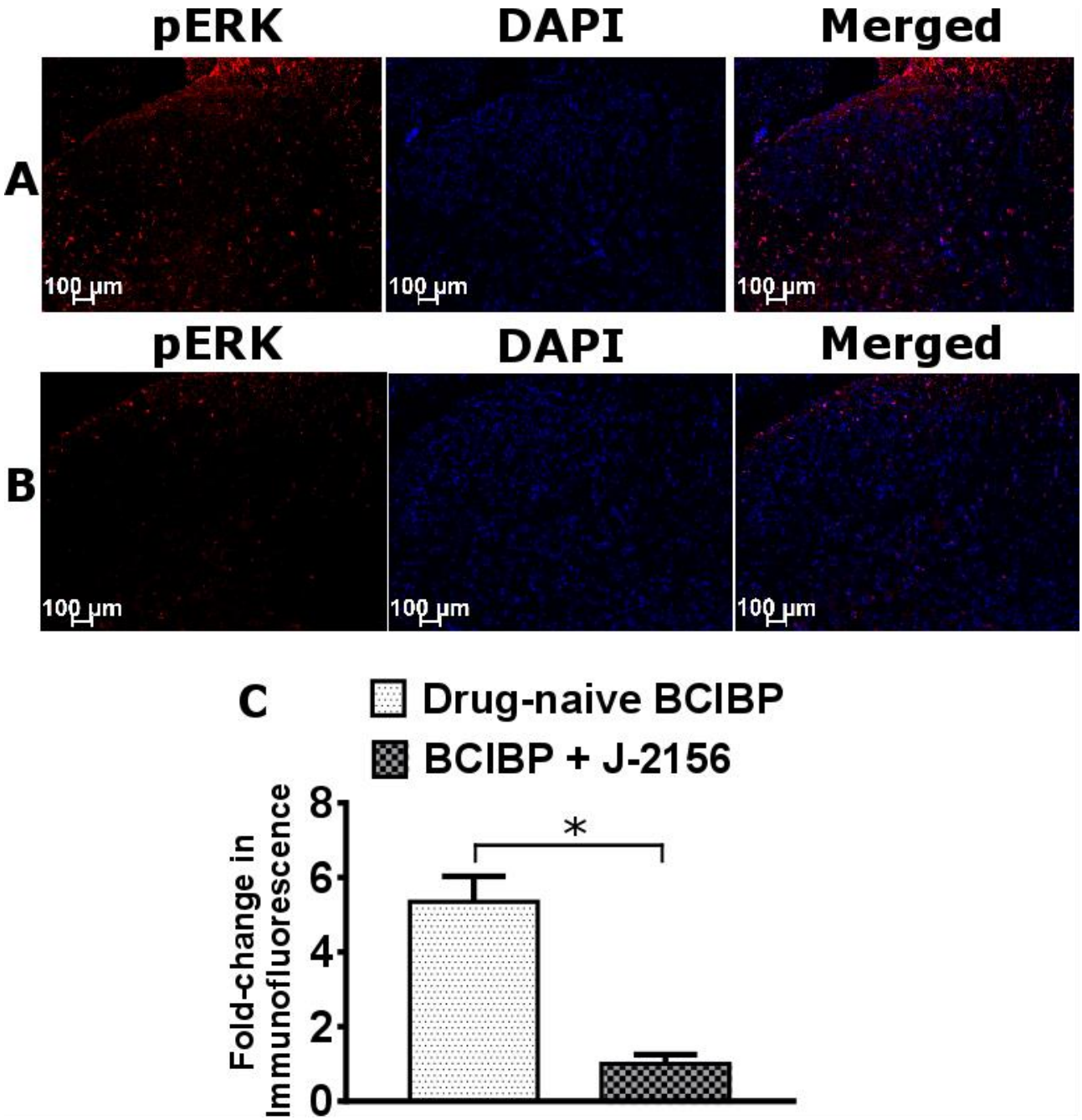

Figure 4.7. Effect of a single bolus dose of J-2156 (10 mg/kg, i.p.) on expression levels of phosphorylated extracellular signal-regulated kinase (pERK) in lumbar L4-L6 spinal dorsal horns of BCIBP-rats (n=3-4/group). Panels in the figure show (A) representative section from a drug-naïve BCIBP-rat, (B) representative section from a BCIBP-rat administered J-2156 (10 mg/kg, i.p.) and (C) fold-change in immunofluorescence of sections from the BCIBP group administered J-2156 relative to the corresponding sections from the drug-naïve BCIBP group. *$p \leq 0.05$ (Mann-Whitney test).

4.5. Discussion

We are the first to show that the small molecule SST4 receptor agonist, J-2156 (Prevot et al., 2017), evokes dose-dependent relief of both mechanical allodynia and mechanical hyperalgesia in the bilateral hindpaws in a rat model of BCIBP. For the ipsilateral hindpaws, the ED_{50} values for J-2156 induced anti-allodynia and anti-hyperalgesia were 3.7 mg/kg and 8.0 mg/kg, respectively. Consistent with these pharmacology data, the SST4 receptor was expressed by the majority of peripheral somatosensory neurons in the ipsilateral lumbar DRGs in BCIBP-rats. The distribution pattern of the SST4 receptor is consistent with its proposed role in modulating pain and transducing endogenous pain relief. Additionally, our findings herein show, for the first time, that a single bolus dose of J-2156 at 10 mg/kg reduces pERK expression levels in the lumbar spinal dorsal horn of BCIBP-rats.

In the Walker 256 cell induced BCIBP model used in the present study, bilateral (ipsilateral and contralateral) hindpaw hypersensitivities were developed following unilateral (ipsilateral) injection of cancer cells. This is in agreement with previously published studies using this pain model (Mao-Ying et al., 2006, Mao-Ying et al., 2012). Peripheral mechanisms like circulating factors and transmedian sprouting as well as centrally acting mechanisms like involvement of signalling via commissural interneurons of spinal cords may underpin contralateral mirror effects associated with unilateral injury (Koltzenburg et al., 1999). Breast cancer cells in the bone cause sprouting of sensory nerve fibres innervating the periosteum and these persistent peripheral noxious inputs can sensitise certain parts of the brain to trigger bilateral hypersensitivities via modulation of descending pain control signalling (Ikeda et al., 2007, Meeus and Nijs, 2007). Activation of spinal glial cells and secretion of proinflammatory cytokines can also be responsible for the contralateral effects (Chacur et al., 2001).

The SST4 receptor is present in multiple tissues including brain, pancreas, stomach, lungs, placenta and kidney (Weckbecker et al., 2003, Caron et al., 1997, Selmer et al., 2000a, Bhandari et al., 2008, Selmer et al., 2000b). Additionally, SST4 receptor mRNA is widely distributed in both the periphery and the central nervous system (Fehlmann et al., 2000, Bruno et al., 1993, Ludvigsen et al., 2015). In female Lewis rats at approximately 10 weeks of age, SST4 receptor immunoreactivity was present in about 40% of DRG neurons as well as in some satellite cells of the peripheral nervous system (Bär et al., 2004). SST4 receptor immunoreactivity has been shown to be present in both the dorsal and ventral horns of the rat spinal cord (Somvanshi and Kumar, 2014), as well as in astrocytes (Feindt et al., 1995) and microglia (Feindt et al., 1998). Our findings of expression of the SST4 receptor in lumbar spinal cord and ipsilateral lumbar DRGs of rats are aligned with work by

others, showing the presence of the SST4 receptor in both the central and peripheral nervous system. These findings herein are in agreement with previous work by others, showing that the SST4 receptor mediates pain relief in rodent models of both inflammatory and neuropathic pain (Elekes et al., 2008, Helyes et al., 2006, Helyes et al., 2009, Sándor et al., 2006, Schuelert et al., 2015, Szolcsanyi et al., 2011, Varecza et al., 2009). In other work, the δ-opioid receptor was heterodimerized with the SST4 receptor, thereby raising the possibility of potentiated endogenous pain relief (Somvanshi and Kumar, 2014). In support of this notion, SST4 receptor gene knockout mice exhibited exaggerated inflammation and hyperalgesia compared with their wild-type counterparts (Helyes et al., 2009). Using gene knockout mice, the SST4 receptor was shown to be coupled to the K^+ M-current (Qiu et al., 2008), which has the potential to modulate pain behaviours (Tsantoulas and McMahon, 2014). All somatostatin receptors, including the SST4 receptor, signal via the inhibition of the adenylyl cyclase-cAMP pathway (Bruns et al., 1995). This pathway is the best characterized effector system associated with opioid receptor signalling (Law et al., 2000, Lantero et al., 2014) and its role in pain pathobiology and analgesia is very well established (Sadana and Dessauer, 2009, Pierre et al., 2009). Using radioligand binding assays, we confirmed that J-2156 has high affinity not only for the human SST4 receptor, but also for the rat SST4 receptor. The potencies of J-2156 towards human and rat SST4 receptors were comparable, with an observed difference of less than 3-fold between the two species. Using cAMP assays, we also found that J-2156 was potent in functionally activating both the human and rat SST4 receptor. The data from radioligand binding assays and cAMP inhibition assays overall suggest that J-2156 is a selective and potent SST4 receptor agonist, and hence it represents a valid preclinical tool compound to investigate the physiological role of the SST4 receptor in preclinical models of pain hypersensitivities.

Administration of single bolus doses of J-2156 (i.p.) alleviated Complete Freund's adjuvant (CFA) induced- inflammatory pain at 0.1 - 1.0 mg/kg in male Han-Wistar rats (Schuelert et al., 2015) and at 0.001 - 0.01 mg/kg in male Lewis rats (Sándor et al., 2006). Similarly, J-2156 at 0.1 mg/kg alleviated carrageenan-induced inflammatory pain (Helyes et al., 2009) and at 0.01 - 0.1 mg/kg (i.p.) alleviated formalin-induced inflammatory pain in mice (Sándor et al., 2006). Additionally, J-2156 at 0.01 - 0.1 mg/kg (i.p.) alleviated neuropathic pain behaviours in rats with sciatic nerve ligation (Sándor et al., 2006). However, we required higher doses of J-2156 to observe alleviation of BCIBP in this model. This could perhaps be due to the fact that, unlike other pain models, cancer-associated pain pathophysiology concurrently involves inflammatory, neuropathic and tumour-specific components.

In the present study in BCIBP-rats, there were no changes in the expression levels of either the SST4 receptor or its ligand, somatostatin, in neural tissue sections analysed. Our findings are in agreement with those of a previous study whereby neither expression levels of the SST4 receptor nor the proportion of neurons expressing the SST4 receptor changed in the lumbar DRGs of rats with unilateral antigen-induced arthritis in the knee joint (Bär et al., 2004).

Sensory nerve fibres are in close proximity with cancer cells colonising the bones, in a micro-environment that is suitable for activation and sensitization of these primary afferents (Voss and Entschladen, 2010, Mancino et al., 2011, Cole et al., 2015, Sroka et al., 2010, di Mola and di Sebastiano, 2008, Jobling et al., 2015, Yoneda et al., 2015). Functional interactions with cancer cells result in hyperexcitability and changes to the morphology of peripheral nerves (Cain et al., 2001), thereby causing pain hypersensitivities (Sughrue et al., 2008). Tumour tissue and immune cell derived endogenous substances such as nerve growth factor have the potential to cause sprouting of primary sensory nerve fibres with the net effect being bone pain (Tong et al., 2010b). Specifically, Walker 256 cells also secrete pro-inflammatory mediators (Rebeca et al., 2008, Pavlaki et al., 2009). Furthermore, cancer invasion and bone loss causes destruction of nerve endings of sensory neurons innervating the bones and the bone marrow, thereby causing intense hypersensitivities (Kane et al., 2015). Following intravenous administration of J-2156 at 5 mg/kg in rats with CFA- induced inflammatory pain, there was significant inhibition of primary afferent nerve firing, however, J-2156 showed no effect in the corresponding group of sham rats (Schuelert et al., 2015, Gorham et al., 2014b). Thus, J-2156 does not affect neuronal transmission under normal physiological conditions (Schuelert et al., 2015, Gorham et al., 2014b). While the endogenous ligand, somatostatin is well-known for its inhibitory actions on primary afferent nerve fibres (Luo et al., 2010, Wang et al., 2011a, Guo et al., 2008, Wang et al., 2009a, Carlton et al., 2004), the peptidomimetic compound- J-2156 (Sándor et al., 2006) inhibits TRPV1 currents, activates GIRK and inhibits voltage stimulated calcium channels in rat DRG neurons by specifically acting on SST4 receptors (Gorham et al., 2014b, Gorham et al., 2014a). However, as knowledge on the DRG neuronal subtypes that express SST4 receptors was lacking, we performed co-localisation experiments with subtype specific markers to address this open question. Here we show for the first time that the SST4 receptor is expressed by the vast majority of small diameter peptidergic and non-peptidergic lumbar DRG neuronal cell bodies as well as cell bodies from medium/large diameter lumbar DRG neurons.

The adenylyl cyclase-cAMP pathway, coupled to the extracellular signal-regulated kinase pathway via a small G-protein, Rap1, acts upstream of ERK activation and contributes to the induction of

pERK in the spinal cord (Kawasaki et al., 2004, Wei et al., 2006). pERK is a prominent player in the development of neural plasticity in the spinal cord, which is a key pathobiological event in the development and maintenance of chronic pain (Ji et al., 2009a). pERK is only induced by noxious stimuli and not by normally innocuous stimuli and its inhibition is generally utilized in the assessment of analgesic efficacy and pain relief mechanisms of novel analgesic compounds (Ji et al., 2009a). pERK is very dynamic in nature as the levels of this protein can elevate as well as deplete within a few minutes (Ji et al., 1999, Muralidharan et al., 2014, Gao and Ji, 2009). Both somatostatin and SST4 receptor-specific agonism can reduce pERK levels (Somvanshi and Kumar, 2014, Hubina et al., 2006). We are the first to show that administration of a SST4 receptor specific agonist J-2156, reduces pERK levels in the spinal dorsal horn of BCIBP-rats. In this context, it is plausible that J-2156 decreases primary afferent hyper-excitability, thereby reducing expression levels of pERK in the lumbar spinal dorsal horn.

Assessing whether the anti-hypersensitivity effects of J-2156 are ablated by pre-treating the animals with an SST4 receptor antagonist, would have been an interesting additional experiment to this work. However, fully characterised SST4 receptor selective antagonists are not yet available (Helyes et al., 2009) and this is one of the shortcomings of the present study. The doses of J-2156 that produced pain relief were higher in BCIBP-rats than those reported previously in other rodent pain models. Importantly however, there were no discernible side effects observed in any BCIBP-rat dosed with J-2156. This good tolerability of J-2156 is consistent with the findings in humans showing that intravenous infusion of somatostatin in patients with abdominal pain associated with pancreatitis, was well-tolerated (Concepcion-Martin et al., 2014). Similarly, administration of TT232, a somatostatin analogue acting through peripheral SST4 receptors was devoid of significant toxicity or side effects in humans (Szokoloczi et al., 2005, Szolcsanyi et al., 2004). After intraperitoneal administration of J-2156 at 1 mg/kg to adult male Han-Wistar rats, the cerebrospinal fluid (CSF) concentration of J-2156 was below the detection limit, thereby indicating that this compound is unlikely to penetrate the blood-brain barrier to a significant extent, consistent with its lack of discernible CNS side-effects in the present study (Schuelert et al., 2015). It was confirmed that J-2156 is an SST4 receptor selective agonist with nanomolar affinity and over 300-fold selectivity for the SST4 receptor, compared to other receptors of the somatostatin family, which was consistent with a previous study by others (Engstrom et al., 2005). Selectivity profile assessment of J-2156 against a standard panel of 67 targets at a single concentration of 10 µM, showed that none of the targets were inhibited or stimulated at / above the pre-defined significance level of 50 %. Minor partial modulation was observed for a few targets ranging from 20 to 35 %. However, at the doses found to be efficacious in the present study (3-10 mg/kg; i.p.), the peak plasma concentration

of J-2156 is expected to be between 300 and 1000 nM, based on the in house pharmacokinetic studies in satellite Wistar Han naive rats conducted by Boehringer Ingelheim (Schuelert et al., 2015). At these concentrations, the non-specific binding of J-2156 to these off-targets is very low. Hence, in the *in vivo* experimental conditions reported herein the possible effect of J-2156 on these non-cognate targets is negligible and the effect of J-2156 is predominantly mediated via SST4 receptor only. This notion is consistent with a pharmacological study by others showing that the pain-relieving effects of J-2156 are abolished in mice null for the SST4 receptor (Helyes et al., 2009). However, other somatostatin receptor subtypes are also expressed in the anatomical regions like DRGs, spinal cord and brain that are involved in the process of nociception (Bär et al., 2004, Kumar, 2009). Hence, a very minor contribution by these receptors to the observed effects of J-2156 cannot be completely ruled out. However, agonists of other somatostatin receptor subtypes have not been assessed for their efficacy to alleviate breast cancer-induced bone pain. The findings presented herein, for the first time, show significant potential of the SST4 receptor in alleviating the complex symptomatology of BCIBP.

Supplementary Table 4.1. J-2156 mediated non-cognate stimulation or inhibition of various pharmacological targets.

Pharmacological Target	**Species**	**Percent (%) inhibition**
Adenosine A_1	human	19
Adenosine A_{2A}	human	-3
Adenosine A_3	human	-13
Adrenergic α_{1A}	rat	-11
Adrenergic α_{1B}	rat	8
Adrenergic α_{1D}	human	17
Adrenergic α_{2A}	human	4
Adrenergic β_1	human	0
Adrenergic β_2	human	6
Androgen (Testosterone) AR	rat	-2
Bradykinin B_1	human	23
Bradykinin B_2	human	-6
Calcium Channel L-Type, Benzothiazepine	rat	9
Calcium Channel L-Type, Dihydropyridine	rat	12
Calcium Channel N-Type	rat	-19
Cannabinoid CB_1	human	-4
Dopamine D_1	human	3
Dopamine D_{25}	human	9

Dopamine D_3	human	10
Dopamine $D_{4.2}$	human	-4
Endothelin ET_A	human	10
Endothelin ET_B	human	-1
Epidermal Growth Factor (EGF)	human	5
$GABA_A$, Flunitrazepam, Central	rat	6
$GABA_A$, Muscimol, Central	rat	-1
$GABA_{B1A}$	human	4
Glucocorticoid	human	6
Glutamate, Kainate	rat	-22
Glutamate, NMDA, Agonism	rat	14
Glutamate, NMDA, Glycine	rat	0
Glutamate, NMDA, Phencyclidine	rat	2
Histamine H_1	human	-6
Histamine H_2	human	4
Histamine H_3	human	2
Imidazoline I_2, Central	rat	-5
Interleukin IL-1	mouse	-4
Leukotriene, Cysteinyl $CysLT_1$	human	-2
Melatonin MT_1	human	-1
Muscarinic M_1	human	-1
Muscarinic M_2	human	5
Muscarinic M_3	human	0
Neuropeptide Y Y_1	human	-1
Neuropeptide Y Y_2	human	-5

Nicotinic Acetylcholine	human	-2
Nicotinic Acetylcholine α1, Bungarotoxin	human	2
Opiate δ (OP1, DOP)	human	20
Opiate κ (OP2, KOP)	human	16
Opiate μ (OP3, MOP)	human	7
Phorbol Ester	mouse	-7
Platelet Activating Factor (PAF)	human	21
Potassium Channel [K_{ATP}]	hamster	0
Potassium Channel hERG	human	11
Prostanoid EP_4	human	-1
Purinergic P_{2X}	rabbit	5
Purinergic P_{2Y}	rat	-6
Rolipram	rat	9
Serotonin (5- Hydroxytryptamine) 5-HT_{1A}	human	24
Serotonin (5- Hydroxytryptamine) 5-HT_{2B}	human	1
Serotonin (5- Hydroxytryptamine) 5-HT_3	human	13
Sigma σ_1	human	-2
Sodium Channel, Site 2	rat	35
Tachykinin NK_1	human	25
Thyroid Hormone	rat	-4
Transporter, Dopamine (DAT)	human	6
Transporter, GABA	rat	6
Transporter, Norepinephrine (NET)	human	-19
Transporter, Serotonin (5-Hydroxytryptamine) (SERT)	human	-3

n=2; concentration=10 uM; +, inhibition of binding; -, enhanced binding

Supplementary Table 4.2. Extent and duration of action (ΔPWT AUC) of J-2156 for the relief of mechanical allodynia in the bilateral hindpaws of BCIBP-rats.

Dose of J-2156 (i.p.)	**Time (h)**				**Mean ΔPWT at peak effect (g)**		**ΔPWT AUC (g.h)**	
	Peak effect		**~Duration of action**					
	Ipsilateral	**Contralateral**	**Ipsilateral**	**Contralateral**	**Ipsilateral**	**Contralateral**	**Ipsilateral**	**Contralateral**
1 mg/kg	1.25	1.25	2	2	1.8 (± 0.44)	2.2 (± 0.76)	2.9 (± 0.80)	3.1 (± 1.21)
3 mg/kg	1	1 – 1.5	3	3	2.8 (± 0.76)	3.2 (± 0.53)	6.4 (± 1.27)	6.2 (± 1.31)
10 mg/kg	0.75 – 1.25	0.75 -1.25	>3	>3	4.5 (± 0.56)	3.9 (± 0.80)	10.2 (± 1.22)*	8.6 (± 1.64)*
Vehicle	NA	NA	NA	NA	NA	NA	2.3 (± 1.02)	1.01 (± 0.95)

i.p., intraperitoneal; NA, not applicable; *$p \leq 0.05$ (ipsilateral- $F_{(3,15)} = 10.2$; contralateral- $F_{(3,15)} = 9.3$), One-way ANOVA, *posthoc* Dunnett's multiple comparisons test *c.f.* BCIBP-rats that received single bolus doses of vehicle

Supplementary Table 4.3. Time courses of the anti-allodynic effect of J-2156 in BCIBP-rats.

Dose of J-2156 (i.p.)	**Hindpaws**	**Time courses (h) of the anti-allodynic effect of J-2156 (i.p.) post-treatment**	
		Effect on PWT	**Effect on ΔPWT**
1 mg/kg	Ipsilateral	NE [a]($p > 0.05$)	NE [c]($p > 0.05$)
1 mg/kg	Contralateral	NE [b]($p > 0.05$)	NE [d]($p > 0.05$)
3 mg/kg	Ipsilateral	0.75 h to 1.25 h [a]($p \leq 0.05$)	0.75 h to 1.5 h [c]($p \leq 0.05$)
3 mg/kg	Contralateral	1 h to 1.5 h [b]($p \leq 0.05$)	1 h to 1.5 h [d]($p \leq 0.05$)
10 mg/kg	Ipsilateral	0.25 h to 2 h [a]($p \leq 0.05$)	0.25 h to 2 h [c]($p \leq 0.05$)
10 mg/kg	Contralateral	0.5 h to at least 3 h [b]($p \leq 0.05$)	0.25 h to 2 h [d]($p \leq 0.05$)

NE, no significant effect; Two-way ANOVA, *posthoc* Bonferroni test *c.f.* BCIBP-rats administered vehicle; [a]($F(3, 8, 24/160) = 20.5, 6.4, 1.5$); [b]($F(3, 8, 24/160) = 21.6, 8.0, 1.8$); [c]($F(3, 8, 24/160) = 13.9, 8.6, 1.5$); [d]($F(3, 8, 24/160) = 8.4, 10.5, 1.7$)

Supplementary Table 4.4. Extent and duration of action (ΔPPT AUC) of single i.p. bolus doses of J-2156 for the relief of mechanical hyperalgesia in the bilateral hindpaws of BCIBP-rats.

Dose of J-2156 (i.p.)	**Time (h)**				**Mean ΔPPT at peak effect (g)**		**ΔPPT AUC (g.h)**	
	Peak effect		**~Duration of action**					
	Ipsilateral	**Contralateral**	**Ipsilateral**	**Contralateral**	**Ipsilateral**	**Contralateral**	**Ipsilateral**	**Contralateral**
1 mg/kg	1	1	2	2	15.8 (± 4.10)	21.7 (± 5.43)	21.5 (± 4.75)	35.7 (± 5.38)
3 mg/kg	1	1	3	3	31.9 (± 8.81)	42.2 (± 8.78)	54.1 (± 14.82)*	74.3 (± 11.85)*
10 mg/kg	1.25	1.25	>3	>3	59.7 (± 5.55)	64.7 (± 4.86)	117.4 (± 25.26)*	126.8 (± 18.94)*
Vehicle	NA	NA	NA	NA	NA	NA	12.5 (± 3.47)	26.3 (± 6.94)

i.p., intraperitoneal; NA, not applicable; *$p \leq 0.05$ (ipsilateral- $F_{(3,15)} = 13.5$; contralateral- $F_{(3,15)} = 16.9$), One-way ANOVA, *posthoc* Dunnett's multiple comparisons test *c.f.* BCIBP-rats that received single bolus doses of vehicle

Supplementary Table 4.5. Time courses of the anti-hyperalgesic effect of J-2156 in BCIBP-rats.

Dose of J-2156 (i.p.)	**Hindpaws**	**Timeline (h) of anti-hyperalgesic effect of J-2156 (i.p.) post-treatment**	
		Effect on PPT	**Effect on ΔPPT**
1 mg/kg	Ipsilateral	NE [a]($p > 0.05$)	NE [c]($p > 0.05$)
1 mg/kg	Contralateral	NE [b]($p > 0.05$)	NE [d]($p > 0.05$)
3 mg/kg	Ipsilateral	1 h to 1.5 h [a]($p \leq 0.05$)	1 h to 1.5 h [c]($p \leq 0.05$)
3 mg/kg	Contralateral	1 h to 1.5 h [b]($p \leq 0.05$)	1 h to 1.5 h [d]($p \leq 0.05$)
10 mg/kg	Ipsilateral	0.5 h to at least 3 h [a]($p \leq 0.05$)	0.5 h to at least 3 h [c]($p \leq 0.05$)
10 mg/kg	Contralateral	0.5 h to at least 3 h [b]($p \leq 0.05$)	0.5 h to at least 3 h [d]($p \leq 0.05$)

NE, no significant effect; Two-way ANOVA, *posthoc* Bonferroni test *c.f.* BCIBP-rats administered vehicle; [a]($F(3, 8, 24/160) = 15.0, 10.1, 3.1$); [b]($F(3, 8, 24/160) = 19.3, 13.2, 2.5$); [c]($F(3, 8, 24/160) = 11.4, 17.1, 4.3$); [d]($F(3, 8, 24/160) = 14.0, 21.0, 3.2$)

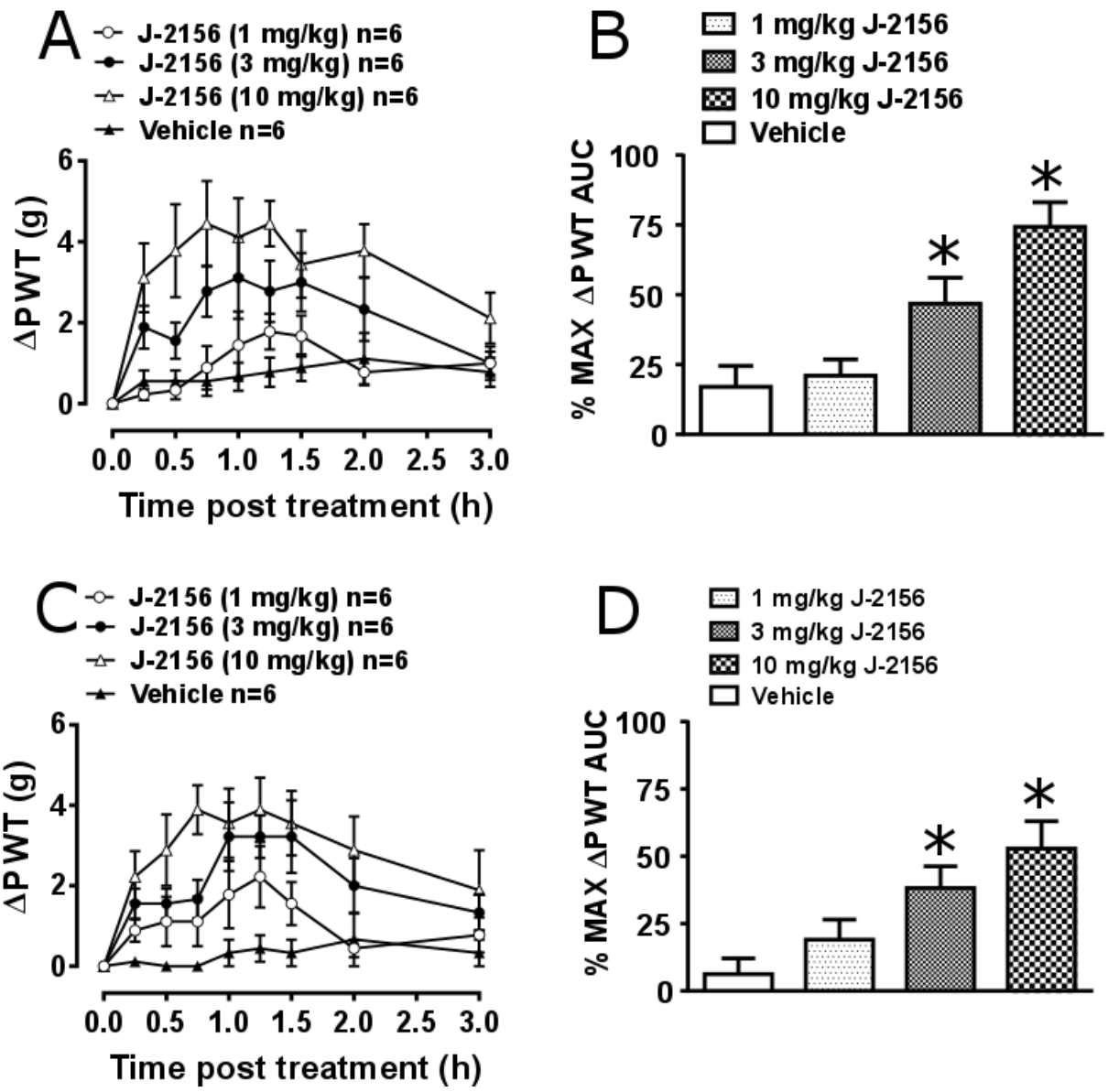

Supplementary Figure 4.1. Anti-allodynic effect of single bolus doses (i.p.) of J-2156 on ipsilateral and contralateral ΔPWT and % MAX ΔPWT AUC values in BCIBP-rats. Panels in the figure show (A) ipsilateral ΔPWT versus time curves, (B) ipsilateral % MAX ΔPWT AUC at each dose, (C) contralateral ΔPWT versus time curves and (D) contralateral % MAX ΔPWT AUC at each dose. Panel B: *$p \leq 0.05$ ($F_{(3,20)} = 11.0$) and Panel D: *$p \leq 0.05$ ($F_{(3,20)} = 6.6$), One-way ANOVA, *posthoc* Dunnett's multiple comparisons test *c.f.* BCIBP-rats that received single bolus doses of vehicle.

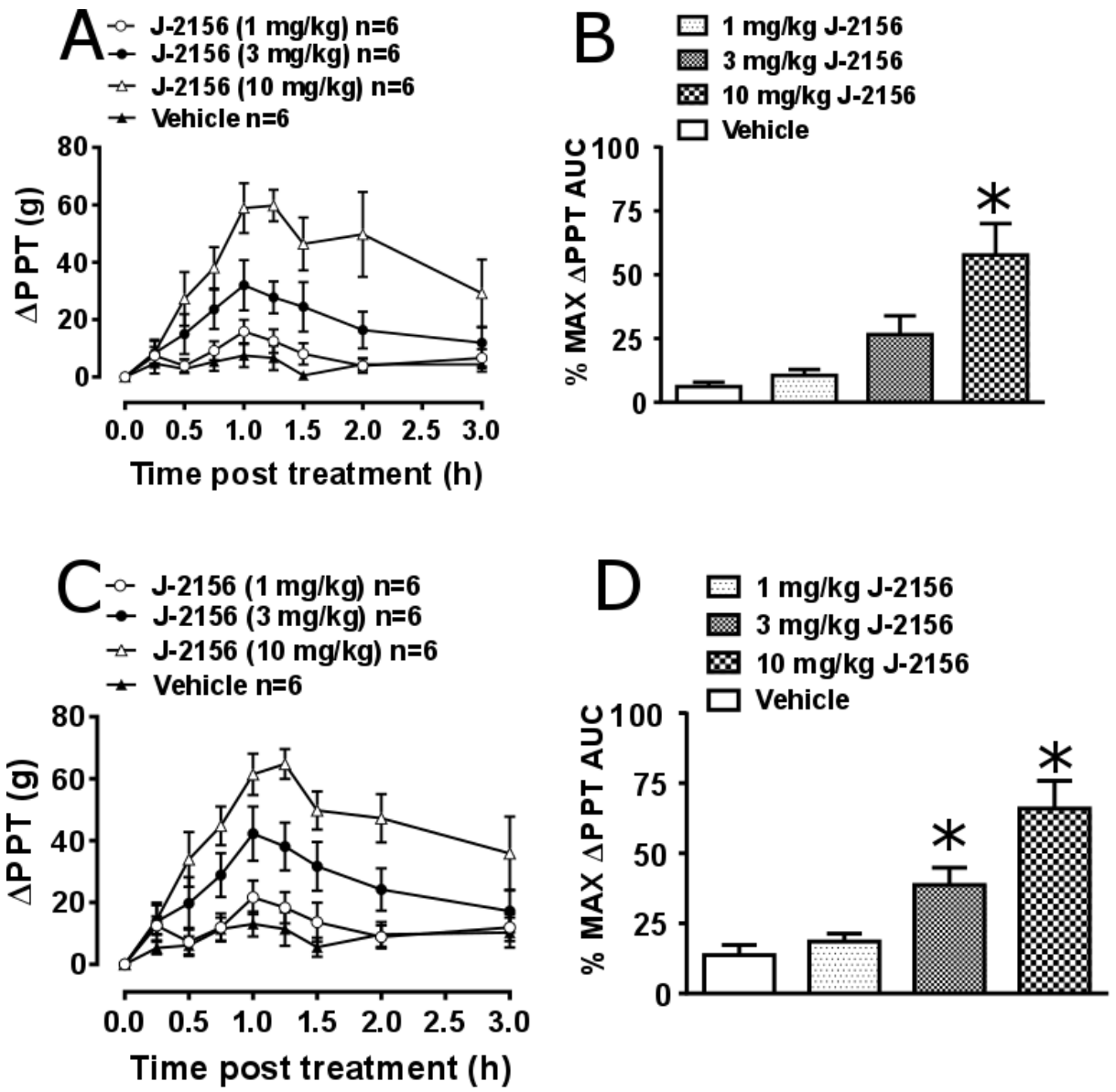

Supplementary Figure 4.2. Anti-hyperalgesic effect of single bolus doses (i.p.) of J-2156 on ipsilateral and contralateral ΔPPT and % MAX ΔPPT AUC values in BCIBP-rats. Panels in the figure show (A) ipsilateral ΔPPT versus time curves, (B) ipsilateral % MAX ΔPPT AUC at each dose, (C) contralateral ΔPPT versus time curves and (D) contralateral % MAX ΔPPT AUC at each dose. Panel B: *p≤0.05 ($F_{(3,20)}$ = 10.1) and Panel D: *p≤0.05 ($F_{(3,20)}$ = 14.5), One-way ANOVA, *posthoc* Dunnett's multiple comparisons test *c.f.* BCIBP-rats that received single bolus doses of vehicle.

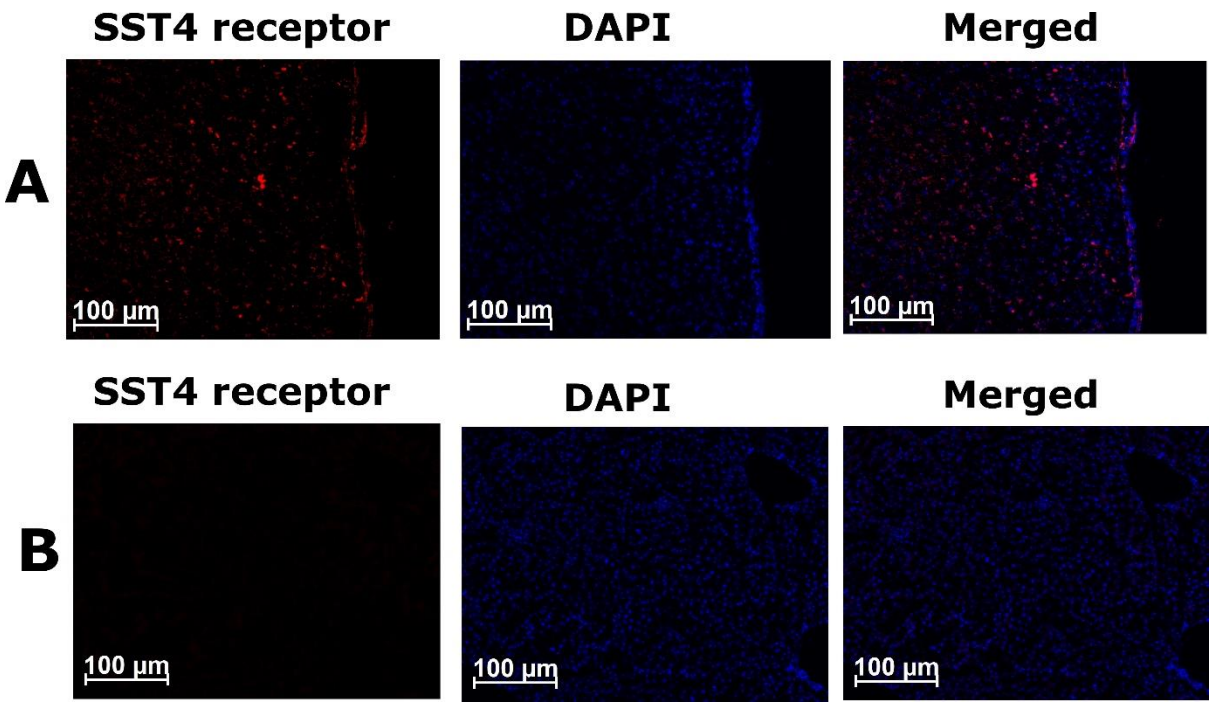

Supplementary Figure 4.3. Validation of the anti-SST4 receptor antibody using IHC staining. Panels in the figure show (A) a representative coronal section of rat brain used as a positive control for the SST4 receptor and (B) a representative rat liver section used as a negative control for the SST4 receptor.

Chapter 5

Summary, conclusions and future directions

5.1. Summary and Conclusions

Pain is a significant medical problem that co-exists with several diseases including various types of cancer. Breast cancer cells metastasize from the tissue of origin and establish themselves in distant parts of the axial skeleton. The cancer cells growing in the bone microenvironment cause osteolysis and sensitisation of the peripheral nerve endings innervating the bones, thereby causing excruciating pain. Breast cancer-induced bone pain causes severe morbidity because of the heterogeneous combination of inflammatory, neuropathic and cancer-specific components. The existing analgesic/adjuvant medications are often insufficiently efficacious to combat this pain condition. Thus it is very important to develop and characterize suitable preclinical models of breast cancer induced bone pain so as to assist in drug discovery programs aimed at identifying novel compounds having potential to mitigate this often intractable pain condition.

This thesis describes the successful establishment, optimization and characterization of a rat model of Walker 256 breast cancer cell-induced bone pain. The health of experimental animals used in cancer research is of prime importance. The work described herein involved systematic assessment and documentation of clinical health parameters in animals following intra-tibial injection of Walker 256 cells. Using female Wistar Han rats, it was found that the severity (magnitude/extent) of Walker 256 cell-induced mechanical allodynia and mechanical hyperalgesia in the hindpaws, is directly correlated with the initial number of cancer cells inoculated in the tibiae. The number of Walker 256 cells injected in the tibiae was found to be a predisposing factor influencing the nature of pain hypersensitivities developed. With lower number of cells inoculated, the pain hypersensitivities developed are unilateral in nature (developed in ipsilateral hindpaws). By increasing the number of cells, pain hypersensitivities become bilateral in nature (in both ipsilateral and contralateral hindpaws). While all the existing studies using this model typically assess the pain behaviors only until around 20-25 days after injection of cancer cells, the findings reported in this thesis are the first to successfully investigate the model for up to ~66 days. It was found that the Walker 256 cell-induced bone pain apparently resolves spontaneously at later stages despite the ongoing presence of cancer cells, similar to the clinical situation in humans. Histological and radiological assessments were used to provide evidence that the cancer disease remains persistent in the rat tibiae, despite apparent resolution of pain hypersensitivities at later stages of this model. Unlike H&E staining of histology, immunohistochemical staining with a specific antibody is a

direct method for detecting the presence of cancer cells in the tibiae. Immunohistochemical staining of the cancer cells in tibiae of rats in this model has not been previously reported. The work described in this thesis uses immunohistochemistry to provide direct evidence of the presence of cancer cells in tibial sections of rats with Walker 256 cell-induced bone pain, not only during the pain-state, but also at the apparently resolved-pain state. Also, the injection of naloxone at the resolved-pain state of the rats with Walker 256 cell-induced bone pain, rescued the pain phenotype, thereby indicating a possible role of endogenous opioidergic signaling in the self-resolution of pain hypersensitivities at later stages. The model was further pharmacologically characterized and it was found that the model is responsive to clinically used analgesic drugs that have diverse mechanisms of action, including morphine, gabapentin, meloxicam and amitriptyline. This shows that the optimized model has considerable potential for use in the process of drug discovery of new analgesics against breast cancer induced bone pain.

The transcriptomic characterization of the model was performed so as to gain insights into the gene level changes occurring in breast cancer induced bone pain. It was found that several genes known to be involved in the pathophysiology of pain hypersensitivities were differentially expressed in neural tissues in the BCIBP state. Additionally, the transcriptomic characterization of the Walker 256 cell line revealed that the genetic composition of this cell line resembles the basal-B subtype of human breast cancer cell lines. Basal-B cell lines are known to be highly invasive in nature. These cell lines may resemble basal tumours / triple negative tumours or Erbb2 tumours or even display stem cell like characteristics, and hence are not yet well-characterized.

Finally, the work described in this thesis also shows that the SST4 receptor mediates analgesia in the state of breast cancer induced bone pain. J-2156, a SST4 receptor agonist, was found to be effective in alleviating the mechanical allodynia and mechanical hyperalgesia in the optimized Walker 256 cell- induced bone pain model. Interestingly, the SST4 receptor was found to be expressed by the majority of the cell bodies of somatosensory neurons in the ipsilateral lumbar DRGs, including peptidergic and non-peptidergic small C-fibre neurons and medium-large diameter fibre neurons, consistent with the role of SST4 receptors in the pain processing pathway. Administration of J-2156 in rats with breast cancer- induced bone pain reduced the levels of pERK in the lumbar spinal dorsal horn. Considering the fact that J-2156 is unlikely to cross the blood brain barrier, this reduction of pERK levels can be assumed to be mediated by the action of J-2156 on peripheral SST4 receptors. Hence, J-2156 can be considered to be a novel analgesic compound which is unlikely to develop side effects of the central nervous system.

5.2. Future Directions

In future, it might be a suitable complementary experiment to assess the ambulatory pain or pain evoked by weight bearing on the hindpaws of rats in this model. Allodynia and gait behaviours are two independent phenomena; allodynia (measured by von Frey testing) being a more reliable measure of the neuropathic pain component rather than gait behaviours (weight bearing or spontaneous pain during ambulation) (Mogil et al., 2010). Neuropathic pain is one of the key components of cancer induced bone pain (Cao et al., 2010). Changes in gait parameters can typically be due to the tendency of animals to avoid allodynia produced by the contact of the paw with the floor (Coulthard et al., 2003). The gait changes do not necessarily relate well to pain hypersensitivities (Mogil et al., 2010, Piesla et al., 2009, Gabriel et al., 2009, Fernihough et al., 2004, Boettger et al., 2009, Aihara et al., 2017). There are several strong evidences available to say that changes in gait parameters like guarding the hindpaw during ambulation or changes in weight bearing are significantly driven by the adaptive changes and psychological influences (pain-avoidance and fear due to cognition), rather than the current levels of pain intensity (Mogil et al., 2010, Vlaeyen and Linton, 2000, Feinstein et al., 2017, Fingleton et al., 2015, Somers et al., 2009, Keefe et al., 2000, Tichonova et al., 2016, Niederstrasser et al., 2015, Haddas et al., 2017, Al-Obaidi et al., 2003, Vincent et al., 2013). Whereas, both the von Frey and Randall-Selitto tests, that are also used in humans to assess pain hypersensitivities, detect the current levels of pain and have high clinical relevance (Tena et al., 2012, Reitz et al., 2016, Abrams et al., 2007, Prabhavathi et al., 2014, Levine et al., 1988, Neuvonen et al., 1985). This is probably one of the most important reasons why large number of published studies used stimuli-evoked methods like the von Frey and Randall-Selitto tests to assess pain hypersensitivities in the hindpaws of animals following unilateral tibial inoculation of cancer cells.

Importantly, a previous study (Sabino et al., 2003) highlights the fact that neither spontaneous pain nor ambulatory pain is the best measure of cancer induced bone pain for all models. It showed that intra-osseous injection of B16-F10 melanoma cell line in the femur did not produce either the spontaneous pain or the ambulatory pain. The bone pain induced by B16-F10 cell line manifested only as hindpaw skin hypersensitivity. Similarly, C26 colon cancer cell line did not produce spontaneous pain behavior. This clearly highlights a very important fact that spontaneous or ambulatory pain are not the universal measures of bone pain at least in some models like B16 cell model and C26 cell model. In alignment to this pre-clinical animal based study, a clinical study of cancer induced bone pain also reported that in patients with breakthrough pain, which is commonly triggered by a stimulus (Caraceni et al., 2013), patients were not more likely to experience pain at the weight-bearing bone sites, compared to patients without pain (Laird et al., 2011).

As per the previous studies published in journals like *PAIN* (Fang et al., 2015, Liu et al., 2013a, Zheng et al., 2013), *The Journal of Pain* (Shih et al., 2012, Li et al., 2016), *European Journal of Pain* (Li et al., 2014b, Liu et al., 2014a, Zhang et al., 2008), *Pain Medicine* (Muralidharan et al., 2014), *Molecular Pain* (Wang et al., 2011b, Pan et al., 2010) and *Nature Neuroscience* (Chen et al., 2017), it is a traditional practice within the pain research fratenerity to test the pain hypersensitivities in the "paw", following inoculation of cancer cells in the "tibia", without deploying gait or weight bearing parameters as a measure of pain. Along these lines, a recent report suggested that a vast majority of around ~90 % of the cancer induced bone pain studies in the literature using MRMT-1 cells in rats used the response evoked by the cutaneous stimuli applied to the foot as a measure of bone pain (De Felice et al., 2016). Based on the experience in our laboratory and from the vast literature available on Walker 256 cell induced bone pain model in rats, inoculation of Walker 256 cell in the tibia always manifests as hypersensitivities in the hindpaws, without any discordance between paw-tibia correlation being reported in the literature to the best of our knowledge (Shenoy et al., 2017, Shenoy et al., 2016). Reportedly, there was a dissociation of skeletal pain behaviors and skin hypersensitivity in a male C3H mouse model of intra-femoral injection of NCTC 2472 osteosarcoma cells in another study (Guedon et al., 2016). However, it is known that different types of cell lines / tumours exhibit distinct pain behavioral patterns (Sabino et al., 2003). It is the unique interaction between each of the cancers colonising the bone and the nerve innervation that predominantly decides the nature of pain manifestation (Lozano-Ondoua et al., 2013b). Importantly, the majority of studies in the literature that used the Walker 256 breast cancer cell-induced bone pain model in rats, used the hind "paw" as a location to test hypersensitivity to evoked pain such as that induced by the von Frey test, rather than spontaneous or movement evoked pain (Cheng et al., 2016, Yao et al., 2011, Sima et al., 2016, Pan et al., 2016, Fu et al., 2016, Luo et al., 2016, Huang et al., 2016, Du et al., 2016, Wang et al., 2016a, Pan et al., 2010, Shenoy et al., 2016). There are many different studies recently published in 2017 to date, that used Walker 256 cells to induce bone pain in rats that only used stimuli evoked behavioural measures such as von Frey paw withdrawal thresholds in the hindpaws, but not spontaneous movement evoked or weight bearing measures to assess pain hypersensitivities (Liu et al., 2017b, Liu et al., 2017a, Song et al., 2017, Yao et al., 2017, Sun et al., 2017b, Sun et al., 2017a, Guo et al., 2017, Dai et al., 2017, Hou et al., 2017, Hang et al., 2017, Liang et al., 2017, Zhou et al., 2018, Hu et al., 2017, Chen et al., 2017). However, in the preclinical research field of cancer induced bone pain, pioneering efforts are being made to introduce novel methods to assess hypersensitivity, like application of stimulus directly to the tibia (Falk et al., 2015a) or assessment of grid climbing behaviours (Falk et al., 2017).

The plantar hindpaw of rats (the anatomical region where von Frey and Randall-Selitto stimuli are applied) is mainly innervated by the tibial nerve (Kambiz et al., 2014, Cobianchi et al., 2014, De Koning et al., 1986), and hence tibial bone pain sensations manifest as hypersensitivities in the plantar aspect of the hindpaws (Yang et al., 2011). Hence, the traditional and most commonly used method to measure tibial bone pain is assessment in the "paws", with hundreds of studies prevailing in the literature using this protocol. By using intra-tibial injections of complete Freund's adjuvant in the tibiae of female Wistar rats, a study has elegantly established that the bone pain induced by activation of tibial nerves directly manifests as hindpaw skin hypersensitivity (Yang et al., 2011).

Cutaneous tests like the von Frey testing and Randall-Selitto testings detect the current levels of pain and have high clinical relevance as used in humans (Tena et al., 2012, Reitz et al., 2016, Abrams et al., 2007, Prabhavathi et al., 2014, Levine et al., 1988, Neuvonen et al., 1985). A study involving the Department of Medicine of the University of Florida (Gainesville, USA) has validated that mechanically evoked pain is a highly relevant measure of the clinical pain intensity in patients with deep pain of muco-skeletal origin (Staud et al., 2012). Similarly, a study conducted in Edinburgh Cancer Centre (Edinburgh, UK) also validated that assessing mechanical allodynia using von Frey filaments is a direct measure of cancer induced bone pain in humans (Scott et al., 2012). Hence the behavioural tests that we have employed are physiologically relevant assessment techniques for assessing bone pain. However, a complementary work could be performed in the future to assess the ambulatory pain or pain evoked by weight bearing on the hindpaws of rats.

My findings in this thesis show that Walker 256 breast cancer cell-induced bone pain appears to resolve spontaneously after around 25 days post-injection of cancer cells and that the administration of naloxone, a non-selective opioid receptor antagonist, rescues the pain phenotype. Future studies can be directed to investigate the endogenous opioid proteins that are involved in resolution of pain hypersensitivities in this model. Other than the DRGs, on which transcriptomic characterization was performed, it will be of interest to assess the changes in the spinal cord and brain compartments, both in neuronal and non-neuronal cells that may give important information on the self-resolving nature of pain hypersensitivities in this model.

Assessing the possible phenotypic and genotypic changes occurring in the cancer cells after bone engraftment will be an interesting area to address. Heterogeneity of cancer cells by themselves is well known. In breast cancer, it may be difficult to clearly classify the cancer cells as marker-receptor- "positive" or "negative", as there can be significant intra-tumoral heterogeneity in their

expression (Allott et al., 2016, Bedard et al., 2013). Her2, Muc1 and cytokeratins are some of the classical breast cancer markers (Sturgeon et al., 2008, Olofsson et al., 2007). Intra-tumoral heterogeneity can typically be observed with such classical markers too, including Her2 (Buckley et al., 2016, Kurozumi et al., 2016, Onsum et al., 2013), MUC1 (Rahn et al., 2001) and cytokeratins (Cimpean et al., 2008, Orito et al., 1989). Such intra-tumoral heterogeneity in breast cancer occurs both at the genetic and morphological levels (Lichy et al., 2000, Denisov et al., 2014, Hiley et al., 2014, Badve and Nakshatri, 2012, Marusyk et al., 2012). Due to the existence of mixed cell populations in the breast cancer tumours, they have the potential to differentially grow into diverse types like epithelial and fibroblastic, subject to different growth conditions (Whitescarver, 1974).

One of the hallmark features of cancer cells is their genomic instability and this is what makes a cancer a cancer (Hanahan and Weinberg, 2011, Negrini et al., 2010). Cancer immunoediting comprises three Es- Elimination (immunosurveillance), Equilibrium and Escape; and the process leading from immunosurveillance to tumour escape in the immunocompetent host is well known (Dunn et al., 2002). As per the Darwinian selection theory, tumor-specific immune responses are responsible for eliminating highly immunogenic tumor cells, while the tumor variants with reduced immunogenicity have a better chance of survival in the immunocompetent host (Kmieciak et al., 2007, Dunn et al., 2004, Dunn et al., 2002). Tumour cells have the ability to shed or restrict the presentation of ligands / antigens involved in their recognition by the host's immune system or down-regulate the expression of factors that promote activation of tumour-specific immune responses (Mohme et al., 2016). Due to the immune pressure, tumour cell variants with loss of such antigens emerge as a consequence of epigenetic mechanisms within the tumor (Sanchez-Perez et al., 2005, Liu et al., 2005). Likewise, the anti-tumor immune responses themselves can induce changes in antigen-positive cells, converting them into antigen-negative cells (Beatty and Paterson, 2000, Beatty and Paterson, 2001). Hence, discordance in receptor or biomarker status and genotypic heterogeneity between primary breast cancer cells and their metastasised lesions or circulating cells in the body is very common, because the biomarker expression of primary tumour cells can change significantly during the disease progression (Singh et al., 2013, Thompson et al., 2010, Aktas et al., 2016, Somlo et al., 2011, Millner et al., 2013, Zhang et al., 2016, Vlems et al., 2003, Deng et al., 2014, Fehm et al., 2008, El Nemr Esmail et al., 2015). Similarly antigens that can be targeted by the immune system are also found to be lost in other types of human cancers (Hanagiri et al., 2013, Mendez et al., 2007, Rivoltini et al., 2002). Such immunoediting processes can be strong enough to induce very significant changes in morphology and microarray of the breast cancer cells, leading to failure in detection of earlier version of cells (Knutson et al., 2006, Gorges et al., 2012, Larue and

Bellacosa, 2005, Voulgari and Pintzas, 2009, Foroni et al., 2012, Wu et al., 2016c, Bill and Christofori, 2015, Palma et al., 2016).

For example, Muc1 has several major limitations as a breast cancer marker (Duffy et al., 2010) and most cancer-expert panels around the world recommend against its use as a reliable marker even in the post-operative clinical setup in humans (Sturgeon et al., 2008). Its expression is not always constant and its expression changes massively based on the changes in endogenous biological processes (DeSouza et al., 1998). Muc1 is known to serve as a target molecule in the killing of breast cancer cells by the body's immune system (Barnd et al., 1989, Agrawal et al., 1996, Pecher and Finn, 1996, Magarian-Blander et al., 1998) and hence is also assumed to be a good candidate for immunotherapy against human cancers (Akagi et al., 1997). So as to avoid being detected and killed by the immune system, the cancer cells can undergo epigenetic changes (Wachowska et al., 2015) such that they lose Muc1 expression or modulate its antigenicity (Kontani et al., 2001, Lakshminarayanan et al., 2016, Anandkumar and Devaraj, 2013, Oudejans et al., 2003, Mukherjee et al., 2000, Villalba et al., 2013, Julian et al., 2009, Sanchez et al., 2013). Similarly, downregulation of Muc1 can also be induced in cancer cells subjected to anti-cancer drugs, which in turn might protect tumours against host's immunity (Roulois et al., 2012, Dorn et al., 2004). It has also been seen in some cases that Muc1 is highly expressed in the normal mammary gland of an animal but not in a mammary tumour of the same animal, which suggests that in vivo factors could be down regulating the Muc1 expression (Adriance and Gendler, 2004). Similar is the case with Her2. Cultured circulating tumour cells maintain discrete Her2+ and Her2− subpopulations and these cells can interconvert spontaneously in vivo just within few cell doublings (Jordan et al., 2016, Wood, 2016). There can be certain factors that selectively pressurise the tumour niche such that breast cancer cells in vivo acquire a change in their Her2 status (Arteaga and Engelman, 2014, Krawczyk et al., 2009). The cancer cells may express Her2 primarily, but there could be discordance as the same cells that are metastasizing or circulating in vivo may not express Her2 or the reverse may be possible as well (Houssami et al., 2011, Turner and Di Leo, 2013, Bidard et al., 2014, Krishnamurthy et al., 2013, Jäger et al., 2015, Pusztai et al., 2010, St. Romain et al., 2012, Sighoko et al., 2014). So, in principle, the Her2 status of cancer cells in bone marrow is independent of the primary tumour (Hartkopf et al., 2013). Her-2/neu antigen loss can actively occur in primary tumors (epigenetic changes) due to the neu-targeted anti-tumor immune responses, which might be a part of the selection process of a tumor variant that has reduced ability to induce danger signals (Kmieciak et al., 2007, Worschech et al., 2008, Manjili et al., 2006, Knutson et al., 2006, Kmieciak et al., 2008, Marth et al., 1990). Neu antigen-negative variants have been reported to be generated after neu-specific antibody therapy in a neu transgenic mice model of breast cancer (Knutson et al.,

2004) and a similar loss of Her2 is observed in humans with gastric or gastroesophageal cancer following trastuzumab therapy (Pietrantonio et al., 2016). On similar grounds dysregulation of expression of cytokeratins is also possible in cancer cells. For example, downregulation of cytokeratin 18 in breast cancer cells is observed in some cases (Woelfle et al., 2004) and such dysregulation might also be triggered due to the effect of drugs (Yin et al., 2016a). The anti-tumour action drives the process of epithelial-mesenchymal transformation of cancer cells, causing downregulation of epithelial markers such as cytokeratins (Mego et al., 2012). Downregulation of cytokeratin 18 in metastatic cancer cells in bone marrow can also commonly occur (Pantel et al., 1994).

Additionally, breast cancer cells can change *in vivo* such that they are present in a non-proliferative state and might possess stem-cell like characteristics (Kasimir-Bauer et al., 2016, Balic et al., 2006, Reuben et al., 2011, Kasimir-Bauer et al., 2012, Lawson et al., 2015). Transdifferentiation of cells from one cell type to another is another commonly observed phenomenon with cancer cells (Shekhani et al., 2013, Huang et al., 2015, Syder et al., 2004, Zelivianski et al., 2001, Choi et al., 2012, Chen and Wu, 2016, Cerasuolo et al., 2015, Ha et al., 2010, Marcu et al., 2010, Xu et al., 2016, Fehrenbach et al., 2016). Transdifferentiated cells thus formed can still be malignant in nature (Gattenlöhner et al., 2008, Cichon et al., 2013, Mori et al., 2010, Han et al., 2014b, Scully et al., 2012, Ul-Mulk et al., 2012, Terry and Beltran, 2014, Polyak and Weinberg, 2009, Hayakawa et al., 2016, Gao et al., 2014, Kong et al., 2010, Stoecker and Wang, 2013, Pilarski et al., 2010, Ratei et al., 2010, Abdul Aziz et al., 2010). Breast cancer cell lines can co-express several types of differentiation markers, leading to aberrant multi-lineage transdifferentiation or lineage infidelity (Zhang et al., 2010). Hence, in the immunocompetent host, the possible dynamic nature of genotypic and phenotypic variations occurring in engrafted breast cancer cells, makes it extremely difficult to predict the molecular nature of breast tumour developed *in vivo* by inoculation of a given breast cancer cell line. To obtain insights into these variations, one will require to perform comparative genomic and proteomic assessments of cell line cultured *in vitro* and bone-colonising tumour developed *in vivo.*

My findings show that J-2156 can alleviate hypersensitivities associated with breast cancer induced bone pain. The ability of J-2156 to cross the blood-brain barrier and blood-spinal cord barrier at concentrations used in this study, needs to be investigated. This will give valuable information on whether the J-2156 mediated anti-hypersensitivity effects are also underpinned by its effects on SST4 receptors in the central nervous system as well as the peripheral nervous system.

Tumour cells and nerves closely interact with each other and cancer cells colonising the bone create an environment suitable for activation of sensory neurons innervating the bone and the tumour (Voss and Entschladen, 2010, Mancino et al., 2011, Cole et al., 2015, Sroka et al., 2010, di Mola and di Sebastiano, 2008, Jobling et al., 2015, Yoneda et al., 2015). Functional interactions between tumour and peripheral nerves cause changes in excitability and morphology of primary afferent fibres (Cain et al., 2001), thereby producing pain hypersensitivity (Sughrue et al., 2008). Tumour tissue derived endogenous substances activate sensory nerve fibres to induce bone pain (Tong et al., 2010b). Drugs can reach and directly act on the breast cancer cells colonised in the bones to reduce secretion of inflammatory mediators and algogenic substances, thereby inhibiting pain hypersensitivities (Lozano-Ondoua et al., 2013a, Fazzari et al., 2015, Ungard et al., 2014). SST4 receptor, activated by somatostatin, is a target known to reduce expression of inflammatory mediators (Helyes et al., 2009). Breast cancer tumours as well as breast cancer cell lines like MCF-7 and MDA-MB-231 commonly express SST4 receptor (Watt and Kumar, 2006, Kumar et al., 2005, Frati et al., 2014). Additionally, Walker 256 cells are commonly known to secrete pro-inflammatory mediators (Rebeca et al., 2008, Pavlaki et al., 2009). Like somatostatin (Andoh et al., 2002, Chowers et al., 2000), J-2156 also inhibits the production of inflammatory mediators (Helyes et al., 2006). Hence, it will be an interesting area to assess which analgesic targets are expressed on the tumour cells and whether drugs might act on tumour cells colonised in the bones to aid the process of analgesia. The ability of analgesic drugs like SST4 agonists to acutely inhibit the cancer cell mediated secretion of pro-inflammatory mediators and to contribute towards analgesia can be investigated in future.

BIBLIOGRAPHY

ABBADIE, C. & BESSON, J. M. 1992. c-fos expression in rat lumbar spinal cord during the development of adjuvant-induced arthritis. *Neuroscience,* 48**,** 985-93.

ABDEL-MAGID, A. F. 2015. Treating pain with somatostatin receptor subtype 4 agonists. *ACS Med Chem Lett,* 6**,** 110-1.

ABDUL AZIZ, M., SULLIVAN, F., KERIN, M. J. & CALLAGY, G. 2010. Malignant Phyllodes Tumour with Liposarcomatous Differentiation, Invasive Tubular Carcinoma, and Ductal and Lobular Carcinoma In Situ: Case Report and Review of the Literature. *Pathology Research International,* 2010**,** 501274.

ABRAIRA, V. E. & GINTY, D. D. 2013. The sensory neurons of touch. *Neuron,* 79**,** 618-39.

ABRAMS, D. I., JAY, C. A., SHADE, S. B., VIZOSO, H., REDA, H., PRESS, S., KELLY, M. E., ROWBOTHAM, M. C. & PETERSEN, K. L. 2007. Cannabis in painful HIV-associated sensory neuropathy: a randomized placebo-controlled trial. *Neurology,* 68**,** 515-21.

ADRIANCE, M. C. & GENDLER, S. J. 2004. Downregulation of Muc1 in MMTV-c-Neu tumors. *Oncogene,* 23**,** 697-705.

AGARWAL, N., PACHER, P., TEGEDER, I., AMAYA, F., CONSTANTIN, C. E., BRENNER, G. J., RUBINO, T., MICHALSKI, C. W., MARSICANO, G., MONORY, K., MACKIE, K., MARIAN, C., BATKAI, S., PAROLARO, D., FISCHER, M. J., REEH, P., KUNOS, G., KRESS, M., LUTZ, B., WOOLF, C. J. & KUNER, R. 2007. Cannabinoids mediate analgesia largely via peripheral type 1 cannabinoid receptors in nociceptors. *Nat Neurosci,* 10**,** 870-9.

AGRAWAL, B., REDDISH, M. A. & LONGENECKER, B. M. 1996. In vitro induction of MUC-1 peptide-specific type 1 T lymphocyte and cytotoxic T lymphocyte responses from healthy multiparous donors. *J Immunol,* 157**,** 2089-95.

AGUIRRE, J., DEL MORAL, A., COBO, I., BORGEAT, A. & BLUMENTHAL, S. 2012. The role of continuous peripheral nerve blocks. *Anesthesiol Res Pract,* 2012**,** 560879.

AIHARA, K., ONO, T., UMEI, N., TSUMIYAMA, W., TASAKA, A., ISHIKURA, H., SATO, Y., MATSUMOTO, T. & OKI, S. 2017. A study of the relationships of changes in pain and gait after tourniquet-induced ischemia-reperfusion in rats. *J Phys Ther Sci,* 29**,** 98-101.

AKAGI, J., HODGE, J. W., MCLAUGHLIN, J. P., GRITZ, L., MAZZARA, G., KUFE, D., SCHLOM, J. & KANTOR, J. A. 1997. Therapeutic antitumor response after immunization with an admixture of recombinant vaccinia viruses expressing a modified MUC1 gene and the murine T-cell costimulatory molecule B7. *J Immunother,* 20**,** 38-47.

AKOPIAN, A. N., SOUSLOVA, V., ENGLAND, S., OKUSE, K., OGATA, N., URE, J., SMITH, A., KERR, B. J., MCMAHON, S. B., BOYCE, S., HILL, R., STANFA, L. C., DICKENSON, A. H. & WOOD, J. N. 1999. The tetrodotoxin-resistant sodium channel SNS has a specialized function in pain pathways. *Nat Neurosci,* 2**,** 541-8.

AKTAS, B., KASIMIR-BAUER, S., MÜLLER, V., JANNI, W., FEHM, T., WALLWIENER, D., PANTEL, K. & TEWES, M. 2016. Comparison of the HER2, estrogen and progesterone

receptor expression profile of primary tumor, metastases and circulating tumor cells in metastatic breast cancer patients. *BMC Cancer,* 16.

AL-HASANI, R. & BRUCHAS, M. R. 2011. Molecular Mechanisms of Opioid Receptor-Dependent Signaling and Behavior. *Anesthesiology,* 115**,** 1363-81.

AL-MAGHREBI, M., ANIM, J. T. & OLALU, A. A. 2005. Up-regulation of eukaryotic elongation factor-1 subunits in breast carcinoma. *Anticancer Res,* 25**,** 2573-7.

AL-OBAIDI, S. M., AL-ZOABI, B., AL-SHUWAIE, N., AL-ZAABIE, N. & NELSON, R. M. 2003. The influence of pain and pain-related fear and disability beliefs on walking velocity in chronic low back pain. *Int J Rehabil Res,* 26**,** 101-8.

AL-REJAIE, S. S., ABUOHASHISH, H. M., AHMED, M. M., ARREJAIE, A. S., ALEISA, A. M. & ALSHARARI, S. D. 2015. Telmisartan inhibits hyperalgesia and inflammatory progression in a diabetic neuropathic pain model of Wistar rats. *Neurosciences (Riyadh),* 20**,** 115-23.

ALBRECHT, P. & RICE, F. 2010. Role of Small-Fiber Afferents in Pain Mechanisms With Implications on Diagnosis and Treatment. *Current Pain and Headache Reports,* 14**,** 179-188.

ALESKANDARANY, M. A., SORIA, D., GREEN, A. R., NOLAN, C., DIEZ-RODRIGUEZ, M., ELLIS, I. O. & RAKHA, E. A. 2015. Markers of progression in early-stage invasive breast cancer: a predictive immunohistochemical panel algorithm for distant recurrence risk stratification. *Breast Cancer Research and Treatment,* 151**,** 325-333.

ALLOTT, E. H., GERADTS, J., SUN, X., COHEN, S. M., ZIRPOLI, G. R., KHOURY, T., BSHARA, W., CHEN, M., SHERMAN, M. E., PALMER, J. R., AMBROSONE, C. B., OLSHAN, A. F. & TROESTER, M. A. 2016. Intratumoral heterogeneity as a source of discordance in breast cancer biomarker classification. *Breast Cancer Research,* 18**,** 1-11.

ANANDKUMAR, A. & DEVARAJ, H. 2013. Tumour immunomodulation: mucins in resistance to initiation and maturation of immune response against tumours. *Scand J Immunol,* 78**,** 1-7.

ANDOH, A., HATA, K., SHIMADA, M., FUJINO, S., TASAKI, K., BAMBA, S., ARAKI, Y., FUJIYAMA, Y. & BAMBA, T. 2002. Inhibitory effects of somatostatin on tumor necrosis factor-alpha-induced interleukin-6 secretion in human pancreatic periacinar myofibroblasts. *Int J Mol Med,* 10**,** 89-93.

ARGOFF, C. 2011. Mechanisms of pain transmission and pharmacologic management. *Curr Med Res Opin,* 27**,** 2019-31.

ARTEAGA, CARLOS L. & ENGELMAN, JEFFREY A. 2014. ERBB Receptors: From Oncogene Discovery to Basic Science to Mechanism-Based Cancer Therapeutics. *Cancer Cell,* 25**,** 282-303.

ASHRAFUZZAMAN, M. & TUSZYNSKI, J. 2013. The Membrane as a Transporter, Ion Channels and Membrane Pumps. *Membrane Biophysics.* Springer Berlin Heidelberg.

AVENALI, L., NARAYANAN, P., ROUWETTE, T., CERVELLINI, I., SEREDA, M., GOMEZ-VARELA, D. & SCHMIDT, M. 2014. Annexin A2 Regulates TRPA1-Dependent Nociception. *J Neurosci,* 34**,** 14506-16.

BAAMONDE, A., LASTRA, A., JUAREZ, L., GARCIA-SUAREZ, O., MEANA, A., HIDALGO, A. & MENENDEZ, L. 2006. Endogenous beta-endorphin induces thermal analgesia at the initial stages of a murine osteosarcoma. *Peptides,* 27**,** 2778-85.

BADRAOUI, R., BLOUIN, S., MOREAU, M. F., GALLOIS, Y., REBAI, T., SAHNOUN, Z., BASLE, M. & CHAPPARD, D. 2009. Effect of alpha tocopherol acetate in Walker 256/B cells-induced oxidative damage in a rat model of breast cancer skeletal metastases. *Chem Biol Interact,* 182**,** 98-105.

BADVE, S. & NAKSHATRI, H. 2012. Breast-cancer stem cells—beyond semantics. *The Lancet Oncology,* 13**,** e43-e48.

BALIC, M., LIN, H., YOUNG, L., HAWES, D., GIULIANO, A., MCNAMARA, G., DATAR, R. H. & COTE, R. J. 2006. Most early disseminated cancer cells detected in bone marrow of breast cancer patients have a putative breast cancer stem cell phenotype. *Clin Cancer Res,* 12**,** 5615-21.

BALLANTYNE, J. C. & SULLIVAN, M. D. 2015. Intensity of Chronic Pain--The Wrong Metric? *N Engl J Med,* 373**,** 2098-9.

BAO, Y., GAO, Y., HOU, W., YANG, L., KONG, X., ZHENG, H., LI, C. & HUA, B. 2015a. Engagement of signaling pathways of protease-activated receptor 2 and mu-opioid receptor in bone cancer pain and morphine tolerance. *Int J Cancer,* 137**,** 1475-83.

BAO, Y., HOU, W., LIU, R., GAO, Y., KONG, X., YANG, L., SHI, Z., LI, W., ZHENG, H., JIANG, S., LI, C., QIN, Y. & HUA, B. 2014a. PAR2-mediated upregulation of BDNF contributes to central sensitization in bone cancer pain. *Mol Pain,* 10**,** 28.

BAO, Y., HOU, W., YANG, L., KONG, X., DU, M., ZHENG, H., GAO, Y. & HUA, B. 2015b. Protease-activated receptor 2 antagonist potentiates analgesic effects of systemic morphine in a rat model of bone cancer pain. *Reg Anesth Pain Med,* 40**,** 158-65.

BAO, Y., HOU, W., YANG, L., LIU, R., GAO, Y., KONG, X., SHI, Z., LI, W., ZHENG, H., JIANG, S. & HUA, B. 2015c. Increased expression of protease-activated receptor 2 and 4 within dorsal root ganglia in a rat model of bone cancer pain. *J Mol Neurosci,* 55**,** 706-14.

BAO, Y., HUA, B., HOU, W., SHI, Z., LI, W., LI, C., CHEN, C., LIU, R. & QIN, Y. 2014b. Involvement of protease-activated receptor 2 in nociceptive behavior in a rat model of bone cancer. *J Mol Neurosci,* 52**,** 566-76.

BÄR, K. J., SCHURIGT, U., SCHOLZE, A., SEGOND VON BANCHET, G., STOPFEL, N., BRÄUER, R., HALBHUBER, K. J. & SCHAIBLE, H. G. 2004. The expression and localization of somatostatin receptors in dorsal root ganglion neurons of normal and monoarthritic rats. *Neuroscience,* 127**,** 197-206.

BARND, D. L., LAN, M. S., METZGAR, R. S. & FINN, O. J. 1989. Specific, major histocompatibility complex-unrestricted recognition of tumor-associated mucins by human cytotoxic T cells. *Proc Natl Acad Sci U S A,* 86**,** 7159-63.

BARON, R. 2006. Mechanisms of Disease: neuropathic pain[mdash]a clinical perspective. *Nat Clin Pract Neuro,* 2**,** 95-106.

BARRY, I. 2009. The regression question. *Nat Rev Cancer,* 9**,** 8-8.

BASBAUM, A. I., BAUTISTA, D. M., SCHERRER, G. & JULIUS, D. 2009. Cellular and molecular mechanisms of pain. *Cell,* 139**,** 267-84.

BASU, S., RAY, A. & DITTEL, B. N. 2011. Cannabinoid Receptor 2 Is Critical for the Homing and Retention of Marginal Zone B Lineage Cells and for Efficient T-Independent Immune Responses. *The Journal of Immunology,* 187**,** 5720-5732.

BAUTISTA, D. M., SIEMENS, J., GLAZER, J. M., TSURUDA, P. R., BASBAUM, A. I., STUCKY, C. L., JORDT, S. E. & JULIUS, D. 2007. The menthol receptor TRPM8 is the principal detector of environmental cold. *Nature,* 448**,** 204-8.

BEAN, B. P. 2007. The action potential in mammalian central neurons. *Nat Rev Neurosci,* 8**,** 451-65.

BEATTY, G. L. & PATERSON, Y. 2000. IFN-gamma can promote tumor evasion of the immune system in vivo by down-regulating cellular levels of an endogenous tumor antigen. *J Immunol,* 165**,** 5502-8.

BEATTY, G. L. & PATERSON, Y. 2001. Regulation of tumor growth by IFN-gamma in cancer immunotherapy. *Immunol Res,* 24**,** 201-10.

BEDARD, P. L., HANSEN, A. R., RATAIN, M. J. & SIU, L. L. 2013. Tumour heterogeneity in the clinic. *Nature,* 501**,** 355-64.

BEGGS, S., TRANG, T. & SALTER, M. W. 2012. P2X4R+ microglia drive neuropathic pain. *Nat Neurosci,* 15**,** 1068-73.

BEKESI, J. G. & WINZLER, R. J. 1970. Inhibitory Effects of d-Glucosamine on the Growth of Walker 256 Carcinosarcoma and on Protein, RNA, and DNA Synthesis. *Cancer Research,* 30**,** 2905-2912.

BELCHEVA, M. M., HAAS, P. D., TAN, Y., HEATON, V. M. & COSCIA, C. J. 2002. The fibroblast growth factor receptor is at the site of convergence between mu-opioid receptor and growth factor signaling pathways in rat C6 glioma cells. *J Pharmacol Exp Ther,* 303**,** 909-18.

BELCHEVA, M. M., SZUCS, M., WANG, D., SADEE, W. & COSCIA, C. J. 2001. mu-Opioid receptor-mediated ERK activation involves calmodulin-dependent epidermal growth factor receptor transactivation. *J Biol Chem,* 276**,** 33847-53.

BEN-ARI, Y., GAIARSA, J.-L., TYZIO, R. & KHAZIPOV, R. 2007. *GABA: A Pioneer Transmitter That Excites Immature Neurons and Generates Primitive Oscillations*.

BENGSCH, F., BUCK, A., GUNTHER, S. C., SEIZ, J. R., TACKE, M., PFEIFER, D., VON ELVERFELDT, D., SEVENICH, L., HILLEBRAND, L. E., KERN, U., SAMENI, M., PETERS,

C., SLOANE, B. F. & REINHECKEL, T. 2014. Cell type-dependent pathogenic functions of overexpressed human cathepsin B in murine breast cancer progression. *Oncogene,* 33**,** 4474-4484.

BHANDARI, S., WATSON, N., LONG, E., SHARPE, S., ZHONG, W., XU, S. Z. & ATKIN, S. L. 2008. Expression of somatostatin and somatostatin receptor subtypes 1-5 in human normal and diseased kidney. *J Histochem Cytochem,* 56**,** 733-43.

BIAN, J., ZHU, S., MA, W., LI, C. & ASHRAF, M. A. 2016. Analgesic effect and possible mechanism of SCH772984 intrathecal injection on rats with bone cancer pain. *Saudi Pharm J,* 24**,** 354-62.

BIDARD, F.-C., PEETERS, D. J., FEHM, T., NOLÉ, F., GISBERT-CRIADO, R., MAVROUDIS, D., GRISANTI, S., GENERALI, D., GARCIA-SAENZ, J. A., STEBBING, J., CALDAS, C., GAZZANIGA, P., MANSO, L., ZAMARCHI, R., DE LASCOITI, A. F., DE MATTOS-ARRUDA, L., IGNATIADIS, M., LEBOFSKY, R., VAN LAERE, S. J., MEIER-STIEGEN, F., SANDRI, M.-T., VIDAL-MARTINEZ, J., POLITAKI, E., CONSOLI, F., BOTTINI, A., DIAZ-RUBIO, E., KRELL, J., DAWSON, S.-J., RAIMONDI, C., RUTTEN, A., JANNI, W., MUNZONE, E., CARAÑANA, V., AGELAKI, S., ALMICI, C., DIRIX, L., SOLOMAYER, E.-F., ZORZINO, L., JOHANNES, H., REIS-FILHO, J. S., PANTEL, K., PIERGA, J.-Y. & MICHIELS, S. 2014. Clinical validity of circulating tumour cells in patients with metastatic breast cancer: a pooled analysis of individual patient data. *The Lancet Oncology,* 15**,** 406-414.

BILL, R. & CHRISTOFORI, G. 2015. The relevance of EMT in breast cancer metastasis: Correlation or causality? *FEBS Letters,* 589**,** 1577-1587.

BINSHTOK, A. M., WANG, H., ZIMMERMANN, K., AMAYA, F., VARDEH, D., SHI, L., BRENNER, G. J., JI, R. R., BEAN, B. P., WOOLF, C. J. & SAMAD, T. A. 2008. Nociceptors are interleukin-1beta sensors. *J Neurosci,* 28**,** 14062-73.

BLACK, J. A., CUMMINS, T. R., PLUMPTON, C., CHEN, Y. H., HORMUZDIAR, W., CLARE, J. J. & WAXMAN, S. G. 1999. Upregulation of a silent sodium channel after peripheral, but not central, nerve injury in DRG neurons. *J Neurophysiol,* 82**,** 2776-85.

BLOOM, A. P., JIMENEZ-ANDRADE, J. M., TAYLOR, R. N., CASTANEDA-CORRAL, G., KACZMARSKA, M. J., FREEMAN, K. T., COUGHLIN, K. A., GHILARDI, J. R., KUSKOWSKI, M. A. & MANTYH, P. W. 2011. Breast cancer-induced bone remodeling, skeletal pain, and sprouting of sensory nerve fibers. *J Pain,* 12**,** 698-711.

BLOUIN, S., BASLE, M. F. & CHAPPARD, D. 2005. Rat models of bone metastases. *Clin Exp Metastasis,* 22**,** 605-14.

BOETTGER, M. K., WEBER, K., SCHMIDT, M., GAJDA, M., BRÄUER, R. & SCHAIBLE, H.-G. 2009. Gait abnormalities differentially indicate pain or structural joint damage in monoarticular antigen-induced arthritis. *PAIN®,* 145**,** 142-150.

BRIGATTE, P., FAIAD, O. J., FERREIRA NOCELLI, R. C., LANDGRAF, R. G., PALMA, M. S., CURY, Y., CURI, R. & SAMPAIO, S. C. 2016. Walker 256 Tumor Growth Suppression by Crotoxin Involves Formyl Peptide Receptors and Lipoxin A4. *Mediators Inflamm,* 2016**,** 2457532.

BRIGATTE, P., SAMPAIO, S. C., GUTIERREZ, V. P., GUERRA, J. L., SINHORINI, I. L., CURI, R. & CURY, Y. 2007. Walker 256 tumor-bearing rats as a model to study cancer pain. *J Pain,* 8**,** 412-21.

BRINGS, V. E. & ZYLKA, M. J. 2015. Sex, drugs and pain control. *Nat Neurosci,* 18**,** 1059-60.

BRUNO, J. F., XU, Y., SONG, J. & BERELOWITZ, M. 1993. Tissue distribution of somatostatin receptor subtype messenger ribonucleic acid in the rat. *Endocrinology,* 133**,** 2561-7.

BRUNS, C., WECKBECKER, G., RAULF, F., LUBBERT, H. & HOYER, D. 1995. Characterization of somatostatin receptor subtypes. *Ciba Found Symp,* 190**,** 89-101; discussion 101-10.

BU, H., SHU, B., GAO, F., LIU, C., GUAN, X., KE, C., CAO, F., HINTON, A. O., JR., XIANG, H., YANG, H., TIAN, X. & TIAN, Y. 2014. Spinal IFN-gamma-induced protein-10 (CXCL10) mediates metastatic breast cancer-induced bone pain by activation of microglia in rat models. *Breast Cancer Res Treat,* 143**,** 255-63.

BUCHHEIT, T., VAN DE VEN, T. & SHAW, A. 2012. Epigenetics and the Transition from Acute to Chronic Pain. *Pain Medicine,* 13**,** 1474-1490.

BUCKLEY, N. E., FORDE, C., MCART, D. G., BOYLE, D. P., MULLAN, P. B., JAMES, J. A., MAXWELL, P., MCQUAID, S. & SALTO-TELLEZ, M. 2016. Quantification of HER2 heterogeneity in breast cancer–implications for identification of sub-dominant clones for personalised treatment. *Sci Rep,* 6.

BUEHRING, G. C., EBY, E. A. & EBY, M. J. 2004. Cell line cross-contamination: how aware are Mammalian cell culturists of the problem and how to monitor it? *In Vitro Cell Dev Biol Anim,* 40**,** 211-5.

BUI, J. D. & SCHREIBER, R. D. 2007. Cancer immunosurveillance, immunoediting and inflammation: independent or interdependent processes? *Curr Opin Immunol,* 19**,** 203-8.

BURNSIDE, E. S., TRENTHAM-DIETZ, A., KELCZ, F. & COLLINS, J. 2006. An Example of Breast Cancer Regression on Imaging. *Radiology Case Reports,* 1**,** 27-37.

CAHILL, L. & ASWAD, D. 2015. Sex Influences on the Brain: An Issue Whose Time Has Come. *Neuron,* 88**,** 1084-1085.

CAIN, D. M., WACNIK, P. W., TURNER, M., WENDELSCHAFER-CRABB, G., KENNEDY, W. R., WILCOX, G. L. & SIMONE, D. A. 2001. Functional interactions between tumor and peripheral nerve: changes in excitability and morphology of primary afferent fibers in a murine model of cancer pain. *J Neurosci,* 21**,** 9367-76.

CAMPOS-FERRAZ, P. L., GUALANO, B., DAS NEVES, W., ANDRADE, I. T., HANGAI, I., PEREIRA, R. T., BEZERRA, R. N., DEMINICE, R., SEELAENDER, M. & LANCHA, A. H. 2016. Exploratory studies of the potential anti-cancer effects of creatine. *Amino Acids*.

CAMPRUBI-ROBLES, M., MAIR, N., ANDRATSCH, M., BENETTI, C., BEROUKAS, D., RUKWIED, R., LANGESLAG, M., PROIA, R. L., SCHMELZ, M., FERRER MONTIEL, A. V., HABERBERGER, R. V. & KRESS, M. 2013. Sphingosine-1-phosphate-induced nociceptor excitation and ongoing pain behavior in mice and humans is largely mediated by S1P3 receptor. *J Neurosci,* 33**,** 2582-92.

CAO, F., GAO, F., XU, A. J., CHEN, Z. J., CHEN, S. S., YANG, H., YU, H. H., MEI, W., LIU, X. J., XIAO, X. P., YANG, S. B., TIAN, X. B., WANG, X. R. & TIAN, Y. K. 2010. Regulation of spinal neuroimmune responses by prolonged morphine treatment in a rat model of cancer induced bone pain. *Brain Res,* 1326**,** 162-73.

CARACENI, A., DAVIES, A., POULAIN, P., CORTES-FUNES, H., PANCHAL, S. J. & FANELLI, G. 2013. Guidelines for the management of breakthrough pain in patients with cancer. *J Natl Compr Canc Netw,* 11 Suppl 1**,** S29-36.

CARLTON, S. M., ZHOU, S., DU, J., HARGETT, G. L., JI, G. & COGGESHALL, R. E. 2004. Somatostatin modulates the transient receptor potential vanilloid 1 (TRPV1) ion channel. *Pain,* 110**,** 616-27.

CARON, P., BUSCAIL, L., BECKERS, A., ESTEVE, J. P., IGOUT, A., HENNEN, G. & SUSINI, C. 1997. Expression of somatostatin receptor SST4 in human placenta and absence of octreotide effect on human placental growth hormone concentration during pregnancy. *J Clin Endocrinol Metab,* 82**,** 3771-6.

CARTER, B. C. & BEAN, B. P. 2009. Sodium entry during action potentials of mammalian central neurons: incomplete inactivation and reduced metabolic efficiency in fast-spiking neurons. *Neuron,* 64**,** 898-909.

CATTERALL, W. A. 2000. From ionic currents to molecular mechanisms: the structure and function of voltage-gated sodium channels. *Neuron,* 26**,** 13-25.

CATTERALL, W. A. 2011. Voltage-Gated Calcium Channels. *Cold Spring Harb Perspect Biol,* 3.

CAVALCANTI, T. C., GREGORINI, C. C., GUIMARAES, F., RETTORI, O. & VIEIRA-MATOS, A. N. 2003. Changes in red blood cell osmotic fragility induced by total plasma and plasma fractions obtained from rats bearing progressive and regressive variants of the Walker 256 tumor. *Braz J Med Biol Res,* 36**,** 887-95.

CERASUOLO, M., PARIS, D., IANNOTTI, F. A., MELCK, D., VERDE, R., MAZZARELLA, E., MOTTA, A. & LIGRESTI, A. 2015. Neuroendocrine Transdifferentiation in Human Prostate Cancer Cells: An Integrated Approach. *Cancer Research*.

CHACUR, M., MILLIGAN, E. D., GAZDA, L. S., ARMSTRONG, C., WANG, H., TRACEY, K. J., MAIER, S. F. & WATKINS, L. R. 2001. A new model of sciatic inflammatory neuritis (SIN): induction of unilateral and bilateral mechanical allodynia following acute unilateral peri-sciatic immune activation in rats. *Pain,* 94**,** 231-44.

CHANG-LIU, C. M. & WOLOSCHAK, G. E. 1997. Effect of passage number on cellular response to DNA-damaging agents: cell survival and gene expression. *Cancer Lett,* 113**,** 77-86.

CHEN, G., KIM, Y. H., LI, H., LUO, H., LIU, D.-L., ZHANG, Z.-J., LAY, M., CHANG, W., ZHANG, Y.-Q. & JI, R.-R. 2017. PD-L1 inhibits acute and chronic pain by suppressing nociceptive neuron activity via PD-1. *Nat Neurosci,* 20**,** 917-926.

CHEN, H. F. & WU, K. J. 2016. Endothelial Transdifferentiation of Tumor Cells Triggered by the Twist1-Jagged1-KLF4 Axis: Relationship between Cancer Stemness and Angiogenesis. *Stem Cells Int,* 2016**,** 6439864.

CHEN, J., GONG, Z., YAN, H., QIAO, Z. & QIN, B. 2012a. Neuroplastic alteration of TTX-resistant sodium channel with visceral pain and morphine-induced hyperalgesia. *J Pain Res,* 5**,** 491-502.

CHEN, J., WANG, L., ZHANG, Y. & YANG, J. 2012b. P2Y1 purinoceptor inhibition reduces extracellular signal-regulated protein kinase 1/2 phosphorylation in spinal cord and dorsal root ganglia: implications for cancer-induced bone pain. *Acta Biochim Biophys Sin (Shanghai),* 44**,** 367-72.

CHEN, L., WANG, K., YANG, T., WANG, W., MEI, X. P., ZHU, C., WANG, W., ZHANG, F. X. & LI, Y. Q. 2015. Downregulation of spinal endomorphin-2 correlates with mechanical allodynia in a rat model of tibia cancer. *Neuroscience,* 286**,** 151-161.

CHEN, L., ZHU, L., WANG, K., WANG, W., MEI, X. P., LIU, T., ZHANG, F. X., WANG, W., CHEN, T. & LI, Y. Q. 2013a. Antinociceptive effect of prostatic acid phosphatase in a rat model of cancer-induced bone pain. *Pain Physician,* 16**,** 533-46.

CHEN, X., TALLEY, E. M., PATEL, N., GOMIS, A., MCINTIRE, W. E., DONG, B., VIANA, F., GARRISON, J. C. & BAYLISS, D. A. 2006. Inhibition of a background potassium channel by Gq protein alpha-subunits. *Proc Natl Acad Sci U S A,* 103**,** 3422-7.

CHEN, Y. C., PRISTERÁ, A., AYUB, M., SWANWICK, R. S., KARU, K., HAMADA, Y., RICE, A. S. C. & OKUSE, K. 2013b. Identification of a Receptor for Neuropeptide VGF and Its Role in Neuropathic Pain. *J Biol Chem,* 288**,** 34638-46.

CHENG, H. Y., PITCHER, G. M., LAVIOLETTE, S. R., WHISHAW, I. Q., TONG, K. I., KOCKERITZ, L. K., WADA, T., JOZA, N. A., CRACKOWER, M., GONCALVES, J., SAROSI, I., WOODGETT, J. R., OLIVEIRA-DOS-SANTOS, A. J., IKURA, M., VAN DER KOOY, D., SALTER, M. W. & PENNINGER, J. M. 2002. DREAM is a critical transcriptional repressor for pain modulation. *Cell,* 108**,** 31-43.

CHENG, W., CHEN, Y. L., WU, L., MIAO, B., YIN, Q., WANG, J. F. & FU, Z. J. 2016. Inhibition of spinal UCHL1 attenuates pain facilitation in a cancer-induced bone pain model by inhibiting ubiquitin and glial activation. *Am J Transl Res,* 8**,** 3041-8.

CHENG, W., ZHAO, Y., LIU, H., FAN, Q., LU, F. F., LI, J., YIN, Q. & YAN, C. D. 2014. Resveratrol attenuates bone cancer pain through the inhibition of spinal glial activation and CX3CR1 upregulation. *Fundam Clin Pharmacol,* 28**,** 661-70.

CHENG, Y.-C. & PRUSOFF, W. H. 1973. Relationship between the inhibition constant (KI) and the concentration of inhibitor which causes 50 per cent inhibition (I50) of an enzymatic reaction. *Biochemical Pharmacology,* 22**,** 3099-3108.

CHIANG, N., ARITA, M. & SERHAN, C. N. 2005. Anti-inflammatory circuitry: lipoxin, aspirin-triggered lipoxins and their receptor ALX. *Prostaglandins Leukot Essent Fatty Acids,* 73**,** 163-77.

CHO, H., YANG, Y. D., LEE, J., LEE, B., KIM, T., JANG, Y., BACK, S. K., NA, H. S., HARFE, B. D., WANG, F., RAOUF, R., WOOD, J. N. & OH, U. 2012. The calcium-activated chloride channel anoctamin 1 acts as a heat sensor in nociceptive neurons. *Nat Neurosci,* 15**,** 1015-21.

CHOI, S. Y., GOUT, P. W., COLLINS, C. C. & WANG, Y. 2012. Epithelial immune cell-like transition (EIT): a proposed transdifferentiation process underlying immune-suppressive activity of epithelial cancers. *Differentiation,* 83**,** 293-8.

CHOWERS, Y., CAHALON, L., LAHAV, M., SCHOR, H., TAL, R., BAR-MEIR, S. & LEVITE, M. 2000. Somatostatin Through Its Specific Receptor Inhibits Spontaneous and TNF-α- and Bacteria-Induced IL-8 and IL-1β Secretion from Intestinal Epithelial Cells. *The Journal of Immunology,* 165**,** 2955-2961.

CHUNG, M. K., LEE, H., MIZUNO, A., SUZUKI, M. & CATERINA, M. J. 2004. 2-aminoethoxydiphenyl borate activates and sensitizes the heat-gated ion channel TRPV3. *J Neurosci,* 24**,** 5177-82.

CHUNG, M. K., PARK, J., ASGAR, J. & RO, J. Y. 2016. Transcriptome analysis of trigeminal ganglia following masseter muscle inflammation in rats. *Mol Pain,* 12.

CIANFROCCA, M. & GRADISHAR, W. 2009. New molecular classifications of breast cancer. *CA Cancer J Clin,* 59**,** 303-13.

CICHON, L., GAEDE, J., SPORN, T., REHDER, C. & LAGOO, A. S. 2013. The Transdifferentiation of Mediastinal Germ Cell Tumor into a Myeloid Neoplasm in the Bone Marrow-Report of a Case and Short Review of a Diagnostic Pitfall. *2013,* 2.

CIMPEAN, A. M., SUCIU, C., CEAUSU, R., TATUCU, D., MURESAN, A. M. & RAICA, M. 2008. Relevance of the immunohistochemical expression of cytokeratin 8/18 for the diagnosis and classification of breast cancer. *Rom J Morphol Embryol,* 49**,** 479-83.

CLARK, A. K. & MALCANGIO, M. 2012. Microglial signalling mechanisms: Cathepsin S and Fractalkine. *Experimental Neurology,* 234**,** 283-292.

CLARK, A. K., STANILAND, A. A., MARCHAND, F., KAAN, T. K., MCMAHON, S. B. & MALCANGIO, M. 2010a. P2X7-dependent release of interleukin-1beta and nociception in the spinal cord following lipopolysaccharide. *J Neurosci,* 30**,** 573-82.

CLARK, A. K., WODARSKI, R., GUIDA, F., SASSO, O. & MALCANGIO, M. 2010b. Cathepsin S release from primary cultured microglia is regulated by the P2X7 receptor. *Glia,* 58**,** 1710-26.

CLARK, A. K., YIP, P. K., GRIST, J., GENTRY, C., STANILAND, A. A., MARCHAND, F., DEHVARI, M., WOTHERSPOON, G., WINTER, J., ULLAH, J., BEVAN, S. & MALCANGIO, M. 2007. Inhibition of spinal microglial cathepsin S for the reversal of neuropathic pain. *Proceedings of the National Academy of Sciences,* 104**,** 10655-10660.

CLARK, A. K., YIP, P. K. & MALCANGIO, M. 2009. The liberation of fractalkine in the dorsal horn requires microglial cathepsin S. *J Neurosci,* 29**,** 6945-54.

CLEELAND, C., VON MOOS, R., WALKER, M. S., WANG, Y., GAO, J., CHAVEZ-MACGREGOR, M., LIEDE, A., ARELLANO, J., BALAKUMARAN, A. & QIAN, Y. 2016. Burden of symptoms associated with development of metastatic bone disease in patients with breast cancer. *Support Care Cancer,* 24**,** 3557-65.

COBIANCHI, S., DE CRUZ, J. & NAVARRO, X. 2014. Assessment of sensory thresholds and nociceptive fiber growth after sciatic nerve injury reveals the differential contribution of collateral reinnervation and nerve regeneration to neuropathic pain. *Exp Neurol,* 255**,** 1-11.

COGHILL, R. C., MCHAFFIE, J. G. & YEN, Y. F. 2003. Neural correlates of interindividual differences in the subjective experience of pain. *Proc Natl Acad Sci U S A,* 100**,** 8538-42.

COLE, S. W., NAGARAJA, A. S., LUTGENDORF, S. K., GREEN, P. A. & SOOD, A. K. 2015. Sympathetic nervous system regulation of the tumour microenvironment. *Nat Rev Cancer,* 15**,** 563-572.

COLEMAN, R. E. 2006. Clinical features of metastatic bone disease and risk of skeletal morbidity. *Clin Cancer Res,* 12**,** 6243s-6249s.

COLVIN, L. & FALLON, M. 2008. Challenges in cancer pain management--bone pain. *Eur J Cancer,* 44**,** 1083-90.

CONCEPCION-MARTIN, M., GOMEZ-OLIVA, C., JUANES, A., DIEZ, X., PRIETO-ALHAMBRA, D., TORRAS, X., SAINZ, S., VILLANUEVA, C., FARRE, A., GUARNER-ARGENTE, C. & GUARNER, C. 2014. Somatostatin for prevention of post-ERCP pancreatitis: a randomized, double-blind trial. *Endoscopy,* 46**,** 851-6.

CONNOR, M., OSBORNE, P. B. & CHRISTIE, M. J. 2004. μ-Opioid receptor desensitization: Is morphine different? *British Journal of Pharmacology,* 143**,** 685-696.

COSTE, B., MATHUR, J., SCHMIDT, M., EARLEY, T. J., RANADE, S., PETRUS, M. J., DUBIN, A. E. & PATAPOUTIAN, A. 2010. Piezo1 and Piezo2 are essential components of distinct mechanically activated cation channels. *Science,* 330**,** 55-60.

COSTELLOE, C. M., ROHREN, E. M., MADEWELL, J. E., HAMAOKA, T., THERIAULT, R. L., YU, T. K., LEWIS, V. O., MA, J., STAFFORD, R. J., TARI, A. M., HORTOBAGYI, G. N. & UENO, N. T. 2009. Imaging bone metastases in breast cancer: techniques and recommendations for diagnosis. *Lancet Oncol,* 10**,** 606-14.

COULL, J. A., BOUDREAU, D., BACHAND, K., PRESCOTT, S. A., NAULT, F., SIK, A., DE KONINCK, P. & DE KONINCK, Y. 2003. Trans-synaptic shift in anion gradient in spinal lamina I neurons as a mechanism of neuropathic pain. *Nature,* 424**,** 938-42.

COULTHARD, P., SIMJEE, S. U. & PLEUVRY, B. J. 2003. Gait analysis as a correlate of pain induced by carrageenan intraplantar injection. *Journal of Neuroscience Methods,* 128**,** 95-102.

COX, J. J., REIMANN, F., NICHOLAS, A. K., THORNTON, G., ROBERTS, E., SPRINGELL, K., KARBANI, G., JAFRI, H., MANNAN, J., RAASHID, Y., AL-GAZALI, L., HAMAMY, H., VALENTE, E. M., GORMAN, S., WILLIAMS, R., MCHALE, D. P., WOOD, J. N., GRIBBLE, F. M. & WOODS, C. G. 2006. An SCN9A channelopathy causes congenital inability to experience pain. *Nature,* 444**,** 894-8.

CRANER, M. J., DAMARJIAN, T. G., LIU, S., HAINS, B. C., LO, A. C., BLACK, J. A., NEWCOMBE, J., CUZNER, M. L. & WAXMAN, S. G. 2005. Sodium channels contribute to microglia/macrophage activation and function in EAE and MS. *Glia,* 49**,** 220-9.

CRANER, M. J., HAINS, B. C., LO, A. C., BLACK, J. A. & WAXMAN, S. G. 2004a. Co-localization of sodium channel Nav1.6 and the sodium-calcium exchanger at sites of axonal injury in the spinal cord in EAE. *Brain,* 127**,** 294-303.

CRANER, M. J., NEWCOMBE, J., BLACK, J. A., HARTLE, C., CUZNER, M. L. & WAXMAN, S. G. 2004b. Molecular changes in neurons in multiple sclerosis: altered axonal expression of Nav1.2 and Nav1.6 sodium channels and Na+/Ca2+ exchanger. *Proc Natl Acad Sci U S A,* 101**,** 8168-73.

CRIDER, A. M. & WITT, K. A. 2007. Somatostatin sst4 ligands: chemistry and pharmacology. *Mini Rev Med Chem,* 7**,** 213-20.

CRUZ, B. L., DA SILVA, P. C., TOMASIN, R., OLIVEIRA, A. G., VIANA, L. R., SALOMAO, E. M. & GOMES-MARCONDES, M. C. 2016. Dietary leucine supplementation minimises tumour-induced damage in placental tissues of pregnant, tumour-bearing rats. *BMC Cancer,* 16**,** 58.

CUMMINS, T. R., AGLIECO, F., RENGANATHAN, M., HERZOG, R. I., DIB-HAJJ, S. D. & WAXMAN, S. G. 2001. Nav1.3 sodium channels: rapid repriming and slow closed-state inactivation display quantitative differences after expression in a mammalian cell line and in spinal sensory neurons. *J Neurosci,* 21**,** 5952-61.

CUMMINS, T. R., HOWE, J. R. & WAXMAN, S. G. 1998. Slow closed-state inactivation: a novel mechanism underlying ramp currents in cells expressing the hNE/PN1 sodium channel. *J Neurosci,* 18**,** 9607-19.

CURRIE, G. L., DELANEY, A., BENNETT, M. I., DICKENSON, A. H., EGAN, K. J., VESTERINEN, H. M., SENA, E. S., MACLEOD, M. R., COLVIN, L. A. & FALLON, M. T. 2013. Animal models of bone cancer pain: systematic review and meta-analyses. *Pain,* 154**,** 917-26.

CURRIE, G. L., SENA, E. S., FALLON, M. T., MACLEOD, M. R. & COLVIN, L. A. 2014. Using animal models to understand cancer pain in humans. *Curr Pain Headache Rep,* 18**,** 423.

D'MELLO, R. & DICKENSON, A. H. 2008. Spinal cord mechanisms of pain. *British Journal of Anaesthesia,* 101**,** 8-16.

DAI, W. L., YAN, B., JIANG, N., WU, J. J., LIU, X. F., LIU, J. H. & YU, B. Y. 2017. Simultaneous inhibition of NMDA and mGlu1/5 receptors by levo-Corydalmine in rat spinal cord attenuates bone cancer pain. *Int J Cancer*.

DANSER, A. H. J. & ANAND, P. 2014. The Angiotensin II Type 2 Receptor for Pain Control. *Cell,* 157**,** 1504-1506.

DE FELICE, M., LAMBERT, D., HOLEN, I., ESCOTT, K. J. & ANDREW, D. 2016. Effects of Src-kinase inhibition in cancer-induced bone pain. *Mol Pain,* 12.

DE KONINCK, Y. 2007. Altered chloride homeostasis in neurological disorders: a new target. *Curr Opin Pharmacol,* 7**,** 93-9.

DE KONING, P., BRAKKEE, J. H. & GISPEN, W. H. 1986. Methods for producing a reproducible crush in the sciatic and tibial nerve of the rat and rapid and precise testing of return of sensory function. *Journal of the Neurological Sciences,* 74**,** 237-246.

DELANEY, A., FLEETWOOD-WALKER, S. M., COLVIN, L. A. & FALLON, M. 2008. Translational medicine: cancer pain mechanisms and management. *Br J Anaesth,* 101**,** 87-94.

DELLA ROCCA, G. J., VAN BIESEN, T., DAAKA, Y., LUTTRELL, D. K., LUTTRELL, L. M. & LEFKOWITZ, R. J. 1997. Ras-dependent mitogen-activated protein kinase activation by G protein-coupled receptors. Convergence of Gi- and Gq-mediated pathways on calcium/calmodulin, Pyk2, and Src kinase. *J Biol Chem,* 272**,** 19125-32.

DELMAS, P., HAO, J. & RODAT-DESPOIX, L. 2011. Molecular mechanisms of mechanotransduction in mammalian sensory neurons. *Nat Rev Neurosci,* 12**,** 139-153.

DEMINICE, R., CELLA, P. S., PADILHA, C. S., BORGES, F. H., DA SILVA, L. E., CAMPOS-FERRAZ, P. L., JORDAO, A. A., ROBINSON, J. L., BERTOLO, R. F., CECCHINI, R. & GUARNIER, F. A. 2016a. Creatine supplementation prevents hyperhomocysteinemia, oxidative stress and cancer-induced cachexia progression in Walker-256 tumor-bearing rats. *Amino Acids*.

DEMINICE, R., PADILHA, C. D. S., BORGES, F., DA SILVA, L. E. C. M., ROSA, F. T., ROBINSON, J. L., CECCHINI, R., GUARNIER, F. A. & FRAJACOMO, F. T. 2016b. Resistance exercise prevents impaired homocysteine metabolism and hepatic redox capacity in Walker-256 tumor-bearing male Wistar rats. *Nutrition*.

DENG, G., KRISHNAKUMAR, S., POWELL, A. A., ZHANG, H., MINDRINOS, M. N., TELLI, M. L., DAVIS, R. W. & JEFFREY, S. S. 2014. Single cell mutational analysis of PIK3CA in circulating tumor cells and metastases in breast cancer reveals heterogeneity, discordance, and mutation persistence in cultured disseminated tumor cells from bone marrow. *BMC Cancer,* 14**,** 456.

DENISOV, E. V., LITVIAKOV, N. V., ZAVYALOVA, M. V., PERELMUTER, V. M., VTORUSHIN, S. V., TSYGANOV, M. M., GERASHCHENKO, T. S., GARBUKOV, E. Y., SLONIMSKAYA, E. M. & CHERDYNTSEVA, N. V. 2014. Intratumoral morphological heterogeneity of breast

cancer: neoadjuvant chemotherapy efficiency and multidrug resistance gene expression. *Sci Rep,* 4**,** 4709.

DESANTIS, C. E., BRAY, F., FERLAY, J., LORTET-TIEULENT, J., ANDERSON, B. O. & JEMAL, A. 2015. International Variation in Female Breast Cancer Incidence and Mortality Rates. *Cancer Epidemiol Biomarkers Prev,* 24**,** 1495-506.

DESOUZA, M. M., MANI, S. K., JULIAN, J. & CARSON, D. D. 1998. Reduction of mucin-1 expression during the receptive phase in the rat uterus. *Biol Reprod,* 58**,** 1503-7.

DEUIS, J. R., DVORAKOVA, L. S. & VETTER, I. 2017. Methods Used to Evaluate Pain Behaviors in Rodents. *Frontiers in Molecular Neuroscience,* 10**,** 284.

DEVOR, M. 2006. Sodium channels and mechanisms of neuropathic pain. *J Pain,* 7**,** S3-s12.

DEWYS, W., PORIES, W. J., RICHTER, M. C. & STRAIN, W. H. 1970. Inhibition of Walker 256 carcinosarcoma growth of dietary zinc deficiency. *Proc Soc Exp Biol Med,* 135**,** 17-22.

DI MOLA, F. F. & DI SEBASTIANO, P. 2008. Pain and pain generation in pancreatic cancer. *Langenbeck's Archives of Surgery,* 393**,** 919-922.

DIB-HAJJ, S., BLACK, J. A., FELTS, P. & WAXMAN, S. G. 1996. Down-regulation of transcripts for Na channel alpha-SNS in spinal sensory neurons following axotomy. *Proc Natl Acad Sci U S A,* 93**,** 14950-4.

DIB-HAJJ, S. D., BLACK, J. A., CUMMINS, T. R., KENNEY, A. M., KOCSIS, J. D. & WAXMAN, S. G. 1998. Rescue of alpha-SNS sodium channel expression in small dorsal root ganglion neurons after axotomy by nerve growth factor in vivo. *J Neurophysiol,* 79**,** 2668-76.

DIB-HAJJ, S. D., CUMMINS, T. R., BLACK, J. A. & WAXMAN, S. G. 2010. Sodium channels in normal and pathological pain. *Annu Rev Neurosci,* 33**,** 325-47.

DING, Z., XU, W., ZHANG, J., ZOU, W., GUO, Q., HUANG, C., LIU, C., ZHONG, T., ZHANG, J. M. & SONG, Z. 2017. Normalizing GDNF expression in the spinal cord alleviates cutaneous hyperalgesia but not ongoing pain in a rat model of bone cancer pain. *Int J Cancer,* 140**,** 411-422.

DOMAGALA, W., STRIKER, G., SZADOWSKA, A., DUKOWICZ, A., HAREZGA, B. & OSBORN, M. 1994. p53 protein and vimentin in invasive ductal NOS breast carcinoma--relationship with survival and sites of metastases. *Eur J Cancer,* 30a**,** 1527-34.

DONG, Y., MAO-YING, Q. L., CHEN, J. W., YANG, C. J., WANG, Y. Q. & TAN, Z. M. 2011. Involvement of EphB1 receptor/ephrinB1 ligand in bone cancer pain. *Neurosci Lett,* 496**,** 163-7.

DONOVAN-RODRIGUEZ, T., DICKENSON, A. H. & URCH, C. E. 2004. Superficial dorsal horn neuronal responses and the emergence of behavioural hyperalgesia in a rat model of cancer-induced bone pain. *Neurosci Lett,* 360**,** 29-32.

DONOVAN-RODRIGUEZ, T., DICKENSON, A. H. & URCH, C. E. 2005. Gabapentin normalizes spinal neuronal responses that correlate with behavior in a rat model of cancer-induced bone pain. *Anesthesiology,* 102**,** 132-40.

DORN, D. C., HARNACK, U. & PECHER, G. 2004. Down-regulation of the human tumor antigen mucin by gemcitabine on the pancreatic cancer cell line capan-2. *Anticancer Res,* 24**,** 821-5.

DU, J., FANG, J., CHEN, Y., WU, S., LIANG, Y. & FANG, J. 2015. [Parametric optimization of electroacupuncture against bone-cancer pain in rats and its intervention on mRNA expression of opioid receptor and precursor]. *Zhongguo Zhen Jiu,* 35**,** 161-8.

DU, J. Y., LIANG, Y., FANG, J. F., JIANG, Y. L., SHAO, X. M., HE, X. F. & FANG, J. Q. 2016. Effect of systemic injection of heterogenous and homogenous opioids on peripheral cellular immune response in rats with bone cancer pain: A comparative study. *Exp Ther Med,* 12**,** 2568-2576.

DUAN, K. Z., XU, Q., ZHANG, X. M., ZHAO, Z. Q., MEI, Y. A. & ZHANG, Y. Q. 2012. Targeting A-type K(+) channels in primary sensory neurons for bone cancer pain in a rat model. *Pain,* 153**,** 562-74.

DUBIN, A. E. & PATAPOUTIAN, A. 2010. Nociceptors: the sensors of the pain pathway. *J Clin Invest,* 120**,** 3760-72.

DUFFY, M. J., EVOY, D. & MCDERMOTT, E. W. 2010. CA 15-3: Uses and limitation as a biomarker for breast cancer. *Clinica Chimica Acta,* 411**,** 1869-1874.

DUNN, G. P., BRUCE, A. T., IKEDA, H., OLD, L. J. & SCHREIBER, R. D. 2002. Cancer immunoediting: from immunosurveillance to tumor escape. *Nat Immunol,* 3**,** 991-8.

DUNN, G. P., KOEBEL, C. M. & SCHREIBER, R. D. 2006. Interferons, immunity and cancer immunoediting. *Nat Rev Immunol,* 6**,** 836-48.

DUNN, G. P., OLD, L. J. & SCHREIBER, R. D. 2004. The three Es of cancer immunoediting. *Annu Rev Immunol,* 22**,** 329-60.

EARLE, W. R. 1935. A Study of the Walker Rat Mammary Carcinoma 256, in vivo and in vitro. *The American Journal of Cancer,* 24**,** 566-612.

EDMONDS, B. T., WYCKOFF, J., YEUNG, Y. G., WANG, Y., STANLEY, E. R., JONES, J., SEGALL, J. & CONDEELIS, J. 1996. Elongation factor-1 alpha is an overexpressed actin binding protein in metastatic rat mammary adenocarcinoma. *Journal of Cell Science,* 109**,** 2705-2714.

EL NEMR ESMAIL, R. S., EL FAROUK ABDEL-SALAM, L. O. & ABD EL ELLAH, M. M. 2015. Could the Breast Prognostic Biomarker Status Change During Disease Progression? An Immunohistochemical Comparison between Primary Tumors and Synchronous Nodal Metastasis. *Asian Pac J Cancer Prev,* 16**,** 4317-21.

ELEKES, K., HELYES, Z., KERESKAI, L., SANDOR, K., PINTER, E., POZSGAI, G., TEKUS, V., BANVOLGYI, A., NEMETH, J., SZUTS, T., KERI, G. & SZOLCSANYI, J. 2008. Inhibitory effects of synthetic somatostatin receptor subtype 4 agonists on acute and chronic airway inflammation and hyperreactivity in the mouse. *Eur J Pharmacol,* 578**,** 313-22.

ENDO, M. 2000. Springer Berlin Heidelberg.

ENGSTRÖM, M., SAVOLA, J.-M. & WURSTER, S. 2006. Differential Efficacies of Somatostatin Receptor Agonists for G-Protein Activation and Desensitization of Somatostatin Receptor Subtype 4-Mediated Responses. *Journal of Pharmacology and Experimental Therapeutics,* 316**,** 1262-1268.

ENGSTROM, M., TOMPERI, J., EL-DARWISH, K., AHMAN, M., SAVOLA, J. M. & WURSTER, S. 2005. Superagonism at the human somatostatin receptor subtype 4. *J Pharmacol Exp Ther,* 312**,** 332-8.

ERCHEGYI, J., PENKE, B., SIMON, L., MICHAELSON, S., WENGER, S., WASER, B., CESCATO, R., SCHAER, J. C., REUBI, J. C. & RIVIER, J. 2003a. Novel sst(4)-selective somatostatin (SRIF) agonists. 2. Analogues with beta-methyl-3-(2-naphthyl)alanine substitutions at position 8. *J Med Chem,* 46**,** 5587-96.

ERCHEGYI, J., WASER, B., SCHAER, J. C., CESCATO, R., BRAZEAU, J. F., RIVIER, J. & REUBI, J. C. 2003b. Novel sst(4)-selective somatostatin (SRIF) agonists. 3. Analogues amenable to radiolabeling. *J Med Chem,* 46**,** 5597-605.

ESQUIVEL-VELAZQUEZ, M., OSTOA-SALOMA, P., PALACIOS-ARREOLA, M. I., NAVA-CASTRO, K. E., CASTRO, J. I. & MORALES-MONTOR, J. 2015. The role of cytokines in breast cancer development and progression. *J Interferon Cytokine Res,* 35**,** 1-16.

FALK, S. & DICKENSON, A. H. 2014. Pain and nociception: mechanisms of cancer-induced bone pain. *J Clin Oncol,* 32**,** 1647-54.

FALK, S., GALLEGO-PEDERSEN, S. & C. PETERSEN, N. 2017. Grid-climbing Behaviour as a Pain Measure for Cancer-induced Bone Pain and Neuropathic Pain. *In Vivo,* 31**,** 619-623.

FALK, S., IPSEN, D. H., APPEL, C. K., UGARAK, A., DURUP, D., DICKENSON, A. H. & HEEGAARD, A. M. 2015a. Randall Selitto pressure algometry for assessment of bone-related pain in rats. *Eur J Pain,* 19**,** 305-12.

FALK, S., SCHWAB, S. D., FROSIG-JORGENSEN, M., CLAUSEN, R. P., DICKENSON, A. H. & HEEGAARD, A. M. 2015b. P2X7 receptor-mediated analgesia in cancer-induced bone pain. *Neuroscience,* 291**,** 93-105.

FALLON, M., HOSKIN, P. J., COLVIN, L. A., FLEETWOOD-WALKER, S. M., ADAMSON, D., BYRNE, A., MURRAY, G. D. & LAIRD, B. J. 2016. Randomized Double-Blind Trial of Pregabalin Versus Placebo in Conjunction With Palliative Radiotherapy for Cancer-Induced Bone Pain. *J Clin Oncol,* 34**,** 550-6.

FAN, H.-B., ZHANG, T., SUN, K., SONG, S.-P., CAO, S.-B., ZHANG, H.-L. & SHEN, W. 2015. Corticotropin-releasing factor mediates bone cancer induced pain through neuronal activation in rat spinal cord. *Tumor Biology***,** 1-7.

FAN, H., XIAO-LING, S., YALIU, S., MING-MING, L., XUE, F., XIAN-SHENG, M. & LI, F. 2016. Comparative Pharmacokinetics of Ginsenoside Rg3 and Ginsenoside Rh2 after Oral Administration of Ginsenoside Rg3 in Normal and Walker 256 Tumor-bearing Rats. *Pharmacogn Mag,* 12**,** 21-4.

FANG, D., KONG, L.-Y., CAI, J., LI, S., LIU, X.-D., HAN, J.-S. & XING, G.-G. 2015. Interleukin-6-mediated functional upregulation of TRPV1 receptors in dorsal root ganglion neurons through the activation of JAK/PI3K signaling pathway: roles in the development of bone cancer pain in a rat model. *PAIN,* 156**,** 1124-1144.

FAZZARI, J., LIN, H., MURPHY, C., UNGARD, R. & SINGH, G. 2015. Inhibitors of glutamate release from breast cancer cells; new targets for cancer-induced bone-pain. *Scientific Reports,* 5**,** 8380.

FEHLMANN, D., LANGENEGGER, D., SCHUEPBACH, E., SIEHLER, S., FEUERBACH, D. & HOYER, D. 2000. Distribution and characterisation of somatostatin receptor mRNA and binding sites in the brain and periphery. *J Physiol Paris,* 94**,** 265-81.

FEHM, T., KRAWCZYK, N., SOLOMAYER, E.-F., BECKER-PERGOLA, G., DÜRR-STÖRZER, S., NEUBAUER, H., SEEGER, H., STAEBLER, A., WALLWIENER, D. & BECKER, S. 2008. ERalpha-status of disseminated tumour cells in bone marrow of primary breast cancer patients. *Breast Cancer Research,* 10**,** 1-8.

FEHRENBACH, S., NOVAK, D., BERNHARDT, M., LARRIBERE, L., BOUKAMP, P., UMANSKY, V. & UTIKAL, J. 2016. Loss of tumorigenic potential upon transdifferentiation from keratinocytic into melanocytic lineage. *Sci Rep,* 6.

FEINDT, J., BECKER, I., BLOMER, U., HUGO, H. H., MEHDORN, H. M., KRISCH, B. & MENTLEIN, R. 1995. Expression of somatostatin receptor subtypes in cultured astrocytes and gliomas. *J Neurochem,* 65**,** 1997-2005.

FEINDT, J., SCHMIDT, A. & MENTLEIN, R. 1998. Receptors and effects of the inhibitory neuropeptide somatostatin in microglial cells. *Brain Res Mol Brain Res,* 60**,** 228-33.

FEINSTEIN, A. B., STURGEON, J. A., DARNALL, B. D., DUNN, A. L., RICO, T., KAO, M. C. & BHANDARI, R. P. 2017. The Effect of Pain Catastrophizing on Outcomes: A Developmental Perspective Across Children, Adolescents, and Young Adults With Chronic Pain. *J Pain,* 18**,** 144-154.

FERNANDES, C., MONTEIRO, S., BELCHIOR, A., MARQUES, F., GANO, L., CORREIA, J. D. & SANTOS, I. 2016. Novel (188)Re multi-functional bone-seeking compounds: Synthesis, biological and radiotoxic effects in metastatic breast cancer cells. *Nucl Med Biol,* 43**,** 150-7.

FERNIHOUGH, J., GENTRY, C., MALCANGIO, M., FOX, A., REDISKE, J., PELLAS, T., KIDD, B., BEVAN, S. & WINTER, J. 2004. Pain related behaviour in two models of osteoarthritis in the rat knee. *Pain,* 112**,** 83-93.

FERRARELLI, L. 2015. Why women feel more pain. *Science Signaling,* 8**,** ec212-ec212.

FERRARI, L. F., ARALDI, D., GREEN, P. & LEVINE, J. D. 2017. Age-dependent sexual dimorphism in susceptibility to develop chronic pain in the rat. *Neuroscience*.

FERTLEMAN, C. R., BAKER, M. D., PARKER, K. A., MOFFATT, S., ELMSLIE, F. V., ABRAHAMSEN, B., OSTMAN, J., KLUGBAUER, N., WOOD, J. N., GARDINER, R. M. &

REES, M. 2006. SCN9A mutations in paroxysmal extreme pain disorder: allelic variants underlie distinct channel defects and phenotypes. *Neuron,* 52**,** 767-74.

FIDLER, I. J. 1978. Tumor heterogeneity and the biology of cancer invasion and metastasis. *Cancer Res,* 38**,** 2651-60.

FINGLETON, C., SMART, K., MOLONEY, N., FULLEN, B. M. & DOODY, C. 2015. Pain sensitization in people with knee osteoarthritis: a systematic review and meta-analysis. *Osteoarthritis and Cartilage,* 23**,** 1043-1056.

FITZGERALD, M. 2005. The development of nociceptive circuits. *Nat Rev Neurosci,* 6**,** 507-520.

FLEMING, I., BAUERSACHS, J. & BUSSE, R. 1997. Calcium-dependent and calcium-independent activation of the endothelial NO synthase. *J Vasc Res,* 34**,** 165-74.

FONTANILLA, D., JOHANNESSEN, M., HAJIPOUR, A. R., COZZI, N. V., JACKSON, M. B. & RUOHO, A. E. 2009. The Hallucinogen N,N-Dimethyltryptamine (DMT) Is an Endogenous Sigma-1 Receptor Regulator. *Science,* 323**,** 934-7.

FORONI, C., BROGGINI, M., GENERALI, D. & DAMIA, G. 2012. Epithelial–mesenchymal transition and breast cancer: Role, molecular mechanisms and clinical impact. *Cancer Treatment Reviews,* 38**,** 689-697.

FRACARO, L., FREZ, F. C., SILVA, B. C., VICENTINI, G. E., DE SOUZA, S. R., MARTINS, H. A., LINDEN, D. R., GUARNIER, F. A. & ZANONI, J. N. 2016. Walker 256 tumor-bearing rats demonstrate altered interstitial cells of Cajal. Effects on ICC in the Walker 256 tumor model. *Neurogastroenterol Motil,* 28**,** 101-15.

FRATI, A., ROUZIER, R., LESIEUR, B., WERKOFF, G., ANTOINE, M., RODENAS, A., DARAI, E. & CHEREAU, E. 2014. Expression of somatostatin type-2 and -4 receptor and correlation with histological type in breast cancer. *Anticancer Res,* 34**,** 3997-4003.

FREEDMAN, L. P. & GIBSON, M. C. 2015. The Impact of Preclinical Irreproducibility on Drug Development. *Clinical Pharmacology & Therapeutics,* 97**,** 16-18.

FREUND, T. F., KATONA, I. & PIOMELLI, D. Role of Endogenous Cannabinoids in Synaptic Signaling. *Physiological reviews,* 83**,** 1017-1066.

FU, Q., SHI, D., ZHOU, Y., ZHENG, H., XIANG, H., TIAN, X., GAO, F., MANYANDE, A., CAO, F., TIAN, Y. & YE, D. 2016. MHC-I promotes apoptosis of GABAergic interneurons in the spinal dorsal horn and contributes to cancer induced bone pain. *Exp Neurol,* 286**,** 12-20.

GABRIEL, A. F., MARCUS, M. A. E., WALENKAMP, G. H. I. M. & JOOSTEN, E. A. J. 2009. The CatWalk method: Assessment of mechanical allodynia in experimental chronic pain. *Behavioural Brain Research,* 198**,** 477-480.

GAGNON, K. B. & DELPIRE, E. 2013. Physiology of SLC12 transporters: lessons from inherited human genetic mutations and genetically engineered mouse knockouts. *American Journal of Physiology - Cell Physiology,* 304**,** C693-C714.

GALAN, A., LAIRD, J. M. & CERVERO, F. 2004. In vivo recruitment by painful stimuli of AMPA receptor subunits to the plasma membrane of spinal cord neurons. *Pain,* 112**,** 315-23.

GALLARDO, M. E., MORENO-LOSHUERTOS, R., LOPEZ, C., CASQUEIRO, M., SILVA, J., BONILLA, F., RODRIGUEZ DE CORDOBA, S. & ENRIQUEZ, J. A. 2006. m.6267G>A: a recurrent mutation in the human mitochondrial DNA that reduces cytochrome c oxidase activity and is associated with tumors. *Hum Mutat,* 27**,** 575-82.

GALUPPO, L. F., DOS REIS LIVERO, F. A., MARTINS, G. G., CARDOSO, C. C., BELTRAME, O. C., KLASSEN, L. M., CANUTO, A. V., ECHEVARRIA, A., TELLES, J. E., KLASSEN, G. & ACCO, A. 2016. Sydnone 1: A Mesoionic Compound with Antitumoral and Haematological Effects In Vivo. *Basic Clin Pharmacol Toxicol,* 119**,** 41-50.

GAMBETA, E., KOPRUSZINSKI, C. M., DOS REIS, R. C., ZANOVELI, J. M. & CHICHORRO, J. G. 2016. Evaluation of heat hyperalgesia and anxiety like-behaviors in a rat model of orofacial cancer. *Neurosci Lett,* 619**,** 100-5.

GANGADHARAN, V. & KUNER, R. 2013. Pain hypersensitivity mechanisms at a glance. *Dis Model Mech,* 6**,** 889-95.

GANGADHARAN, V., WANG, R., ULZHOFER, B., LUO, C., BARDONI, R., BALI, K. K., AGARWAL, N., TEGEDER, I., HILDEBRANDT, U., NAGY, G. G., TODD, A. J., GHIRRI, A., HAUSSLER, A., SPRENGEL, R., SEEBURG, P. H., MACDERMOTT, A. B., LEWIN, G. R. & KUNER, R. 2011. Peripheral calcium-permeable AMPA receptors regulate chronic inflammatory pain in mice. *J Clin Invest,* 121**,** 1608-23.

GAO, H., ZHU, J., LI, Y., FU, P. & SHEN, B. 2016. Inhibitory effect of endostatin gene therapy combined with phosphorus-32 colloid on tumor growth in Wistar rats. *Biosci Rep*.

GAO, Y., ZHANG, W., HAN, X., LI, F., WANG, X., WANG, R., FANG, Z., TONG, X., YAO, S., LI, F., FENG, Y., SUN, Y., HOU, Y., YANG, Z., GUAN, K., CHEN, H., ZHANG, L. & JI, H. 2014. YAP inhibits squamous transdifferentiation of Lkb1-deficient lung adenocarcinoma through ZEB2-dependent DNp63 repression. *Nat Commun,* 5**,** 4629.

GAO, Y. J. & JI, R. R. 2009. c-Fos and pERK, which is a better marker for neuronal activation and central sensitization after noxious stimulation and tissue injury? *Open Pain J,* 2**,** 11-17.

GAO, Y. J. & JI, R. R. 2010a. Chemokines, neuronal-glial interactions, and central processing of neuropathic pain. *Pharmacol Ther,* 126**,** 56-68.

GAO, Y. J. & JI, R. R. 2010b. Targeting astrocyte signaling for chronic pain. *Neurotherapeutics,* 7**,** 482-93.

GATTENLÖHNER , S., BROCKER , E.-B. & MULLER-HERMELINK , H.-K. 2008. Malignant Melanoma with Metastatic Rhabdomyosarcomatoid Transdifferentiation. *New England Journal of Medicine,* 358**,** 649-650.

GERANTON, S. M., MORENILLA-PALAO, C. & HUNT, S. P. 2007. A role for transcriptional repressor methyl-CpG-binding protein 2 and plasticity-related gene serum- and glucocorticoid-inducible kinase 1 in the induction of inflammatory pain states. *J Neurosci,* 27**,** 6163-73.

GIBBS, R. A., WEINSTOCK, G. M., METZKER, M. L., MUZNY, D. M., SODERGREN, E. J., SCHERER, S., SCOTT, G., STEFFEN, D., WORLEY, K. C., BURCH, P. E., OKWUONU, G., HINES, S., LEWIS, L., DERAMO, C., DELGADO, O., DUGAN-ROCHA, S., MINER, G., MORGAN, M., HAWES, A., GILL, R., CELERA, HOLT, R. A., ADAMS, M. D., AMANATIDES, P. G., BADEN-TILLSON, H., BARNSTEAD, M., CHIN, S., EVANS, C. A., FERRIERA, S., FOSLER, C., GLODEK, A., GU, Z., JENNINGS, D., KRAFT, C. L., NGUYEN, T., PFANNKOCH, C. M., SITTER, C., SUTTON, G. G., VENTER, J. C., WOODAGE, T., SMITH, D., LEE, H. M., GUSTAFSON, E., CAHILL, P., KANA, A., DOUCETTE-STAMM, L., WEINSTOCK, K., FECHTEL, K., WEISS, R. B., DUNN, D. M., GREEN, E. D., BLAKESLEY, R. W., BOUFFARD, G. G., DE JONG, P. J., OSOEGAWA, K., ZHU, B., MARRA, M., SCHEIN, J., BOSDET, I., FJELL, C., JONES, S., KRZYWINSKI, M., MATHEWSON, C., SIDDIQUI, A., WYE, N., MCPHERSON, J., ZHAO, S., FRASER, C. M., SHETTY, J., SHATSMAN, S., GEER, K., CHEN, Y., ABRAMZON, S., NIERMAN, W. C., HAVLAK, P. H., CHEN, R., DURBIN, K. J., EGAN, A., REN, Y., SONG, X. Z., LI, B., LIU, Y., QIN, X., CAWLEY, S., WORLEY, K. C., COONEY, A. J., D'SOUZA, L. M., MARTIN, K., WU, J. Q., GONZALEZ-GARAY, M. L., JACKSON, A. R., KALAFUS, K. J., MCLEOD, M. P., MILOSAVLJEVIC, A., VIRK, D., VOLKOV, A., WHEELER, D. A., ZHANG, Z., BAILEY, J. A., EICHLER, E. E., et al. 2004. Genome sequence of the Brown Norway rat yields insights into mammalian evolution. *Nature,* 428**,** 493-521.

GOLAN, N., KARTVELISHVILY, E., SPIEGEL, I., SALOMON, D., SABANAY, H., RECHAV, K., VAINSHTEIN, A., FRECHTER, S., MAIK-RACHLINE, G., ESHED-EISENBACH, Y., MOMOI, T. & PELES, E. 2013. Genetic deletion of Cadm4 results in myelin abnormalities resembling Charcot-Marie-Tooth neuropathy. *J Neurosci,* 33**,** 10950-61.

GOLD, M. S. & GEBHART, G. F. 2010. Nociceptor sensitization in pain pathogenesis. *Nat Med,* 16**,** 1248-57.

GOLD, M. S., ZHANG, L., WRIGLEY, D. L. & TRAUB, R. J. 2002. Prostaglandin E(2) modulates TTX-R I(Na) in rat colonic sensory neurons. *J Neurophysiol,* 88**,** 1512-22.

GOLDBERG, Y. P., MACFARLANE, J., MACDONALD, M. L., THOMPSON, J., DUBE, M. P., MATTICE, M., FRASER, R., YOUNG, C., HOSSAIN, S., PAPE, T., PAYNE, B., RADOMSKI, C., DONALDSON, G., IVES, E., COX, J., YOUNGHUSBAND, H. B., GREEN, R., DUFF, A., BOLTSHAUSER, E., GRINSPAN, G. A., DIMON, J. H., SIBLEY, B. G., ANDRIA, G., TOSCANO, E., KERDRAON, J., BOWSHER, D., PIMSTONE, S. N., SAMUELS, M. E., SHERRINGTON, R. & HAYDEN, M. R. 2007. Loss-of-function mutations in the Nav1.7 gene underlie congenital indifference to pain in multiple human populations. *Clin Genet,* 71**,** 311-9.

GOLDBERG, Y. P., PRICE, N., NAMDARI, R., COHEN, C. J., LAMERS, M. H., WINTERS, C., PRICE, J., YOUNG, C. E., VERSCHOOF, H., SHERRINGTON, R., PIMSTONE, S. N. &

HAYDEN, M. R. 2012. Treatment of Na(v)1.7-mediated pain in inherited erythromelalgia using a novel sodium channel blocker. *Pain,* 153**,** 80-5.

GOLDEN, J. P., HOSHI, M., NASSAR, M. A., ENOMOTO, H., WOOD, J. N., MILBRANDT, J., GEREAU, R. W. T., JOHNSON, E. M., JR. & JAIN, S. 2010. RET signaling is required for survival and normal function of nonpeptidergic nociceptors. *J Neurosci,* 30**,** 3983-94.

GONG, N., XIAO, Q., ZHU, B., ZHANG, C. Y., WANG, Y. C., FAN, H., MA, A. N. & WANG, Y. X. 2014. Activation of spinal glucagon-like peptide-1 receptors specifically suppresses pain hypersensitivity. *J Neurosci,* 34**,** 5322-34.

GORGES, T. M., TINHOFER, I., DROSCH, M., RÖSE, L., ZOLLNER, T. M., KRAHN, T. & VON AHSEN, O. 2012. Circulating tumour cells escape from EpCAM-based detection due to epithelial-to-mesenchymal transition. *BMC Cancer,* 12**,** 1-13.

GORHAM, L., JUST, S. & DOODS, H. 2014a. Somatostatin 4 receptor activation modulates G-protein coupled inward rectifying potassium channels and voltage stimulated calcium signals in dorsal root ganglion neurons. *European Journal of Pharmacology,* 736**,** 101-106.

GORHAM, L., JUST, S. & DOODS, H. 2014b. Somatostatin 4 receptor activation modulates TRPV1[correction of TPRV1] currents in dorsal root ganglion neurons. *Neurosci Lett,* 573**,** 35-9.

GRACE, C. R., KOERBER, S. C., ERCHEGYI, J., REUBI, J. C., RIVIER, J. & RIEK, R. 2003. Novel sst(4)-selective somatostatin (SRIF) agonists. 4. Three-dimensional consensus structure by NMR. *J Med Chem,* 46**,** 5606-18.

GRAHAM, T. J., BOX, G., TUNARIU, N., CRESPO, M., SPINKS, T. J., MIRANDA, S., ATTARD, G., DE BONO, J., ECCLES, S. A., DAVIES, F. E. & ROBINSON, S. P. 2014. Preclinical Evaluation of Imaging Biomarkers for Prostate Cancer Bone Metastasis and Response to Cabozantinib. *Journal of the National Cancer Institute*.

GRIGGS, R. B., DONAHUE, R. R., ADKINS, B. G., ANDERSON, K. L., THIBAULT, O. & TAYLOR, B. K. 2016. Pioglitazone Inhibits the Development of Hyperalgesia and Sensitization of Spinal Nociresponsive Neurons in Type 2 Diabetes. *The Journal of Pain,* 17**,** 359-373.

GUAN, X. H., FU, Q. C., SHI, D., BU, H. L., SONG, Z. P., XIONG, B. R., SHU, B., XIANG, H. B., XU, B., MANYANDE, A., CAO, F. & TIAN, Y. K. 2015. Activation of spinal chemokine receptor CXCR3 mediates bone cancer pain through an Akt-ERK crosstalk pathway in rats. *Exp Neurol,* 263**,** 39-49.

GUEDON, J. M. G., LONGO, G., MAJUTA, L. A., THOMSPON, M. L., FEALK, M. N. & MANTYH, P. W. 2016. Dissociation between the relief of skeletal pain behaviors and skin hypersensitivity in a model of bone cancer pain. *Pain,* 157**,** 1239-47.

GUERRERO, M., PODDUTOORI, R., PINACHO-CRISOSTOMO, F., SCHAEFFER, M. T., BROWN, S. J., SPICER, T., CHASE, P., FERGUSON, J., ROBERTS, E., SANNA, G., HODDER, P. & ROSEN, H. 2010a. Probe Development Efforts for an Allosteric Agonist of

the Sphingosine 1-phosphate Receptor 3 (S1P3). *Probe Reports from the NIH Molecular Libraries Program.* Bethesda (MD): National Center for Biotechnology Information (US).

GUERRERO, M., URBANO, M., VELAPARTHI, S., ZHAO, J., SCHAEFFER, M. T., BROWN, S. J., CRISP, M., FERGUSON, J., ROBERTS, E., OLDSTONE, M., HODDER, P. & ROSEN, H. 2010b. Probe Development Efforts to Identify Novel Agonists of the Sphingosine 1-phosphate Receptor 4 (S1P4). *Probe Reports from the NIH Molecular Libraries Program.* Bethesda (MD): National Center for Biotechnology Information (US).

GUI, Q., XU, C., LI, D., ZHUANG, L., XIA, S. & YU, S. 2015. Urinary N telopeptide levels in predicting the anti-nociceptive responses of zoledronic acid and paclitaxel in a rat model of bone metastases. *Mol Med Rep,* 12**,** 4243-9.

GUI, Q., XU, C., ZHUANG, L., XIA, S., CHEN, Y., PENG, P. & YU, S. 2013. A new rat model of bone cancer pain produced by rat breast cancer cells implantation of the shaft of femur at the third trochanter level. *Cancer Biol Ther,* 14**,** 193-9.

GUIMARÃES, F., SCHANOSKI, A. S., CAVALCANTI, T. C. S., JULIANO, P. B., VIERA-MATOS, A. N. & RETTORI, O. 2010. Tumor growth characteristics of the Walker 256 AR tumor, a regressive variant of the rat Walker 256 A tumor. *Brazilian Archives of Biology and Technology,* 53**,** 1101-1108.

GUO, C., LIU, S., WANG, J., SUN, M.-Z. & GREENAWAY, F. T. 2013. ACTB in cancer. *Clinica Chimica Acta,* 417**,** 39-44.

GUO, G., PENG, Y., XIONG, B., LIU, D., BU, H., TIAN, X., YANG, H., WU, Z., CAO, F. & GAO, F. 2017. Involvement of chemokine CXCL11 in the development of morphine tolerance in rats with cancer-induced bone pain. *J Neurochem,* 141**,** 553-564.

GUO, Y., YAO, F.-R., CAO, D.-Y., PICKAR, J. G., ZHANG, Q., WANG, H.-S. & ZHAO, Y. 2008. Somatostatin inhibits activation of dorsal cutaneous primary afferents induced by antidromic stimulation of primary afferents from an adjacent thoracic segment in the rat. *Brain Research,* 1229**,** 61-71.

GUREVICH, V. V. & GUREVICH, E. V. 2017. Molecular Mechanisms of GPCR Signaling: A Structural Perspective. *Int J Mol Sci,* 18.

HA, S.-A., KIM, H. K., YOO, J., KIM, S., SHIN, S. M., LEE, Y. S., HUR, S. Y., KIM, Y. W., KIM, T. E., CHUNG, Y. J., JEUN, S. S., KIM, D. W., PARK, Y. G., KIM, J., SHIN, S. Y., LEE, Y. H. & KIM, J. W. 2010. Transdifferentiation-inducing HCCR-1 oncogene. *BMC Cell Biology,* 11**,** 49.

HADDAS, R., LIEBERMAN, I. H. & BLOCK, A. 2017. The Relationship between Fear-Avoidance and Objective Biomechanical Measures of Function in Patients with Adult Degenerative Scoliosis. *Spine (Phila Pa 1976)*.

HAGGERTY, G. C. 1991. Strategy for and Experience with Neurotoxicity Testing of New Pharmaceuticals. *International Journal of Toxicology,* 10**,** 677-688.

HAHN, T., SZABO, L., GOLD, M., RAMANATHAPURAM, L., HURLEY, L. H. & AKPORIAYE, E. T. 2006. Dietary administration of the proapoptotic vitamin E analogue alpha-tocopheryloxyacetic acid inhibits metastatic murine breast cancer. *Cancer Res,* 66**,** 9374-8.

HAINS, B. C., KLEIN, J. P., SAAB, C. Y., CRANER, M. J., BLACK, J. A. & WAXMAN, S. G. 2003. Upregulation of sodium channel Nav1.3 and functional involvement in neuronal hyperexcitability associated with central neuropathic pain after spinal cord injury. *J Neurosci,* 23**,** 8881-92.

HAINS, B. C., SAAB, C. Y., KLEIN, J. P., CRANER, M. J. & WAXMAN, S. G. 2004. Altered sodium channel expression in second-order spinal sensory neurons contributes to pain after peripheral nerve injury. *J Neurosci,* 24**,** 4832-9.

HALD, A., HANSEN, R. R., THOMSEN, M. W., DING, M., CROUCHER, P. I., GALLAGHER, O., EBETINO, F. H., KASSEM, M. & HEEGAARD, A. M. 2009. Cancer-induced bone loss and associated pain-related behavior is reduced by risedronate but not its phosphonocarboxylate analog NE-10790. *Int J Cancer,* 125**,** 1177-85.

HAN, F. Y., WYSE, B. D. & SMITH, M. T. 2014a. Optimization and pharmacological characterization of a refined cisplatin-induced rat model of peripheral neuropathic pain. *Behav Pharmacol,* 25**,** 732-40.

HAN, X., LI, F., FANG, Z., GAO, Y., LI, F., FANG, R., YAO, S., SUN, Y., LI, L., ZHANG, W., MA, H., XIAO, Q., GE, G., FANG, J., WANG, H., ZHANG, L., WONG, K. K., CHEN, H., HOU, Y. & JI, H. 2014b. Transdifferentiation of lung adenocarcinoma in mice with Lkb1 deficiency to squamous cell carcinoma. *Nat Commun,* 5**,** 3261.

HANAGIRI, T., SHIGEMATSU, Y., SHINOHARA, S., TAKENAKA, M., OKA, S., CHIKAISHI, Y., NAGATA, Y., BABA, T., URAMOTO, H., SO, T. & YAMADA, S. 2013. Clinical significance of expression of cancer/testis antigen and down-regulation of HLA class-I in patients with stage I non-small cell lung cancer. *Anticancer Res,* 33**,** 2123-8.

HANAHAN, D. & WEINBERG, ROBERT A. 2011. Hallmarks of Cancer: The Next Generation. *Cell,* 144**,** 646-674.

HANG, L.-H., LI, S.-N., LUO, H., SHU, W.-W., MAO, Z.-M., CHEN, Y.-F., SHI, L.-L. & SHAO, D.-H. 2015a. Connexin 43 Mediates CXCL12 Production from Spinal Dorsal Horn to Maintain Bone Cancer Pain in Rats. *Neurochemical Research***,** 1-9.

HANG, L.-H., SHAO, D.-H., CHEN, Z., CHEN, Y.-F., SHU, W.-W. & ZHAO, Z.-G. 2013a. Involvement of Spinal CC Chemokine Ligand 5 in the Development of Bone Cancer Pain in Rats. *Basic & Clinical Pharmacology & Toxicology,* 113**,** 325-328.

HANG, L. H., LI, S. N., DAN, X., SHU, W. W., LUO, H. & SHAO, D. H. 2017. Involvement of Spinal CCR5/PKCgamma Signaling Pathway in the Maintenance of Cancer-Induced Bone Pain. *Neurochem Res,* 42**,** 563-571.

HANG, L. H., LI, S. N., SHAO, D. H., CHEN, Z., CHEN, Y. F. & SHU, W. W. 2014. Evidence for involvement of spinal RANTES in the antinociceptive effects of triptolide, a diterpene triepoxide, in a rat model of bone cancer pain. *Basic Clin Pharmacol Toxicol,* 115**,** 477-80.

HANG, L. H., LUO, H., LI, S. N., SHU, W. W., CHEN, Z., CHEN, Y. F., YUAN, J. F., SHI, L. L. & SHAO, D. H. 2015b. Involvement of Spinal Bv8/Prokineticin 2 in a Rat Model of Cancer-Induced Bone Pain. *Basic Clin Pharmacol Toxicol*.

HANG, L. H., SHAO, D. H., CHEN, Z. & SUN, W. J. 2013b. Spinal RhoA/Rho kinase signalling pathway may participate in the development of bone cancer pain. *Basic Clin Pharmacol Toxicol,* 113**,** 87-91.

HANG, L. H., YANG, J. P., SHAO, D. H., CHEN, Z. & WANG, H. 2013c. Involvement of spinal PKA/CREB signaling pathway in the development of bone cancer pain. *Pharmacol Rep,* 65**,** 710-6.

HANG, L. H., YANG, J. P., YIN, W., WANG, L. N., GUO, F., JI, F. H., SHAO, D. H., XU, Q. N., WANG, X. Y. & ZUO, J. L. 2012. Activation of spinal TDAG8 and its downstream PKA signaling pathway contribute to bone cancer pain in rats. *Eur J Neurosci,* 36**,** 2107-17.

HARGREAVES, K., DUBNER, R., BROWN, F., FLORES, C. & JORIS, J. 1988. A new and sensitive method for measuring thermal nociception in cutaneous hyperalgesia. *Pain,* 32**,** 77-88.

HARTKOPF, A. D., BANYS, M., MEIER-STIEGEN, F., HAHN, M., RÖHM, C., HOFFMANN, J., HELMS, G., TARAN, F. A., WALLWIENER, M., WALTER, C., NEUBAUER, H., WALLWIENER, D. & FEHM, T. 2013. The HER2 status of disseminated tumor cells in the bone marrow of early breast cancer patients is independent from primary tumor and predicts higher risk of relapse. *Breast Cancer Research and Treatment,* 138**,** 509-517.

HARTMANN, B., AHMADI, S., HEPPENSTALL, P. A., LEWIN, G. R., SCHOTT, C., BORCHARDT, T., SEEBURG, P. H., ZEILHOFER, H. U., SPRENGEL, R. & KUNER, R. 2004. The AMPA receptor subunits GluR-A and GluR-B reciprocally modulate spinal synaptic plasticity and inflammatory pain. *Neuron,* 44**,** 637-50.

HARVEY, R. J., DEPNER, U. B., WASSLE, H., AHMADI, S., HEINDL, C., REINOLD, H., SMART, T. G., HARVEY, K., SCHUTZ, B., ABO-SALEM, O. M., ZIMMER, A., POISBEAU, P., WELZL, H., WOLFER, D. P., BETZ, H., ZEILHOFER, H. U. & MULLER, U. 2004. GlyR alpha3: an essential target for spinal PGE2-mediated inflammatory pain sensitization. *Science,* 304**,** 884-7.

HAYAKAWA, Y., SETHI, N., SEPULVEDA, A. R., BASS, A. J. & WANG, T. C. 2016. Oesophageal adenocarcinoma and gastric cancer: should we mind the gap? *Nat Rev Cancer,* 16**,** 305-318.

HECK, R. K., PEABODY, T. D. & SIMON, M. A. 2006. Staging of Primary Malignancies of Bone. *CA: A Cancer Journal for Clinicians,* 56**,** 366-375.

HELYES, Z., PINTÉR, E., NÉMETH, J., SÁNDOR, K., ELEKES, K., SZABÓ, Á., POZSGAI, G., KESZTHELYI, D., KERESKAI, L., ENGSTRÖM, M., WURSTER, S. & SZOLCSÁNYI, J. 2006. Effects of the somatostatin receptor subtype 4 selective agonist J-2156 on sensory neuropeptide release and inflammatory reactions in rodents. *British Journal of Pharmacology,* 149**,** 405-415.

HELYES, Z., PINTER, E., SANDOR, K., ELEKES, K., BANVOLGYI, A., KESZTHELYI, D., SZOKE, E., TOTH, D. M., SANDOR, Z., KERESKAI, L., POZSGAI, G., ALLEN, J. P., EMSON, P. C., MARKOVICS, A. & SZOLCSANYI, J. 2009. Impaired defense mechanism against inflammation, hyperalgesia, and airway hyperreactivity in somatostatin 4 receptor gene-deleted mice. *Proc Natl Acad Sci U S A,* 106**,** 13088-93.

HENDERSON, G. 2015. The mu-opioid receptor: an electrophysiologist's perspective from the sharp end. *Br J Pharmacol,* 172**,** 260-7.

HENDERSON, J. V., HARRISON, C. M., BRITT, H. C., BAYRAM, C. F. & MILLER, G. C. 2013. Prevalence, Causes, Severity, Impact, and Management of Chronic Pain in Australian General Practice Patients. *Pain Medicine,* 14**,** 1346-1361.

HENDRIX, M. J., SEFTOR, E. A., SEFTOR, R. E. & TREVOR, K. T. 1997. Experimental co-expression of vimentin and keratin intermediate filaments in human breast cancer cells results in phenotypic interconversion and increased invasive behavior. *Am J Pathol,* 150**,** 483-95.

HERZOG, R. I., CUMMINS, T. R., GHASSEMI, F., DIB-HAJJ, S. D. & WAXMAN, S. G. 2003. Distinct repriming and closed-state inactivation kinetics of Nav1.6 and Nav1.7 sodium channels in mouse spinal sensory neurons. *J Physiol,* 551**,** 741-50.

HILEY, C., DE BRUIN, E. C., MCGRANAHAN, N. & SWANTON, C. 2014. Deciphering intratumor heterogeneity and temporal acquisition of driver events to refine precision medicine. *Genome Biol,* 15**,** 453.

HIRAI, T., MULPURI, Y., CHENG, Y., XIA, Z., LI, W., RUANGSRI, S., SPIGELMAN, I. & NISHIMURA, I. 2017. Aberrant plasticity of peripheral sensory axons in a painful neuropathy. *Scientific Reports,* 7**,** 3407.

HOFFMAN, S. A., PASCHKIS, K. E., DEBIAS, D. A., CANTAROW, A. & WILLIAMS, T. L. 1962. The influence of exercise on the growth of transplanted rat tumors. *Cancer Res,* 22**,** 597-9.

HOGAN-CANN, A. D. & ANDERSON, C. M. 2016. Physiological Roles of Non-Neuronal NMDA Receptors. *Trends Pharmacol Sci*.

HOMAYOUNFAR, H., JAMALI-RAEUFY, N., SAHEBGHARANI, M. & ZARRINDAST, M.-R. 2005. Adenosine receptor mediates nicotine-induced antinociception in formalin test. *Pharmacological Research,* 51**,** 197-203.

HONORE, E. 2007. The neuronal background K2P channels: focus on TREK1. *Nat Rev Neurosci,* 8**,** 251-61.

HONORE, P., ROGERS, S. D., SCHWEI, M. J., SALAK-JOHNSON, J. L., LUGER, N. M., SABINO, M. C., CLOHISY, D. R. & MANTYH, P. W. 2000. Murine models of inflammatory, neuropathic and cancer pain each generates a unique set of neurochemical changes in the spinal cord and sensory neurons. *Neuroscience,* 98**,** 585-98.

HOU, X., WENG, Y., OUYANG, B., DING, Z., SONG, Z., ZOU, W., HUANG, C. & GUO, Q. 2017. HDAC inhibitor TSA ameliorates mechanical hypersensitivity and potentiates analgesic effect of morphine in a rat model of bone cancer pain by restoring mu-opioid receptor in spinal cord. *Brain Res*.

HOUSSAMI, N., MACASKILL, P., BALLEINE, R. L., BILOUS, M. & PEGRAM, M. D. 2011. HER2 discordance between primary breast cancer and its paired metastasis: tumor biology or test artefact? Insights through meta-analysis. *Breast Cancer Research and Treatment,* 129**,** 659-674.

HU, H. J., CARRASQUILLO, Y., KARIM, F., JUNG, W. E., NERBONNE, J. M., SCHWARZ, T. L. & GEREAU, R. W. T. 2006. The kv4.2 potassium channel subunit is required for pain plasticity. *Neuron,* 50**,** 89-100.

HU, J. H., WU, M. Y., TAO, M. & YANG, J. P. 2013. Changes in protein expression and distribution of spinal CCR2 in a rat model of bone cancer pain. *Brain Res,* 1509**,** 1-7.

HU, J. H., YANG, J. P., LIU, L., LI, C. F., WANG, L. N., JI, F. H. & CHENG, H. 2012a. Involvement of CX3CR1 in bone cancer pain through the activation of microglia p38 MAPK pathway in the spinal cord. *Brain Res,* 1465**,** 1-9.

HU, J. H., ZHENG, X. Y., YANG, J. P., WANG, L. N. & JI, F. H. 2012b. Involvement of spinal monocyte chemoattractant protein-1 (MCP-1) in cancer-induced bone pain in rats. *Neurosci Lett,* 517**,** 60-3.

HU, S., CHEN, Y., WANG, Z. F., MAO-YING, Q. L., MI, W. L., JIANG, J. W., WU, G. C. & WANG, Y. Q. 2015a. The Analgesic and Antineuroinflammatory Effect of Baicalein in Cancer-Induced Bone Pain. *Evid Based Complement Alternat Med,* 2015**,** 973524.

HU, S., MAO-YING, Q. L., WANG, J., WANG, Z. F., MI, W. L., WANG, X. W., JIANG, J. W., HUANG, Y. L., WU, G. C. & WANG, Y. Q. 2012c. Lipoxins and aspirin-triggered lipoxin alleviate bone cancer pain in association with suppressing expression of spinal proinflammatory cytokines. *J Neuroinflammation,* 9**,** 278.

HU, X. F., HE, X. T., ZHOU, K. X., ZHANG, C., ZHAO, W. J., ZHANG, T., LI, J. L., DENG, J. P. & DONG, Y. L. 2017. The analgesic effects of triptolide in the bone cancer pain rats via inhibiting the upregulation of HDACs in spinal glial cells. *J Neuroinflammation,* 14**,** 213.

HU, X. M., LIU, Y. N., ZHANG, H. L., CAO, S. B., ZHANG, T., CHEN, L. P. & SHEN, W. 2015b. CXCL12/CXCR4 chemokine signaling in spinal glia induces pain hypersensitivity through MAPKs-mediated neuroinflammation in bone cancer rats. *J Neurochem,* 132**,** 452-63.

HUANG, J. L., CHEN, X. L., GUO, C. & WANG, Y. X. 2012. Contributions of spinal D-amino acid oxidase to bone cancer pain. *Amino Acids,* 43**,** 1905-18.

HUANG, Q., MAO, X. F., WU, H. Y., LI, T. F., SUN, M. L., LIU, H. & WANG, Y. X. 2016. Bullatine A stimulates spinal microglial dynorphin A expression to produce anti-hypersensitivity in a variety of rat pain models. *J Neuroinflammation,* 13**,** 214.

HUANG, Z., WU, T., LIU, A. Y. & OUYANG, G. 2015. Differentiation and transdifferentiation potentials of cancer stem cells. *Oncotarget,* 6**,** 39550-63.

HUANG, Z. X., LU, Z. J., MA, W. Q., WU, F. X., ZHANG, Y. Q., YU, W. F. & ZHAO, Z. Q. 2014. Involvement of RVM-expressed P2X7 receptor in bone cancer pain: mechanism of descending facilitation. *Pain,* 155**,** 783-91.

HUBINA, E., NANZER, A. M., HANSON, M. R., CICCARELLI, E., LOSA, M., GAIA, D., PAPOTTI, M., TERRENI, M. R., KHALAF, S., JORDAN, S., CZIRJAK, S., HANZELY, Z., NAGY, G. M., GOTH, M. I., GROSSMAN, A. B. & KORBONITS, M. 2006. Somatostatin analogues stimulate p27 expression and inhibit the MAP kinase pathway in pituitary tumours. *Eur J Endocrinol,* 155**,** 371-9.

HUCHO, T. & LEVINE, J. D. 2007. Signaling pathways in sensitization: toward a nociceptor cell biology. *Neuron,* 55**,** 365-76.

HUNTER, J. C., GOGAS, K. R., HEDLEY, L. R., JACOBSON, L. O., KASSOTAKIS, L., THOMPSON, J. & FONTANA, D. J. 1997. The effect of novel anti-epileptic drugs in rat experimental models of acute and chronic pain. *European Journal of Pharmacology,* 324**,** 153-160.

HUTTER, R. V. P. 1982. Assessment: Is cured early cancer truly cancer? *CA: A Cancer Journal for Clinicians,* 32**,** 2-9.

IBRAHIM, T., FLAMINI, E., MERCATALI, L., SACANNA, E., SERRA, P. & AMADORI, D. 2010. Pathogenesis of osteoblastic bone metastases from prostate cancer. *Cancer,* 116**,** 1406-18.

IBRAHIM, T., MERCATALI, L. & AMADORI, D. 2013. A new emergency in oncology: Bone metastases in breast cancer patients (Review). *Oncology Letters,* 6**,** 306-310.

IBSEN, M. S., CONNOR, M. & GLASS, M. 2017. Cannabinoid CB(1) and CB(2) Receptor Signaling and Bias. *Cannabis and Cannabinoid Research,* 2**,** 48-60.

IKEDA, H., STARK, J., FISCHER, H., WAGNER, M., DRDLA, R., JAGER, T. & SANDKUHLER, J. 2006. Synaptic amplifier of inflammatory pain in the spinal dorsal horn. *Science,* 312**,** 1659-62.

IKEDA, K., KOBAYASHI, T., KUMANISHI, T., NIKI, H. & YANO, R. 2000. Involvement of G-protein-activated inwardly rectifying K (GIRK) channels in opioid-induced analgesia. *Neurosci Res,* 38**,** 113-6.

IKEDA, R., TAKAHASHI, Y., INOUE, K. & KATO, F. 2007. NMDA receptor-independent synaptic plasticity in the central amygdala in the rat model of neuropathic pain. *Pain,* 127**,** 161-172.

INQUIMBERT, P., BARTELS, K., BABANIYI, O. B., BARRETT, L. B., TEGEDER, I. & SCHOLZ, J. 2012. Peripheral nerve injury produces a sustained shift in the balance between glutamate release and uptake in the dorsal horn of the spinal cord. *Pain,* 153**,** 2422-31.

JAGANJAC, M., POLJAK-BLAZI, M., ZARKOVIC, K., SCHAUR, R. J. & ZARKOVIC, N. 2008. The involvement of granulocytes in spontaneous regression of Walker 256 carcinoma. *Cancer Lett,* 260**,** 180-6.

JÄGER, B. A. S., FINKENZELLER, C., BOCK, C., MAJUNKE, L., JUECKSTOCK, J. K., ANDERGASSEN, U., NEUGEBAUER, J. K., PESTKA, A., FRIEDL, T. W. P., JESCHKE, U., JANNI, W., DOISNEAU-SIXOU, S. F. & RACK, B. K. 2015. Estrogen Receptor and HER2 Status on Disseminated Tumor Cells and Primary Tumor in Patients with Early Breast Cancer. *Translational Oncology,* 8**,** 509-516.

JAMIESON, D. G., MOSS, A., KENNEDY, M., JONES, S., NENADIC, G., ROBERTSON, D. L. & SIDDERS, B. 2014. The pain interactome: Connecting pain-specific protein interactions. *Pain,* 155**,** 2243-52.

JANKOWSKI, M. P. & KOERBER, H. R. 2010. Frontiers in Neuroscience

Neurotrophic Factors and Nociceptor Sensitization. *In:* KRUGER, L. & LIGHT, A. R. (eds.) *Translational Pain Research: From Mouse to Man.* Boca Raton, FL: CRC Press/Taylor & Francis

Llc.

JENSEN, G. & MUNTZING, J. 1970. Differences in the growth of the Walker carcinoma in Sprague-Dawley and Wistar rats. *Z Krebsforsch,* 74**,** 55-8.

JI, D., LIANG, Z., LIU, G., ZHAO, G. & FANG, J. 2017. Bufalin attenuates cancer-induced pain and bone destruction in a model of bone cancer. *Naunyn Schmiedebergs Arch Pharmacol*.

JI, R. R., BABA, H., BRENNER, G. J. & WOOLF, C. J. 1999. Nociceptive-specific activation of ERK in spinal neurons contributes to pain hypersensitivity. *Nat Neurosci,* 2**,** 1114-9.

JI, R. R., GEREAU, R. W. T., MALCANGIO, M. & STRICHARTZ, G. R. 2009a. MAP kinase and pain. *Brain Res Rev,* 60**,** 135-48.

JI, R. R., KOHNO, T., MOORE, K. A. & WOOLF, C. J. 2003. Central sensitization and LTP: do pain and memory share similar mechanisms? *Trends Neurosci,* 26**,** 696-705.

JI, R. R., XU, Z. Z., WANG, X. & LO, E. H. 2009b. MMP regulation of neuropathic pain. *Trends Pharmacol Sci,* 30**,** 336-40.

JIANG, J., ZHANG, J., YAO, P., WU, X. & LI, K. 2014. Activation of spinal neuregulin 1-ErbB2 signaling pathway in a rat model of cancer-induced bone pain. *Int J Oncol,* 45**,** 235-44.

JIANG, Z., WU, S., WU, X., ZHONG, J., LV, A., JIAO, J. & CHEN, Z. 2015. Blocking mammalian target of rapamycin alleviates bone cancer pain and morphine tolerance via μ-opioid receptor. *International Journal of Cancer***,** n/a-n/a.

JIANG, Z., WU, S., WU, X., ZHONG, J., LV, A., JIAO, J. & CHEN, Z. 2016. Blocking mammalian target of rapamycin alleviates bone cancer pain and morphine tolerance via micro-opioid receptor. *Int J Cancer,* 138**,** 2013-20.

JIN, D., YANG, J. P., HU, J. H., WANG, L. N. & ZUO, J. L. 2015. MCP-1 stimulates spinal microglia via PI3K/Akt pathway in bone cancer pain. *Brain Res,* 1599**,** 158-67.

JIN, L., NONAKA, Y., MIYAKAWA, S., FUJIWARA, M. & NAKAMURA, Y. 2016. Dual Therapeutic Action of a Neutralizing Anti-FGF2 Aptamer in Bone Disease and Bone Cancer Pain. *Mol Ther*.

JIN, X. H., WANG, L. N., ZUO, J. L., YANG, J. P. & LIU, S. L. 2014. P2X4 receptor in the dorsal horn partially contributes to brain-derived neurotrophic factor oversecretion and toll-like receptor-4 receptor activation associated with bone cancer pain. *J Neurosci Res,* 92**,** 1690-702.

JOBLING, P., PUNDAVELA, J., OLIVEIRA, S. M. R., ROSELLI, S., WALKER, M. M. & HONDERMARCK, H. 2015. Nerve–Cancer Cell Cross-talk: A Novel Promoter of Tumor Progression. *Cancer Research*.

JORDAN, N. V., BARDIA, A., WITTNER, B. S., BENES, C., LIGORIO, M., ZHENG, Y., YU, M., SUNDARESAN, T. K., LICAUSI, J. A., DESAI, R., O'KEEFE, R. M., EBRIGHT, R. Y., BOUKHALI, M., SIL, S., ONOZATO, M. L., IAFRATE, A. J., KAPUR, R., SGROI, D., TING, D. T., TONER, M., RAMASWAMY, S., HAAS, W., MAHESWARAN, S. & HABER, D. A. 2016. HER2 expression identifies dynamic functional states within circulating breast cancer cells. *Nature,* 537**,** 102-106.

JULIAN, J., DHARMARAJ, N. & CARSON, D. D. 2009. MUC1 is a substrate for gamma-secretase. *J Cell Biochem,* 108**,** 802-15.

JULIUS, D. & BASBAUM, A. I. 2001. Molecular mechanisms of nociception. *Nature,* 413**,** 203-10.

JUNG, S., LI, C., JEONG, D., LEE, S., OHK, J., PARK, M., HAN, S., DUAN, J., KIM, C., YANG, Y., KIM, K. I., LIM, J. S., KANG, Y. S. & LEE, M. S. 2013. Oncogenic function of p34SEI-1 via NEDD41mediated PTEN ubiquitination/degradation and activation of the PI3K/AKT pathway. *Int J Oncol,* 43**,** 1587-95.

JUNG, Y., OH, S. H., ZHENG, D., SHUPE, T. D., WITEK, R. P. & PETERSEN, B. E. 2006. A potential role of somatostatin and its receptor SSTR4 in the migration of hepatic oval cells. *Lab Invest,* 86**,** 477-89.

JUSTICE, A. 1985. Review of the effects of stress on cancer in laboratory animals: importance of time of stress application and type of tumor. *Psychol Bull,* 98**,** 108-38.

KAAN, T. K., YIP, P. K., PATEL, S., DAVIES, M., MARCHAND, F., COCKAYNE, D. A., NUNN, P. A., DICKENSON, A. H., FORD, A. P., ZHONG, Y., MALCANGIO, M. & MCMAHON, S. B. 2010. Systemic blockade of P2X3 and P2X2/3 receptors attenuates bone cancer pain behaviour in rats. *Brain,* 133**,** 2549-64.

KALLUNKI, T., OLSEN, O. D. & JAATTELA, M. 2013. Cancer-associated lysosomal changes: friends or foes[quest]. *Oncogene,* 32**,** 1995-2004.

KAMBIZ, S., BAAS, M., DURAKU, L. S., KERVER, A. L., KONING, A. H., WALBEEHM, E. T. & RUIGROK, T. J. 2014. Innervation mapping of the hind paw of the rat using Evans Blue extravasation, Optical Surface Mapping and CASAM. *J Neurosci Methods,* 229**,** 15-27.

KANE, C. M., HOSKIN, P. & BENNETT, M. I. 2015. *Cancer induced bone pain*.

KANZAKI, H., MIZOBUCHI, S., OBATA, N., ITANO, Y., KAKU, R., TOMOTSUKA, N., NAKAJIMA, H., OUCHIDA, M., NAKATSUKA, H., MAESHIMA, K. & MORITA, K. 2012. Expression changes of the neuregulin 1 isoforms in neuropathic pain model rats. *Neuroscience Letters,* 508**,** 78-83.

KAO, J., SALARI, K., BOCANEGRA, M., CHOI, Y. L., GIRARD, L., GANDHI, J., KWEI, K. A., HERNANDEZ-BOUSSARD, T., WANG, P., GAZDAR, A. F., MINNA, J. D. & POLLACK, J. R. 2009. Molecular Profiling of Breast Cancer Cell Lines Defines Relevant Tumor Models and Provides a Resource for Cancer Gene Discovery. *PLoS One,* 4.

KAPTCHUK, T. J. & MILLER, F. G. 2015. Placebo Effects in Medicine. *New England Journal of Medicine,* 373**,** 8-9.

KASIMIR-BAUER, S., HOFFMANN, O., WALLWIENER, D., KIMMIG, R. & FEHM, T. 2012. Expression of stem cell and epithelial-mesenchymal transition markers in primary breast cancer patients with circulating tumor cells. *Breast Cancer Research,* 14**,** 1-9.

KASIMIR-BAUER, S., REITER, K., AKTAS, B., BITTNER, A. K., WEBER, S., KELLER, T., KIMMIG, R. & HOFFMANN, O. 2016. Different prognostic value of circulating and disseminated tumor cells in primary breast cancer: Influence of bisphosphonate intake? *Sci Rep,* 6**,** 26355.

KATZ, J., ROSENBLOOM, B. N. & FASHLER, S. 2015. Chronic Pain, Psychopathology, and DSM-5 Somatic Symptom Disorder. *Can J Psychiatry,* 60**,** 160-7.

KAWASAKI, Y., KOHNO, T. & JI, R. R. 2006. Different effects of opioid and cannabinoid receptor agonists on C-fiber-induced extracellular signal-regulated kinase activation in dorsal horn neurons in normal and spinal nerve-ligated rats. *J Pharmacol Exp Ther,* 316**,** 601-7.

KAWASAKI, Y., KOHNO, T., ZHUANG, Z. Y., BRENNER, G. J., WANG, H., VAN DER MEER, C., BEFORT, K., WOOLF, C. J. & JI, R. R. 2004. Ionotropic and metabotropic receptors, protein kinase A, protein kinase C, and Src contribute to C-fiber-induced ERK activation and cAMP response element-binding protein phosphorylation in dorsal horn neurons, leading to central sensitization. *J Neurosci,* 24**,** 8310-21.

KAWASAKI, Y., XU, Z. Z., WANG, X., PARK, J. Y., ZHUANG, Z. Y., TAN, P. H., GAO, Y. J., ROY, K., CORFAS, G., LO, E. H. & JI, R. R. 2008. Distinct roles of matrix metalloproteases in the early- and late-phase development of neuropathic pain. *Nat Med,* 14**,** 331-6.

KE, C., LI, C., HUANG, X., CAO, F., SHI, D., HE, W., BU, H., GAO, F., CAI, T., HINTON, A. O., JR. & TIAN, Y. 2013. Protocadherin20 promotes excitatory synaptogenesis in dorsal horn and contributes to bone cancer pain. *Neuropharmacology,* 75**,** 181-90.

KE, C. B., HE, W. S., LI, C. J., SHI, D., GAO, F. & TIAN, Y. K. 2012. Enhanced SCN7A/Nax expression contributes to bone cancer pain by increasing excitability of neurons in dorsal root ganglion. *Neuroscience,* 227**,** 80-9.

KEEFE, F. J., LEFEBVRE, J. C., EGERT, J. R., AFFLECK, G., SULLIVAN, M. J. & CALDWELL, D. S. 2000. The relationship of gender to pain, pain behavior, and disability in osteoarthritis patients: the role of catastrophizing. *Pain,* 87**,** 325-334.

KERR, B. J., SOUSLOVA, V., MCMAHON, S. B. & WOOD, J. N. 2001. A role for the TTX-resistant sodium channel Nav 1.8 in NGF-induced hyperalgesia, but not neuropathic pain. *Neuroreport,* 12**,** 3077-80.

KHAN, N., GORDON, R., WOODRUFF, T. M. & SMITH, M. T. 2015. Antiallodynic effects of alpha lipoic acid in an optimized RR-EAE mouse model of MS-neuropathic pain are accompanied by attenuation of upregulated BDNF-TrkB-ERK signaling in the dorsal horn of the spinal cord. *Pharmacology Research & Perspectives,* 3**,** n/a-n/a.

KHAN, N., WOODRUFF, T. M. & SMITH, M. T. 2014. Establishment and characterization of an optimized mouse model of multiple sclerosis-induced neuropathic pain using behavioral, pharmacologic, histologic and immunohistochemical methods. *Pharmacology Biochemistry and Behavior,* 126**,** 13-27.

KHEGAI, II 2013. [Concordance between vasopressin gene expression and growth of Walker 256 carcinosarcoma in rats]. *Genetika,* 49**,** 538-40.

KHEGAY, II & IVANOVA, L. N. 2015. Regression of Walker 256 carcinosarcoma in vasopressin-deficient Brattleboro rats is accompanied by a changed laminin pattern. *Biochem Genet,* 53**,** 1-7.

KHONG, H. T. & RESTIFO, N. P. 2002. Natural selection of tumor variants in the generation of "tumor escape" phenotypes. *Nat Immunol,* 3**,** 999-1005.

KIM, C. H., OH, Y., CHUNG, J. M. & CHUNG, K. 2001. The changes in expression of three subtypes of TTX sensitive sodium channels in sensory neurons after spinal nerve ligation. *Brain Res Mol Brain Res,* 95**,** 153-61.

KIMBUNG, S., LOMAN, N. & HEDENFALK, I. 2015. Clinical and molecular complexity of breast cancer metastases. *Seminars in Cancer Biology,* 35**,** 85-95.

KINSEY, S. G., LONG, J. Z., O'NEAL, S. T., ABDULLAH, R. A., POKLIS, J. L., BOGER, D. L., CRAVATT, B. F. & LICHTMAN, A. H. 2009. Blockade of endocannabinoid-degrading enzymes attenuates neuropathic pain. *J Pharmacol Exp Ther,* 330**,** 902-10.

KISCHEL, P., WALTREGNY, D., DUMONT, B., TURTOI, A., GREFFE, Y., KIRSCH, S., DE PAUW, E. & CASTRONOVO, V. 2010. Versican overexpression in human breast cancer lesions: known and new isoforms for stromal tumor targeting. *Int J Cancer,* 126**,** 640-50.

KLUGBAUER, N., LACINOVA, L., FLOCKERZI, V. & HOFMANN, F. 1995. Structure and functional expression of a new member of the tetrodotoxin-sensitive voltage-activated sodium channel family from human neuroendocrine cells. *Embo j,* 14**,** 1084-90.

KMIECIAK, M., KNUTSON, K. L., DUMUR, C. I. & MANJILI, M. H. 2007. HER-2/neu antigen loss and relapse of mammary carcinoma are actively induced by T cell-mediated anti-tumor immune responses. *Eur J Immunol,* 37**,** 675-85.

KMIECIAK, M., MORALES, J. K., MORALES, J., BOLESTA, E., GRIMES, M. & MANJILI, M. H. 2008. Danger signals and nonself entity of tumor antigen are both required for eliciting effective immune responses against HER-2/neu positive mammary carcinoma: implications for vaccine design. *Cancer Immunol Immunother,* 57**,** 1391-8.

KNUTSON, K. L., ALMAND, B., DANG, Y. & DISIS, M. L. 2004. Neu antigen-negative variants can be generated after neu-specific antibody therapy in neu transgenic mice. *Cancer Res,* 64**,** 1146-51.

KNUTSON, K. L., LU, H., STONE, B., REIMAN, J. M., BEHRENS, M. D., PROSPERI, C. M., GAD, E. A., SMORLESI, A. & DISIS, M. L. 2006. Immunoediting of cancers may lead to epithelial to mesenchymal transition. *J Immunol,* 177**,** 1526-33.

KOHNO, T., WANG, H., AMAYA, F., BRENNER, G. J., CHENG, J. K., JI, R. R. & WOOLF, C. J. 2008. Bradykinin enhances AMPA and NMDA receptor activity in spinal cord dorsal horn neurons by activating multiple kinases to produce pain hypersensitivity. *J Neurosci,* 28**,** 4533-40.

KOLTZENBURG, M., WALL, P. D. & MCMAHON, S. B. 1999. Does the right side know what the left is doing? *Trends Neurosci,* 22**,** 122-7.

KONG, B., MICHALSKI, C. W., HONG, X., VALKOVSKAYA, N., RIEDER, S., ABIATARI, I., STREIT, S., ERKAN, M., ESPOSITO, I., FRIESS, H. & KLEEFF, J. 2010. AZGP1 is a tumor suppressor in pancreatic cancer inducing mesenchymal-to-epithelial transdifferentiation by inhibiting TGF-beta-mediated ERK signaling. *Oncogene,* 29**,** 5146-58.

KONTANI, K., TAGUCHI, O., NARITA, T., IZAWA, M., HIRAIWA, N., ZENITA, K., TAKEUCHI, T., MURAI, H., MIURA, S. & KANNAGI, R. 2001. Modulation of MUC1 mucin as an escape mechanism of breast cancer cells from autologous cytotoxic T-lymphocytes. *Br J Cancer,* 84**,** 1258-64.

KORZH, A., KEREN, O., GAFNI, M., BAR-JOSEF, H. & SARNE, Y. 2008. Modulation of extracellular signal-regulated kinase (ERK) by opioid and cannabinoid receptors that are expressed in the same cell. *Brain Research,* 1189**,** 23-32.

KOSTI, I., JAIN, N., ARAN, D., BUTTE, A. J. & SIROTA, M. 2016. Cross-tissue Analysis of Gene and Protein Expression in Normal and Cancer Tissues. *Sci Rep,* 6**,** 24799.

KRAWCZYK, N., BANYS, M., NEUBAUER, H., SOLOMAYER, E. F., GALL, C., HAHN, M., BECKER, S., BACHMANN, R., WALLWIENER, D. & FEHM, T. 2009. HER2 status on

persistent disseminated tumor cells after adjuvant therapy may differ from initial HER2 status on primary tumor. *Anticancer Res,* 29**,** 4019-24.

KRESS, G. J. & MENNERICK, S. 2009. Action potential initiation and propagation: upstream influences on neurotransmission. *Neuroscience,* 158**,** 211-22.

KRISHNAMURTHY, S., BISCHOFF, F., ANN MAYER, J., WONG, K., PHAM, T., KUERER, H., LODHI, A., BHATTACHARYYA, A., HALL, C. & LUCCI, A. 2013. Discordance in HER2 gene amplification in circulating and disseminated tumor cells in patients with operable breast cancer. *Cancer Med,* 2**,** 226-33.

KUDO-SAITO, C. 2013. FSTL1 promotes bone metastasis by causing immune dysfunction. *Oncoimmunology,* 2.

KUDO-SAITO, C., FUWA, T., MURAKAMI, K. & KAWAKAMI, Y. 2013. Targeting FSTL1 Prevents Tumor Bone Metastasis and Consequent Immune Dysfunction. *Cancer Research,* 73**,** 6185-6193.

KUMAR, U. 2009. Role of Somatostatin and Somatostatin Receptors in Pain. *Peripheral Receptor Targets for Analgesia.* John Wiley & Sons, Inc.

KUMAR, U., GRIGORAKIS, S. I., WATT, H. L., SASI, R., SNELL, L., WATSON, P. & CHAUDHARI, S. 2005. Somatostatin receptors in primary human breast cancer: quantitative analysis of mRNA for subtypes 1--5 and correlation with receptor protein expression and tumor pathology. *Breast Cancer Res Treat,* 92**,** 175-86.

KUNER, R. 2010. Central mechanisms of pathological pain. *Nat Med,* 16**,** 1258-66.

KUO, A., WYSE, B. D., MEUTERMANS, W. & SMITH, M. T. 2015. In vivo profiling of seven common opioids for antinociception, constipation and respiratory depression: no two opioids have the same profile. *Br J Pharmacol,* 172**,** 532-48.

KUROZUMI, S., PADILLA, M., KUROSUMI, M., MATSUMOTO, H., INOUE, K., HORIGUCHI, J., TAKEYOSHI, I., OYAMA, T., RANGER-MOORE, J., ALLRED, D. C., DENNIS, E. & NITTA, H. 2016. HER2 intratumoral heterogeneity analyses by concurrent HER2 gene and protein assessment for the prognosis of HER2 negative invasive breast cancer patients. *Breast Cancer Res Treat,* 158**,** 99-111.

KURTH, A. A., KIM, S. Z., SEDLMEYER, I., BAUSS, F. & SHEA, M. 2002. Ibandronate treatment decreases the effects of tumor-associated lesions on bone density and strength in the rat. *Bone,* 30**,** 300-6.

KURTH, A. H., KIM, S. Z., SEDLMEYER, I., HOVY, L. & BAUSS, F. 2000. Treatment with ibandronate preserves bone in experimental tumour-induced bone loss. *J Bone Joint Surg Br,* 82**,** 126-30.

KURTH, A. H., WANG, C., HAYES, W. C. & SHEA, M. 2001. The evaluation of a rat model for the analysis of densitometric and biomechanical properties of tumor-induced osteolysis. *J Orthop Res,* 19**,** 200-5.

KWAN, K. Y., ALLCHORNE, A. J., VOLLRATH, M. A., CHRISTENSEN, A. P., ZHANG, D. S., WOOLF, C. J. & COREY, D. P. 2006. TRPA1 contributes to cold, mechanical, and chemical nociception but is not essential for hair-cell transduction. *Neuron,* 50**,** 277-89.

KWAN, K. Y. & COREY, D. P. 2009. Burning cold: involvement of TRPA1 in noxious cold sensation. *J Gen Physiol,* 133**,** 251-6.

KWONG, E., NESHEIM, M. C. & DILLS, W. L., JR. 1984. The influence of diet on the regression of the Walker carcinosarcoma 256 in rats. *J Nutr,* 114**,** 2324-30.

LACROIX-FRALISH, M. L., TAWFIK, V. L., SPRATT, K. F. & DELEO, J. A. 2006. Sex differences in lumbar spinal cord gene expression following experimental lumbar radiculopathy. *Journal of Molecular Neuroscience,* 30**,** 283-295.

LAIRD, B. J., WALLEY, J., MURRAY, G. D., CLAUSEN, E., COLVIN, L. A. & FALLON, M. T. 2011. Characterization of cancer-induced bone pain: an exploratory study. *Support Care Cancer,* 19**,** 1393-401.

LAKSHMINARAYANAN, V., SUPEKAR, N. T., WEI, J., MCCURRY, D. B., DUECK, A. C., KOSIOREK, H. E., TRIVEDI, P. P., BRADLEY, J. M., MADSEN, C. S., PATHANGEY, L. B., HOELZINGER, D. B., WOLFERT, M. A., BOONS, G. J., COHEN, P. A. & GENDLER, S. J. 2016. MUC1 Vaccines, Comprised of Glycosylated or Non-Glycosylated Peptides or Tumor-Derived MUC1, Can Circumvent Immunoediting to Control Tumor Growth in MUC1 Transgenic Mice. *PLoS One,* 11**,** e0145920.

LAN, L. S., PING, Y. J., NA, W. L., MIAO, J., CHENG, Q. Q., NI, M. Z., LEI, L., FANG, L. C., GUANG, R. C., JIN, Z. & WEI, L. 2010. Down-regulation of Toll-like receptor 4 gene expression by short interfering RNA attenuates bone cancer pain in a rat model. *Mol Pain,* 6**,** 2.

LANTERO, A., TRAMULLAS, M., PILAR-CUELLAR, F., VALDIZAN, E., SANTILLAN, R., ROQUES, B. P. & HURLE, M. A. 2014. TGF-beta and opioid receptor signaling crosstalk results in improvement of endogenous and exogenous opioid analgesia under pathological pain conditions. *J Neurosci,* 34**,** 5385-95.

LARUE, L. & BELLACOSA, A. 2005. Epithelial-mesenchymal transition in development and cancer: role of phosphatidylinositol 3[prime] kinase//AKT pathways. *Oncogene,* 24**,** 7443-7454.

LAW, P. Y., WONG, Y. H. & LOH, H. H. 2000. Molecular mechanisms and regulation of opioid receptor signaling. *Annu Rev Pharmacol Toxicol,* 40**,** 389-430.

LAWSON, D. A., BHAKTA, N. R., KESSENBROCK, K., PRUMMEL, K. D., YU, Y., TAKAI, K., ZHOU, A., EYOB, H., BALAKRISHNAN, S., WANG, C.-Y., YASWEN, P., GOGA, A. & WERB, Z. 2015. Single-cell analysis reveals a stem-cell program in human metastatic breast cancer cells. *Nature,* 526**,** 131-135.

LE PICHON, C. E. & CHESLER, A. T. 2014. The functional and anatomical dissection of somatosensory subpopulations using mouse genetics. *Frontiers in Neuroanatomy,* 8.

LECHNER, S. G. & LEWIN, G. R. 2009. Peripheral sensitisation of nociceptors via G-protein-dependent potentiation of mechanotransduction currents. *J Physiol,* 587**,** 3493-503.

LEGENDRE, P. 2001. The glycinergic inhibitory synapse. *Cellular and Molecular Life Sciences CMLS,* 58**,** 760-793.

LEONG, K. G., WANG, B. E., JOHNSON, L. & GAO, W. Q. 2008. Generation of a prostate from a single adult stem cell. *Nature,* 456**,** 804-8.

LESNIAK, A., BOCHYNSKA-CZYZ, M., SACHARCZUK, M., BENHYE, S., MISICKA, A., BUJALSKA-ZADROZNY, M. & LIPKOWSKI, A. W. 2016. Biphalin preferentially recruits peripheral opioid receptors to facilitate analgesia in a mouse model of cancer pain - A comparison with morphine. *Eur J Pharm Sci,* 89**,** 39-49.

LEVER, I. J., ROBINSON, M., CIBELLI, M., PAULE, C., SANTHA, P., YEE, L., HUNT, S. P., CRAVATT, B. F., ELPHICK, M. R., NAGY, I. & RICE, A. S. 2009. Localization of the endocannabinoid-degrading enzyme fatty acid amide hydrolase in rat dorsal root ganglion cells and its regulation after peripheral nerve injury. *J Neurosci,* 29**,** 3766-80.

LEVINE, J. D., GORDON, N. C., TAIWO, Y. O. & CODERRE, T. J. 1988. Potentiation of pentazocine analgesia by low-dose naloxone. *J Clin Invest,* 82**,** 1574-7.

LEWIS, K. M., HARFORD-WRIGHT, E., VINK, R. & GHABRIEL, M. N. 2013. Characterisation of Walker 256 breast carcinoma cells from two tumour cell banks as assessed using two models of secondary brain tumours. *Cancer Cell Int,* 13**,** 5.

LEWISON, E. F. 1976. Spontaneous regression of breast cancer. *Natl Cancer Inst Monogr,* 44**,** 23-6.

LI, T. F., FAN, H. & WANG, Y. X. 2016. Aconitum-Derived Bulleyaconitine A Exhibits Antihypersensitivity Through Direct Stimulating Dynorphin A Expression in Spinal Microglia. *J Pain,* 17**,** 530-48.

LI, X.-Y. & TOYODA, H. 2015. Role of leak potassium channels in pain signaling. *Brain Research Bulletin,* 119**,** 73-79.

LI, X., LI, G., WU, S., ZHANG, B., WAN, Q., YU, D., ZHOU, R. & MA, C. 2014a. Antinociceptive effect of intrathecal microencapsulated human pheochromocytoma cell in a rat model of bone cancer pain. *Int J Mol Sci,* 15**,** 12135-48.

LI, X., WANG, X. W., FENG, X. M., ZHOU, W. J., WANG, Y. Q. & MAO-YING, Q. L. 2013. Stage-dependent anti-allodynic effects of intrathecal Toll-like receptor 4 antagonists in a rat model of cancer induced bone pain. *J Physiol Sci,* 63**,** 203-9.

LI, Y., CAI, J., HAN, Y., XIAO, X., MENG, X. L., SU, L., LIU, F. Y., XING, G. G. & WAN, Y. 2014b. Enhanced function of TRPV1 via up-regulation by insulin-like growth factor-1 in a rat model of bone cancer pain. *European Journal of Pain,* 18**,** 774-784.

LIANG, Y., DU, J. Y., FANG, J. F., FANG, R. Y., ZHOU, J., SHAO, X. M., JIANG, Y. L., CHEN, Y. T. & FANG, J. Q. 2017. Alleviating Mechanical Allodynia and Modulating Cellular Immunity

Contribute to Electroacupuncture's Dual Effect on Bone Cancer Pain. *Integr Cancer Ther*, 1534735417728335.

LICHY, J. H., DALBEGUE, F., ZAVAR, M., WASHINGTON, C., TSAI, M. M., SHENG, Z.-M. & TAUBENBERGER, J. K. 2000. Genetic Heterogeneity in Ductal Carcinoma of the Breast. *Lab Invest,* 80, 291-301.

LINDIA, J. A., KOHLER, M. G., MARTIN, W. J. & ABBADIE, C. 2005. Relationship between sodium channel NaV1.3 expression and neuropathic pain behavior in rats. *Pain,* 117, 145-53.

LISCOVITCH, M. & RAVID, D. 2007. A case study in misidentification of cancer cell lines: MCF-7/AdrR cells (re-designated NCI/ADR-RES) are derived from OVCAR-8 human ovarian carcinoma cells. *Cancer Lett,* 245, 350-2.

LIU, C., SONG, J., MAO, Y. & LIU, X. 2015. Bone metastatic pain palliation in a modified rat bone cancer pain model using 188Re-HEDP therapy. *Journal of Nuclear Medicine,* 56, 1199.

LIU, H., LIU, Z., DU, J., HE, J., LIN, P., AMINI, B., STARBUCK, M. W., NOVANE, N., SHAH, J. J., DAVIS, R. E., HOU, J., GAGEL, R. F. & YANG, J. 2016. Thymidine phosphorylase exerts complex effects on bone resorption and formation in myeloma. *Science Translational Medicine,* 8, 353ra113-353ra113.

LIU, K., CALDWELL, S. A. & ABRAMS, S. I. 2005. Immune selection and emergence of aggressive tumor variants as negative consequences of Fas-mediated cytotoxicity and altered IFN-gamma-regulated gene expression. *Cancer Res,* 65, 4376-88.

LIU, L., GAO, X. J., REN, C. G., HU, J. H., LIU, X. W., ZHANG, P., ZHANG, Z. W. & FU, Z. J. 2017a. Monocyte chemoattractant protein-1 contributes to morphine tolerance in rats with cancer-induced bone pain. *Exp Ther Med,* 13, 461-466.

LIU, M., YANG, H., FANG, D., YANG, J.-J., CAI, J., WAN, Y., CHUI, D.-H., HAN, J.-S. & XING, G.-G. 2013a. Upregulation of P2X3 receptors by neuronal calcium sensor protein VILIP-1 in dorsal root ganglions contributes to the bone cancer pain in rats. *PAIN®,* 154, 1551-1568.

LIU, M., YAO, M., WANG, H., XU, L., ZHENG, Y., HUANG, B., NI, H., XU, S., ZHOU, X. & LIAN, Q. 2017b. P2Y12 receptor-mediated activation of spinal microglia and p38MAPK pathway contribute to cancer-induced bone pain. *J Pain Res,* 10, 417-426.

LIU, S., LIU, W. T., LIU, Y. P., DONG, H. L., HENKEMEYER, M., XIONG, L. Z. & SONG, X. J. 2011. Blocking EphB1 receptor forward signaling in spinal cord relieves bone cancer pain and rescues analgesic effect of morphine treatment in rodents. *Cancer Res,* 71, 4392-402.

LIU, S., LIU, Y. P., SONG, W. B. & SONG, X. J. 2013b. EphrinB-EphB receptor signaling contributes to bone cancer pain via Toll-like receptor and proinflammatory cytokines in rat spinal cord. *Pain,* 154, 2823-35.

LIU, S., LIU, Y. P., YUE, D. M. & LIU, G. J. 2014a. Protease-activated receptor 2 in dorsal root ganglion contributes to peripheral sensitization of bone cancer pain. *European Journal of Pain,* 18, 326-337.

LIU, S., YANG, J., WANG, L., JIANG, M., QIU, Q., MA, Z., LIU, L., LI, C., REN, C., ZHOU, J. & LI, W. 2010. Tibia tumor-induced cancer pain involves spinal p38 mitogen-activated protein kinase activation via TLR4-dependent mechanisms. *Brain Res,* 1346**,** 213-23.

LIU, S., ZHANG, M. Y., CHEN, L. P., LIU, Y. P. & LIU, G. J. 2014b. cGMP and cGMP-dependent protein kinase I pathway in dorsal root ganglia contributes to bone cancer pain in rats. *Spine (Phila Pa 1976),* 39**,** 1533-41.

LIU, X., BU, H., LIU, C., GAO, F., YANG, H., TIAN, X., XU, A., CHEN, Z., CAO, F. & TIAN, Y. 2012. Inhibition of glial activation in rostral ventromedial medulla attenuates mechanical allodynia in a rat model of cancer-induced bone pain. *J Huazhong Univ Sci Technolog Med Sci,* 32**,** 291-8.

LIU, X. D., YANG, J. J., FANG, D., CAI, J., WAN, Y. & XING, G. G. 2014c. Functional upregulation of nav1.8 sodium channels on the membrane of dorsal root Ganglia neurons contributes to the development of cancer-induced bone pain. *PLoS One,* 9**,** e114623.

LOW, L. A. 2013. The impact of pain upon cognition: what have rodent studies told us? *Pain,* 154.

LOZANO-ONDOUA, A. N., HANLON, K. E., SYMONS-LIGUORI, A. M., LARGENT-MILNES, T. M., HAVELIN, J. J., FERLAND, H. L., 3RD, CHANDRAMOULI, A., OWUSU-ANKOMAH, M., NIKOLICH-ZUGICH, T., BLOOM, A. P., JIMENEZ-ANDRADE, J. M., KING, T., PORRECA, F., NELSON, M. A., MANTYH, P. W. & VANDERAH, T. W. 2013a. Disease modification of breast cancer-induced bone remodeling by cannabinoid 2 receptor agonists. *J Bone Miner Res,* 28**,** 92-107.

LOZANO-ONDOUA, A. N., SYMONS-LIGUORI, A. M. & VANDERAH, T. W. 2013b. Cancer-induced bone pain: Mechanisms and models. *Neurosci Lett,* 557 Pt A**,** 52-9.

LU, C., LIU, Y., SUN, B., SUN, Y., HOU, B., ZHANG, Y., MA, Z. & GU, X. 2015. Intrathecal Injection of JWH-015 Attenuates Bone Cancer Pain Via Time-Dependent Modification of Pro-inflammatory Cytokines Expression and Astrocytes Activity in Spinal Cord. *Inflammation*.

LU, C., SHI, L., SUN, B., ZHANG, Y., HOU, B., SUN, Y., MA, Z. & GU, X. 2016. A Single Intrathecal or Intraperitoneal Injection of CB2 Receptor Agonist Attenuates Bone Cancer Pain and Induces a Time-Dependent Modification of GRK2. *Cell Mol Neurobiol*.

LUDVIGSEN, E., CARLSSON, C., TIENSUU JANSON, E., SANDLER, S. & STRIDSBERG, M. 2015. Somatostatin receptor 1-5; expression profiles during rat development. *Ups J Med Sci,* 120**,** 157-68.

LUO, C., GANGADHARAN, V., BALI, K. K., XIE, R. G., AGARWAL, N., KUREJOVA, M., TAPPE-THEODOR, A., TEGEDER, I., FEIL, S., LEWIN, G., POLGAR, E., TODD, A. J., SCHLOSSMANN, J., HOFMANN, F., LIU, D. L., HU, S. J., FEIL, R., KUNER, T. & KUNER, R. 2012. Presynaptically localized cyclic GMP-dependent protein kinase 1 is a key determinant of spinal synaptic potentiation and pain hypersensitivity. *PLoS Biol,* 10**,** e1001283.

LUO, J., HUANG, X., LI, Y., LI, Y., XU, X., GAO, Y., SHI, R., YAO, W., LIU, J. & KE, C. 2016. GPR30 disrupts the balance of GABAergic and glutamatergic transmission in the spinal cord driving to the development of bone cancer pain. *Oncotarget*.

LUO, R., GUO, Y., CAO, D.-Y., PICKAR, J. G., LI, L., WANG, J. & ZHAO, Y. 2010. Local effects of octreotide on glutamate-evoked activation of Aδ and C afferent fibers in rat hairy skin. *Brain Research,* 1322**,** 50-58.

LUSSIER, D., HUSKEY, A. G. & PORTENOY, R. K. 2004. Adjuvant analgesics in cancer pain management. *Oncologist,* 9**,** 571-91.

LUTY, M., KWIECIEN, E., FIRLEJ, M., LABEDZ-MASLOWSKA, A., PAW, M., MADEJA, Z. & CZYZ, J. 2016. Curcumin augments the cytostatic and anti-invasive effects of mitoxantrone on carcinosarcoma cells in vitro. *Acta Biochim Pol*.

LYNN, B. 1996. Neurogenic inflammation caused by cutaneous polymodal receptors. *Prog Brain Res,* 113**,** 361-8.

MAGARIAN-BLANDER, J., CIBOROWSKI, P., HSIA, S., WATKINS, S. C. & FINN, O. J. 1998. Intercellular and intracellular events following the MHC-unrestricted TCR recognition of a tumor-specific peptide epitope on the epithelial antigen MUC1. *J Immunol,* 160**,** 3111-20.

MAGUIRE, D. R., YANG, W. & FRANCE, C. P. 2013. Interactions between μ-Opioid Receptor Agonists and Cannabinoid Receptor Agonists in Rhesus Monkeys: Antinociception, Drug Discrimination, and Drug Self-Administration. *J Pharmacol Exp Ther,* 345**,** 354-62.

MALHOTRA, G. K., ZHAO, X., BAND, H. & BAND, V. 2010. Histological, molecular and functional subtypes of breast cancers. *Cancer Biol Ther,* 10**,** 955-60.

MANCINO, M., AMETLLER, E., GASCÓN, P. & ALMENDRO, V. 2011. The neuronal influence on tumor progression. *Biochimica et Biophysica Acta (BBA) - Reviews on Cancer,* 1816**,** 105-118.

MANJILI, M. H., ARNOUK, H., KNUTSON, K. L., KMIECIAK, M., DISIS, M. L., SUBJECK, J. R. & KAZIM, A. L. 2006. Emergence of immune escape variant of mammary tumors that has distinct proteomic profile and a reduced ability to induce "danger signals". *Breast Cancer Res Treat,* 96**,** 233-41.

MANTYH, P. W. 2006. Cancer pain and its impact on diagnosis, survival and quality of life. *Nat Rev Neurosci,* 7**,** 797-809.

MANTYH, P. W. 2014. Bone cancer pain: from mechanism to therapy. *Curr Opin Support Palliat Care,* 8**,** 83-90.

MANTYH, P. W., CLOHISY, D. R., KOLTZENBURG, M. & HUNT, S. P. 2002. Molecular mechanisms of cancer pain. *Nat Rev Cancer,* 2**,** 201-9.

MAO-YING, Q. L., WANG, X. W., YANG, C. J., LI, X., MI, W. L., WU, G. C. & WANG, Y. Q. 2012. Robust spinal neuroinflammation mediates mechanical allodynia in Walker 256 induced bone cancer rats. *Mol Brain,* 5**,** 16.

MAO-YING, Q. L., ZHAO, J., DONG, Z. Q., WANG, J., YU, J., YAN, M. F., ZHANG, Y. Q., WU, G. C. & WANG, Y. Q. 2006. A rat model of bone cancer pain induced by intra-tibia inoculation of Walker 256 mammary gland carcinoma cells. *Biochem Biophys Res Commun,* 345**,** 1292-8.

MARCU, M., RADU, E. & SAJIN, M. 2010. Neuroendocrine transdifferentiation of prostate carcinoma cells and its prognostic significance. *Rom J Morphol Embryol,* 51**,** 7-12.

MARTH, C., MULLER-HOLZNER, E., GREITER, E., CRONAUER, M. V., ZEIMET, A. G., DOPPLER, W., EIBL, B., HYNES, N. E. & DAXENBICHLER, G. 1990. Gamma-interferon reduces expression of the protooncogene c-erbB-2 in human ovarian carcinoma cells. *Cancer Res,* 50**,** 7037-41.

MARUSYK, A., ALMENDRO, V. & POLYAK, K. 2012. Intra-tumour heterogeneity: a looking glass for cancer? *Nat Rev Cancer,* 12**,** 323-334.

MARX, V. 2014. Cell-line authentication demystified. *Nat Meth,* 11**,** 483-488.

MCDONALD, J. & LAMBERT, D. 2005. Opioid receptors. *Continuing Education in Anaesthesia, Critical Care & Pain,* 5**,** 22-25.

MCEUEN, C. S. & THOMSON, D. L. 1933. *The Effect of Hypophysectomy on the Growth of the Walker Rat Tumour*, Br J Exp Pathol. 1933 Dec;14(6):384-91.

MCKELVEY, R., BERTA, T., OLD, E., JI, R. R. & FITZGERALD, M. 2015. Neuropathic pain is constitutively suppressed in early life by anti-inflammatory neuroimmune regulation. *J Neurosci,* 35**,** 457-66.

MCKIERNAN, E., MCDERMOTT, E. W., EVOY, D., CROWN, J. & DUFFY, M. J. 2011. The role of S100 genes in breast cancer progression. *Tumour Biol,* 32**,** 441-50.

MCMAHON, S. B. & MALCANGIO, M. 2009. Current challenges in glia-pain biology. *Neuron,* 64**,** 46-54.

MEDHURST, S. J., WALKER, K., BOWES, M., KIDD, B. L., GLATT, M., MULLER, M., HATTENBERGER, M., VAXELAIRE, J., O'REILLY, T., WOTHERSPOON, G., WINTER, J., GREEN, J. & URBAN, L. 2002. A rat model of bone cancer pain. *Pain,* 96**,** 129-40.

MEEUS, M. & NIJS, J. 2007. Central sensitization: a biopsychosocial explanation for chronic widespread pain in patients with fibromyalgia and chronic fatigue syndrome. *Clin Rheumatol,* 26**,** 465-73.

MEGO, M., MANI, S. A., LEE, B. N., LI, C., EVANS, K. W., COHEN, E. N., GAO, H., JACKSON, S. A., GIORDANO, A., HORTOBAGYI, G. N., CRISTOFANILLI, M., LUCCI, A. & REUBEN, J. M. 2012. Expression of epithelial-mesenchymal transition-inducing transcription factors in primary breast cancer: The effect of neoadjuvant therapy. *Int J Cancer,* 130**,** 808-16.

MENDEZ, R., RUIZ-CABELLO, F., RODRIGUEZ, T., DEL CAMPO, A., PASCHEN, A., SCHADENDORF, D. & GARRIDO, F. 2007. Identification of different tumor escape mechanisms in several metastases from a melanoma patient undergoing immunotherapy. *Cancer Immunol Immunother,* 56**,** 88-94.

MENENDEZ, L., HIDALGO, A., MEANA, A., PORAS, H., FOURNIE-ZALUSKI, M. C., ROQUES, B. P. & BAAMONDE, A. 2008. Inhibition of osteosarcoma-induced thermal hyperalgesia in mice by the orally active dual enkephalinase inhibitor PL37. Potentiation by gabapentin. *Eur J Pharmacol,* 596**,** 50-5.

MENENDEZ, L., LASTRA, A., FRESNO, M. F., LLAMES, S., MEANA, A., HIDALGO, A. & BAAMONDE, A. 2003. Initial thermal heat hypoalgesia and delayed hyperalgesia in a murine model of bone cancer pain. *Brain Res,* 969**,** 102-9.

MENEZES, A. H. & AHMED, R. 2014. Primary atlantoaxial bone tumors in children: management strategies and long-term follow-up. *J Neurosurg Pediatr,* 13**,** 260-72.

MERCADO, J., GORDON-SHAAG, A., ZAGOTTA, W. N. & GORDON, S. E. 2010. Ca2+-dependent desensitization of TRPV2 channels is mediated by hydrolysis of phosphatidylinositol 4,5-bisphosphate. *J Neurosci,* 30**,** 13338-47.

MERTENS, W. C., FILIPCZAK, L. A., BEN-JOSEF, E., DAVIS, L. P. & PORTER, A. T. 1998. Systemic bone-seeking radionuclides for palliation of painful osseous metastases: current concepts. *CA Cancer J Clin,* 48**,** 361-74, 321.

MI, H., MURUGANUJAN, A., CASAGRANDE, J. T. & THOMAS, P. D. 2013a. Large-scale gene function analysis with the PANTHER classification system. *Nat. Protocols,* 8**,** 1551-1566.

MI, H., MURUGANUJAN, A. & THOMAS, P. D. 2013b. PANTHER in 2013: modeling the evolution of gene function, and other gene attributes, in the context of phylogenetic trees. *Nucleic Acids Res,* 41**,** D377-86.

MIAO, X. R., GAO, X. F., WU, J. X., LU, Z. J., HUANG, Z. X., LI, X. Q., HE, C. & YU, W. F. 2010. Bilateral downregulation of Nav1.8 in dorsal root ganglia of rats with bone cancer pain induced by inoculation with Walker 256 breast tumor cells. *BMC Cancer,* 10**,** 216.

MICHAELSON, S. & ORCUTT, J. A. 1957. Observations on some growth characteristics of the Walker carcinoma 256. *Cancer,* 10**,** 416-8.

MIDDLEMISS, T., LAIRD, B. J. & FALLON, M. T. 2011. Mechanisms of cancer-induced bone pain. *Clin Oncol (R Coll Radiol),* 23**,** 387-92.

MIFFLIN, K. & KERR, B. 2014. The transition from acute to chronic pain: understanding how different biological systems interact. *Canadian Journal of Anesthesia/Journal canadien d'anesthésie,* 61**,** 112-122.

MILGROM, D. P., LAD, N. L., KONIARIS, L. G. & ZIMMERS, T. A. 2017. Bone Pain and Muscle Weakness in Cancer Patients. *Current Osteoporosis Reports,* 15**,** 76-87.

MILLAN, M. J. 2002. Descending control of pain. *Progress in Neurobiology,* 66**,** 355-474.

MILLER, A., SANDERSON, K., BRUNO, R., BRESLIN, M. & NEIL, A. L. 2017. The prevalence of pain and analgesia use in the Australian population: Findings from the 2011 to 2012 Australian National Health Survey. *Pharmacoepidemiology and Drug Safety,* 26**,** 1403-1410.

MILLNER, L. M., LINDER, M. W. & VALDES, R., JR. 2013. Circulating tumor cells: a review of present methods and the need to identify heterogeneous phenotypes. *Ann Clin Lab Sci,* 43**,** 295-304.

MINETT, M. S., FALK, S., SANTANA-VARELA, S., BOGDANOV, Y. D., NASSAR, M. A., HEEGAARD, A. M. & WOOD, J. N. 2014. Pain without nociceptors? Nav1.7-independent pain mechanisms. *Cell Rep,* 6**,** 301-12.

MITRA, R. & JONES, S. 2012. Adjuvant analgesics in cancer pain: a review. *Am J Hosp Palliat Care,* 29**,** 70-9.

MOGIL, J. S. 2009. Animal models of pain: progress and challenges. *Nat Rev Neurosci,* 10**,** 283-294.

MOGIL, J. S., GRAHAM, A. C., RITCHIE, J., HUGHES, S. F., AUSTIN, J.-S., SCHORSCHER-PETCU, A., LANGFORD, D. J. & BENNETT, G. J. 2010. Hypolocomotion, asymmetrically directed behaviors (licking, lifting, flinching, and shaking) and dynamic weight bearing (gait) changes are not measures of neuropathic pain in mice. *Molecular Pain,* 6**,** 34.

MOGIL, J. S. & GRISEL, J. E. 1998. Transgenic studies of pain. *Pain,* 77**,** 107-28.

MOHME, M., RIETHDORF, S. & PANTEL, K. 2016. Circulating and disseminated tumour cells [mdash] mechanisms of immune surveillance and escape. *Nat Rev Clin Oncol,* advance online publication.

MORGAN, M. M., FOSSUM, E. N., STALDING, B. M. & KING, M. M. 2006. Morphine Antinociceptive Potency on Chemical, Mechanical, and Thermal Nociceptive Tests in the Rat. *The Journal of Pain,* 7**,** 358-366.

MORI, M., MATSUSHITA, A., TAKIUCHI, Y., ARIMA, H., NAGANO, S., SHIMOJI, S., KIMURA, T., INOUE, D., TABATA, S., YANAGITA, S., NAGAI, K., IMAI, Y. & TAKAHASHI, T. 2010. Histiocytic sarcoma and underlying chronic myelomonocytic leukemia: a proposal for the developmental classification of histiocytic sarcoma. *International Journal of Hematology,* 92**,** 168-173.

MOSER, V. C. & MACPHAIL, R. C. 1990. Comparative sensitivity of neurobehavioral tests for chemical screening. *Neurotoxicology,* 11**,** 335-44.

MUKHERJEE, P., GINARDI, A. R., MADSEN, C. S., STERNER, C. J., ADRIANCE, M. C., TEVETHIA, M. J. & GENDLER, S. J. 2000. Mice with Spontaneous Pancreatic Cancer Naturally Develop MUC-1-Specific CTLs That Eradicate Tumors When Adoptively Transferred. *The Journal of Immunology,* 165**,** 3451-3460.

MULLINS, L. J. & MULLINS, J. J. 2004. Insights from the rat genome sequence. *Genome Biology,* 5**,** 221.

MURALIDHARAN, A. & SMITH, M. T. 2013. Pathobiology and management of prostate cancer-induced bone pain: recent insights and future treatments. *Inflammopharmacology,* 21**,** 339-63.

MURALIDHARAN, A., WYSE, B. D. & SMITH, M. T. 2013. Optimization and characterization of a rat model of prostate cancer-induced bone pain using behavioral, pharmacological, radiological, histological and immunohistochemical methods. *Pharmacol Biochem Behav,* 106**,** 33-46.

MURALIDHARAN, A., WYSE, B. D. & SMITH, M. T. 2014. Analgesic Efficacy and Mode of Action of a Selective Small Molecule Angiotensin II Type 2 Receptor Antagonist in a Rat Model of Prostate Cancer-Induced Bone Pain. *Pain Medicine,* 15**,** 93-110.

MUROI, Y. & UNDEM, B. J. 2014. Targeting Voltage Gated Sodium Channels Na(V)1.7, Na(V)1.8, and Na(V)1.9 for Treatment of Pathological Cough. *Lung,* 192**,** 15-20.

MURPHY, A. Z., SUCKOW, S. K., JOHNS, M. & TRAUB, R. J. 2009. Sex differences in the activation of the spinoparabrachial circuit by visceral pain. *Physiol Behav,* 97**,** 205-12.

MURRAY, R. D., KIM, K., REN, S. G., CHELLY, M., UMEHARA, Y. & MELMED, S. 2004. Central and peripheral actions of somatostatin on the growth hormone-IGF-I axis. *J Clin Invest,* 114**,** 349-56.

NASSAR, M. A., LEVATO, A., STIRLING, L. C. & WOOD, J. N. 2005. Neuropathic pain develops normally in mice lacking both Na(v)1.7 and Na(v)1.8. *Mol Pain,* 1**,** 24.

NASSAR, M. A., STIRLING, L. C., FORLANI, G., BAKER, M. D., MATTHEWS, E. A., DICKENSON, A. H. & WOOD, J. N. 2004. Nociceptor-specific gene deletion reveals a major role for Nav1.7 (PN1) in acute and inflammatory pain. *Proc Natl Acad Sci U S A,* 101**,** 12706-11.

NEGRINI, S., GORGOULIS, V. G. & HALAZONETIS, T. D. 2010. Genomic instability [mdash] an evolving hallmark of cancer. *Nat Rev Mol Cell Biol,* 11**,** 220-228.

NEGUS, S. S., MORRISSEY, E. M., FOLK, J. E. & RICE, K. C. 2012. Interaction between Mu and Delta Opioid Receptor Agonists in an Assay of Capsaicin-Induced Thermal Allodynia in Rhesus Monkeys. *Pain Res Treat,* 2012.

NEUVONEN, P. J., TOKOLA, O., TOIVONEN, M. L. & SIMELL, O. 1985. Methionine in paracetamol tablets, a tool to reduce paracetamol toxicity. *Int J Clin Pharmacol Ther Toxicol,* 23**,** 497-500.

NEVE, R. M., CHIN, K., FRIDLYAND, J., YEH, J., BAEHNER, F. L., FEVR, T., CLARK, L., BAYANI, N., COPPE, J. P., TONG, F., SPEED, T., SPELLMAN, P. T., DEVRIES, S., LAPUK, A., WANG, N. J., KUO, W. L., STILWELL, J. L., PINKEL, D., ALBERTSON, D. G., WALDMAN, F. M., MCCORMICK, F., DICKSON, R. B., JOHNSON, M. D., LIPPMAN, M., ETHIER, S., GAZDAR, A. & GRAY, J. W. 2006. A collection of breast cancer cell lines for the study of functionally distinct cancer subtypes. *Cancer Cell,* 10**,** 515-27.

NIEDERSTRASSER, N. G., MEULDERS, A., MEULDERS, M., SLEPIAN, P. M., VLAEYEN, J. W. S. & SULLIVAN, M. J. L. 2015. Pain Catastrophizing and Fear of Pain Predict the Experience of Pain in Body Parts Not Targeted by a Delayed-Onset Muscle Soreness Procedure. *The Journal of Pain,* 16**,** 1065-1076.

NIMS, R. W., SYKES, G., COTTRILL, K., IKONOMI, P. & ELMORE, E. 2010. Short tandem repeat profiling: part of an overall strategy for reducing the frequency of cell misidentification. *In Vitro Cell Dev Biol Anim,* 46**,** 811-9.

NOBLE, S. & BALFOUR, J. A. 1996. Meloxicam. *Drugs,* 51**,** 424-30; discussion 431-32.

NORTH, R. A. 2002. Molecular physiology of P2X receptors. *Physiol Rev,* 82**,** 1013-67.

O'SULLIVAN, G. J., CARTY, F. L. & CRONIN, C. G. 2015. Imaging of bone metastasis: An update. *World Journal of Radiology,* 7**,** 202-211.

OJI, Y., TATSUMI, N., FUKUDA, M., NAKATSUKA, S., AOYAGI, S., HIRATA, E., NANCHI, I., FUJIKI, F., NAKAJIMA, H., YAMAMOTO, Y., SHIBATA, S., NAKAMURA, M., HASEGAWA, K., TAKAGI, S., FUKUDA, I., HOSHIKAWA, T., MURAKAMI, Y., MORI, M., INOUE, M., NAKA, T., TOMONAGA, T., SHIMIZU, Y., NAKAGAWA, M., HASEGAWA, J., NEZU, R., INOHARA, H., IZUMOTO, S., NONOMURA, N., YOSHIMINE, T., OKUMURA, M., MORII, E., MAEDA, H., NISHIDA, S., HOSEN, N., TSUBOI, A., OKA, Y. & SUGIYAMA, H. 2014. The translation elongation factor eEF2 is a novel tumorassociated antigen overexpressed in various types of cancers. *Int J Oncol,* 44**,** 1461-9.

OLIVEIRA, A. G. & GOMES-MARCONDES, M. C. 2016. Metformin treatment modulates the tumour-induced wasting effects in muscle protein metabolism minimising the cachexia in tumour-bearing rats. *BMC Cancer,* 16**,** 418.

OLOFSSON, M. H., UENO, T., PAN, Y., XU, R., CAI, F., VAN DER KUIP, H., MUERDTER, T. E., SONNENBERG, M., AULITZKY, W. E., SCHWARZ, S., ANDERSSON, E., SHOSHAN, M. C., HAVELKA, A. M., TOI, M. & LINDER, S. 2007. Cytokeratin-18 is a useful serum biomarker for early determination of response of breast carcinomas to chemotherapy. *Clin Cancer Res,* 13**,** 3198-206.

ONSUM, M. D., GERETTI, E., PARAGAS, V., KUDLA, A. J., MOULIS, S. P., LUUS, L., WICKHAM, T. J., MCDONAGH, C. F., MACBEATH, G. & HENDRIKS, B. S. 2013. Single-cell quantitative HER2 measurement identifies heterogeneity and distinct subgroups within traditionally defined HER2-positive patients. *Am J Pathol,* 183**,** 1446-60.

ONUIGBO, W. I. 2012. Spontaneous regression of breast carcinoma: review of English publications from 1753 to 1897. *Oncol Rev,* 6**,** e22.

ORITO, T., SHINOHARA, H., OKADA, Y. & MORI, M. 1989. Heterogeneity of Keratin Expression in Epithelial Tumor Cells of Adenolymphoma in Paraffin Sections. *Pathology - Research and Practice,* 184**,** 600-608.

OUDEJANS, J. J., TEN BERGE, R. L. & MEIJER, C. 2003. Immune escape mechanisms in ALCL. *J Clin Pathol,* 56**,** 423-5.

PACHARINSAK, C. & BEITZ, A. 2008. Animal models of cancer pain. *Comp Med,* 58**,** 220-33.

PALEY, C. A., BENNETT, M. I. & JOHNSON, M. I. 2011. Acupuncture for Cancer-Induced Bone Pain? *Evid Based Complement Alternat Med,* 2011.

PALMA, C. D. S., GRASSI, M. L., THOMÉ, C. H., FERREIRA, G. A., ALBUQUERQUE, D., PINTO, M. T., MELO, F. U. F., KASHIMA, S., COVAS, D. T., PITTERI, S. J. & FACA, V. M. 2016. Proteomic analysis of epithelial to mesenchymal transition reveals crosstalk between SNAIL and HDAC1 in breast cancer cells. *Molecular & Cellular Proteomics*.

PAN, H.-L., ZHANG, Y.-Q. & ZHAO, Z.-Q. 2010. Involvement of lysophosphatidic acid in bone cancer pain by potentiation of TRPV1 via PKCϵ pathway in dorsal root ganglion neurons. *Molecular Pain,* 6**,** 85.

PAN, H. L., LIU, B. L., LIN, W. & ZHANG, Y. Q. 2016. Modulation of Nav1.8 by Lysophosphatidic Acid in the Induction of Bone Cancer Pain. *Neurosci Bull,* 32**,** 445-54.

PAN, R., DI, H., ZHANG, J., HUANG, Z., SUN, Y., YU, W. & WU, F. 2015. Inducible Lentivirus-Mediated siRNA against TLR4 Reduces Nociception in a Rat Model of Bone Cancer Pain. *Mediators Inflamm,* 2015**,** 523896.

PANTEL, K., SCHLIMOK, G., ANGSTWURM, M., WECKERMANN, D., SCHMAUS, W., GATH, H., PASSLICK, B., IZBICKI, J. R. & RIETHMULLER, G. 1994. Methodological analysis of immunocytochemical screening for disseminated epithelial tumor cells in bone marrow. *J Hematother,* 3**,** 165-73.

PAQUERON, X., CONKLIN, D. & EISENACH, J. C. 2003. Plasticity in action of intrathecal clonidine to mechanical but not thermal nociception after peripheral nerve injury. *Anesthesiology,* 99**,** 199-204.

PARDOLL, D. M. & TOPALIAN, S. L. 1998. The role of CD4+ T cell responses in antitumor immunity. *Curr Opin Immunol,* 10**,** 588-94.

PARK, C. K., LU, N., XU, Z. Z., LIU, T., SERHAN, C. N. & JI, R. R. 2011. Resolving TRPV1- and TNF-alpha-mediated spinal cord synaptic plasticity and inflammatory pain with neuroprotectin D1. *J Neurosci,* 31**,** 15072-85.

PARK, J. & JEONG, S. 2015. Wnt activated beta-catenin and YAP proteins enhance the expression of non-coding RNA component of RNase MRP in colon cancer cells. *Oncotarget,* 6**,** 34658-68.

PARK, J. S., VOITENKO, N., PETRALIA, R. S., GUAN, X., XU, J. T., STEINBERG, J. P., TAKAMIYA, K., SOTNIK, A., KOPACH, O., HUGANIR, R. L. & TAO, Y. X. 2009. Persistent inflammation induces GluR2 internalization via NMDA receptor-triggered PKC activation in dorsal horn neurons. *J Neurosci,* 29**,** 3206-19.

PAVLAKI, M., GIANNOPOULOU, E., NIARAKIS, A., RAVAZOULA, P. & ALETRAS, A. J. 2009. Walker 256 cancer cells secrete tissue inhibitor of metalloproteinase-free metalloproteinase-9. *Molecular and Cellular Biochemistry,* 328**,** 189-199.

PECHER, G. & FINN, O. J. 1996. Induction of cellular immunity in chimpanzees to human tumor-associated antigen mucin by vaccination with MUC-1 cDNA-transfected Epstein-Barr virus-immortalized autologous B cells. *Proc Natl Acad Sci U S A,* 93**,** 1699-704.

PEROU, C. M., JEFFREY, S. S., VAN DE RIJN, M., REES, C. A., EISEN, M. B., ROSS, D. T., PERGAMENSCHIKOV, A., WILLIAMS, C. F., ZHU, S. X., LEE, J. C., LASHKARI, D., SHALON, D., BROWN, P. O. & BOTSTEIN, D. 1999. Distinctive gene expression patterns in human mammary epithelial cells and breast cancers. *Proc Natl Acad Sci U S A,* 96**,** 9212-7.

PETERS, C. M., GHILARDI, J. R., KEYSER, C. P., KUBOTA, K., LINDSAY, T. H., LUGER, N. M., MACH, D. B., SCHWEI, M. J., SEVCIK, M. A. & MANTYH, P. W. 2005. Tumor-induced injury of primary afferent sensory nerve fibers in bone cancer pain. *Exp Neurol,* 193**,** 85-100.

PETRUS, M., PEIER, A. M., BANDELL, M., HWANG, S. W., HUYNH, T., OLNEY, N., JEGLA, T. & PATAPOUTIAN, A. 2007. A role of TRPA1 in mechanical hyperalgesia is revealed by pharmacological inhibition. *Mol Pain,* 3**,** 40.

PHANPHAISARN, A., PATUMANOND, J., SETTAKORN, J., CHAIYAWAT, P., KLANGJORHOR, J. & PRUKSAKORN, D. 2016. Prevalence and Survival Patterns of Patients with Bone Metastasis from Common Cancers in Thailand. *Asian Pac J Cancer Prev,* 17**,** 4335-4340.

PIERRE, S., ESCHENHAGEN, T., GEISSLINGER, G. & SCHOLICH, K. 2009. Capturing adenylyl cyclases as potential drug targets. *Nat Rev Drug Discov,* 8**,** 321-335.

PIESLA, M. J., LEVENTHAL, L., STRASSLE, B. W., HARRISON, J. E., CUMMONS, T. A., LU, P. & WHITESIDE, G. T. 2009. Abnormal gait, due to inflammation but not nerve injury, reflects enhanced nociception in preclinical pain models. *Brain Research,* 1295**,** 89-98.

PIETRANTONIO, F., CAPORALE, M., MORANO, F., SCARTOZZI, M., GLOGHINI, A., DE VITA, F., GIOMMONI, E., FORNARO, L., APRILE, G., MELISI, D., BERENATO, R., MENNITTO, A., VOLPI, C. C., LATERZA, M. M., PUSCEDDU, V., ANTONUZZO, L., VASILE, E., ONGARO, E., SIMIONATO, F., DE BRAUD, F., TORRI, V. & DI BARTOLOMEO, M. 2016. HER2 loss in HER2-positive gastric or gastroesophageal cancer after trastuzumab therapy: Implication for further clinical research. *Int J Cancer,* 139**,** 2859-2864.

PIGATTO, M. C., DE ARAUJO, B. V., TORRES, B. G., SCHMIDT, S., MAGNI, P. & DALLA COSTA, T. 2016. Population Pharmacokinetic Modeling of Etoposide Free Concentrations in Solid Tumor. *Pharm Res*.

PILARSKI, L. M., PILARSKI, P. M. & BELCH, A. R. 2010. Multiple myeloma may include microvessel endothelial cells of malignant origin. *Leuk Lymphoma,* 51**,** 592-7.

POLYAK, K. & WEINBERG, R. A. 2009. Transitions between epithelial and mesenchymal states: acquisition of malignant and stem cell traits. *Nat Rev Cancer,* 9**,** 265-273.

POSTE, G., DOLL, J., BROWN, A. E., TZENG, J. & ZEIDMAN, I. 1982a. Comparison of the metastatic properties of B16 melanoma clones isolated from cultured cell lines, subcutaneous tumors, and individual lung metastases. *Cancer Res,* 42**,** 2770-8.

POSTE, G., TZENG, J., DOLL, J., GREIG, R., RIEMAN, D. & ZEIDMAN, I. 1982b. Evolution of tumor cell heterogeneity during progressive growth of individual lung metastases. *Proc Natl Acad Sci U S A,* 79**,** 6574-8.

PRABHAVATHI, K., CHANDRA, U. S., SOANKER, R. & RANI, P. U. 2014. A randomized, double blind, placebo controlled, cross over study to evaluate the analgesic activity of Boswellia serrata in healthy volunteers using mechanical pain model. *Indian J Pharmacol,* 46**,** 475-9.

PREVOT, T. D., GASTAMBIDE, F., VIOLLET, C., HENKOUS, N., MARTEL, G., EPELBAUM, J., BERACOCHEA, D. & GUILLOU, J.-L. 2017. Roles of Hippocampal Somatostatin Receptor Subtypes in Stress Response and Emotionality. *Neuropsychopharmacology,* 42**,** 1647-1656.

PUSZTAI, L., VIALE, G., KELLY, C. M. & HUDIS, C. A. 2010. Estrogen and HER-2 Receptor Discordance Between Primary Breast Cancer and Metastasis. *The Oncologist,* 15**,** 1164-1168.

QIU, C., ZEYDA, T., JOHNSON, B., HOCHGESCHWENDER, U., DE LECEA, L. & TALLENT, M. K. 2008. Somatostatin receptor subtype 4 couples to the M-current to regulate seizures. *J Neurosci,* 28**,** 3567-76.

QIU, F., JIANG, Y., ZHANG, H., LIU, Y. & MI, W. 2012. Increased expression of tetrodotoxin-resistant sodium channels Nav1.8 and Nav1.9 within dorsal root ganglia in a rat model of bone cancer pain. *Neurosci Lett,* 512**,** 61-6.

QIU, F., WEI, X., ZHANG, S., YUAN, W. & MI, W. 2014. Increased expression of acid-sensing ion channel 3 within dorsal root ganglia in a rat model of bone cancer pain. *Neuroreport,* 25**,** 887-93.

QU, K., ZABA, LISA C., GIRESI, PAUL G., LI, R., LONGMIRE, M., KIM, YOUN H., GREENLEAF, WILLIAM J. & CHANG, HOWARD Y. 2015. Individuality and Variation of Personal Regulomes in Primary Human T Cells. *Cell Systems,* 1**,** 51-61.

RADES, D., SCHILD, S. E. & ABRAHM, J. L. 2010. Treatment of painful bone metastases. *Nat Rev Clin Oncol,* 7**,** 220-9.

RAHN, J. J., DABBAGH, L., PASDAR, M. & HUGH, J. C. 2001. The importance of MUC1 cellular localization in patients with breast carcinoma. *Cancer,* 91**,** 1973-1982.

RAMOS, F. S., SERINO, L. T., CARVALHO, C. M., LIMA, R. S., URBAN, C. A., CAVALLI, I. J. & RIBEIRO, E. M. 2015. PDIA3 and PDIA6 gene expression as an aggressiveness marker in primary ductal breast cancer. *Genet Mol Res,* 14**,** 6960-7.

RANDALL, L. O., SELITTO, J. J. & VALDES, J. 1957. Anti-inflammatory effects of xylopropamine. *Arch Int Pharmacodyn Ther,* 113**,** 233-49.

RAOUF, R., QUICK, K. & WOOD, J. N. 2010. Pain as a channelopathy. *J Clin Invest,* 120**,** 3745-52.

RATEI, R., HUMMEL, M., ANAGNOSTOPOULOS, I., JAHNE, D., ARNOLD, R., DORKEN, B., MATHAS, S., BENTER, T., DUDECK, O., LUDWIG, W. D. & STEIN, H. 2010. Common

clonal origin of an acute B-lymphoblastic leukemia and a Langerhans' cell sarcoma: evidence for hematopoietic plasticity. *Haematologica,* 95**,** 1461-6.

REBECA, R., BRACHT, L., NOLETO, G. R., MARTINEZ, G. R., CADENA, S. M., CARNIERI, E. G., ROCHA, M. E. & DE OLIVEIRA, M. B. 2008. Production of cachexia mediators by Walker 256 cells from ascitic tumors. *Cell Biochem Funct,* 26**,** 731-8.

REES, R. C. & MIAN, S. 1999. Selective MHC expression in tumours modulates adaptive and innate antitumour responses. *Cancer Immunol Immunother,* 48**,** 374-81.

REITZ, M. C., HRNCIC, D., TREEDE, R. D. & CASPANI, O. 2016. A comparative behavioural study of mechanical hypersensitivity in 2 pain models in rats and humans. *Pain,* 157**,** 1248-58.

REN, F., JIAO, H. & CAI, H. 2015. Analgesic Effect of Intrathecal Administration of Chemokine Receptor CCR2 Antagonist is Related to Change in Spinal NR2B, nNOS, and SIGIRR Expression in Rat with Bone Cancer Pain. *Cell Biochem Biophys,* 72**,** 611-6.

REN, K. 1999. An Improved Method for Assessing Mechanical Allodynia in the Rat. *Physiology & Behavior,* 67**,** 711-716.

REUBEN, J. M., LEE, B. N., GAO, H., COHEN, E. N., MEGO, M., GIORDANO, A., WANG, X., LODHI, A., KRISHNAMURTHY, S., HORTOBAGYI, G. N., CRISTOFANILLI, M., LUCCI, A. & WOODWARD, W. A. 2011. Primary breast cancer patients with high risk clinicopathologic features have high percentages of bone marrow epithelial cells with ALDH activity and CD44(+)CD24lo cancer stem cell phenotype. *Eur J Cancer,* 47**,** 1527-36.

REYNAERT, H., ROMBOUTS, K., VANDERMONDE, A., URBAIN, D., KUMAR, U., BIOULAC-SAGE, P., PINZANI, M., ROSENBAUM, J. & GEERTS, A. 2004. Expression of somatostatin receptors in normal and cirrhotic human liver and in hepatocellular carcinoma. *Gut,* 53**,** 1180-9.

RICCIOTTI, E. & FITZGERALD, G. A. 2011. Prostaglandins and Inflammation. *Arterioscler Thromb Vasc Biol,* 31**,** 986-1000.

RINGE, J. D. & BODY, J. J. 2007. A review of bone pain relief with ibandronate and other bisphosphonates in disorders of increased bone turnover. *Clin Exp Rheumatol,* 25**,** 766-74.

RIVOLTINI, L., CARRABBA, M., HUBER, V., CASTELLI, C., NOVELLINO, L., DALERBA, P., MORTARINI, R., ARANCIA, G., ANICHINI, A., FAIS, S. & PARMIANI, G. 2002. Immunity to cancer: attack and escape in T lymphocyte-tumor cell interaction. *Immunol Rev,* 188**,** 97-113.

ROBERSON, D. P., BINSHTOK, A. M., BLASL, F., BEAN, B. P. & WOOLF, C. J. 2011. Targeting of sodium channel blockers into nociceptors to produce long-duration analgesia: a systematic study and review. *Br J Pharmacol,* 164**,** 48-58.

ROBERT, C. & WATSON, M. 2015. Errors in RNA-Seq quantification affect genes of relevance to human disease. *Genome Biology,* 16**,** 177.

ROBERTS, L. A. & CONNOR, M. 2006. TRPV1 antagonists as a potential treatment for hyperalgesia. *Recent Pat CNS Drug Discov,* 1**,** 65-76.

RODRIGUEZ PARKITNA, J., KOROSTYNSKI, M., KAMINSKA-CHOWANIEC, D., OBARA, I., MIKA, J., PRZEWLOCKA, B. & PRZEWLOCKI, R. 2006. Comparison of gene expression profiles in neuropathic and inflammatory pain. *J Physiol Pharmacol,* 57**,** 401-14.

ROJEWSKA, E., KOROSTYNSKI, M., PRZEWLOCKI, R., PRZEWLOCKA, B. & MIKA, J. 2014. Expression profiling of genes modulated by minocycline in a rat model of neuropathic pain. *Mol Pain,* 10**,** 47.

ROQUES, B. P., FOURNIÉ-ZALUSKI, M.-C. & WURM, M. 2012. Inhibiting the breakdown of endogenous opioids and cannabinoids to alleviate pain. *Nat Rev Drug Discov,* 11**,** 292-310.

ROSENBLUM, A., MARSCH, L. A., JOSEPH, H. & PORTENOY, R. K. 2008. Opioids and the Treatment of Chronic Pain: Controversies, Current Status, and Future Directions. *Experimental and clinical psychopharmacology,* 16**,** 405-416.

ROULOIS, D., BLANQUART, C., PANTERNE, C., GUEUGNON, F., GREGOIRE, M. & FONTENEAU, J. F. 2012. Downregulation of MUC1 expression and its recognition by CD8(+) T cells on the surface of malignant pleural mesothelioma cells treated with HDACi. *Eur J Immunol,* 42**,** 783-9.

ROYCHOWDHURY, S. & CHINNAIYAN, A. M. 2016. Translating cancer genomes and transcriptomes for precision oncology. *CA Cancer J Clin,* 66**,** 75-88.

ROZA, C., LAIRD, J. M. A., SOUSLOVA, V., WOOD, J. N. & CERVERO, F. 2003. The Tetrodotoxin-Resistant Na(+) Channel Nav1.8 is Essential for the Expression of Spontaneous Activity in Damaged Sensory Axons of Mice. *J Physiol,* 550**,** 921-6.

RUBOVITCH, V., GAFNI, M. & SARNE, Y. 2004. The involvement of VEGF receptors and MAPK in the cannabinoid potentiation of Ca2+ flux into N18TG2 neuroblastoma cells. *Brain Res Mol Brain Res,* 120**,** 138-44.

RUSH, A. M. & WAXMAN, S. G. 2004. PGE2 increases the tetrodotoxin-resistant Nav1.9 sodium current in mouse DRG neurons via G-proteins. *Brain Res,* 1023**,** 264-71.

SABINO, M. A., LUGER, N. M., MACH, D. B., ROGERS, S. D., SCHWEI, M. J. & MANTYH, P. W. 2003. Different tumors in bone each give rise to a distinct pattern of skeletal destruction, bone cancer-related pain behaviors and neurochemical changes in the central nervous system. *Int J Cancer,* 104**,** 550-8.

SACCHI, A., MAURO, F. & ZUPI, G. 1984. Changes of phenotypic characteristics of variants derived from Lewis lung carcinoma during long-term in vitro growth. *Clin Exp Metastasis,* 2**,** 171-8.

SADANA, R. & DESSAUER, C. W. 2009. Physiological roles for G protein-regulated adenylyl cyclase isoforms: insights from knockout and overexpression studies. *Neurosignals,* 17**,** 5-22.

SAITOH, S., AKASHI, S., YAMADA, T., TANIMURA, N., MATSUMOTO, F., FUKASE, K., KUSUMOTO, S., KOSUGI, A. & MIYAKE, K. 2004. Ligand-dependent Toll-like receptor 4 (TLR4)-oligomerization is directly linked with TLR4-signaling. *J Endotoxin Res,* 10**,** 257-60.

SAMAL, S. K., ROUTRAY, S., VEERAMACHANENI, G. K., DASH, R. & BOTLAGUNTA, M. 2015. Ketorolac salt is a newly discovered DDX3 inhibitor to treat oral cancer. *Sci Rep,* 5**,** 9982.

SANCHEZ-PEREZ, L., KOTTKE, T., DIAZ, R. M., AHMED, A., THOMPSON, J., CHONG, H., MELCHER, A., HOLMEN, S., DANIELS, G. & VILE, R. G. 2005. Potent Selection of Antigen Loss Variants of B16 Melanoma following Inflammatory Killing of Melanocytes In vivo. *Cancer Research,* 65**,** 2009-2017.

SANCHEZ, C., CHAN, R., BAJGAIN, P., RAMBALLY, S., PALAPATTU, G., MIMS, M., ROONEY, C. M., LEEN, A. M., BRENNER, M. K. & VERA, J. F. 2013. Combining T-cell immunotherapy and anti-androgen therapy for prostate cancer. *Prostate Cancer Prostatic Dis,* 16**,** 123-31, s1.

SANDKUHLER, J. 2009. Models and mechanisms of hyperalgesia and allodynia. *Physiol Rev,* 89**,** 707-58.

SÁNDOR, K., ELEKES, K., SZABÓ, Á., PINTÉR, E., ENGSTRÖM, M., WURSTER, S., SZOLCSÁNYI, J. & HELYES, Z. 2006. Analgesic effects of the somatostatin sst4 receptor selective agonist J-2156 in acute and chronic pain models. *European Journal of Pharmacology,* 539**,** 71-75.

SCHAIBLE, H. G. 2007. Peripheral and central mechanisms of pain generation. *Handb Exp Pharmacol***,** 3-28.

SCHAIBLE, H. G., DEL ROSSO, A. & MATUCCI-CERINIC, M. 2005. Neurogenic aspects of inflammation. *Rheum Dis Clin North Am,* 31**,** 77-101, ix.

SCHANOSKI, A. S., CAVALCANTI, T. C., CAMPOS, C. B., VIERA-MATOS, A. N., RETTORI, O. & GUIMARAES, F. 2004. Walker 256 tumor MHC class I expression during the shift from A variant to the immunogenic AR variant. *Cancer Lett,* 211**,** 119-27.

SCHMIDT, B. L. 2014. The Neurobiology of Cancer Pain. *Neuroscientist,* 20**,** 546-62.

SCHMIDTKO, A., GAO, W., SAUSBIER, M., RAUHMEIER, I., SAUSBIER, U., NIEDERBERGER, E., SCHOLICH, K., HUBER, A., NEUHUBER, W., ALLESCHER, H. D., HOFMANN, F., TEGEDER, I., RUTH, P. & GEISSLINGER, G. 2008. Cysteine-rich protein 2, a novel downstream effector of cGMP/cGMP-dependent protein kinase I-mediated persistent inflammatory pain. *J Neurosci,* 28**,** 1320-30.

SCHNEIDER, E. R., ANDERSON, E. O., GRACHEVA, E. O. & BAGRIANTSEV, S. N. 2014. Temperature sensitivity of two-pore (K2P) potassium channels. *Curr Top Membr,* 74**,** 113-33.

SCHUELERT, N., JUST, S., KUELZER, R., CORRADINI, L., GORHAM, L. C. J. & DOODS, H. 2015. The somatostatin receptor 4 agonist J-2156 reduces mechanosensitivity of peripheral

nerve afferents and spinal neurons in an inflammatory pain model. *European Journal of Pharmacology,* 746**,** 274-281.

SCHWAB, J. M. & SERHAN, C. N. 2006. Lipoxins and new lipid mediators in the resolution of inflammation. *Curr Opin Pharmacol,* 6**,** 414-20.

SCHWEI, M. J., HONORE, P., ROGERS, S. D., SALAK-JOHNSON, J. L., FINKE, M. P., RAMNARAINE, M. L., CLOHISY, D. R. & MANTYH, P. W. 1999. Neurochemical and cellular reorganization of the spinal cord in a murine model of bone cancer pain. *J Neurosci,* 19**,** 10886-97.

SCHWEIZERHOF, M., STOSSER, S., KUREJOVA, M., NJOO, C., GANGADHARAN, V., AGARWAL, N., SCHMELZ, M., BALI, K. K., MICHALSKI, C. W., BRUGGER, S., DICKENSON, A., SIMONE, D. A. & KUNER, R. 2009. Hematopoietic colony-stimulating factors mediate tumor-nerve interactions and bone cancer pain. *Nat Med,* 15**,** 802-7.

SCOTT, A. C., MCCONNELL, S., LAIRD, B., COLVIN, L. & FALLON, M. 2012. Quantitative Sensory Testing to assess the sensory characteristics of cancer-induced bone pain after radiotherapy and potential clinical biomarkers of response. *Eur J Pain,* 16**,** 123-33.

SCULLY, S., FRANCESCONE, R., FAIBISH, M., BENTLEY, B., TAYLOR, S. L., OH, D., SCHAPIRO, R., MORAL, L., YAN, W. & SHAO, R. 2012. Transdifferentiation of Glioblastoma Stem-Like Cells into Mural Cells Drives Vasculogenic Mimicry in Glioblastomas. *The Journal of Neuroscience,* 32**,** 12950-12960.

SELMER, I.-S., SCHINDLER, M., HUMPHREY, P. P. A., WALDVOGEL, H. J., FAULL, R. L. M. & EMSON, P. C. 2000a. First localisation of somatostatin sst4 receptor protein in selected human brain areas: an immunohistochemical study. *Molecular Brain Research,* 82**,** 114-125.

SELMER, I. S., SCHINDLER, M., HUMPHREY, P. P. A. & EMSON, P. C. 2000b. Immunohistochemical localization of the somatostatin sst4 receptor in rat brain. *Neuroscience,* 98**,** 523-533.

SERHAN, C. N. & SAVILL, J. 2005. Resolution of inflammation: the beginning programs the end. *Nat Immunol,* 6**,** 1191-7.

SEVCIK, M. A., JONAS, B. M., LINDSAY, T. H., HALVORSON, K. G., GHILARDI, J. R., KUSKOWSKI, M. A., MUKHERJEE, P., MAGGIO, J. E. & MANTYH, P. W. 2006. Endogenous opioids inhibit early-stage pancreatic pain in a mouse model of pancreatic cancer. *Gastroenterology,* 131**,** 900-10.

SHANKAR, J., MESSENBERG, A., CHAN, J., UNDERHILL, T. M., FOSTER, L. J. & NABI, I. R. 2010. Pseudopodial actin dynamics control epithelial-mesenchymal transition in metastatic cancer cells. *Cancer Res,* 70**,** 3780-90.

SHARMA, G. N., DAVE, R., SANADYA, J., SHARMA, P. & SHARMA, K. K. 2010. VARIOUS TYPES AND MANAGEMENT OF BREAST CANCER: AN OVERVIEW. *J Adv Pharm Technol Res,* 1**,** 109-26.

SHEKHANI, M. T., JAYANTHY, A. S., MADDODI, N. & SETALURI, V. 2013. Cancer stem cells and tumor transdifferentiation: implications for novel therapeutic strategies. *Am J Stem Cells,* 2**,** 52-61.

SHEN, W., HU, X. M., LIU, Y. N., HAN, Y., CHEN, L. P., WANG, C. C. & SONG, C. 2014. CXCL12 in astrocytes contributes to bone cancer pain through CXCR4-mediated neuronal sensitization and glial activation in rat spinal cord. *J Neuroinflammation,* 11**,** 75.

SHENOY, P., KUO, A., VETTER, I. & SMITH, M. T. 2017. Optimization and In Vivo Profiling of a Refined Rat Model of Walker 256 Breast Cancer Cell-Induced Bone Pain Using Behavioral, Radiological, Histological, Immunohistochemical and Pharmacological Methods. *Frontiers in Pharmacology,* 8.

SHENOY, P. A., KUO, A., VETTER, I. & SMITH, M. T. 2016. The Walker 256 Breast Cancer Cell-Induced Bone Pain Model in Rats. *Frontiers in Pharmacology,* 7.

SHI, L.-L., ZHANG, N., XIE, X.-M., CHEN, Y.-J., WANG, R., SHEN, L., ZHOU, J.-S., HU, J.-G. & LÜ, H.-Z. 2017. Transcriptome profile of rat genes in injured spinal cord at different stages by RNA-sequencing. *BMC Genomics,* 18**,** 173.

SHIH, L. Y., SHIH, H. N. & CHEN, T. H. 2004. Bone resorption activity of osteolytic metastatic lung and breast cancers. *J Orthop Res,* 22**,** 1161-7.

SHIH, M.-H., KAO, S.-C., WANG, W., YASTER, M. & TAO, Y.-X. 2012. Spinal Cord NMDA Receptor-Mediated Activation of Mammalian Target of Rapamycin Is Required for the Development and Maintenance of Bone Cancer-Induced Pain Hypersensitivities in Rats. *The Journal of Pain,* 13**,** 338-349.

SIGHOKO, D., LIU, J., HOU, N., GUSTAFSON, P. & HUO, D. 2014. Discordance in Hormone Receptor Status Among Primary, Metastatic, and Second Primary Breast Cancers: Biological Difference or Misclassification? *Oncologist,* 19**,** 592-601.

SILLS, G. J. 2006. The mechanisms of action of gabapentin and pregabalin. *Curr Opin Pharmacol,* 6**,** 108-13.

SIMA, L., FAN, B., YAN, L. & SHUI, Y. 2016. Effects of Electroacupuncture Treatment on Bone Cancer Pain Model with Morphine Tolerance. *Evid Based Complement Alternat Med,* 2016**,** 8028474.

SIMMONS, J. K., HILDRETH, B. E., SUPSAVHAD, W., ELSHAFAE, S. M., HASSAN, B. B., DIRKSEN, W. P., TORIBIO, R. E. & ROSOL, T. J. 2015. Animal Models of Bone Metastasis. *Vet Pathol,* 52**,** 827-41.

SIMONETTI, M., HAGENSTON, A. M., VARDEH, D., FREITAG, H. E., MAUCERI, D., LU, J., SATAGOPAM, V. P., SCHNEIDER, R., COSTIGAN, M., BADING, H. & KUNER, R. 2013. Nuclear calcium signaling in spinal neurons drives a genomic program required for persistent inflammatory pain. *Neuron,* 77**,** 43-57.

SIMPKINS, H., LEHMAN, J. M., MAZURKIEWICZ, J. E. & DAVIS, B. H. 1991. A morphological and phenotypic analysis of Walker 256 cells. *Cancer Res,* 51**,** 1334-8.

SINGH, A., SIROHI, B. & GUPTA, S. 2013. Biomarkers in Breast Cancer and the Implications of Their Discordance. *Current Breast Cancer Reports,* 5**,** 266-274.

SLADE, M. J. & COOMBES, R. C. 2007. The clinical significance of disseminated tumor cells in breast cancer. *Nat Clin Prac Oncol,* 4**,** 30-41.

SLOSKY, L. M., LARGENT-MILNES, T. M. & VANDERAH, T. W. 2015. Use of Animal Models in Understanding Cancer-induced Bone Pain. *Cancer Growth Metastasis,* 8**,** 47-62.

SMITH, M. T., WYSE, B. D. & EDWARDS, S. R. 2013. Small molecule angiotensin II type 2 receptor (AT(2)R) antagonists as novel analgesics for neuropathic pain: comparative pharmacokinetics, radioligand binding, and efficacy in rats. *Pain Med,* 14**,** 692-705.

SOMERS, T. J., KEEFE, F. J., PELLS, J. J., DIXON, K. E., WATERS, S. J., RIORDAN, P. A., BLUMENTHAL, J. A., MCKEE, D. C., LACAILLE, L., TUCKER, J. M., SCHMITT, D., CALDWELL, D. S., KRAUS, V. B., SIMS, E. L., SHELBY, R. A. & RICE, J. R. 2009. Pain Catastrophizing and Pain-Related Fear in Osteoarthritis Patients: Relationships to Pain and Disability. *Journal of Pain and Symptom Management,* 37**,** 863-872.

SOMLO, G., LAU, S. K., FRANKEL, P., HSIEH, H. B., LIU, X., YANG, L., KRIVACIC, R. & BRUCE, R. H. 2011. Multiple biomarker expression on circulating tumor cells in comparison to tumor tissues from primary and metastatic sites in patients with locally advanced/inflammatory, and stage IV breast cancer, using a novel detection technology. *Breast Cancer Res Treat,* 128**,** 155-63.

SOMVANSHI, R. K. & KUMAR, U. 2014. delta-opioid receptor and somatostatin receptor-4 heterodimerization: possible implications in modulation of pain associated signaling. *PLoS One,* 9**,** e85193.

SONG, H., HAN, Y., PAN, C., DENG, X., DAI, W., HU, L., JIANG, C., YANG, Y., CHENG, Z., LI, F., ZHANG, G., WU, X. & LIU, W. 2015. Activation of Adenosine Monophosphate-activated Protein Kinase Suppresses Neuroinflammation and Ameliorates Bone Cancer Pain: Involvement of Inhibition on Mitogen-activated Protein Kinase. *Anesthesiology,* 123**,** 1170-85.

SONG, S. H., LENG, X. S., LI, T., QIN, Z. Z., PENG, J. R., ZHAO, L., WEI, Y. H. & YU, X. 2004. Expression of subtypes of somatostatin receptors in hepatic stellate cells. *World J Gastroenterol,* 10**,** 1663-5.

SONG, Z., XIONG, B., ZHENG, H., MANYANDE, A., GUAN, X., CAO, F., REN, L., ZHOU, Y., YE, D. & TIAN, Y. 2017. STAT1 as a downstream mediator of ERK signaling contributes to bone cancer pain by regulating MHC II expression in spinal microglia. *Brain Behav Immun,* 60**,** 161-173.

SONG, Z. P., XIONG, B. R., GUAN, X. H., CAO, F., MANYANDE, A., ZHOU, Y. Q., ZHENG, H. & TIAN, Y. K. 2016. Minocycline attenuates bone cancer pain in rats by inhibiting NF-kappaB in spinal astrocytes. *Acta Pharmacol Sin,* 37**,** 753-62.

SORGE, R. E., MAPPLEBECK, J. C. S., ROSEN, S., BEGGS, S., TAVES, S., ALEXANDER, J. K., MARTIN, L. J., AUSTIN, J.-S., SOTOCINAL, S. G., CHEN, D., YANG, M., SHI, X. Q., HUANG, H., PILLON, N. J., BILAN, P. J., TU, Y., KLIP, A., JI, R.-R., ZHANG, J., SALTER, M. W. & MOGIL, J. S. 2015. Different immune cells mediate mechanical pain hypersensitivity in male and female mice. *Nat Neurosci,* 18**,** 1081-1083.

SORGE, R. E., MARTIN, L. J., ISBESTER, K. A., SOTOCINAL, S. G., ROSEN, S., TUTTLE, A. H., WIESKOPF, J. S., ACLAND, E. L., DOKOVA, A., KADOURA, B., LEGER, P., MAPPLEBECK, J. C. S., MCPHAIL, M., DELANEY, A., WIGERBLAD, G., SCHUMANN, A. P., QUINN, T., FRASNELLI, J., SVENSSON, C. I., STERNBERG, W. F. & MOGIL, J. S. 2014. Olfactory exposure to males, including men, causes stress and related analgesia in rodents. *Nat Meth,* 11**,** 629-632.

SOUTH, S. M., EDWARDS, S. R. & SMITH, M. T. 2009. Antinociception versus serum concentration relationships following acute administration of intravenous morphine in male and female Sprague-Dawley rats: differences between the tail flick and hot plate nociceptive tests. *Clin Exp Pharmacol Physiol,* 36**,** 20-8.

SROKA, I. C., ANDERSON, T. A., MCDANIEL, K. M., NAGLE, R. B., GRETZER, M. B. & CRESS, A. E. 2010. The Laminin Binding Integrin α6β1 in Prostate Cancer Perineural Invasion. *J Cell Physiol,* 224**,** 283-8.

SROKA, J., KRECIOCH, I., ZIMOLAG, E., LASOTA, S., RAK, M., KEDRACKA-KROK, S., BOROWICZ, P., GAJEK, M. & MADEJA, Z. 2016. Lamellipodia and Membrane Blebs Drive Efficient Electrotactic Migration of Rat Walker Carcinosarcoma Cells WC 256. *PLoS One,* 11**,** e0149133.

ST. ROMAIN, P., MADAN, R., TAWFIK, O. W., DAMJANOV, I. & FAN, F. 2012. Organotropism and prognostic marker discordance in distant metastases of breast carcinoma: fact or fiction? A clinicopathologic analysis. *Human Pathology,* 43**,** 398-404.

STAUD, R., WEYL, E. E., PRICE, D. D. & ROBINSON, M. E. 2012. Mechanical and Heat Hyperalgesia Highly Predict Clinical Pain Intensity in Patients With Chronic Musculoskeletal Pain Syndromes. *J Pain,* 13**,** 725-35.

STEIN, C. & LANG, L. J. 2009. Peripheral mechanisms of opioid analgesia. *Curr Opin Pharmacol,* 9**,** 3-8.

STOECKER, M. M. & WANG, E. 2013. Histiocytic/dendritic cell transformation of B-cell neoplasms: pathologic evidence of lineage conversion in differentiated hematolymphoid malignancies. *Arch Pathol Lab Med,* 137**,** 865-70.

STONE, L. S. & MOLLIVER, D. C. 2009. In search of analgesia: emerging roles of GPCRs in pain. *Mol Interv,* 9**,** 234-51.

STRØBÆK, D., BROWN, D., JENKINS, D., CHEN, Y., COLEMAN, N., ANDO, Y., CHIU, P., JØRGENSEN, S., DEMNITZ, J., WULFF, H. & CHRISTOPHERSEN, P. 2013. NS6180, a

new K(Ca)3.1 channel inhibitor prevents T-cell activation and inflammation in a rat model of inflammatory bowel disease. *Br J Pharmacol,* 168**,** 432-44.

STURGEON, C. M., DUFFY, M. J., STENMAN, U.-H., LILJA, H., BRÜNNER, N., CHAN, D. W., BABAIAN, R., BAST, R. C., DOWELL, B., ESTEVA, F. J., HAGLUND, C., HARBECK, N., HAYES, D. F., HOLTEN-ANDERSEN, M., KLEE, G. G., LAMERZ, R., LOOIJENGA, L. H., MOLINA, R., NIELSEN, H. J., RITTENHOUSE, H., SEMJONOW, A., SHIH, I.-M., SIBLEY, P., SÖLÉTORMOS, G., STEPHAN, C., SOKOLL, L., HOFFMAN, B. R. & DIAMANDIS, E. P. 2008. National Academy of Clinical Biochemistry Laboratory Medicine Practice Guidelines for Use of Tumor Markers in Testicular, Prostate, Colorectal, Breast, and Ovarian Cancers. *Clinical Chemistry,* 54**,** e11-e79.

SUDO, H., TSUJI, A. B., SUGYO, A., ABE, M., HINO, O. & SAGA, T. 2014. AHNAK is highly expressed and plays a key role in cell migration and invasion in mesothelioma. *Int J Oncol,* 44**,** 530-8.

SUGHRUE, M. E., LEVINE, J. & BARBARO, N. M. 2008. Pain as a symptom of peripheral nerve sheath tumors: clinical significance and future therapeutic directions. *J Brachial Plex Peripher Nerve Inj,* 3**,** 6.

SUN, Y., TIAN, Y., LI, H., ZHANG, D. & SUN, Q. 2017a. Antinociceptive Effect of Intrathecal Injection of Genetically Engineered Human Bone Marrow Stem Cells Expressing the Human Proenkephalin Gene in a Rat Model of Bone Cancer Pain. *Pain Research and Management,* 2017**,** 11.

SUN, Y., WU, Y. X., ZHANG, P., PENG, G. & YU, S. Y. 2017b. Anti-rheumatic drug iguratimod protects against cancer-induced bone pain and bone destruction in a rat model. *Oncol Lett,* 13**,** 4849-4856.

SYDER, A. J., KARAM, S. M., MILLS, J. C., IPPOLITO, J. E., ANSARI, H. R., FAROOK, V. & GORDON, J. I. 2004. A transgenic mouse model of metastatic carcinoma involving transdifferentiation of a gastric epithelial lineage progenitor to a neuroendocrine phenotype. *Proceedings of the National Academy of Sciences of the United States of America,* 101**,** 4471-4476.

SZKLARCZYK, D., FRANCESCHINI, A., WYDER, S., FORSLUND, K., HELLER, D., HUERTA-CEPAS, J., SIMONOVIC, M., ROTH, A., SANTOS, A., TSAFOU, K. P., KUHN, M., BORK, P., JENSEN, L. J. & VON MERING, C. 2015. STRING v10: protein-protein interaction networks, integrated over the tree of life. *Nucleic Acids Res,* 43**,** D447-52.

SZOKOLOCZI, O., SCHWAB, R., PETAK, I., ORFI, L., PAP, A., EBERLE, A. N., SZUTS, T. & KERIL, G. 2005. TT232, a novel signal transduction inhibitory compound in the therapy of cancer and inflammatory diseases. *J Recept Signal Transduct Res,* 25**,** 217-35.

SZOLCSANYI, J., BOLCSKEI, K., SZABO, A., PINTER, E., PETHO, G., ELEKES, K., BORZSEI, R., ALMASI, R., SZUTS, T., KERI, G. & HELYES, Z. 2004. Analgesic effect of TT-232, a

heptapeptide somatostatin analogue, in acute pain models of the rat and the mouse and in streptozotocin-induced diabetic mechanical allodynia. *Eur J Pharmacol,* 498**,** 103-9.

SZOLCSANYI, J., PINTER, E., HELYES, Z. & PETHO, G. 2011. Inhibition of the function of TRPV1-expressing nociceptive sensory neurons by somatostatin 4 receptor agonism: mechanism and therapeutical implications. *Curr Top Med Chem,* 11**,** 2253-63.

TAIPALEENMÄKI, H., BROWNE, G., AKECH, J., ZUSTIN, J., VAN WIJNEN, A. J., STEIN, J. L., HESSE, E., STEIN, G. S. & LIAN, J. B. 2015. Targeting of Runx2 by miR-135 and miR-203 Impairs Progression of Breast Cancer and Metastatic Bone Disease. *Cancer Research,* 75**,** 1433-1444.

TAPPE-THEODOR, A., CONSTANTIN, C. E., TEGEDER, I., LECHNER, S. G., LANGESLAG, M., LEPCYNZSKY, P., WIROTANSENG, R. I., KUREJOVA, M., AGARWAL, N., NAGY, G., TODD, A., WETTSCHURECK, N., OFFERMANNS, S., KRESS, M., LEWIN, G. R. & KUNER, R. 2012. Galpha(q/11) signaling tonically modulates nociceptor function and contributes to activity-dependent sensitization. *Pain,* 153**,** 184-96.

TARAZONA, S., GARCÍA-ALCALDE, F., DOPAZO, J., FERRER, A. & CONESA, A. 2011. Differential expression in RNA-seq: A matter of depth. *Genome Res,* 21**,** 2213-23.

TATE, S., BENN, S., HICK, C., TREZISE, D., JOHN, V., MANNION, R. J., COSTIGAN, M., PLUMPTON, C., GROSE, D., GLADWELL, Z., KENDALL, G., DALE, K., BOUNTRA, C. & WOOLF, C. J. 1998. Two sodium channels contribute to the TTX-R sodium current in primary sensory neurons. *Nat Neurosci,* 1**,** 653-5.

TATSUMI, S., MABUCHI, T., KATANO, T., MATSUMURA, S., ABE, T., HIDAKA, H., SUZUKI, M., SASAKI, Y., MINAMI, T. & ITO, S. 2005. Involvement of Rho-kinase in inflammatory and neuropathic pain through phosphorylation of myristoylated alanine-rich C-kinase substrate (MARCKS). *Neuroscience,* 131**,** 491-8.

TENA, B., ESCOBAR, B., ARGUIS, M. J., CANTERO, C., RIOS, J. & GOMAR, C. 2012. Reproducibility of Electronic Von Frey and Von Frey monofilaments testing. *Clin J Pain,* 28**,** 318-23.

TERRY, S. & BELTRAN, H. 2014. The Many Faces of Neuroendocrine Differentiation in Prostate Cancer Progression. *Frontiers in Oncology,* 4.

THOMPSON, A. M., JORDAN, L. B., QUINLAN, P., ANDERSON, E., SKENE, A., DEWAR, J. A. & PURDIE, C. A. 2010. Prospective comparison of switches in biomarker status between primary and recurrent breast cancer: the Breast Recurrence In Tissues Study (BRITS). *Breast Cancer Res,* 12**,** R92.

TIAN, H., LIU, X., HAN, W., ZHAO, L., YUAN, B. & YUAN, C. 2013. Differential expression of filamin A and its clinical significance in breast cancer. *Oncol Lett,* 6**,** 681-6.

TICHONOVA, A., RIMDEIKIENĖ, I., PETRUŠEVIČIENĖ, D. & LENDRAITIENĖ, E. 2016. The relationship between pain catastrophizing, kinesiophobia and subjective knee function

during rehabilitation following anterior cruciate ligament reconstruction and meniscectomy: A pilot study. *Medicina,* 52**,** 229-237.

TOMURA, H., MOGI, C., SATO, K. & OKAJIMA, F. 2005. Proton-sensing and lysolipid-sensitive G-protein-coupled receptors: a novel type of multi-functional receptors. *Cell Signal,* 17**,** 1466-76.

TONETO, A. T., FERREIRA RAMOS, L. A., SALOMAO, E. M., TOMASIN, R., AEREAS, M. A. & GOMES-MARCONDES, M. C. 2016. Nutritional leucine supplementation attenuates cardiac failure in tumour-bearing cachectic animals. *J Cachexia Sarcopenia Muscle*.

TONG, W., WANG, W., HUANG, J., REN, N., WU, S. X. & LI, Y. Q. 2010a. Spinal high-mobility group box 1 contributes to mechanical allodynia in a rat model of bone cancer pain. *Biochem Biophys Res Commun,* 395**,** 572-6.

TONG, Z., LUO, W., WANG, Y., YANG, F., HAN, Y., LI, H., LUO, H., DUAN, B., XU, T., MAOYING, Q., TAN, H., WANG, J., ZHAO, H., LIU, F. & WAN, Y. 2010b. Tumor tissue-derived formaldehyde and acidic microenvironment synergistically induce bone cancer pain. *PLoS One,* 5**,** e10234.

TORRANO, V., VALCARCEL-JIMENEZ, L., CORTAZAR, A. R., LIU, X., UROSEVIC, J., CASTILLO-MARTIN, M., FERNANDEZ-RUIZ, S., MORCIANO, G., CARO-MALDONADO, A., GUIU, M., ZUNIGA-GARCIA, P., GRAUPERA, M., BELLMUNT, A., PANDYA, P., LORENTE, M., MARTIN-MARTIN, N., DAVID SUTHERLAND, J., SANCHEZ-MOSQUERA, P., BOZAL-BASTERRA, L., ZABALA-LETONA, A., ARRUABARRENA-ARISTORENA, A., BERENGUER, A., EMBADE, N., UGALDE-OLANO, A., LACASA-VISCASILLAS, I., LOIZAGA-IRIARTE, A., UNDA-URZAIZ, M., SCHULTZ, N., ARANSAY, A. M., SANZ-MORENO, V., BARRIO, R., VELASCO, G., PINTON, P., CORDON-CARDO, C., LOCASALE, J. W., GOMIS, R. R. & CARRACEDO, A. 2016. The metabolic co-regulator PGC1[alpha] suppresses prostate cancer metastasis. *Nat Cell Biol,* 18**,** 645-656.

TORRE, L. A., BRAY, F., SIEGEL, R. L., FERLAY, J., LORTET-TIEULENT, J. & JEMAL, A. 2015. Global cancer statistics, 2012. *CA: A Cancer Journal for Clinicians,* 65**,** 87-108.

TOZAKI-SAITOH, H., TSUDA, M., MIYATA, H., UEDA, K., KOHSAKA, S. & INOUE, K. 2008. P2Y12 receptors in spinal microglia are required for neuropathic pain after peripheral nerve injury. *J Neurosci,* 28**,** 4949-56.

TRASHKOV, A. P., VASIL'EV, A. G., KOVALENKO, A. L., PETROV, A. Y. & VALEEV, V. V. 2016. [INFLUENCE OF ANGIOPROTECTOR DRUGS ON THE EFFICACY OF CYTOSTATIC THERAPY (EXPERIMENTAL STUDY)]. *Eksp Klin Farmakol,* 79**,** 34-9.

TSANTOULAS, C. & MCMAHON, S. B. 2014. Opening paths to novel analgesics: the role of potassium channels in chronic pain. *Trends Neurosci,* 37**,** 146-58.

TSUDA, M., KOIZUMI, S., KITA, A., SHIGEMOTO, Y., UENO, S. & INOUE, K. 2000. Mechanical allodynia caused by intraplantar injection of P2X receptor agonist in rats: involvement of

heteromeric P2X2/3 receptor signaling in capsaicin-insensitive primary afferent neurons. *J Neurosci,* 20**,** Rc90.

TSUZUKI, S., PARK, S. H., EBER, M. R., PETERS, C. M. & SHIOZAWA, Y. 2016. Skeletal complications in cancer patients with bone metastases. *Int J Urol*.

TU, J. C., XIAO, B., YUAN, J. P., LANAHAN, A. A., LEOFFERT, K., LI, M., LINDEN, D. J. & WORLEY, P. F. 1998. Homer binds a novel proline-rich motif and links group 1 metabotropic glutamate receptors with IP3 receptors. *Neuron,* 21**,** 717-26.

TURA, B. & TURA, S. M. 1990. The analgesic effect of tricyclic antidepressants. *Brain Res,* 518**,** 19-22.

TURNER, N. H. & DI LEO, A. 2013. HER2 discordance between primary and metastatic breast cancer: assessing the clinical impact. *Cancer Treat Rev,* 39**,** 947-57.

TUTTLE, A. H., TOHYAMA, S., RAMSAY, T., KIMMELMAN, J., SCHWEINHARDT, P., BENNETT, G. J. & MOGIL, J. S. 2015. Increasing placebo responses over time in U.S. clinical trials of neuropathic pain. *Pain,* 156**,** 2616-26.

UL-MULK, J., RASMUSSEN, H., BREITING, L. & SIIM, E. 2012. A case of collision tumor or transdifferentiation between malignant melanoma and leiomyosarcoma. *Indian Journal of Pathology and Microbiology,* 55**,** 538-539.

UNGARD, R. G., SEIDLITZ, E. P. & SINGH, G. 2014. Inhibition of breast cancer-cell glutamate release with sulfasalazine limits cancer-induced bone pain. *Pain,* 155**,** 28-36.

URCH, C. 2004. The pathophysiology of cancer-induced bone pain: current understanding. *Palliat Med,* 18**,** 267-74.

URCH, C. E., DONOVAN-RODRIGUEZ, T. & DICKENSON, A. H. 2003. Alterations in dorsal horn neurones in a rat model of cancer-induced bone pain. *Pain,* 106**,** 347-56.

UTRERAS, E., KELLER, J., TERSE, A., PROCHAZKOVA, M., IADAROLA, M. J. & KULKARNI, A. B. 2012. Transforming growth factor-beta1 regulates Cdk5 activity in primary sensory neurons. *J Biol Chem,* 287**,** 16917-29.

VACCA, V., MARINELLI, S., PIERONI, L., URBANI, A., LUVISETTO, S. & PAVONE, F. 2014. Higher pain perception and lack of recovery from neuropathic pain in females: a behavioural, immunohistochemical, and proteomic investigation on sex-related differences in mice. *Pain,* 155**,** 388-402.

VACCA, V., MARINELLI, S., PIERONI, L., URBANI, A., LUVISETTO, S. & PAVONE, F. 2016. 17beta-estradiol counteracts neuropathic pain: a behavioural, immunohistochemical, and proteomic investigation on sex-related differences in mice. *Sci Rep,* 6**,** 18980.

VAN DORP, E., YASSEN, A. & DAHAN, A. 2007. Naloxone treatment in opioid addiction: the risks and benefits. *Expert Opin Drug Saf,* 6**,** 125-32.

VARAMINI, P., MANSFELD, F. M., BLANCHFIELD, J. T., WYSE, B. D., SMITH, M. T. & TOTH, I. 2012. Lipo-endomorphin-1 derivatives with systemic activity against neuropathic pain without producing constipation. *PLoS One,* 7**,** e41909.

VARECZA, Z., ELEKES, K., LÁSZLÓ, T., PERKECZ, A., PINTÉR, E., SÁNDOR, Z., SZOLCSÁNYI, J., KESZTHELYI, D., SZABÓ, Á., SÁNDOR, K., MOLNÁR, T. F., SZÁNTÓ, Z., PONGRÁCZ, J. E. & HELYES, Z. 2009. Expression of the Somatostatin Receptor Subtype 4 in Intact and Inflamed Pulmonary Tissues. *Journal of Histochemistry & Cytochemistry,* 57**,** 1127-1137.

VARGO-GOGOLA, T. & ROSEN, J. M. 2007. Modelling breast cancer: one size does not fit all. *Nat Rev Cancer,* 7**,** 659-672.

VILLALBA, M., RATHORE, M. G., LOPEZ-ROYUELA, N., KRZYWINSKA, E., GARAUDE, J. & ALLENDE-VEGA, N. 2013. From tumor cell metabolism to tumor immune escape. *Int J Biochem Cell Biol,* 45**,** 106-13.

VINCENT, H. K., ADAMS, M. C., VINCENT, K. R. & HURLEY, R. W. 2013. Musculoskeletal pain, fear avoidance behaviors, and functional decline in obesity: potential interventions to manage pain and maintain function. *Reg Anesth Pain Med,* 38**,** 481-91.

VLAEYEN, J. W. S. & LINTON, S. J. 2000. Fear-avoidance and its consequences in chronic musculoskeletal pain: a state of the art. *Pain,* 85**,** 317-332.

VLEMS, F. A., RUERS, T. J. M., PUNT, C. J. A., WOBBES, T. & VAN MUIJEN, G. N. P. 2003. Relevance of disseminated tumour cells in blood and bone marrow of patients with solid epithelial tumours in perspective. *European Journal of Surgical Oncology (EJSO),* 29**,** 289-302.

VOSS, M. J. & ENTSCHLADEN, F. 2010. Tumor interactions with soluble factors and the nervous system. *Cell Communication and Signaling,* 8**,** 1-6.

VOULGARI, A. & PINTZAS, A. 2009. Epithelial–mesenchymal transition in cancer metastasis: Mechanisms, markers and strategies to overcome drug resistance in the clinic. *Biochimica et Biophysica Acta (BBA) - Reviews on Cancer,* 1796**,** 75-90.

VRIENS, J., OWSIANIK, G., HOFMANN, T., PHILIPP, S. E., STAB, J., CHEN, X., BENOIT, M., XUE, F., JANSSENS, A., KERSELAERS, S., OBERWINKLER, J., VENNEKENS, R., GUDERMANN, T., NILIUS, B. & VOETS, T. 2011. TRPM3 is a nociceptor channel involved in the detection of noxious heat. *Neuron,* 70**,** 482-94.

WACHOWSKA, M., MUCHOWICZ, A. & GOLAB, J. 2015. Targeting Epigenetic Processes in Photodynamic Therapy-Induced Anticancer Immunity. *Frontiers in Oncology,* 5.

WAGNER, R., DELEO, J. A., COOMBS, D. W., WILLENBRING, S. & FROMM, C. 1993. Spinal dynorphin immunoreactivity increases bilaterally in a neuropathic pain model. *Brain Res,* 629**,** 323-6.

WALKER, K., FOX, A. J. & URBAN, L. A. 1999. Animal models for pain research. *Mol Med Today,* 5**,** 319-21.

WALPOLE, A. L. 1951. The Walker carcinoma 256 in the screening of tumour inhibitors. *Br J Pharmacol Chemother,* 6**,** 135-43.

WANG, J., CAO, D. Y., GUO, Y., MA, S. J., LUO, R., PICKAR, J. G. & ZHAO, Y. 2011a. Octreotide inhibits capsaicin-induced activation of C and Adelta afferent fibres in rat hairy skin in vivo. *Clin Exp Pharmacol Physiol,* 38**,** 521-7.

WANG, J., GUO, Y., CAO, D. Y., LUO, R., MA, S. J., WANG, H. S., PICKAR, J. G. & ZHAO, Y. 2009a. Tonic inhibition of somatostatin on C and Adelta afferent fibers in rat dorsal skin in vivo. *Brain Res,* 1288**,** 50-9.

WANG, J., ZHANG, R., DONG, C., JIAO, L., XU, L., LIU, J., WANG, Z. & LAO, L. 2015. Transient Receptor Potential Channel and Interleukin-17A Involvement in LTTL Gel Inhibition of Bone Cancer Pain in a Rat Model. *Integrative Cancer Therapies,* 14**,** 381-393.

WANG, J., ZHANG, R., DONG, C., JIAO, L., XU, L., LIU, J., WANG, Z., MAO YING, Q. L., FONG, H. & LAO, L. 2012a. Topical treatment with Tong-Luo-San-Jie gel alleviates bone cancer pain in rats. *J Ethnopharmacol,* 143**,** 905-13.

WANG, L. N., YANG, J. P., JI, F. H., ZHAN, Y., JIN, X. H., XU, Q. N., WANG, X. Y. & ZUO, J. L. 2012b. Brain-derived neurotrophic factor modulates N-methyl-D-aspartate receptor activation in a rat model of cancer-induced bone pain. *J Neurosci Res,* 90**,** 1249-60.

WANG, L. N., YANG, J. P., ZHAN, Y., JI, F. H., WANG, X. Y., ZUO, J. L. & XU, Q. N. 2012c. Minocycline-induced reduction of brain-derived neurotrophic factor expression in relation to cancer-induced bone pain in rats. *J Neurosci Res,* 90**,** 672-81.

WANG, L. N., YAO, M., YANG, J. P., PENG, J., PENG, Y., LI, C. F., ZHANG, Y. B., JI, F. H., CHENG, H., XU, Q. N., WANG, X. Y. & ZUO, J. L. 2011b. Cancer-induced bone pain sequentially activates the ERK/MAPK pathway in different cell types in the rat spinal cord. *Mol Pain,* 7**,** 48.

WANG, S. F., DONG, C. G., YANG, X. & YIN, J. J. 2016a. Upregulation of (C-X-C motif) Ligand 13 (CXCL13) Attenuates Morphine Analgesia in Rats with Cancer-Induced Bone Pain. *Med Sci Monit,* 22**,** 4612-4622.

WANG, W., GU, J., LI, Y. Q. & TAO, Y. X. 2011c. Are voltage-gated sodium channels on the dorsal root ganglion involved in the development of neuropathic pain? *Mol Pain,* 7**,** 16.

WANG, X., KRUITHOF-DE JULIO, M., ECONOMIDES, K. D., WALKER, D., YU, H., HALILI, M. V., HU, Y. P., PRICE, S. M., ABATE-SHEN, C. & SHEN, M. M. 2009b. A luminal epithelial stem cell that is a cell of origin for prostate cancer. *Nature,* 461**,** 495-500.

WANG, X. W., HU, S., MAO-YING, Q. L., LI, Q., YANG, C. J., ZHANG, H., MI, W. L., WU, G. C. & WANG, Y. Q. 2012d. Activation of c-jun N-terminal kinase in spinal cord contributes to breast cancer induced bone pain in rats. *Mol Brain,* 5**,** 21.

WANG, X. W., LI, T. T., ZHAO, J., MAO-YING, Q. L., ZHANG, H., HU, S., LI, Q., MI, W. L., WU, G. C., ZHANG, Y. Q. & WANG, Y. Q. 2012e. Extracellular signal-regulated kinase activation in spinal astrocytes and microglia contributes to cancer-induced bone pain in rats. *Neuroscience,* 217**,** 172-81.

WANG, Z. L., DU, T. T. & ZHANG, R. G. 2016b. JNK in spinal cord facilitates bone cancer pain in rats through modulation of CXCL1. *J Huazhong Univ Sci Technolog Med Sci,* 36**,** 88-94.

WARNECKE, M., OSTER, H., REVELLI, J. P., ALVAREZ-BOLADO, G. & EICHELE, G. 2005. Abnormal development of the locus coeruleus in Ear2(Nr2f6)-deficient mice impairs the functionality of the forebrain clock and affects nociception. *Genes Dev,* 19**,** 614-25.

WASZKIELEWICZ, A., GUNIA, A., SZKARADEK, N., SŁOCZYŃSKA, K., KRUPIŃSKA, S. & MARONA, H. 2013. Ion Channels as Drug Targets in Central Nervous System Disorders. *Curr Med Chem,* 20**,** 1241-85.

WATANABE, H., VRIENS, J., SUH, S. H., BENHAM, C. D., DROOGMANS, G. & NILIUS, B. 2002. Heat-evoked activation of TRPV4 channels in a HEK293 cell expression system and in native mouse aorta endothelial cells. *J Biol Chem,* 277**,** 47044-51.

WATT, H. L. & KUMAR, U. 2006. Colocalization of somatostatin receptors and epidermal growth factor receptors in breast cancer cells. *Cancer Cell International,* 6**,** 5.

WEBB, T. E., SIMON, J., BATESON, A. N. & BARNARD, E. A. 1994. Transient expression of the recombinant chick brain P2y1 purinoceptor and localization of the corresponding mRNA. *Cell Mol Biol (Noisy-le-grand),* 40**,** 437-42.

WECKBECKER, G., LEWIS, I., ALBERT, R., SCHMID, H. A., HOYER, D. & BRUNS, C. 2003. Opportunities in somatostatin research: biological, chemical and therapeutic aspects. *Nat Rev Drug Discov,* 2**,** 999-1017.

WEI, F., VADAKKAN, K. I., TOYODA, H., WU, L. J., ZHAO, M. G., XU, H., SHUM, F. W., JIA, Y. H. & ZHUO, M. 2006. Calcium calmodulin-stimulated adenylyl cyclases contribute to activation of extracellular signal-regulated kinase in spinal dorsal horn neurons in adult rats and mice. *J Neurosci,* 26**,** 851-61.

WENG, T. Y., WANG, C. Y., HUNG, Y. H., CHEN, W. C., CHEN, Y. L. & LAI, M. D. 2016. Differential Expression Pattern of THBS1 and THBS2 in Lung Cancer: Clinical Outcome and a Systematic-Analysis of Microarray Databases. *PLoS One,* 11**,** e0161007.

WHITESCARVER, J. 1974. Problems of In Vitro Culture of Human Mammary Tumor Cells. *Journal of Investigative Dermatology,* 63**,** 58-64.

WHITESIDE, G. T., HARRISON, J., BOULET, J., MARK, L., PEARSON, M., GOTTSHALL, S. & WALKER, K. 2004. Pharmacological characterisation of a rat model of incisional pain. *Br J Pharmacol,* 141**,** 85-91.

WIESENFELD-HALLIN, Z. 2005. Sex differences in pain perception. *Gender Medicine,* 2**,** 137-145.

WILSON, S. G. & MOGIL, J. S. 2001. Measuring pain in the (knockout) mouse: big challenges in a small mammal. *Behav Brain Res,* 125**,** 65-73.

WITTMACK, E. K., RUSH, A. M., HUDMON, A., WAXMAN, S. G. & DIB-HAJJ, S. D. 2005. Voltage-gated sodium channel Nav1.6 is modulated by p38 mitogen-activated protein kinase. *J Neurosci,* 25**,** 6621-30.

WOELFLE, U., SAUTER, G., SANTJER, S., BRAKENHOFF, R. & PANTEL, K. 2004. Down-regulated expression of cytokeratin 18 promotes progression of human breast cancer. *Clin Cancer Res,* 10**,** 2670-4.

WOOD, J. N., BOORMAN, J. P., OKUSE, K. & BAKER, M. D. 2004. Voltage-gated sodium channels and pain pathways. *J Neurobiol,* 61**,** 55-71.

WOOD, K. C. 2016. Two faces of circulating breast cancer cells. *Science Translational Medicine,* 8**,** 356ec149-356ec149.

WOOLF, C. J. & MA, Q. 2007. Nociceptors—Noxious Stimulus Detectors. *Neuron,* 55**,** 353-364.

WOOLF, C. J. & SALTER, M. W. 2000. Neuronal plasticity: increasing the gain in pain. *Science,* 288**,** 1765-9.

WOOLF, D. K., PADHANI, A. R. & MAKRIS, A. 2015. Assessing response to treatment of bone metastases from breast cancer: what should be the standard of care? *Ann Oncol,* 26**,** 1048-57.

WORSCHECH, A., KMIECIAK, M., KNUTSON, K. L., BEAR, H. D., SZALAY, A. A., WANG, E., MARINCOLA, F. M. & MANJILI, M. H. 2008. Signatures associated with rejection or recurrence in HER-2/neu-positive mammary tumors. *Cancer Res,* 68**,** 2436-46.

WU, D. F., CHANDRA, D., MCMAHON, T., WANG, D., DADGAR, J., KHARAZIA, V. N., LIANG, Y. J., WAXMAN, S. G., DIB-HAJJ, S. D. & MESSING, R. O. 2012a. PKCepsilon phosphorylation of the sodium channel NaV1.8 increases channel function and produces mechanical hyperalgesia in mice. *J Clin Invest,* 122**,** 1306-15.

WU, J., MAO, X., CAI, T., LUO, J. & WEI, L. 2006. KOBAS server: a web-based platform for automated annotation and pathway identification. *Nucleic Acids Res,* 34**,** W720-4.

WU, J. X., XU, M. Y., MIAO, X. R., LU, Z. J., YUAN, X. M., LI, X. Q. & YU, W. F. 2012b. Functional up-regulation of P2X3 receptors in dorsal root ganglion in a rat model of bone cancer pain. *Eur J Pain,* 16**,** 1378-88.

WU, J. X., YUAN, X. M., WANG, Q., WEI, W. & XU, M. Y. 2016a. Rho/ROCK acts downstream of lysophosphatidic acid receptor 1 in modulating P2X3 receptor-mediated bone cancer pain in rats. *Mol Pain,* 12.

WU, M., LU, L., ZHANG, Q., GUO, Q., ZHAO, F., LI, T. & ZHANG, X. 2016b. Relating Doses of Contrast Agent Administered to TIC and Semi-Quantitative Parameters on DCE-MRI: Based on a Murine Breast Tumor Model. *PLoS One,* 11**,** e0149279.

WU, Y., SARKISSYAN, M. & VADGAMA, J. 2016c. Epithelial-Mesenchymal Transition and Breast Cancer. *Journal of Clinical Medicine,* 5**,** 13.

XIA, H., ZHANG, D., YANG, S., WANG, Y., XU, L., WU, J., REN, J., YAO, W., FAN, L., ZHANG, C., TIAN, Y., PAN, H. L. & WANG, X. 2014. Role of ATP-sensitive potassium channels in modulating nociception in rat model of bone cancer pain. *Brain Res,* 1554**,** 29-35.

XIE, C., MAO, X., HUANG, J., DING, Y., WU, J., DONG, S., KONG, L., GAO, G., LI, C. Y. & WEI, L. 2011. KOBAS 2.0: a web server for annotation and identification of enriched pathways and diseases. *Nucleic Acids Res,* 39**,** W316-22.

XU, B., O'DONNELL, M., O'DONNELL, J., YU, J., ZHANG, Y., SARTOR, M. A. & KOENIG, R. J. 2016. Adipogenic differentiation of thyroid cancer cells through the Pax8-PPARgamma fusion protein is regulated by thyroid transcription factor 1 (TTF-1). *Journal of Biological Chemistry*.

XU, J.-Y., JIANG, Y., LIU, W. & HUANG, Y.-G. 2015. *Calpain Inhibitor Reduces Cancer-induced Bone Pain Possibly Through Inhibition of Osteoclastogenesis in Rat Cancer-induced Bone Pain Model*.

XU, Q., ZHANG, X. M., DUAN, K. Z., GU, X. Y., HAN, M., LIU, B. L., ZHAO, Z. Q. & ZHANG, Y. Q. 2013. Peripheral TGF-beta1 signaling is a critical event in bone cancer-induced hyperalgesia in rodents. *J Neurosci,* 33**,** 19099-111.

YALOVENKO, T. M., TODOR, I. M., LUKIANOVA, N. Y. & CHEKHUN, V. F. 2016. Hepcidin as a possible marker in determination of malignancy degree and sensitivity of breast cancer cells to cytostatic drugs. *Exp Oncol,* 38**,** 84-8.

YANG, C. J., WANG, X. W., LI, X., WU, G. C., WANG, Y. Q. & MAO-YING, Q. L. 2011. A rat model of bone inflammation-induced pain by intra-tibial complete Freund's adjuvant injection. *Neurosci Lett,* 490**,** 175-9.

YANG, L., LI, Q., LIU, X. & LIU, S. 2016. Roles of Voltage-Gated Tetrodotoxin-Sensitive Sodium Channels Na(V)1.3 and Na(V)1.7 in Diabetes and Painful Diabetic Neuropathy. *International Journal of Molecular Sciences,* 17**,** 1479.

YANG, X., JIA, M., LI, Z., LU, S., QI, X., ZHAO, B., WANG, X., RONG, Y., SHI, J., ZHANG, Z., XU, W., GAO, Y., ZHANG, S. & YU, G. 2014. Bioinformatics analysis of aggressive behavior of breast cancer via an integrated gene regulatory network. *J Cancer Res Ther,* 10**,** 1013-8.

YANG, Y., LI, H., LI, T. T., LUO, H., GU, X. Y., LU, N., JI, R. R. & ZHANG, Y. Q. 2015. Delayed activation of spinal microglia contributes to the maintenance of bone cancer pain in female Wistar rats via P2X7 receptor and IL-18. *J Neurosci,* 35**,** 7950-63.

YANG, Z., LV, Q., WANG, Z., DONG, X., YANG, R. & ZHAO, W. 2017. Identification of crucial genes associated with rat traumatic spinal cord injury. *Mol Med Rep,* 15**,** 1997-2006.

YAO, M., CHANG, X. Y., CHU, Y. X., YANG, J. P., WANG, L. N., CAO, H. Q., LIU, M. J. & XU, Q. N. 2011. Antiallodynic effects of propentofylline Elicited by interrupting spinal glial function in a rat model of bone cancer pain. *J Neurosci Res,* 89**,** 1877-86.

YAO, M., YANG, J. P., WANG, L. N., CHENG, H., ZHANG, Y. B., XU, Q. N. & WU, Y. W. 2008. [Feasibility of establishment of rat model of bone cancer pain by using Walker 256 cells cultured in vitro or in vivo]. *Zhonghua Yi Xue Za Zhi,* 88**,** 880-4.

YAO, P., DING, Y., WANG, Z., MA, J., HONG, T., ZHU, Y., LI, H. & PAN, S. 2016. Impacts of anti-nerve growth factor antibody on pain-related behaviors and expressions of opioid receptor

in spinal dorsal horn and dorsal root ganglia of rats with cancer-induced bone pain. *Mol Pain,* 12.

YAO, W., ZHAO, H., SHI, R., LI, X., LI, Y., KE, C. & LIU, J. 2017. Recombinant protein transduction domain-Cu/Zn superoxide dismutase alleviates bone cancer pain via peroxiredoxin 4 modulation and antioxidation. *Biochemical and Biophysical Research Communications,* 486**,** 1143-1148.

YE, D., BU, H., GUO, G., SHU, B., WANG, W., GUAN, X., YANG, H., TIAN, X., XIANG, H. & GAO, F. 2014a. Activation of CXCL10/CXCR3 signaling attenuates morphine analgesia: involvement of Gi protein. *J Mol Neurosci,* 53**,** 571-9.

YE, X., WANG, L., SHANG, B., WANG, Z. & WEI, W. 2014b. NEDD4: A Promising Target for Cancer Therapy. *Curr Cancer Drug Targets,* 14**,** 549-56.

YE, Y., BAE, S. S., VIET, C. T., TROOB, S., BERNABÉ, D. & SCHMIDT, B. L. 2014c. IB4(+) and TRPV1(+) sensory neurons mediate pain but not proliferation in a mouse model of squamous cell carcinoma. *Behav Brain Funct,* 10**,** 5.

YEKKIRALA, A. S., ROBERSON, D. P., BEAN, B. P. & WOOLF, C. J. 2017. Breaking barriers to novel analgesic drug development. *Nat Rev Drug Discov,* advance online publication.

YERSAL, O. & BARUTCA, S. 2014. Biological subtypes of breast cancer: Prognostic and therapeutic implications. *World J Clin Oncol,* 5**,** 412-24.

YIN, B., ZHANG, M., ZENG, Y., LI, Y., ZHANG, C. & SONG, Y. 2016a. Downregulation of cytokeratin 18 is associated with paclitaxelresistance and tumor aggressiveness in prostate cancer. *Int J Oncol,* 48**,** 1730-6.

YIN, K., BAILLIE, G. J. & VETTER, I. 2016b. Neuronal cell lines as model dorsal root ganglion neurons: A transcriptomic comparison. *Mol Pain,* 12.

YIN, K., DEUIS, J. R., LEWIS, R. J. & VETTER, I. 2016c. Transcriptomic and behavioural characterisation of a mouse model of burn pain identify the cholecystokinin 2 receptor as an analgesic target. *Mol Pain,* 12.

YIN, Q., CHENG, W., CHENG, M. Y., FAN, S. Z. & SHEN, W. 2010. Intrathecal injection of anti-CX3CR1 neutralizing antibody delayed and attenuated pain facilitation in rat tibial bone cancer pain model. *Behav Pharmacol,* 21**,** 595-601.

YONEDA, T., HIASA, M., NAGATA, Y., OKUI, T. & WHITE, F. A. 2015. Acidic microenvironment and bone pain in cancer-colonized bone. *Bonekey Rep,* 4**,** 690.

YU, S., PENG, H. D., JU, D. W., WEI, P. K., XU, L., LAO, L. X. & LI, J. 2009. Mechanisms of treatment of cancer pain with a topical Chinese herbal formula in rats. *Chin Med J (Engl),* 122**,** 2027-31.

ZAHA, D. C. 2014. Significance of immunohistochemistry in breast cancer. *World J Clin Oncol,* 5**,** 382-92.

ZAMBELLI, V. O., CHIOATO, L., GUTIERREZ, V. P., WARD, R. J. & CURY, Y. 2017. Structural determinants of the hyperalgesic activity of myotoxic Lys49-phospholipase A2. *Journal of Venomous Animals and Toxins including Tropical Diseases,* 23**,** 7.

ZELIVIANSKI, S., VERNI, M., MOORE, C., KONDRIKOV, D., TAYLOR, R. & LIN, M.-F. 2001. Multipathways for transdifferentiation of human prostate cancer cells into neuroendocrine-like phenotype. *Biochimica et Biophysica Acta (BBA) - Molecular Cell Research,* 1539**,** 28-43.

ZHANG, C., GUAN, Y., SUN, Y., AI, D. & GUO, Q. 2016. Tumor heterogeneity and circulating tumor cells. *Cancer Lett,* 374**,** 216-23.

ZHANG, C., ZHU, Y., WANG, S., WEI, Z. Z., JIANG MICHAEL, Q., ZHANG, Y., PAN, Y., TAO, S., LI, J. & WEI, L. 2017. Temporal Gene Expression Profiles after Focal Cerebral Ischemia in Mice. *A&D***,** 0-.

ZHANG, G. & YANG, P. 2017. Bioinformatics Genes and Pathway Analysis for Chronic Neuropathic Pain after Spinal Cord Injury. *BioMed Research International,* 2017**,** 6423021.

ZHANG, J. Y., GONG, N., HUANG, J. L., GUO, L. C. & WANG, Y. X. 2013. Gelsemine, a principal alkaloid from Gelsemium sempervirens Ait., exhibits potent and specific antinociception in chronic pain by acting at spinal alpha3 glycine receptors. *Pain,* 154**,** 2452-62.

ZHANG, M. Y., LIU, Y. P., ZHANG, L. Y., YUE, D. M., QI, D. Y., LIU, G. J. & LIU, S. 2015. Levo-Tetrahydropalmatine Attenuates Bone Cancer Pain by Inhibiting Microglial Cells Activation. *Mediators Inflamm,* 2015**,** 752512.

ZHANG, Q., FAN, H., SHEN, J., HOFFMAN, R. M. & XING, H. R. 2010. Human Breast Cancer Cell Lines Co-Express Neuronal, Epithelial, and Melanocytic Differentiation Markers In Vitro and In Vivo. *PLoS ONE,* 5**,** e9712.

ZHANG, R.-X., LI, A., LIU, B., WANG, L., XIN, J., REN, K., QIAO, J.-T., BERMAN, B. M. & LAO, L. 2008. Electroacupuncture attenuates bone cancer-induced hyperalgesia and inhibits spinal preprodynorphin expression in a rat model. *European Journal of Pain,* 12**,** 870-878.

ZHANG, X., HUANG, J. & MCNAUGHTON, P. A. 2005. NGF rapidly increases membrane expression of TRPV1 heat-gated ion channels. *Embo j,* 24**,** 4211-23.

ZHANG, X., MAK, S., LI, L., PARRA, A., DENLINGER, B., BELMONTE, C. & MCNAUGHTON, P. A. 2012. Direct inhibition of the cold-activated TRPM8 ion channel by Galphaq. *Nat Cell Biol,* 14**,** 851-8.

ZHAO, C., TALL, J. M., MEYER, R. A. & RAJA, S. N. 2004. Antiallodynic effects of systemic and intrathecal morphine in the spared nerve injury model of neuropathic pain in rats. *Anesthesiology,* 100**,** 905-11.

ZHAO, D., PLOTNIKOFF, N., GRIFFIN, N., SONG, T. & SHAN, F. 2016. Methionine enkephalin, its role in immunoregulation and cancer therapy. *Int Immunopharmacol,* 37**,** 59-64.

ZHAO, J., PAN, H. L., LI, T. T., ZHANG, Y. Q., WEI, J. Y. & ZHAO, Z. Q. 2010. The sensitization of peripheral C-fibers to lysophosphatidic acid in bone cancer pain. *Life Sci,* 87**,** 120-5.

ZHAO, P., WAXMAN, S. G. & HAINS, B. C. 2006. Sodium channel expression in the ventral posterolateral nucleus of the thalamus after peripheral nerve injury. *Mol Pain,* 2**,** 27.

ZHAO, Y. & BOULANT, J. A. 2005. Temperature effects on neuronal membrane potentials and inward currents in rat hypothalamic tissue slices. *J Physiol,* 564**,** 245-57.

ZHAO, Y., TIAN, L., SHENG, W., MIAO, J. & YANG, J. 2013. Hypalgesia effect of IL-24, a quite new mechanism for IL-24 application in cancer treatment. *J Interferon Cytokine Res,* 33**,** 606-11.

ZHENG, Q., FANG, D., LIU, M., CAI, J., WAN, Y., HAN, J.-S. & XING, G.-G. 2013. Suppression of KCNQ/M (Kv7) potassium channels in dorsal root ganglion neurons contributes to the development of bone cancer pain in a rat model. *PAIN®,* 154**,** 434-448.

ZHOU, X., LI, J. & YANG, W. 2014. Calcium/calmodulin-dependent protein kinase II regulates cyclooxygenase-2 expression and prostaglandin E2 production by activating cAMP-response element-binding protein in rat peritoneal macrophages. *Immunology,* 143**,** 287-99.

ZHOU, Y.-Q., LIU, D.-Q., CHEN, S.-P., SUN, J., ZHOU, X.-R., RITTNER, H., MEI, W., TIAN, Y.-K., ZHANG, H.-X., CHEN, F. & YE, D.-W. 2018. Reactive oxygen species scavengers ameliorate mechanical allodynia in a rat model of cancer-induced bone pain. *Redox Biology,* 14**,** 391-397.

ZHOU, Y. L., JIANG, G. Q., WEI, J., ZHANG, H. H., CHEN, W., ZHU, H., HU, S., JIANG, X. & XU, G. Y. 2015. Enhanced binding capability of nuclear factor-kappaB with demethylated P2X3 receptor gene contributes to cancer pain in rats. *Pain,* 156**,** 1892-905.

ZHU, B., GONG, N., FAN, H., PENG, C. S., DING, X. J., JIANG, Y. & WANG, Y. X. 2014a. Lamiophlomis rotata, an orally available Tibetan herbal painkiller, specifically reduces pain hypersensitivity states through the activation of spinal glucagon-like peptide-1 receptors. *Anesthesiology,* 121**,** 835-51.

ZHU, G., DONG, Y., HE, X., ZHAO, P., YANG, A., ZHOU, R., MA, J., XIE, Z. & SONG, X. J. 2016. Radiotherapy Suppresses Bone Cancer Pain through Inhibiting Activation of cAMP Signaling in Rat Dorsal Root Ganglion and Spinal Cord. *Mediators Inflamm,* 2016**,** 5093095.

ZHU, G. Q., LIU, S., HE, D. D., LIU, Y. P. & SONG, X. J. 2014b. Activation of the cAMP-PKA signaling pathway in rat dorsal root ganglion and spinal cord contributes toward induction and maintenance of bone cancer pain. *Behav Pharmacol,* 25**,** 267-76.

ZHU, S., WANG, C., HAN, Y., SONG, C., HU, X. & LIU, Y. 2015a. Sigma-1 Receptor Antagonist BD1047 Reduces Mechanical Allodynia in a Rat Model of Bone Cancer Pain through the Inhibition of Spinal NR1 Phosphorylation and Microglia Activation. *Mediators of Inflammation,* 2015.

ZHU, X. C., ZHANG, J. L., GE, C. T., YU, Y. Y., WANG, P., YUAN, T. F. & FU, C. Y. 2015b. Advances in cancer pain from bone metastasis. *Drug Des Devel Ther,* 9**,** 4239-45.

ZIMMERMANN, K., LEFFLER, A., BABES, A., CENDAN, C. M., CARR, R. W., KOBAYASHI, J., NAU, C., WOOD, J. N. & REEH, P. W. 2007. Sensory neuron sodium channel Nav1.8 is essential for pain at low temperatures. *Nature,* 447**,** 855-8.

ZIMMERMANN, K., LENNERZ, J. K., HEIN, A., LINK, A. S., KACZMAREK, J. S., DELLING, M., UYSAL, S., PFEIFER, J. D., RICCIO, A. & CLAPHAM, D. E. 2011. Transient receptor potential cation channel, subfamily C, member 5 (TRPC5) is a cold-transducer in the peripheral nervous system. *Proc Natl Acad Sci U S A,* 108**,** 18114-9.

APPENDICES

Appendix- 1. Percent multi versus unique- mapping of reads in all 15 samples of neuronal tissues from BCIBP and sham rats.

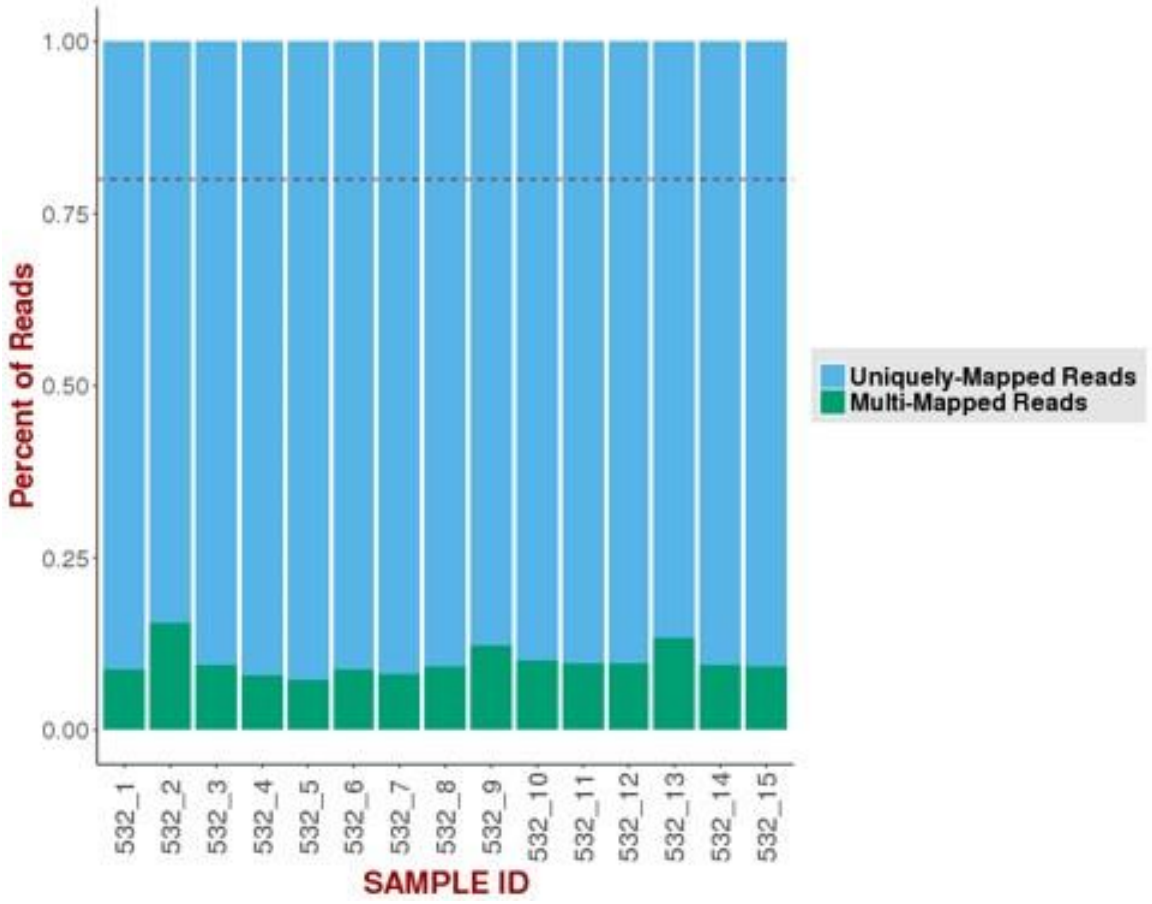

Appendix- 2. The principal component analysis using the read counts for genes in all 15 samples of neuronal tissues from BCIBP and sham rats.

A

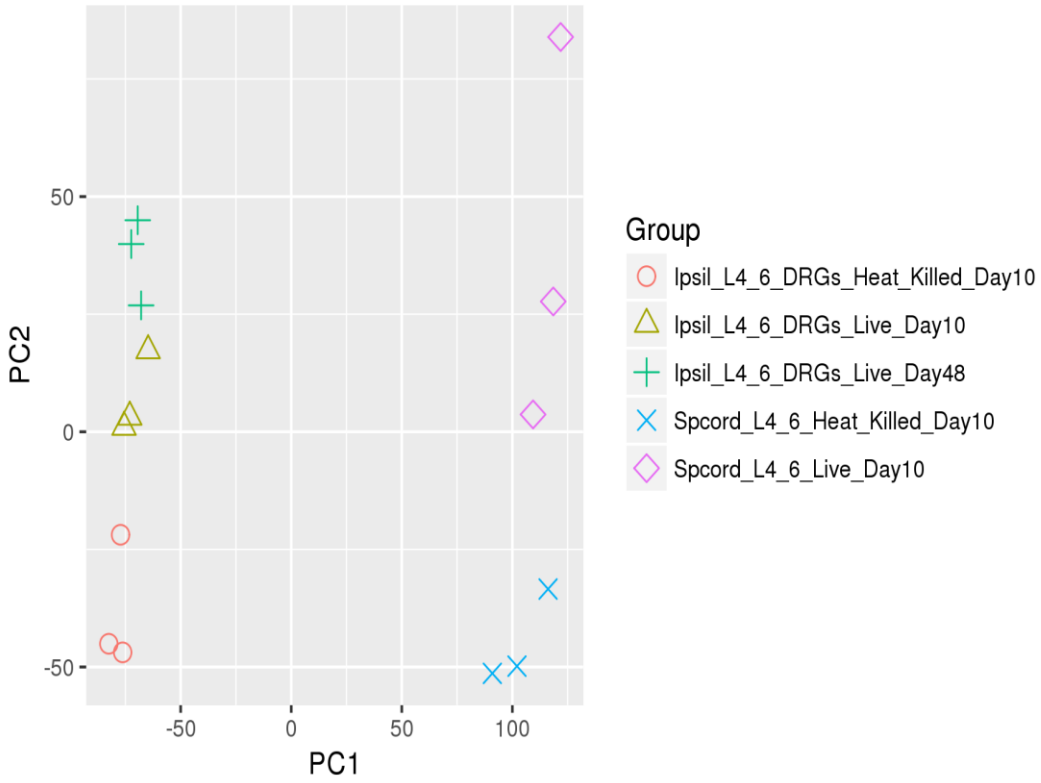

B

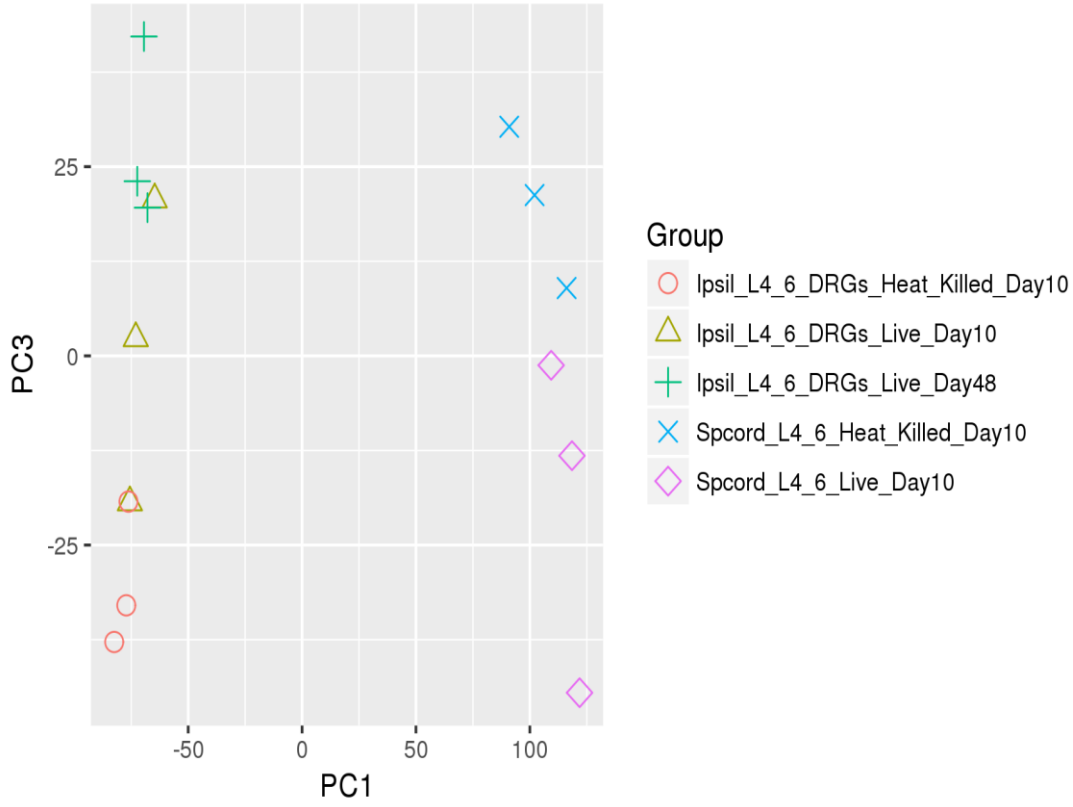

C

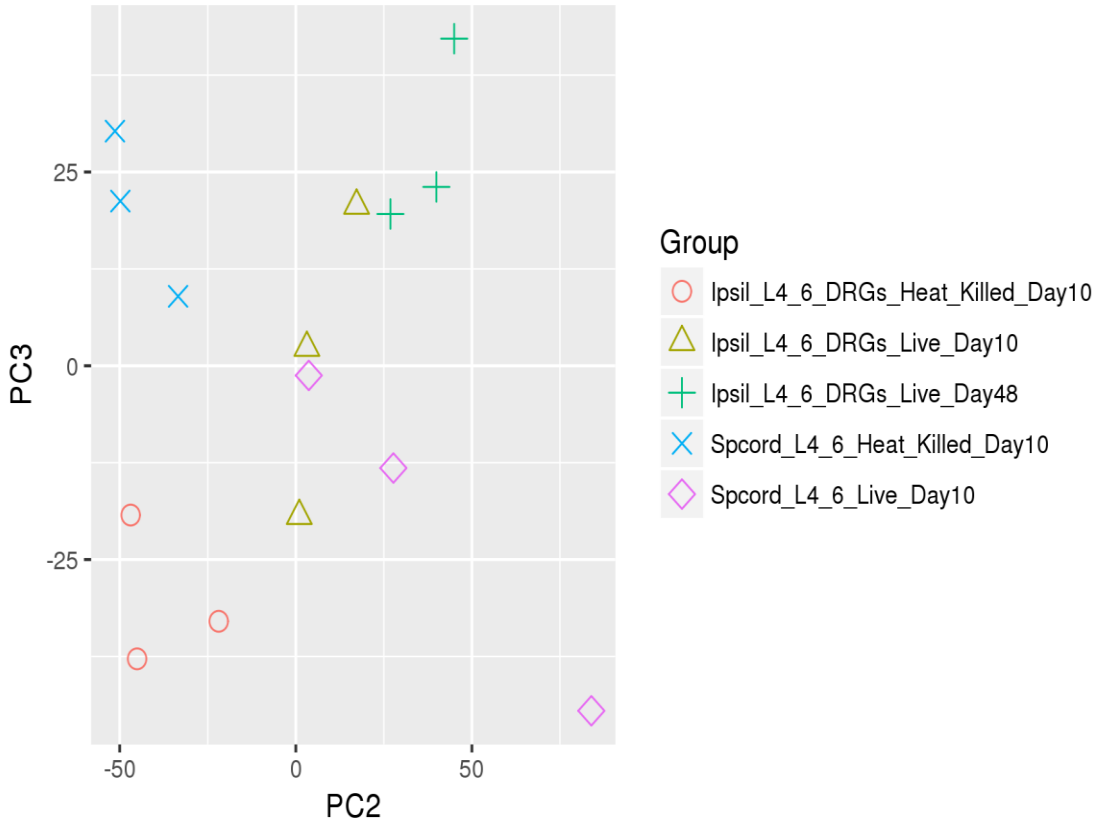
25
0
-25
PC3
-50
0
50
PC2
Group
Ipsil_L4_6_DRGs_Heat_Killed_Day10
Ipsil_L4_6_DRGs_Live_Day10
Ipsil_L4_6_DRGs_Live_Day48
Spcord_L4_6_Heat_Killed_Day10
Spcord_L4_6_Live_Day10

Appendix- 3. List of upregulated genes (abbreviations as per standard gene nomenclature) in lumbar spinal cord of BCIBP rats compared to sham rats given heat-killed cancer cells; day 10 post-ITI.

RGD1563668	Cers4	Hn1l
Igf1	Cggbp1	
Rtkn2	Usp31	
Igf2	Galnt7	
Igfbp3	Marcks	
Depdc1b	Btbd8	
Slc7a11	Cdkl5	
Ago3	Igfbp2	
Gan	Ccne2	
Clca1	Xiap	
Cdkn1c	Tgfb2	
Anlnl1	Klhl28	
Slitrk6	Cyp2j10	
Vps13a	D14Abb1e	
Mob1b	Cpd	
AI429214	RGD1306941	
MT-ND4L	Mylk	
Entpd5	Tmeff1	
Tmem254	Utp14b	
Fam126b	Amot	
Ptar1	Pik3c2a	
Scd1	Cpsf6	
Zdhhc20	Gabrb2	
SPPL2A	St18	
Trove2	Ccdc88a	
Agps	Pank3	
Tgfbr1	Smc2	
Far1	Yes1	
RGD1566380	Fnip1	
Slc7a2	Kdm5a	
Trim59	Reep3	
Hsd17b7	Pus7	
Ctnna3	Tmed5	
Erbb4	Elovl7	
RGD1563888	Lonrf3	
RGD1305938	Fmnl2	
Zdhhc21	Ptpn4	
Lyrm5	MT-ATP8	
Snap23	Slc12a2	
Agmo	Rapgef5	
Fam210a	Rb1	
Prrg1	Rabgap1l	

Appendix- 4. List of downregulated genes (abbreviations as per standard gene nomenclature) in lumbar spinal cord of BCIBP rats compared to sham rats given heat-killed cancer cells; day 10 post-ITI.

Ngef	Hspbp1	Tuba1c	Tmem255b	Gdf1
Atp1a1	Agt	Mif	Mical1	Rab3b
Tmem86a	Tceb2	Ndufs7	Pcbd1	Egfl8
Wash	Ndufb7	Mef2bnb	Nefh	Tspan17
Naglu	Mt3	PQLC1	Rplp1	Impdh1
Serp2	Rpusd3	Isoc2a	Zic1	Nptx2
Tox3	Stmn2	Ckb	Man2b2	Sfrp5
Col9a2	Cldn5	Nefl	Capn1	Cck
Arhgdig	Ssbp4	Dlgap3	Pomgnt2	Tubb3
Atp13a2	RGD1561113	Stk32c	Slc2a6	Syndig1l
Hdac7	Enho	Rac3	TMEM9	Rab3d
Traf3ip2	Dos	Col4a1	Polr3g	Vstm2l
Fam173a	Jag2	Timm13	Acads	Rem2
Rnf208	Inha	Pabpc1l2a	Slc29a4	Sncg
Slc9a3r2	Lppr2	Drp2	Cd24	Fxyd7
Frmpd1	Them6	Fbll1	Kcnd1	Ahnak2
Nell2	Kcnj12	Sema4f	Tesc	Palm3
Samd14	Btbd2	Tmem63c	Tldc1	Cpne6
Hoxd9	Sh3bgrl3	Gpc1	RET	Bmyc
Fbxl16	Ndufa13	S100a10	Fbln2	Shh
Arvcf	Mfng	Fam189b	BCL7B	Anxa2
Fam213b	Spire2	Jund	Cacnb3	Uts2
Tmem151b	Nrgn	COL4A2	Crip2	Ncmap
Bok	Bid	Map1s	Flywch2	H1fx
Nfkbie	Josd2	Coro2a	Fam69c	Susd2
Tpgs1	Hspb8	Tmem160	Hmgcs2	Dok4
Shc2	Parp3	Vbp1	Serpinb6	Hspb1
Adck3	Rhbdl1	RPL37	DHRSX	Npy2r
Cacna1h	Bag3	Col5a3	Metrnl	Serinc2
Atp5d	Lsm7	Bex1	Alpl	Ppm1j
Nipsnap3b	Mest	Kcnk4	Crym	Kcnf1
Nr2f6	Dohh	Numbl	Trpv2	Prph
Pkdcc	Ndufb4	Bcam	Ifi27	Calcb
MAST1	Chpf	Camk2n2	Lgals1	Calca
Rps15	RGD1562390	Lrfn1	Nrg1	Isl2
Baiap3	Slc7a4	Elfn1	S100a6	
Fam57b	H2afz	Celf4	Dkc1	
Abhd8	Chchd5	Htra1	Ifi27l2b	
Mien1	Syde1	Pafah1b3	Kcnh6	
Hoxc10	Pcbp3	Nefm	Mt2A	
Rarg	Snx21	Dysf	Itga7	
Sync	Cdk5r2	Slc41a3	Rplp2	

Appendix- 5. List of upregulated genes (abbreviations as per standard gene nomenclature) in ipsilateral lumbar DRGs of BCIBP rats at day 48 post-ITI (resolved pain state) compared to BCIBP rats at day 10 post-ITI (pain state).

Cdh19
Abca9
Tef
Crebl2
Ephx1
NR1D2
Per3
Dbp
Nr1d1
RGD1566380

Appendix- 6. List of downregulated genes (abbreviations as per standard gene nomenclature) in ipsilateral lumbar DRGs of BCIBP rats at day 48 post-ITI (resolved pain state) compared to BCIBP rats at day 10 post-ITI (pain state).

Tnc
ARNTL
Col16a1
COL4A2
Gpx7
S1pr3
Heyl
Mmp14
MT-ND4L
Chsy1
Cd93
Cadm4
Lepre1
Adam17